VOLUME 35 | SUPPLEMENT 2 | MARCH 2022

MODERN PATHOLOGY

ABSTRACTS (74–204)

BREAST PATHOLOGY

2022

USCAP 111TH ANNUAL MEETING

REAL INTELLIGENCE

MARCH 19–24, 2022 LOS ANGELES, CALIFORNIA

Published by
SPRINGER NATURE
www.ModernPathology.org

USCAP
Creating a Better Pathologist
AN OFFICIAL JOURNAL OF THE UNITED STATES AND CANADIAN ACADEMY OF PATHOLOGY

EDUCATION COMMITTEE

Rhonda K. Yantiss
Chair

Kristin C. Jensen
Chair, CME Subcommittee

Laura C. Collins
Chair, Interactive Microscopy Subcommittee

Yuri Fedoriw
Short Course Coordinator

Ilan Weinreb
Chair, Subcommittee for Unique Live Course Offerings

Carla L. Ellis
Chair, DEI Subcommittee

Adebowale J. Adeniran
Kimberly H. Allison
Sarah M. Dry
William C. Faquin
Karen J. Fritchie
Jennifer B. Gordetsky
Levon Katsakhyan, Pathologist-in-Training
Melinda J. Lerwill
M. Beatriz S. Lopes
Julia R. Naso, Pathologist-in-Training
Liron Pantanowitz
Carlos Parra-Herran
Rajiv M. Patel
Charles "Matt" Quick
David F. Schaeffer
Lynette M. Sholl
Olga K. Weinberg
Maria Westerhoff

ABSTRACT REVIEW BOARD

Benjamin Adam
Oyedele Adeyi
Mariam Priya Alexander
Daniela Allende
Catalina Amador
Vijayalakshmi Ananthanarayanan
Tatjana Antic
Manju Aron
Roberto Barrios
Gregory R. Bean
Govind Bhagat
Luis Zabala Blanco
Michael Bonert
Alain C. Borczuk
Tamar C. Brandler
Eric Jason Burks
Kelly J. Butnor
Sarah M. Calkins
Weibiao Cao
Wenqing (Wendy) Cao
Barbara Ann Centeno
Joanna SY Chan
Kung-Chao Chang
Hao Chen
Wei Chen
Yunn-Yi Chen
Sarah Chiang
Soo-Jin Cho
Shefali Chopra
Nicole A. Cipriani
Cecilia Clement
Claudiu Cotta
Jennifer A. Cotter
Sonika M. Dahiya
Elizabeth G. Demicco
Katie Dennis
Jasreman Dhillon
Anand S. Dighe
Bojana Djordjevic
Michelle R. Downes
Charles G. Eberhart
Andrew G. Evans
Fang Fan
Julie C. Fanburg-Smith
Gelareh Farshid
Michael Feely
Susan A. Fineberg
Dennis J. Firchau
Gregory A. Fishbein
Agnes B. Fogo
Andrew L. Folpe
Danielle Fortuna
Billie Fyfe-Kirschner
Zeina Ghorab
Giovanna A. Giannico
Anthony J. Gill
Tamar A. Giorgadze
Alessio Giubellino
Carolyn Glass
Carmen R. Gomez-Fernandez
Shunyou Gong
Purva Gopal
Abha Goyal
Christopher C. Griffith
Ian S. Hagemann
Gillian Leigh Hale
Suntrea TG Hammer
Malini Harigopal
Kammi J. Henriksen
Jonas J. Heymann
Carlo Vincent Hojilla
Aaron R. Huber
Jabed Iqbal
Shilpa Jain
Vickie Y. Jo
Ivy John
Dan Jones
Ridas Juskevicius
Meghan E. Kapp
Nora Katabi
Francesca Khani
Joseph D. Khoury
Benjamin Kipp
Veronica E. Klepeis
Christian A. Kunder
Stefano La Rosa
Stephen M. Lagana
Keith K. Lai
Goo Lee
Michael Lee
Vasiliki Leventaki
Madelyn Lew
Faqian Li
Ying Li
Chieh-Yu Lin
Mikhail Lisovsky
Lesley C. Lomo
Fang-I Lu
aDeqin Ma
Varsha Manucha
Rachel Angelica Mariani
Brock Aaron Martin
David S. McClintock
Anne M. Mills
Richard N. Mitchell
Hiroshi Miyamoto
Kristen E. Muller
Priya Nagarajan
Navneet Narula
Michiya Nishino
Maura O'Neil
Scott Roland Owens
Burcin Pehlivanoglu
Deniz Peker Barclift
Avani Anil Pendse
Andre Pinto
Susan Prendeville
Carlos N. Prieto Granada
Peter Pytel
Stephen S. Raab
Emilian V. Racila
Stanley J. Radio
Santiago Ramon Y Cajal
Kaaren K Reichard
Jordan P. Reynolds
Lisa M. Rooper
Andrew Eric Rosenberg
Ozlen Saglam
Ankur R. Sangoi
Kurt B. Schaberg
Qiuying (Judy) Shi
Wonwoo Shon
Pratibha S. Shukla
Gabriel Sica
Alexa Siddon
Anthony Sisk
Kalliopi P. Siziopikou
Stephanie Lynn Skala
Maxwell L. Smith
Isaac H. Solomon
Wei Song
Simona Stolnicu
Adrian Suarez
Paul E. Swanson
Benjamin Jack Swanson
Sara Szabo
Gary H. Tozbikian
Gulisa Turashvili
Andrew T. Turk
Efsevia Vakiani
Paul VanderLaan
Hanlin L. Wang
Stephen C. Ward
Kevin M. Waters
Jaclyn C. Watkins
Shi Wei
Hannah Y. Wen
Kwun Wah Wen
Kristy Wolniak
Deyin Xing
Ya Xu
Shaofeng N. Yan
Zhaohai Yang
Yunshin Albert Yeh
Huina Zhang
Xuchen Zhang
Bihong Zhao
Lei Zhao

To cite abstracts in this publication, please use the following format: **Author A, Author B, Author C, et al. Abstract title (abs#). In "File Title."** ***Modern Pathology*** **2022; 35 (suppl 2): page#**

74 Estrogen Receptor Status May Have Prognostic Relevance In Metaplastic Breast Carcinoma

Evi Abada[1], Keion Dozier[1], Seongho Kim[2], Hyejeong Jang[2], Omar Fehmi[3], Othuke Abada[4], Ziad Fehmi[5], Deepti Jain[1], Reema Smadi[1], Mohamed Garada[6], Tala Tawil[1], Sudeshna Bandyopadhyay[1]
[1]Wayne State University, Detroit, MI, [2]Karmanos Cancer Institute, Detroit, MI, [3]University of Michigan, Ann Arbor, MI, [4]Ascension St. John Hospital, Detroit, MI, [5]University of Michigan, Detroit, MI, [6]Michigan State University, Detroit, MI

Disclosures: Evi Abada: None; Keion Dozier: None; Seongho Kim: None; Hyejeong Jang: None; Omar Fehmi: None; Othuke Abada: None; Ziad Fehmi: None; Deepti Jain: None; Reema Smadi: None; Mohamed Garada: None; Tala Tawil: None; Sudeshna Bandyopadhyay: None

Background: Metaplastic breast carcinoma (MBC) is a rare histologic variant of breast cancer characterized by the presence of glandular and non-glandular components with the majority of cases being triple negative. The prognostic significance of estrogen receptor (ER) status has been scarcely studied in these tumors. We, therefore, aimed to study the prognostic relevance of ER status in MBC within our patient population.

Design: We reviewed MBC cases (n = 125) from our institution between January 2000 and September 2019. Histologic slides were reviewed for variables including tumor morphology and hormonal status. Additional clinical information was obtained from the electronic medical records and pathology reports to include demographic information, size, grade, stage, treatment received, and comorbidities. Fisher's exact test and Wilcoxon rank-sum test were used to compare patient characteristics by ER status and Cox analysis was used to assess the association between overall survival (OS) and ER status.

Results: Of the 125 patients, 15 (12%) had ER-positive tumors and 110 (82%) had ER negative tumors. Ninety-three (74%) patients had triple negative tumors, 17 (14%) patients had progesterone (PR) positive tumors and 9 (7%) patients had HER2 positive tumors. Of the ER positive tumors, 11 (73%) had ER positivity > 10% and 4 (27%) had ER positivity $\leq$ 10%. MBC was more likely to be high-grade (115; 92%) regardless of hormonal status. Heterologous histology was the predominant pattern in ER positive tumors (40%). ER positive tumors also had a smaller median tumor size of 2.5cm (range: 0.6-11.5). Patients with ER-positive tumors were more likely to present with stage II disease (53%) and metastatic disease only occurred in one patient (7%) with ER positive tumors. There was no difference between ER positive and ER negative tumors in terms of age at diagnosis, tumor size, HER2 expression, fibrocystic breast disease, or coexistent ductal carcinoma in situ. ER-positive tumors were however more likely to also be PR positive ($p<0.001$). Additionally, ER positive tumors were also more likely to receive hormonal therapy ($p<0.001$). Compared with ER negative tumors, ER positive tumors appear to have a better OS, however, this finding was not statistically significant (HR=0.35, 95% CI, 0.003-2.67, P=0.39). Additional clinicopathologic characteristics are summarized in Table 1.

Table 1: Patient Characteristics

	All (n=125)	ER negative (n=110)	ER positive (n=15)	P value*
Age at diagnosis, median (range)	57 (27,92)	57 (27,92)	53 (33,88)	.27
Race, no. (%)				>.99
White	43 (34)	38 (35)	5 (33)	
Black/African American	71 (57)	62 (56)	9 (60)	
Other	11 (9)	10 (9)	1 (7)	
Tumor size (cm), median (range)	3 (0.5-21.5)	3.05 (0.5-21.5)	2.5 (0.6-11.5)	.82
Histologic grade, no. (%)				.34
Low	3 (2)	2 (2)	1 (7)	
Intermediate	7 (6)	6 (5)	1 (7)	
High	115 (92)	102 (93)	13 (87)	
Histologic type, no. (%)				.65
Squamous	36 (29)	31 (28)	5 (33)	
Spindle/Sarcomatoid	32 (26)	30 (27)	2 (13)	
Heterologous	38 (30)	32 (29)	6 (40)	
Mixed metaplastic	19 (15)	17 (15)	2 (13)	
AJCC Stage, no (%)				>.99
Stage I	27 (22)	24 (22)	3 (20)	
Stage II	59 (47)	51 (46)	8 (53)	
Stage III	21 (17)	19 (17)	2 (13)	
Stage IV	18 (14)	16 (15)	2 (13)	
HER2, no. (%)				.29
Positive	9 (7)	7 (6)	2 (13)	
Negative	116 (93)	103 (94)	13 (87)	
Progesterone receptor, no. (%)				***<.001***
Positive	17 (14)	8 (7)	9 (60)	
Negative	108 (86)	102 (93)	6 (40)	
Metastatic disease, no (%)				.69
Yes	18 (14)	17 (15)	1 (7)	
No	107 (86)	93 (85)	14 (93)	
Additional Treatment, no. (%)				.18
Not recorded	24 (19)	22 (20)	2 (13)	
Chemotherapy	91 (73)	81 (74)	10 (67)	
Without chemotherapy	10 (8)	7 (6)	3 (20)	
Hormonal therapy, no. (%)				***<.001***
Yes	26 (21)	17 (15)	9 (60)	
No	99 (79)	93 (85)	6 (40)	

*Fisher's exact test or Wilcox rank-sum test as appropriate

Figure 1 - 74

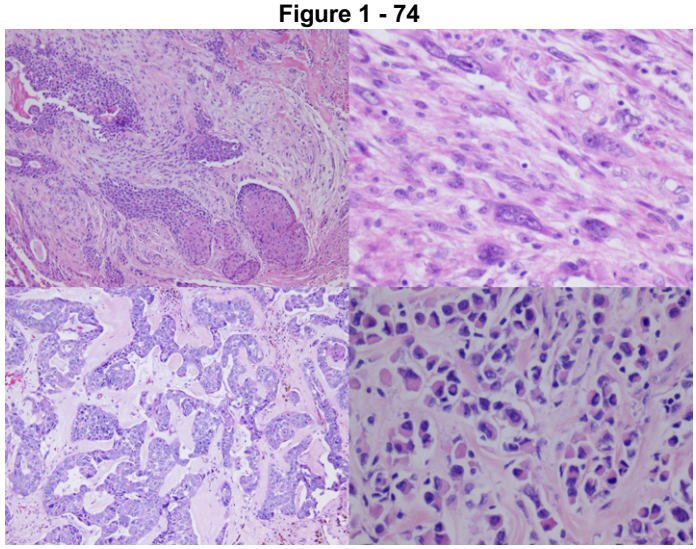

Figure 2 – 74

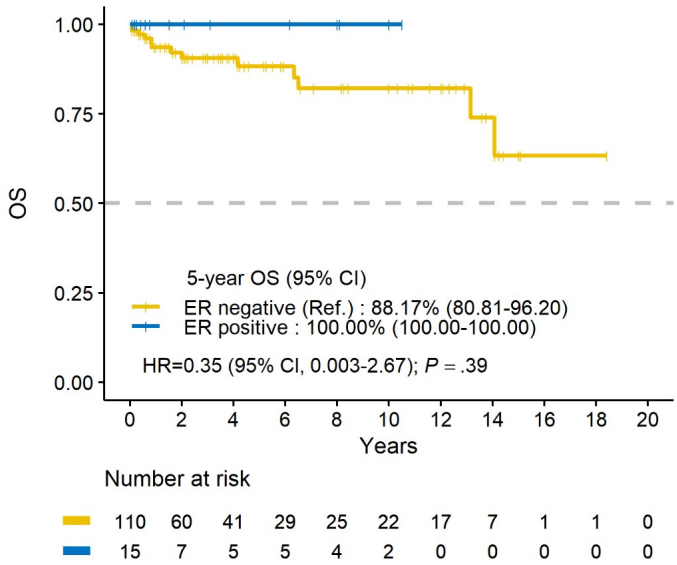

Conclusions: Our experience suggests that even though most cases of MBC are histologically high grade, ER positive status may have prognostic relevance in terms of OS and thus may have a role to play in the management of these patients. Additional research is needed to further elucidate the clinical implications of this finding.

75 Breast Markers TRPS1, GATA3 and Mammoglobin Expression in Triple Negative Breast Cancers (TNBC) and Implications in the Distant Metastatic (DM) Carcinoma Setting

Hala Abdelwahab[1], Zhiyan Fu[2], Saleh Najjar[3], Ammoura Ibrahim[1], Christopher Hsu[1], Sandra Shin[1]
[1]Albany Medical College, Albany, NY, [2]H. Lee Moffitt Cancer Center & Research Institute, Tampa, FL, [3]The University of Texas MD Anderson Cancer Center, Houston, TX

Disclosures: Hala Abdelwahab: None; Zhiyan Fu: None; Saleh Najjar: None; Ammoura Ibrahim: None; Christopher Hsu: None; Sandra Shin: None

Background: Ai et al. reported that TRPS1 was a superior breast marker than GATA3 in primary (PRI) TNBCs (*Mod Pathol* 2021:34;710–719). While most DM breast cancers are ER+ in the DM setting, TNBC could be missed if the PRI is unknown and TRPS1 is not used in the IHC work-up. We compared TRPS1, GATA3 and mammoglobin (MG) in TNBC and further, in matched PRI and DM TNBCs.

Design: TRPS1, GATA3 and MG were stained on TMA or whole tissue slides for 98 TNBC [PRI (84) and DM (14)], 6 of which were matched PRI and DM TNBCs. An additional 2 matched cases were TNBC (PRI) but DM tumor was non-TNBC. IHC was performed using commercially available antibodies TRPS1, GATA3, MG and automated staining protocols with appropriate positive (pos)/negative(neg) controls. Nuclear pos for TRPS1 and GATA3 was assessed with semi-quantitative scoring: % pos cells (0, <1%; 1, 1-10%; 2, 11-50%; 3, 51-100%) X staining intensity (0, neg: 1, weak; 2, moderate; 3, strong), resulting in overall score/final interpretation (0-1, neg; 2, pos; 3-4, intermediate pos or 6-9, high pos). For MG, >5% cytoplasmic/membranous staining of moderate or strong or 100% of weak staining intensity was deemed pos.

Results: TRPS1, GATA3 and MG was pos in 82/98 (84%), 56/98 (57%) and 52/96 (54%), respectively. TRPS1 was pos while GATA3 was neg in 30/98 (31%); and even less so(16%) if both GATA3 and MG were neg. Conversely, GATA3 was pos while TRPS1 was neg in 8/98 (8%); and even less so (4%) if both TRPS1 and MG were neg. In 4/98 (4%), MG was pos while TRPS1 and GATA3 were neg.

Of 6 matched PRI and DM TNBCs, the triple neg status was unchanged between PRI and DM tumors; status of 1 DM tumor was unknown. TRPS1 and GATA3 was unchanged for each matched case whereas for MG, pos staining was seen in the PRI but neg in the DM tumor in 2.

2 additional matched cases showed a change in triple neg status. While both PRI were TNBC, the DM tumor of 1 was HER2 pos while the other, the DM tumor was pos for both HER2 and progesterone. Also, MG was pos in both PRI TNBCs but then was neg in their matched DM tumors. GATA3 was neg in both PRI TNBCs but pos in their matched DM tumors. TRPS1 remained pos in both matched cases.

Conclusions: TRPS1 is a superior breast marker for TNBC than GATA3 or MG. TRPS1 should be included when evaluating DM tumors of unknown PRI where TNBC is a possibility. In the limited numbers studied here, TRPS1 did not change expression in matched cases of PRI and DM TNBC; a notable finding that did not hold true for GATA3 or MG.

76 The Utility of TRPS1 As a Breast Marker in the Distant Metastatic Carcinoma (DMC) Setting

Hala Abdelwahab[1], Zhiyan Fu[2], Christopher Hsu[1], Sandra Shin[1]
[1]Albany Medical College, Albany, NY, [2]H. Lee Moffitt Cancer Center & Research Institute, Tampa, FL

Disclosures: Hala Abdelwahab: None; Zhiyan Fu: None; Christopher Hsu: None; Sandra Shin: None

Background: Investigating metastatic carcinoma of unknown primary requires reliable breast markers to exclude a breast primary. Moreover, biopsies of DMC are small, requiring careful selection of immunostains to employ. GATA3, GCDFP-15 and mammoglobin (MG) works variably well to identify ER positive (pos) breast cancers. Recently, Ai et al. reported TRPS1 as a breast marker with superior sensitivity in triple negative breast cancers (TNBC) than GATA3 (*Mod Pathol* 2021:34;710–719). We aimed to assess TRPS1, GATA3 and MG in the DMC setting.

Design: TRPS1, GATA3 and MG were performed on TMA or whole tissue slides for 90 DMC of breast origin. IHC was performed using commercially available TRPS1, GATA3, and MG; on automated staining protocols with appropriate pos/negative (neg) controls. Nuclear pos for TRPS1 and GATA3 was assessed using a semi-quantitative scoring system: % cells (0, <1%; 1, 1-10%; 2, 11-50%; 3, 51-100%) X staining intensity (0, neg: 1, weak; 2, moderate; 3, strong), resulting in an overall score/interpretation (0-1, neg; 2, pos; 3-4, intermediate pos or 6-9, high pos). For MG, cases showing >5% of cytoplasmic/membranous staining of either moderate or strong intensity or 100% of weak intensity in cells were pos.

Results: TRPS1, GATA3 and MG were pos in 83/90 (92%), 81/90 (90%), and 55/90 (61%) DMC of breast origin, respectively. In 3/90 (3%), TRPS1 was pos while GATA3 and MG were neg. In 3/90 (3%), GATA3 was pos while TRPS1 and MG were neg. No cases were pos for MG but neg for both TRPS1 and GATA3.

Between metastatic ER+ (59) and TNBC (12) cases, TRPS1 and GATA3 showed comparable staining in ER+ cases with 98% and 100% pos, respectively while MG was pos in 60%. However, in TNBCs, TRPS1 was pos in 83% whereas GATA3 and MG was pos in only 50% and 41%, respectively. Qualitatively, when TRPS1 and GATA3 were both pos, TRPS1 showed less intense and in some, less diffuse staining than GATA3.

Conclusions: TRPS1 is similarly effective to GATA3 in identifying metastasis of breast origin, the majority of which are known to be ER+. However, we show that in metastatic TNBC, TRPS1 is a superior breast marker to GATA3 (and MG). MG was the least effective as no cases were pos while neg for both TRPS1 and GATA3.

GATA3 is an excellent stand alone breast marker in the metastatic setting. However, if metastatic TNBC requires consideration, then TRPS1 would be the superior stain. If sufficient tissue is available, utilizing both TRPS1 and GATA3 would be optimally comprehensive.

77 A Retrospective, Multi-Institutional, Pathologist-Based Assessment of 4 Immunohistochemistry Assays for PD-L1 Expression in Triple Negative Breast Cancer

Rodrigo Abreu[1], Roberto Peixoto[2], Marcelo Corassa[1], Warley Nunes[1], Thiago Rodrigues[1], Tatiane Neotti[3], Dirce Carraro[1], Cynthia Osorio[1], Helenice Gobbi[4], Marina De Brot[1]

[1]A.C.Camargo Cancer Center, Sao Paulo, Brazil, [2]Instituto de Anatomia Patológica, AC Camargo Cancer Center, São Paulo, Brazil, [3]Belém, Brazil, [4]Federal University of Triangulo Mineiro, Uberlandia, Brazil

Disclosures: Rodrigo Abreu: None; Roberto Peixoto: None; Marcelo Corassa: None; Warley Nunes: None; Thiago Rodrigues: None; Tatiane Neotti: None; Dirce Carraro: None; Cynthia Osorio: None; Helenice Gobbi: *Speaker*, Roche Diagnóstica Brasil; Marina De Brot: None

Background: Immunotherapy to inhibit the PD-L1/PD-1 pathway has been used in several types of cancer including triple-negative breast cancer (TNBC). The PD-L1 expression was the best predictor of clinical benefit. This study aims to evaluate the expression of PD-L1 in TNBC and compare expression rates using 4 distinct immunohistochemical antibodies. Further, the association of PD-L1 with clinicopathological features and clinical outcome was examined.

Design: We selected 168 previously tested TNBCs diagnosed between 1987-2016 from 3 institutions. Immunohistochemistry for 4 commercially used PD-L1 monoclonal antibodies (clones 22C3, SP142, 28-8, SP263) was performed in 2 TMAs. PD-L1 expression was assessed in cancer cells (CC) and tumor-infiltrating immune cells (IC). A cut-off of IC ≥1% was applied for SP142 (IMpassion 130), 28-8 and SP263 and combined proportion score (CPS) ≥ 1 for 22C3 and ≥ 10 (Keynote 355).

Results: PD-L1 expression in CC and IC using the 4 antibody clones are presented in the figures. For 22C3, 4.1% showed a CPS≥1 and 0.6% ≥10 (0.6% and 4.2% positivity in CC and IC respectively). For SP142, 2.9% of cases were positive and all positive cases exhibited low expression levels (1-5%) in CC; 88.8% exhibited low expression levels (1-5%) and 11.2% moderate levels (5-20%) in IC. No case showed high levels of positivity (>20%) in IC or CC. Interestingly, most TNBCs with PD-L1 expression in CC also had PD-L1 expression in their IC, with <1% having PD-L1 expression exclusively in CC. For SP263, 9.5%/21% of TNBCs exhibited low expression levels in CC and IC, respectively, 7%/10% showed moderate levels and 10%/24% displayed high levels of positivity. PD-L1-SP263 expression in IC was significantly associated with histologic grade III (p<0.001), whereas a significant correlation between PD-L1-SP263 expression in CC and death rates was demonstrated (p=0.049). However, survival analyses revealed no association with positivity for PD-L1.

Age (years)	**Tumor size (cm)**	**Hystological type (WHO 2019)**	**Histological grade (Notthingham)**	**Lymphovascular invasion**	**Lymph node metastases**
Ranging 25 – 84 y (median 53 y)	Ranging 1.0-16.0 cm (median 4.6 cm)	No special type: 82.6% Special type: 11.9% Mixed: 5.3%	Grade II: 13.7% Grade III: 86.8%	54 cases (32.0%)	82 cases (49.0%)
Stage (AJCC 8th Ed)	**Locoregional recurrence**	**Distant metastasis**	**Metastasis site**	**Final status**	**Survival (months)**
I 7.83% IIA 33.13% IIB 16.86% IIIA 27.71% IIIB 2.40% IIIC 0.60% IV 12.04%	Yes 9.0% No 91%	Yes 12.0% No 88.0%	Brain 24.3% CNS 18.91% Bone 16.21% Breast (contralateral) 5.40% Liver 5.40% Ovarian 2.70% Thyroid 2.70% Mediastinum 2.70%	Alive disease free 67.0% Cancer related death 28.0% Alive with disease 5.0%	**OS** 36.0 mo (1.0-159.0 mo) **DFS** 28.0 mo (0-119.0 mo)

Figure 1 - 77

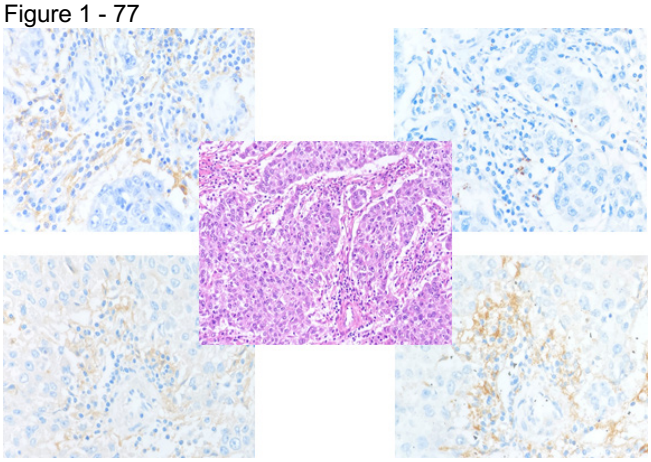

Figure 2 - 77

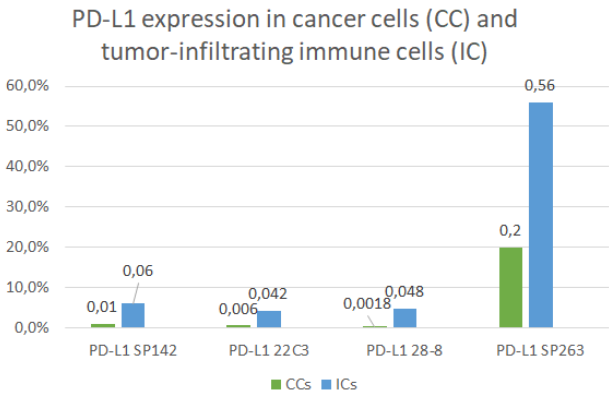

Conclusions: PD-L1 detection in cancer cells and immune cells varied greatly according to antibody clones resulting in different test results. PD-L1 was expressed primarily in tumor-infiltrating immune cells in 51(30%) cases. Positive PD-L1 in IC was associated with a high histologic grade, while expression in CC was connected to a higher frequency of death. We identified 2.4% PD-L1-SP142 and 0.6% PD-L1-22C3 TNBC positive cases, using IMpassion130 and Keynote 355 criteria, respectively. Our findings uncover a relevant proportion of TNBC patients that could benefit from immune checkpoint blockade.

78 Predicted and Genomic Risk in ER+ Invasive Breast Cancer in BRCA Mutation Carriers

Aibek Akmatbekov[1], Poornima Saha[2], Allison DePersia[2], Megan Sullivan[2]
[1]Chicago, IL, [2]NorthShore University HealthSystem, Evanston, IL

Disclosures: Aibek Akmatbekov: None; Poornima Saha: None; Allison DePersia: None; Megan Sullivan: None

Background: Although we associate BRCA mutations with triple negative breast cancer, carriers also develop estrogen receptor (ER) positive invasive carcinoma (IC). About 24% of ICs in BRCA1 and 78% of ICs in BRCA2 mutation carriers are ER+ in comparison to ~70-80% in the general population. Within ER+/HER2- ICs, there are also different intrinsic profiles, luminal A (lumA) and luminal B (lumB), that have different prognoses. In the general population, the majority of ICs (>70%) are lumA. In this study, we identified a cohort of BRCA1/2 carriers with ER+/HER2 negative IC with the goals of: 1) determining their subtype (lumA vs. lumB); 2) predicting risk from pathologic data using the Magee equation; and 3) comparing predicted risk with genomic risk as determined by OncotypeDx testing.

Design: The EMR was searched for women with germline BRCA1 or 2 mutations and ER+/HER2- IC. Slides were reviewed to select the optimal block for Oncotype recurrence score (RS) RT-PCR and/or Ki-67 immunohistochemistry (IHC) when the results were not already available. Manual quantitation of the proliferative index by Ki-67 was performed by a single pathologist. Tumors were subtyped as lumA when PR positive (>= 20%) and Ki-67 <14% and as lumB when either PR <20 to 0% or Ki-67 >=20%. Additional data collected from the pathology report including tumor size, grade, and ER/PR intensity were entered into the online Magee Equation to generate an average score (AS). Low risk (LR) was AS and/or RS <18, intermediate risk (IR) was 18-25 & high risk (HR) was >25.

Results: 39 patients met inclusion criteria and had an available RS. Average age at diagnosis was 51 (range 28-74). 15 were lumA (38%) and 24 were lumB (62%). Two of the lumB were ER low positive (LP; 1-10%). The IHC slides were missing for 3 cases (1 lumA and 2 lumB) so no Magee score could be generated. For lumA ICs, the predicted and genomic risk groups were similar (Table 1) with all 12 predicted LR having a LR RS. The genomic HR case (RS 40) was predicted IR (AS 21). For the lumB ICs, 2 were predicted LR, however only 1 was genomic LR while the other was HR (RS 26). All lumB predicted HR were genomic HR. The majority of lumB were predicted IR; all were genomic HR except 1 LR (RS 9).

	Predicted LR (<18)	Genomic LR	Predicted IR (18-25)	Genomic IR	Predicted HR (>25)	Genomic HR
Lum A	86% (12/14)	80% (12/15)	14% (2/14)	13% (2/15)	0	7% (1/15)
Lum B	10% (2/20)	14% (3/22)	70% (14/20)	0	20% (4/20)	86% (19/22)
Lum B-LP	0	0	0	0	100% (2/2)	100% (2/2)

Conclusions: BRCA mutation carriers with ER+/HER- ICs more frequently have lumB tumors in comparison to the general population. For lumA tumors, there was 100% concordance between predicted and genomic LR. In contrast, lumB genomic HR tumors were present in all 3 predicted risk categories. 86% of lumB tumors were genomic HR but only 20% were predicted HR.

79 Immunohistochemical Staining Characteristics of Well-Differentiated Invasive Ductal Carcinoma Using the ADH5 Cocktail (CK5/14, P63 and CK7/18): a Potential Interpretative Pitfall

Reham Al-Refai[1], Ahmed Bendari[1], Eugene Santagada[2], Rui Soares[1], Sabina Hajiyeva[1]
[1]Northwell Health Lenox Hill Hospital, New York, NY, [2]Lenox Hill Hospital, New York, NY

Disclosures: Reham Al-Refai: None; Ahmed Bendari: None; Eugene Santagada: None; Rui Soares: None; Sabina Hajiyeva: None

Background: In our practice, an antibody cocktail comprising CK5/14, p63, and CK7/18 (ADH5 cocktail) is frequently utilized to distinguish noninvasive from invasive breast lesions and for the delineation of intraductal epithelial proliferations. ADH-5 helps with diagnostic challenges such as differentiating atypical ductal hyperplasia from hyperplasia of the usual type, identifying microinvasion and invasive ductal carcinoma, and distinguishing basal phenotypes in triple negatives.

Design: We have reviewed 23 consecutive excisions of well-differentiated ductal carcinoma and stained with ADH5 cocktail. Additionally, we have stained these cases with more commonly used immunostains: smooth muscle myosin heavy chain (SMMH) and P63. SMMH and P63 are some of the most sensitive and specific myoepithelial cell markers lost around infiltrative glands.

Well-differentiated invasive carcinoma comprises small, round to ovoid or angular glands and tubules with open lumens within a fibrous or fibroelastotic desmoplastic stroma. The cells that line the neoplastic tubules in a single layer have relatively uniform nuclei of small or intermediate size. The tubules in well-differentiated carcinomas have no surrounding myoepithelium, and this is useful in differentiating them from benign conditions. The well-differentiated carcinoma cells have a luminal phenotype (CK8/18-positive, CK5/14-negative).

Results: The expected ADH5 cocktail staining pattern of invasive glands should show positive staining for CK7/18 (red) and negative staining for CK5/14 and P63 (brown).

Interestingly, only 2 cases (8.7%) out of 23 showed an expected staining pattern for ADH5 – loss of brown (P63, CK5/14) staining around invasive glands and diffuse red (CK7/18) expression.

Unexpected (mixture of cytoplasmic brown and red) staining in invasive glands was seen in 21 (91.3%) of 23 well-differentiated ductal carcinomas. In these cases, the ADH5 cocktail showed decreased diagnostic utility due to the ease of interpretation and the necessity for further myoepithelial stains (SMMH and p63) to confirm foci of invasion.

Antibody	**Staining**	**Cell type**	**Stain localization**
Anti-CK 5/14	DAB Brown	Myoepithelial/Luminal basal phenotype	Cytoplasmic
Anti-P63	DAB Brown	Myoepithelial cells	Nuclear
Anti-CK 7/18	FR Red	Luminal epithelium	Cytoplasmic
Anti-SMMH	DAB Brown	Myoepithelial cells	Cytoplasmic

Figure 1 - 79

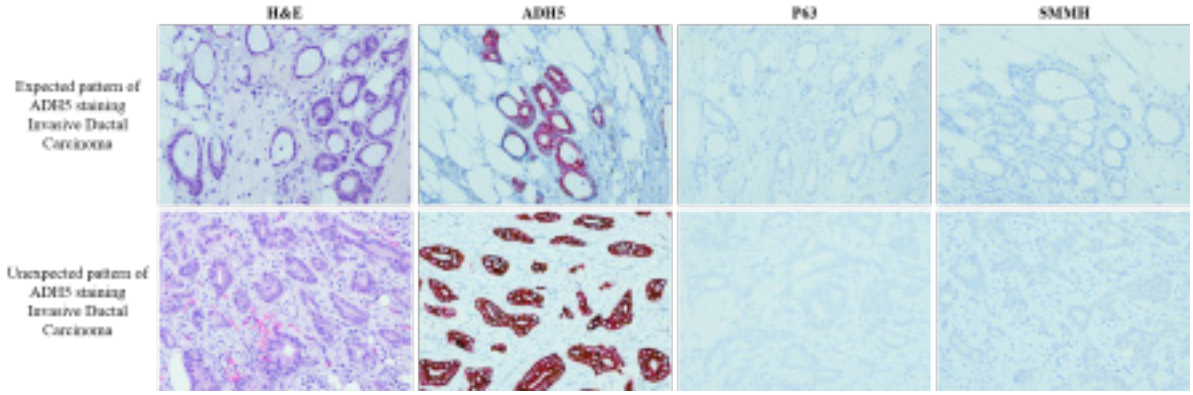

Conclusions: This staining pattern of ADH5 in well-differentiated ductal carcinomas, along with the low-grade cytological atypia, can be misinterpreted as benign glands. This occurrence when using a multiplex stain can confuse, and users should be aware of this potential pitfall.

80 The Spectrum of Breast Lesions Correlating with Non-Mass Enhancement (NME) on Magnetic Resonance Imaging (MRI): A Single Institute Study of 221 Core Needle Biopsies (CNB)

Abdullah Almajnnooni[1], Mariana Solari[1], Ankica Braun[1], Paolo Gattuso[1], Indu Agarwal[1]
[1]Rush University Medical Center, Chicago, IL

Disclosures: Abdullah Almajnnooni: None; Mariana Solari: None; Ankica Braun: None; Paolo Gattuso: None; Indu Agarwal: None

Background: Breast MRI is usually performed in high-risk patients, or to evaluate the extent of disease in patients with diagnosed malignancy, or to evaluate the contralateral breast. NME is a common breast MRI finding and is defined as an area of enhancement that does not meet the criteria for a 3-dimensional mass or has distinct features of a mass. It often undergoes CNB. However, the correlation between CNB findings and NME has not been studied in the literature. Here, we assessed the spectrum of pathologic entities encountered in patients with an MRI reading of NME and whether any specific distribution or internal enhancement patterns are associated with malignancy on biopsy or follow-up excisions.

Design: We retrieved data for NME lesions with associated CNBs (2/2019 - 9/2021) and their follow-up using the electronic medical records system. The majority of these NME lesions did not have a mammographic correlate and if correlate present, was not amenable to targeted biopsy. The lesions were stratified into malignant, high-risk lesions with atypia, and benign where benign also includes high-risk lesions without atypia.

Results: A total of 221 CNBs were identified from 181 patients (age range 34-77 years, median = 50). The majority of CNBs (69.2%) were benign, with pseudo-angiomatous stromal hyperplasia being the most common (12.6%), followed by apocrine metaplasia (9%). The remaining 30.8% were malignant (16.8%) and atypical (14.0%) lesions, where DCIS and invasive carcinoma account for 10.9% and 5.9%, respectively.

On follow-up, all malignant lesions underwent excision, with 1 DCIS case upgraded to invasive carcinoma. All atypical lesions were confirmed on excision with 1 atypical ductal hyperplasia upgraded to DCIS. All benign lesions were concordant by radiology and only excised for other concurrent diagnoses, if at all.

Linear, segmental, and clustered ring NME significantly associated with malignant lesions 25/37 (67.6%) compared with benign lesions 9/153 (5.9%) (p 0.001), but not with atypical lesions (p 0.116). The large size of NME (>1 cm) did not predict malignancy (2.7%) compared with benign lesions (18.9%). Interestingly, hemangioma commonly presented with linear NME (66.7%).

Group	Diagnosis on CNB	Number of cases	Follow up available	Concordant cases with or without excision	Upgrades on excision	Patterns of enhancement			Size
						linear	Segmental	clustered ring	> 1.0 cm
Malignant 37 (16.8%)	Invasive Carcinoma	13 (5.9%)	12/13	12/12 (100%)	0	0	0	6/13 (46.2%)	0
	DCIS	24 (10.9%)	21/24	20/21 (95.2%)	1 (IDC)	4/24 (16.7%)	10/24 (41.6%)	5/24 (20.8%)	1/24 (4.1%)
High-risk lesions with atypia 31 (14%)	ADH	16 (7.2%)	16/16	16/16 (100%)	1 (DCIS)	2/16 (12.5%)	2/16 (12.5%)	0	0
	Lobular neoplasia (ALH, LCIS)	12 (5.4%)	12/12, 10 excised	10/10 (100%)	0	0	0	0	0
	Other atypia (FEA, Atypical apocrine adenosis, atypical lymphoid infiltrate)	3 (1.4%)	3/3, 2 excised	2/2 (100%)	0	0	1/3 (33.3%)	0	0
Benign: High-risk lesions without atypia 27 (12.2%)	Radial scar or complex sclerosing lesions	9 (4.5%)	9/9	9/9 (100%)	0	0	1/9 (11.1%)	0	0
	Intraductal papilloma	18 (8.1%)	18/18, 12 excised	11/12 (91.7%)	1 (ALH)	0	0	0	0
Benign: non High-risk lesions 126 (57%)	PASH	28 (12.6 %)	28/28	Concordant No excision	0	0	0	0	12/28 (42.8%)
	Fibroadenomatous changes	15 (6.7%)	15/15	Concordant No excision	0	0	0	0	2/15 (12.5%)
	Apocrine metaplasia	20 (9.0%)	20/20	Concordant No excision	0	0	0	0	1/20 (5%)
	Previous biopsy/surgical site	12 (5.4 %)	12/12	Concordant No excision	0	1/12 (8.3%)	0	0	2/12 (16.67%)
	Chronic nonspecific inflammation	5 (2.3%)	5/5	Concordant No excision	0	0	0	0	2/5 (40%)
	Lymphocytic mastitis	2 (0.9%)	2/2	Concordant No excision	0	0	1/2 (50%)	0	0
	Hemangioma	3 (1.4 %)	3/3	Concordant No excision	0	2/3 (66.7%)	0	0	0
	Other fibrocystic changes including stromal fibrosis, usual ductal hyperplasia, sclerosing adenosis	39 (17.6 %)	39/39	Concordant No excision	0	0	3/39 (7.5%)	1/39 (2.5%)	10/39 (20.5%)
	Radiation changes	2 (0.9%)	2/2	Concordant No excision	0	0	0	0	0

CNB: Core needle biopsy, DCIS: Ductal carcinoma in situ, ADH: Atypical ductal hyperplasia, ALH: Atypical lobular hyperplasia, LCIS: Lobular carcinoma in situ, FEA: Flat epithelial atypia, PASH: Pseudoangiomatous stromal hyperplasia, IDC: Invasive ductal carcinoma

Figure 1 - 80

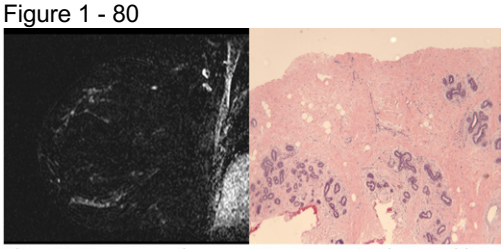

Figure 1: Non-mass enhancement on MRI T1W image with corresponding pseudoangiomatous hyperplasia on histology (10x).

Figure 2 - 80

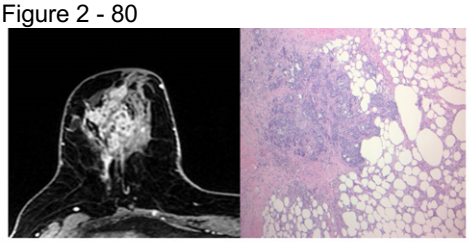

Figure 2: Non-mass clustered ring enhancement on MRI AXIAL Fat Sat T1 Post contrast image with corresponding high grade invasive ductal carcinoma on histology (10x).

Conclusions: The majority of NME (69.2%) correspond to benign lesions, while 30.8% were malignant on CNBs. Clustered ring, linear, or segmental NME were significantly associated with malignancy. The size of NME did not predict malignancy or atypia. Lobular neoplasia did not have any specific patterns of NME.

81 Clinicopathological and Immunohistochemical Features of Histiocytoid Variant of Invasive Lobular Breast Carcinoma. A single institutional study

Rabail Aslam[1], Hannah Gilmore[2], Philip Bomeisl[3], Aparna Harbhajanka[1]

[1]Case Western Reserve University/University Hospitals Cleveland Medical Center, Cleveland, OH, [2]University Hospitals Case Medical Center, Case Western Reserve University, Cleveland, OH, [3]University Hospitals Cleveland Medical Center, Cleveland, OH

Disclosures: Rabail Aslam: None; Hannah Gilmore: *Speaker*, Agendia; *Advisory Board Member*, Sectra; Philip Bomeisl: *Consultant*, PathAI; Aparna Harbhajanka: None

Background: Histiocytoid variant of invasive lobular carcinoma (HV-ILC) is an uncommon cytologic variant showing tumor cells with abundant foamy and/or eosinophilic cytoplasm that resemble macrophages. The bland appearance of the tumor cells, especially in limited samples such as core biopsies, can create a broad differential diagnosis including inflammatory and neoplastic processes. Since HV-ILC is rare and it is difficult to accumulate a large number of cases, the clinicopathology, histiogenesis, immunohistochemical (IHC) and molecular profile are not well-elucidated. The goal of this study is to review the clinicopathologic parameters, characterize the IHC profile and determine outcomes of patients diagnosed with HV-ILC at our institution.

Design: All HC-ILC cases diagnosed at our institution by breast subspecialized pathologists in past two decades were retrieved. Resulting in collection of clinicopathologic parameters and IHC stains data for estrogen receptor (ER), progesterone receptor (PR), and HER-2 status of 18 HV-ILC cases. In addition, IHC stains for monoclonal carcinoembryonic antigen (mCEA), androgen receptor (AR), GATA-3, and gross cystic disease fluid protein (GCDFP-15) were performed.

Results: A total of 38 cases consisting of core needle biopsies and surgical excision were identified in a total of 18 patients (cohort attached: table 1). Of these 18 patients, the majority of the patients were triple negative (TNBC) 50% (9/18), hormonal receptors positive and HER2 negative in 27.8% (5/18) and HER2 positive in 22% (4/18).

Additional IHC panel was performed on 13 cases. mCEA staining was diffusely positive in 15.4% (2/13), focally positive in 23.1% (3/13) and negative in 61.5% (8/13). mCEA was focal positive in 2 out of 6 (33.3%) of TNBC. GCDFP-15 staining was positive in 84.6% (11/13) and negative in 15.4% (2/13) including 6/6 (100%) cases of TNBC. All cases were AR positive (13/13) including 6 TNBC cases. GATA-3 staining was positive in 53.8% (7/13) and negative in 46.2% (6/13). 2 out of 6 (33.3%) of TNBC was positive for GATA-3.

Follow up data was available on 89.5 % (17/18) of the patients. There was no record of any of the patients developing recurrence, distant metastasis and death due to HV-ILC was found.

Table 1. Clinicopathological characteristics of Histiocytoid Breast Carcinoma.

Clinicopathological parameters	TNBC	ER/PR positive;Her2 negative	Her2 positive	Total
Age((yr, mean ± SD)	59.9±9.6	70.6±4.62	74.75±11.41	66.5±10.7
Size(cm, mean ± SD)	1.23.0±1.01	2.48.0±1.55	1.5±1.36	1.64±1.3
IHC based subtypes	9/18	5/18	4/18	13/18 (72.2%)
Angio-lymphatic invasion	1/9 (11%)	2/5(40%)	2/4(50%)	5/18 (27.78%)
GRADE1	0	1/5	0	1/18 (5.56%)
2	8/9	4/5	3/4	15/18(83.33%)
3	1/9	0	1/4	2/18 (11.11%)
LN Metastasis	4/9(44.4%)	2/5(40%)	2/4(50%)	8/18 (44.4%)
Mean Follow Up	45.3 months	60.0 months	36.67 months	47.32 months
LCIS associated with Invasion	4/9(44.4%)	2/5(40%)	2/4(50%)	8/18 (44.4%)
IMMUNOHISTIOCHEMISTRY				
mCEA in Invasive carcinoma				
Negative	4/6 (66.7%)	3/4(75.0%)	1/3(33.3%)	8/13 (61.5%)
Focal positive	2/6(33.3%)	0	1/3(33.3%)	3/13 (23.1%)
Moderate-Strong	0	1/4(25%)	1/3(33.3%)	2/13(15.4%)
mCEA in LCIS				
present	3/4(75%)	0	0	3/13 (23.1%)
absent	1/4(25%)	2/2(100%)	2/2(100%)	5/13(38.5%)
GCDFP15				
absent	0	1/3(33.3%)	1/4(25.0%)	2/13 (15.4%)
present	6/6(100%)	2/3(66.7%)	3/4(75.0%)	11/13(84.6%)
AR				
absent	0	0	0	0
present	6/6(100%)	4/4(100%)	3/3(100%)	13/13(100%)
GATA-3				
absent	4/6(66.7%)	1/4(25.0%)	1/3(33.3%)	6/13(46.2%)
present	2/6(33.3%)	3/4(75.0%)	2/3(66.7%)	7/13 (53.8%)

Conclusions: HV-ILC is a rare variant with deceptively bland histology. Most of HV-ILC in our cohort were TNBC. IHC staining ought to be the great tool for pointing toward right diagnosis with highest sensitivity for AR, followed by GATA3, and mCEA especially in TNBC.

82 Studying p53 Aggregation in Breast Cancer with Conformation-Sensitive Antibodies

Sara Avalos Hernandez[1], Cade Smelley[1], Yusuf Ozcelik[1], Veronica Ramirez-Alcantara[1], Pamela Moore Campbell[2], Eric Wei[2], Guillermo Herrera[1], Elba Turbat-Herrera[1], Luis Del Pozo-Yauner[1]
[1]University of South Alabama, Mobile, AL, [2]University of South Alabama College of Medicine, Mobile, AL

Disclosures: Sara Avalos Hernandez: None; Cade Smelley: None; Yusuf Ozcelik: None; Veronica Ramirez-Alcantara: None; Pamela Moore Campbell: None; Eric Wei: None; Guillermo Herrera: None; Elba Turbat-Herrera: None; Luis Del Pozo-Yauner: None

Background: Some cancer-associated mutations destabilize the p53 protein and promote its aggregation as amyloid fibrils and oligomers, an event that is believed to be related to the gain of oncogenic function. Triple-negative breast cancer (TNBC), an aggressive variant of breast cancer (BC), features one of the highest rates of p53 mutations (~80%), significantly higher than the average in human cancers (~50%). However, the relationship between p53 aggregation and breast cancer pathogenesis is not well understood.

Design: We have developed a strategy to produce conformation-sensitive antibodies against amyloid-forming proteins. Based on this strategy, we generated five different rabbit polyclonal antibodies (rpAbs) against five non-overlapping segments of the DNA-binding domain of p53 protein (p53-DBD) that are predicted to undergo extensive changes in both conformation and solvent accessibility during p53 aggregation (Figure 1). We sought to evaluate the ability of these anti-p53 rpAbs to recognize p53 aggregates in BC. We performed immunohistochemical (IHC) analysis of 20 BC, 10 TNBC, and 10 non-TNBC archived biopsies of BC patient. For comparative purposes, the commercial monoclonal anti-p53 antibody DO-7 was also evaluated. A preparation of unrelated rabbit polyclonal IgG was used as negative controls.

Results: IHC performed in TNBC and non-TNBC biopsies showed positive rpAbs staining in the nucleus and cytoplasm of cancer cells. Different patterns of staining in intensity and distribution were observed between the five rpAbs and between biopsies (Figure 2). In contrast, antibody DO-7 yielded positive staining only in the nucleus. RpAbs staining was not observed in normal breast tissue nor non-neoplastic cells surrounding the tumor. Interestingly, intra-tumoral variations were observed, with individual cells or groups of cells staining positively in an otherwise negative stained tumor. Importantly, rpAbs staining was observed in tumors negative to DO-7 antibody, a finding that could be explained by the location of the DO-7´s epitope. Although rpAbs staining was observed in TNBC and non-TNBC tumors, a distinctive IHC pattern was not identified for either BC variant.

Figure 1 - 82

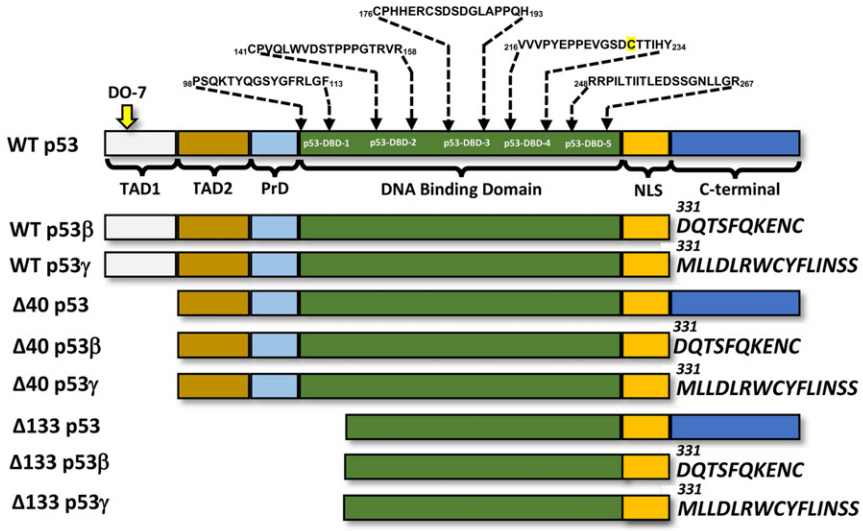

Figure 1. Schematic representation of the structure of the full-length p53 protein (WT p53) and its various isoforms. The yellow downward arrowhead indicates the approximate location of the monoclonal antibody DO-7 epitope. The approximate location in the structure of the DNA-binding domain of p53 and the sequence of the synthetic peptides used as immunogen to produce the conformation-sensitive antibodies p53-DBD 1 to p53-DBD-5 are shown in part top of the figure. TAD1 and TAD2 refer to transactivation domain 1 and 2, respectively. PrD and NLS stand for Proline-rich domain and Nuclear Localization Signal, respectively. *Curr Pharm Biotechnol. 2007 December; 8(6): 332–336.*

Figure 2 – 82

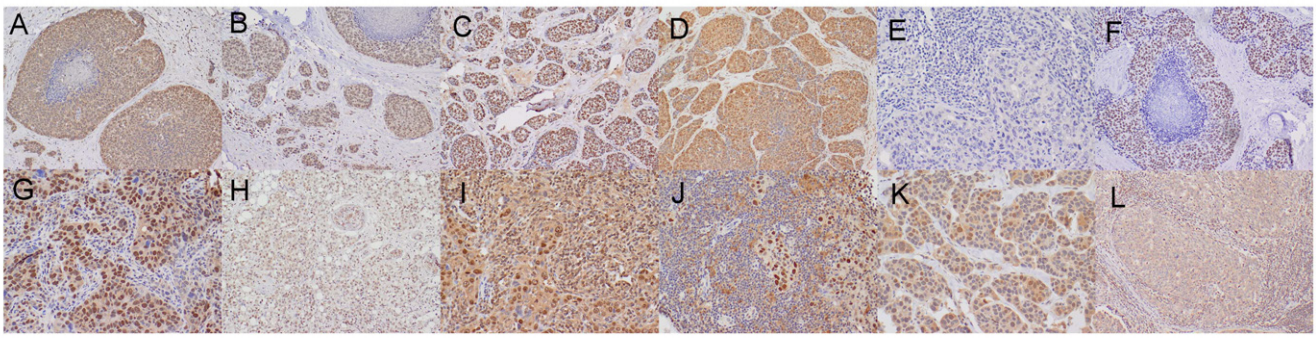

Figure 2. Immunohistochemical analysis of TNBC samples. Panel A to F show the IHC with the antibodies p53-DBD-1, p53-DBD-2, p53-DBD-3, p53-DBD-4, p53-DBD-5, and DO-7, respectively, in the same patient. Panels G to L show the IHC with the p53-DBD-1 antibody in tumor samples from six different patients. Note the differences in the recognition pattern in nucleus and cytoplasm between the five antibodies in the same patient and with the commercial anti-p53 DO-7 antibody. Differences in the recognition pattern generated by antibody p53-DBD-1 in seven different samples of triple negative breast cancer (compare panels A, G to L) are also observed. The secondary antibody was a peroxidase-conjugated specie-specific antibody.

Conclusions: IHC staining pattern suggest that p53 aggregates distribute intracellularly and in a patient-dependent manner. As aggregation of p53 appears to be a frequent phenomenon in breast cancer, its study is warranted to unveil its relevance in the pathogenesis of this disease.

83 Phyllodes Tumors of the Breast: Challenges in Histologic Classification

Sara Bachert[1], Liza Quintana[2], Stuart Schnitt[3]
[1]University of Kentucky College of Medicine, Lexington, KY, [2]Beth Israel Deaconess Medical Center, Boston, MA, [3]Brigham and Women's Hospital, Dana-Farber Cancer Institute, Harvard Medical School, Boston, MA

Disclosures: Sara Bachert: None; Liza Quintana: None; Stuart Schnitt: None

Background: The WHO Classification of Breast Tumors (5TH ed) categorizes phyllodes tumors (PT) as benign, borderline, or malignant based on evaluation of six histologic features: tumor border, stromal cellularity, stromal atypia, mitotic activity, stromal overgrowth, and malignant heterologous elements. However, some tumors are challenging to classify because they have features from more than one category. The frequency with which this occurs has not been previously studied in detail.

Design: The study population consisted of 227 PT from 2 groups. Group 1 consisted of 70 consecutive PT treated at a single institution between January 2000 and June 2015, and the slides were reviewed by 2 of the authors. Group 2 consisted of 157 PT seen on a breast pathology consultation service between July 2017 and June 2021; all of these were reviewed by one of the authors who reviewed the Group 1 cases. For this analysis, the pathology reports of all 227 cases were reviewed and each of the six features used to categorize PT using the WHO criteria was recorded for each case. The number of cases in which all features were from the same category and in which features spanned more than 1 category was tabulated.

Results: Median patient age was 43 years (range: 12-94) and all cases were surgical specimens. Of the 227 PT, only 83 (36.6%) had all histologic features from one category and were readily classifiable based on WHO criteria. These included 61 benign, 13 borderline and 9 malignant PT. The remaining 144 cases (63.4%) demonstrated histologic features that overlapped between two or more categories, and this was significantly more common in Group 2 than in Group 1 cases (68.8% vs 51.4%, p=0.01). The most common overlap was between the benign and borderline categories, seen in ~30% of Group 1 and Group 2 cases. An additional 58 cases (25.6%) had features of borderline and malignant tumors. Thirteen cases (5.7%) had features from all three categories, 11 of which were in Group 2 (Table 1).

Table 1. Frequency of discrepant histologic features in 227 phyllodes tumors.

Histologic Features	Total (n=227)	Group 1: Consecutive Cases (n=70)	Group 2: Consult Cases (n=157)
All one category	83 (36.6%)	34 (48.6%)	49 (31.2%)
Discrepant features	144 (63.4%)	36 (51.4%)	108 (68.8%)
Benign/Borderline	69 (30.4%)	21 (30%)	48 (30.6%)
Borderline/Malignant	58 (25.6%)	11 (15.7%)	47 (29.9%)
Benign/Malignant	4 (1.8%)	2 (2.9%)	2 (1.3%)
All three categories	13 (5.7%)	2 (2.9%)	11 (7.0%)

Conclusions: In this series of 227 PT, 63.4% demonstrated features from more than one category, including 51.4% of cases from a consecutive series and 68.8% from a consultation series. While WHO recommends that cases with some features of borderline and some of malignant PT be classified as borderline, how best to classify the 30% of tumors with features overlapping between the benign and borderline categories remains problematic, particularly since all features used to categorize PT are given equal weight in the WHO classification.

84 Invasive Breast Cancer with Average HER2 Copy Number ≥ 4.0 and < 6.0: Risk Classification and Molecular Typing by a 21-Gene Expression Assay and MammaPrint plus BluePrint Analysis

Qianming Bai[1], Hong Lv[1], Longlong Bao[1], Yu Yang[1], Xiaoyan Zhou[2], Yang Wentao[1]
[1]Fudan University Shanghai Cancer Center, Shanghai, China, [2]Fudan University Shanghai Cancer Center, Shanghai Medical College, Fudan University, Shanghai, China

Disclosures: Qianming Bai: None; Hong Lv: None; Longlong Bao: None; Yu Yang: None; Xiaoyan Zhou: None; Yang Wentao: None

Background: American Society of Clinical Oncology (ASCO)/College of American Pathologists (CAP) updated the guideline for human epidermal growth factor receptor 2 (HER2) testing in breast cancer in 2018. Meanwhile, several publications indicated that almost all breast cancers with a HER2 copy number ≥ 6.0 were considered positive for HER2 amplification, while those with a HER2 copy number < 4.0 were considered negative, regardless of the ratio of HER2 to CEP17. However, the ratio must be considered for breast cancers with average HER2 copy number ≥ 4.0 and < 6.0. HER2 amplification was diagnosed as positive when the ratio is ≥ 2.0, and negative when the ratio < 2.0 and non HER2 3+ by immunohistochemistry (IHC). This judgment and the guidance for subsequent targeted therapies are still controversial.

Design: A total of 40 cases of breast cancer with average HER2 copy number ≥ 4.0 and < 6.0 by FISH in Fudan University Shanghai Cancer Center were collected, and HER2 immunohistochemistry was 1+, or 2+, but not 3+ in all the cases. According to the ratio of HER2 to CEP17, these cases were divided into two groups: Group A, HER2/CEP17 < 2.0 (n=18) and Group B, HER2/CEP17 ≥ 2.0 (n=22). Risk classification and molecular typing were analyzed in all the cases by MammaPrint and BluePrint analysis, and a 21-Gene expression was performed in the cases with hormone receptor (HR) + and pN0-1 (0-3 positive nodes). The flow chart was shown in Figure 1.

Results: As shown in Figure 2, compared with Group A, breast cancers in Group B were significantly younger, and lymph node metastases were more common. Among the breast cancers with HR+ and pN0-1, 86.7% (13/15) of Group A and 93.3% (14/15) of Group B were identified to be a high recurrence risk score (≥ 26) by a 21-Gene expression assay. Similarly, 66.7% (10/15) of Group A and 73.3% (11/15) of Group B were determined to be high risk by MammaPrint analysis. The coincidence rate of the above two methods was 80% (12/15) in both Group A and Group B. Most importantly and unexpectedly, all the breast cancers in both Group A and Group B with HR positivity were classified as Luminal type, which means HER2 negative, and those with HR negativity were Basal type or unknown by BluePrint typing analysis, regardless of the ratio of HER2 to CEP17. Consistently, 10 cases of breast cancer in Group B were treated with anti-HER2 neoadjuvant chemotherapy and assessed the pathological response using the Miller-Payne (MP) system. The results of pathological responses based on the MP system are presented in Table 1. Briefly, only one case with HR negativity showed Grade 5 as pathological complete response (pCR), and all other 9 cases with HR negativity showed Grade 1-4 as partial pathological response (pPR).

Table 1. Assessment of pathological responses using the Miller-Payne (MP) system in Group B breast cancers treated with anti-HER2 neoadjuvant chemotherapy

	TNM stage	IHC-ER/PR/HER2/Ki67	21-Gene Score	MammaPrint	BluePrint	MP grade
Case 1	T1cN1M0	-/-/2+/50%+	ND	High	BASAL	5
Case 2	T1cN1M0	80%+/20%+/1+/10%+	40.7	High	Luminal	3
Case 3	T2N0M0	60%+/0/1+/50%+	50.1	High	Luminal	4
Case 4	T2N0M0	90%+/50%+/2+/80%+	52.7	High	Luminal	3
Case 5	T2N1M0	90%+/90%+/2+/10%+	22	Low	Luminal	2
Case 6	T2N1M0	90%+/0/2+/20%+	48.1	High	Luminal	1
Case 7	T2N2M0	90%+/30%+/2+/30%+	30.3	High	Luminal	2
Case 8	T2N2M0	95%+/50%+/2+/70%+	37.6	High	Luminal	2
Case 9	T2N2M0	95%+/30%+/2+/30%+	37.9	High	Luminal	4
Case 10	T2N2M0	50%+/50%+/2+/20%+	43	High	Luminal	3

IHC, immunochemistry; ND, not detected; MP, Miller-Payne.

Figure 1 - 84

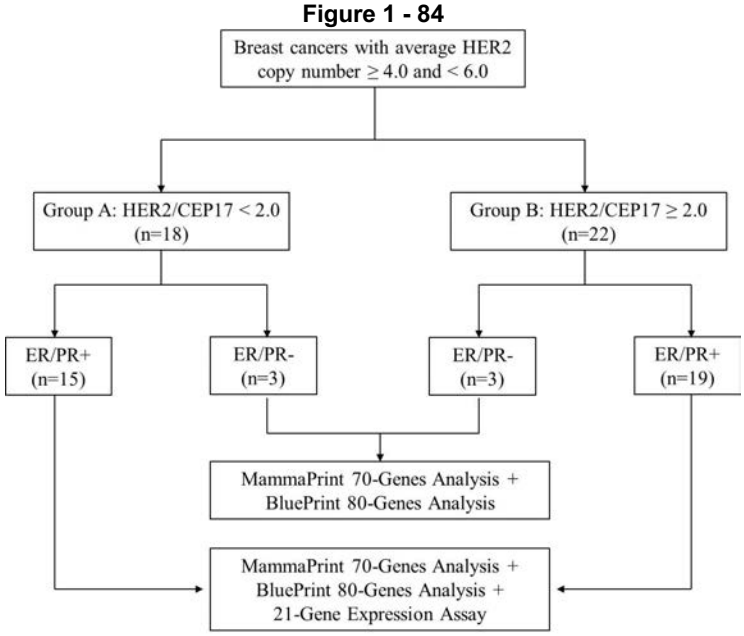

Figure 2 – 84

	21-gene assay			MammaPrint		BluePrint				Coincidence rate
	≥26	16-25	≤15	High (MPI<0)	Low (MPI<0)	Luminal	HER2	Basal	unknown	
Group A: HER2/CEP17 Ratio < 2.0										
ER/PR+ (n=15)										12/15, 80.0%
post-menopausal (n=12)										
pN0 (n=9)	8	1	0	5	4	9	0	0	0	6/9, 66.7%
pN1 (n=3)	2	1	0	2	1	3	0	0	0	3/3, 100%
pre-menopausal (n=3)										
pN0 (n=2)	2	0	0	2	0	2	0	0	0	2/2, 100%
pN1 (n=1)	1	0	0	1	0	1	0	0	0	1/1, 100%
ER/PR- (n=3)	ND	ND	ND	3	0	0	0	3	0	NA
Group B: HER2/CEP17 Ratio ≥ 2.0										
ER/PR+ (n=19)										12/15, 80.0%
post-menopausal (n=8)										
pN0 (n=3)	3	0	0	2	1	3	0	0	0	2/3, 66.7%
pN1 (n=3)	2	1	0	2	1	3	0	0	0	3/3, 100%
pN2 (n=2)	ND	ND	ND	2	0	2	0	0	0	NA
pre-menopausal (n=11)										
pN0 (n=3)	3	0	0	2	1	3	0	0	0	2/3, 66.7%
pN1 (n=6)	6	0	0	5	1	6	0	0	0	5/6, 83.3%
pN2 (n=2)	ND	ND	ND	2	0	2	0	0	0	NA
ER/PR- (n=3)	ND	ND	ND	3	0	0	0	1	2	NA

Conclusions: Both Group A and Group B breast cancers with HR+ and pN0-1 showed a high risk of recurrence at high frequency by a 21-Gene expression assay and MammaPrint analysis, respectively. Breast cancers in Group B (HER2 copy number ≥ 4.0 and < 6.0, and HER2/CEP17≥ 2.0) , which was classical HER2 amplification according to the updated ASCO/CAP guideline, were reclassified as Luminal or Basal type, but not HER2 type, by BluePrint analysis. Breast cancers in Group B derived less benefit

from anti-HER2 neoadjuvant chemotherapy. These results indicate that further studies are needed to clarify the biological feature of Group B breast cancers. This group might be heterogeneous regarding its nature and response to anti-HER2 treatment.

85 Intraepidermal Glands in the Nipple-areolar Complex of Transmasculine Individuals

Gabrielle Baker[1], Vanessa Bret-Mounet[2], Jingxiong Xu[3], Valerie Fein-Zachary[2], Gerburg Wulf[2], Stuart Schnitt[4], Yujing Jan Heng[1]

[1]Beth Israel Deaconess Medical Center, Boston, MA, [2]Beth Israel Deaconess Medical Center, Harvard Medical School, Boston, MA, [3]Mount Sinai Hospital, University of Toronto, Toronto, Canada, [4]Brigham and Women's Hospital, Dana-Farber Cancer Institute, Harvard Medical School, Boston, MA

Disclosures: Gabrielle Baker: None; Vanessa Bret-Mounet: None; Jingxiong Xu: None; Valerie Fein-Zachary: None; Gerburg Wulf: None; Stuart Schnitt: None; Yujing Jan Heng: None

Background: The majority of transmasculine individuals (TM)—assigned female at birth—receive testosterone therapy (TT) to affirm their gender identity. The effect of long-term exposure of the biologically female body to exogenous testosterone remains unclear. We previously reported that alterations in breast histology were generally evident after TM received TT for at least 12 months. In the course of reviewing TM breast tissues, we observed the presence of intraepidermal gland (IEG) formation within the nipple-areolar complex (NAC), sometimes in association with cells morphologically consistent with Toker cells (TCs). TCs with IEG formation have been observed in the cisgender population and this study aims to characterize this unusual feature in a TM cohort.

Design: We established a retrospective TM research cohort consisting of 444 subjects who underwent chest-contouring surgeries at our institution (2013-2019). We collected clinical data including duration of TT in months and breast cancer risk factors commonly studied in cisgender women. A portion of the NAC was excised and available for microscopic evaluation in 82/444 TM subjects. We also reviewed NAC from 55 cisgender women <50 years old who had mastectomies because of genetic susceptibility to breast cancer or cancer in the contralateral breast (2016-2020); women who received neoadjuvant therapy or had atypical lesions in the ipsilateral breast were excluded.

Results: IEG were observed in the NAC of 18/82 (22.0%) TM individuals (see Figure 1) compared to 5/55 (9.1%) cisgender women (p=0.05). In addition, IEG were more likely to be present in TM individuals who were overweight/obese and taking TT (p=0.03; see Table 1). Singly dispersed TCs were present in 5/82 (6.1%) TM individuals compared to 9/55 (16.4%) cisgender women on H&E-stained slides (p=0.05). Immunohistochemical characterization of the IEG are currently in progress.

	IEG present N (%)	IEG absent N (%)
BMI<25 & TT	4 (22.2)	27 (45.0)
BMI<25 & Not using TT	0 (0)	6 (10.0)
BMI>25 & TT	13 (72.2)	20 (33.3)
BMI>25 & Not using TT	1 (5.6)	7 (11.7)

Figure 1 - 85

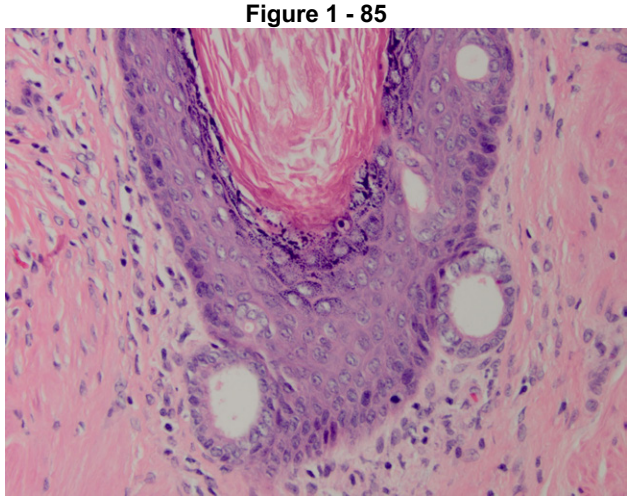

Conclusions: In a TM cohort, the presence of IEG in the NAC was associated with high body mass index and testosterone use. While IEG may represent a gland-forming type of Toker cell proliferation, the clinical significance of this finding is uncertain and immunohistochemical evaluation is in progress to further elucidate their nature.

86 Utility of Smooth Muscle Actin for Differentiating Angiosarcomas of the Breast from Benign Vascular Lesions on Core Needle Biopsy

Ahmed Bakhshwin[1], Lauren Duckworth[2], Raza Hoda[1], Miglena Komforti[1], Gloria Lewis[1], Xiaoyan Cui[1], J. Jordi Rowe[1], Jesse McKenney[1], Erinn Downs-Kelly[1], Patrick McIntire[1]
[1]Cleveland Clinic, Cleveland, OH, [2]Cleveland Clinic Foundation, Cleveland, OH

Disclosures: Ahmed Bakhshwin: None; Lauren Duckworth: None; Raza Hoda: None; Miglena Komforti: None; Gloria Lewis: None; Xiaoyan Cui: None; J. Jordi Rowe: None; Jesse McKenney: None; Erinn Downs-Kelly: *Advisory Board Member*, Lilly Oncology; Patrick McIntire: None

Background: Angiosarcomas (AS) occurring in the breast parenchyma proper are rare and in this location can be diagnostically challenging to differentiate from other benign vascular lesions. Prior work has suggested that smooth muscle actin (SMA) may be useful as an ancillary stain in AS, as the pericyte layer is lost in these lesions. Our study evaluates the utility of SMA staining in primary AS on core needle biopsy (CNB) to differentiate them from benign vascular lesions of the breast.

Design: The anatomic pathology database CoPath Plus™ was searched from 1992-2021 for all cases of AS on CNB. Patient clinical history and follow-up information were obtained via the medical record. A total of 23 control cases were identified in the anatomic pathology database as benign vascular lesions consistent with hemangiomas on CNB. Evaluation of SMA staining in atypical vascular lesions is currently ongoing. Immunohistochemical stain for SMA was performed using the Ventana Medical System Benchmark Special Stainer which performs online slide deparaffinization and uses a temperature-controlled heating block for each slide and compared to their appropriate controls.

Results: A total of 15 cases of AS within breast parenchyma from 10 patients were identified. Of the 15 cases, 12/15 (80%) had at least partial loss of SMA staining (Figure 1). In the control group, 0/20 (0%) had any loss of SMA staining. The sensitivity of partial loss of SMA is 0.80 and the specificity of partial SMA loss is 0.96 (p-value < 0.05). Eleven of the 15 AS cases underwent resection and were confirmed to be AS. One control case underwent excision and was confirmed to be hemangioma; none of the other control benign cases had excision, recurrence, or growth of the lesion.

		Angiosarcoma (n=15)	Benign Vascular Lesions (n=23)	p-value
Median age (years)		69	63	
Laterality	Left	6	11	
	Right	9	12	
SMA Staining	Partial loss	12	1	< 0.05
	Retained	3	22	

Figure 1 - 86

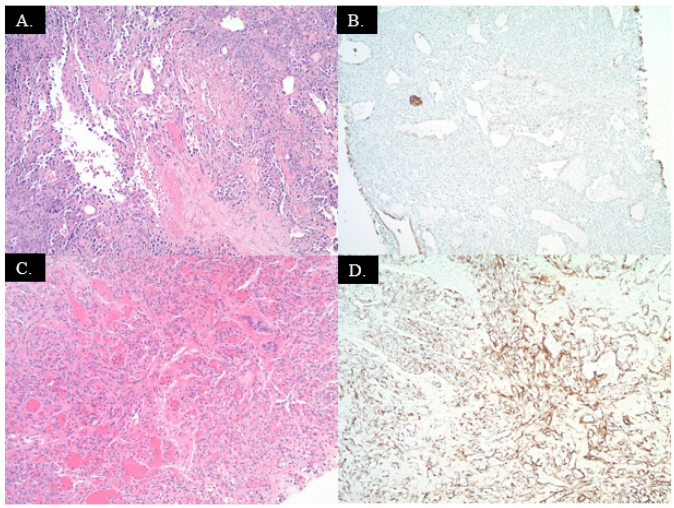

Figure 1. A case of angiosarcoma (A, H&E) demonstrating loss of SMA stain (B) as compared to a benign vascular lesion (C, H&E) which retained SMA (D).

Conclusions: Diagnosis of AS in the breast parenchyma on CNB can be diagnostically challenging. This cohort demonstrates that partial loss of SMA has high sensitivity and specificity for AS and may represent a useful ancillary diagnostic tool in challenging vascular lesions of the breast and can be used diagnostically in these lesions.

87 Male Invasive Lobular Breast Cancer: Clinicopathologic Features and Recurrence Score Results from a Population Based Database

Michael Balatico[1], Ana Ruano[2], Allison Cleary[2], H. Evin Gulbahce[1]
[1]The University of Utah, Salt Lake City, UT, [2]The University of Utah/ARUP Laboratories, Salt Lake City, UT

Disclosures: Michael Balatico: None; Ana Ruano: None; Allison Cleary: None; H. Evin Gulbahce: None

Background: Invasive lobular carcinoma (ILC) is rare in males. Using the surveillance, epidemiology, and results database (SEER) which captures approximately 35% of all cancers in the US, we investigated clinicopathological characteristics and outcomes of male ILC.

Design: We reviewed SEER data from 2004-2015 to identify male ILC patients and compared this to data from female patients with ILC. Bivariate analyses compared male and female patients on clinicopathological characteristics, Recurrence Score (RS) testing, and treatment received. Hazards Ratios (HR) were estimated using Cox proportional hazards model. A Kaplan-Meier survival plot was generated using log-rank test.

Results: 62,714 patients were diagnosed with ILC. Less than 1% were males. Tumor size, stage, grade, hormone receptor status, and tumor subtype were significantly different between male and female ILC patients (Table 1). Breast cancer specific death (BCSD) was significantly different between male and females (p=0.04) (Figure). In multivariate analysis there was no difference in BCSD between males and females in all cases (HR: 1.30, CI: 0.58-2.89) as well as in the hormone receptor +/HER2- subgroup (HR: 1.50; CI: 0.21-10.63)

	Male Lobular BrCa			Female Lobular BrCa		
	N= 56	% *		N=62,658	% *	P
Age Group						
<50	6	10.7		9,050	14.4	0.17
50-64	15	26.8		22,360	35.7	
≥65	35	62.5		31,248	49.9	
Race						
Non-Hispanic White	46	82.1		48,584	77.5	0.70
Black	4	7.1		5,173	8.3	
Others	6	10.8		8,901	14.2	
Tumor Size						
T1 (≤2cm)	17	30.4		30,393	48.5	0.03
T2 (2-≤5 cm)	25	44.6		19,546	31.2	
T3 (>5 cm)	4	7.1		7,606	12.1	
T4	4	7.1		2,083	3.3	
Unknown***	6	10.7		3,030	4.8	
Lymph Node Status						
N0	30	53.6		40,017	63.9	0.13
N1 (1-3 positive nodes)	17	30.4		13,195	21.1	
N2 (4-9 positive nodes)	1	1.8		4,034	6.4	
N3 (≥10 positive nodes)	2	3.6		3,432	5.5	
Unknown***	6	10.7		1,980	3.2	
Stage						
I	11	19.6		24,559	39.2	0.002
II	25	44.6		21,652	34.6	
III	7	12.5		9,691	15.5	
IV	9	16.1		3,900	6.2	
Unknown***	4	7.1		2,856	4.6	
Grade						
1	4	7.1		16,034	25.6	< 0.001
2	23	41.1		32,048	51.2	
3	14	25.0		5,457	8.7	
Unknown***	15	26.8		9,119	14.6	
Hormone Receptor						
Positive (ER and/or PR)	46	82.1		58,100	92.7	0.03
Negative (ER and PR)	4	7.1		1,675	2.7	
Unknown	6	10.7		2,883	4.6	
HER2 Status **						
Negative	21	37.5		31,233	49.9	0.82
Positive	1	1.8		1,668	2.7	
Borderline	0	0		568	0.9	
Unknown***	5	8.9		1,708	2.7	
Diagnosed before 2010**	29	51.8		27,481	43.9	
Tumor Subtype						
Hormone Receptor+/HER2-	19	33.9		30,635	48.9	0.05
Hormone Receptor+/HER2+	1	1.8		1,490	2.4	
Hormone Receptor-/HER2+	0	0		172	0.3	
Triple Negative	2	3.6		532	0.9	
Unknown***	34	60.7		29,829	47.6	
Chemotherapy						
No/Unknown	35	62.5		42,277	67.5	0.43
Yes	21	37.5		20,381	32.5	
RS Testing						
Not Done	48	85.7		49,893	79.6	0.26
Done	8	14.3		12,765	20.4	
TAILORx Risk Group (N=8)						
Low (RS<11)	2	25		2,203	17.3	0.73
Intermediate (RS 11-25)	5	62.5		9,535	74.7	
High (RS>25)	1	12.5		1,027	8.1	

Figure 1 - 87

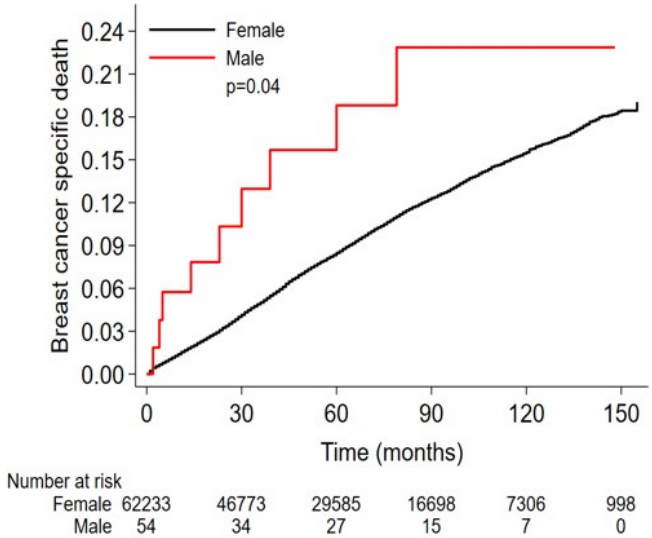

Conclusions: ILC in male patients is more likely to be higher stage, grade 3, hormone receptor negative, and less likely to be hormone receptor +/HER2-, resulting in higher BCSD. These patients are as likely to be tested for RS and have similar RS risk group distribution as females with ILC.

88 Identification of "ER Low Positive" Breast Cancers Is Associated with Immunohistochemical Assay Conditions in CAP Proficiency Testing PM2 Survey

Gregory Bean[1], Rhona Souers[2], Sebastian Fernandez-Pol[3], Andrew Bellizzi[4]
[1]Stanford Medicine/Stanford University, Stanford, CA, [2]College of American Pathologists, Northfield, IL, [3]Stanford University Medical Center, Stanford, CA, [4]University of Iowa Hospitals & Clinics, Iowa City, IA

Disclosures: Gregory Bean: None; Rhona Souers: None; Sebastian Fernandez-Pol: None; Andrew Bellizzi: None

Background: The 2020 ASCO/CAP ER/PgR Guideline Update introduced the new reporting category "ER Low Positive" to address uncommon breast cancers (BCs) with 1-10% ER staining. A heterogeneous group, these tumors often have outcomes and biology more similar to ER-negative BCs, but also demonstrate clinical benefit from endocrine therapy. Accurate stratification is important to select appropriate treatment algorithms for BC patients. The CAP PM2 survey provides semiannual proficiency testing for ER and PgR immunohistochemistry using tissue microarray (TMA) cores of 20 BCs each. Historical data has shown lower agreement between participants among cases near defined thresholds of positivity.

Design: BC cell lines grown in monoculture and co-culture with fibroblasts may offer a more homogeneous and quantitative medium for reliable testing of low ER BCs. The 2021-A mailing of the CAP PM2 survey included 4 supplemental ungraded TMA cores targeting a low percentage of ER staining cells using these methods: cores 11 (pseudotissue of BC cells with fibroblasts, 15% expected positivity), 12 (BT20 cell line, 1.7%), 13 (BT474 cell line, 3%) and 14 (mix of AU565 and T47D cell lines, 5%). Responses were segregated into negative (<1%) and positive (≥1%); ER clone, antigen retrieval pH level (low vs high), and testing platform were compared.

Results: Among 1352 respondents, reported ER positivity rates were 47%, 17%, 27% and 52% for the 4 cores, respectively. Consensus was significantly lower for the ER low cases than the graded cores; core 12 showed the highest agreement with 83% of respondents scoring negative. 43% of participants reported the same result for all cores. In multivariate analysis, differences in pH level and platform impacted scoring of ER low positive cases; use of different clones did not show a significant effect. On Leica platforms, antigen retrieval with high pH was associated with higher rates of positive scoring compared to low pH for all 4 cores. Pairwise tests between platforms using high pH showed significant differences for 3 cores, with higher rates of positive scoring seen on Leica platforms compared to Ventana.

Wildcard core	Platform - pH level	Total # of results	ER Positive # (%)	*P* value
Core 11 (Overall ER+ 47%)	Dako - Low pH	15	10 (66.7)	0.64
	Dako - High pH	96	57 (59.4)	
	Leica - Low pH	102	43 (42.2)	**<0.001**
	Leica - High pH	98	69 (70.4)	
	Ventana - Low pH	12	4 (33.3)	0.64
	Ventana - High pH	859	370 (43.1)	
	Other - Low pH	17	4 (23.5)	0.15
	Other - High pH	10	6 (60.0)	
Core 12 (Overall ER+ 17%)	Dako - Low pH	16	1 (6.3)	0.33
	Dako - High pH	99	20 (20.2)	
	Leica - Low pH	104	8 (7.7)	**<0.001**
	Leica - High pH	102	40 (39.2)	
	Ventana - Low pH	12	2 (16.7)	0.74
	Ventana - High pH	887	139 (15.7)	
	Other - Low pH	18	1 (5.6)	0.22
	Other - High pH	10	3 (30.0)	
Core 13 (Overall ER+ 27%)	Dako - Low pH	16	8 (50.0)	0.60
	Dako - High pH	99	39 (39.4)	
	Leica - Low pH	104	22 (21.2)	**<0.001**
	Leica - High pH	101	60 (59.4)	
	Ventana - Low pH	12	3 (25.0)	0.90
	Ventana - High pH	886	206 (23.3)	
	Other - Low pH	18	2 (11.1)	0.97
	Other - High pH	10	1 (10.0)	
Core 14 (Overall ER+ 52%)	Dako - Low pH	16	9 (56.3)	0.77
	Dako - High pH	98	51 (52.0)	
	Leica - Low pH	104	25 (24.0)	**<0.001**
	Leica - High pH	101	62 (61.4)	
	Ventana - Low pH	12	3 (25.0)	0.22
	Ventana - High pH	888	493 (55.5)	
	Other - Low pH	17	4 (23.5)	0.34
	Other - High pH	10	5 (50.0)	
Additional significant pairwise tests between platforms				
Core 11	Leica - High pH	Ventana - High pH		**<0.001**
	Dako - High pH	Ventana - High pH		**0.007**
Core 12	Leica - High pH	Ventana - High pH		**<0.001**
	Leica - High pH	Dako - High pH		**0.01**
Core 13	Leica - High pH	Ventana - High pH		**<0.001**

Low pH buffers include citrate, Dako TRS pH 6.1, Biocare Diva Decloaker, Leica Bond ER1 and Ventana CC2. High pH buffers include Dako TRS pH 9, Leica Bond ER2, Ventana CC1 and EDTA.

Conclusions: In addition to confirming a low rate of agreement among ER low positive tumors, this study shows that immunohistochemical assay conditions can influence ER reactivity in BCs. For select cases that are near the defined threshold for positivity, factors such as antigen retrieval and platform may alter interpretation above or below a cutoff, with the potential for significant clinical impact. Further optimization of proficiency testing for ER low BCs is likely needed.

89 Mass-Forming Ductal Carcinoma in Situ: An Ultrasonographic and Histopathologic Correlation

Shaza Ben Khadra[1], Sean Hacking[2], Kamaljeet Singh[3], Bianca Carpentier[4], Li Juan Wang[2], Evgeny Yakirevich[4], Yihong Wang[5]

[1]Brown University, Providence, RI, [2]Alpert Medical School of Brown University, Providence, RI, [3]Women and Infants Hospital, Providence, RI, [4]Rhode Island Hospital, Providence, RI, [5]Brown University, Rhode Island Hospital, Providence, RI

Disclosures: Shaza Ben Khadra: None; Sean Hacking: None; Kamaljeet Singh: None; Bianca Carpentier: None; Li Juan Wang: None; Evgeny Yakirevich: None; Yihong Wang: None

Background: A concordant radiology-pathology diagnosis of breast malignancy allows for surgical planning of breast cancer. The clinical application of ultrasound (US) guided core needle biopsy (CNB) for mass lesions is crucial to rule out invasive carcinoma. However, if the lesion is diagnosed as ductal carcinoma in situ (DCIS), it is discordant with radiology and that creates surgical planning difficulty as to whether a sentinel lymph node biopsy is needed. We aimed to characterize the clinical and pathologic features of the concordant mass-forming DCIS and correlate the discordant cases with excision outcomes.

Design: This study included 82 consecutive cases of US-guided CNB undertaken in mass lesions diagnosed as DCIS. We evaluated DCIS histology: architectural patterns, nuclear grades, estrogen receptor (ER) status, comedo necrosis, and stromal desmoplasia. A radiology-pathology correlation was performed. Patient demographics and follow-up surgical excision findings were analyzed.

Results: The average patient age was 68 years (range: 25 to 90). Twenty-nine (35%) cases were high nuclear grade (HG) and the other fifty-three (64.6%) cases were low to intermediate nuclear grade. 13 out of 29 HG DCIS were ER-negative (45%). Fifty-eight of the 82 cases (71%) were radiologically concordant: 21(25%) HG exhibited solid pattern, comedo necrosis, and stromal desmoplasia; 19 (23%) were associated with mass-forming lesions such as radial scar (6), papilloma (9), fibroadenoma (1), sclerosing adenosis (2), ruptured cyst (1); and 18 (22%) had predominantly papillary architecture. Twenty-four (29%) discordant cases had no histologic correlate of a mass lesion in CNB (Table 1). Follow-up excisions were available in 65 cases. Invasive ductal carcinoma (IDC) was identified in 13 cases. 11 were among the 24 radiologically discordant cases (46%), 2 IDC were associated with HG DCIS with desmoplasia. In the 18 papillary architecture DCIS cases, subsequent excision revealed one Encapsulated papillary carcinoma, one Intracystic papillary carcinoma, two Solid papillary carcinoma and fourteen papillary DCIS.

	Total, n (%)	Non-high nuclear grade (n=53)	High nuclear grade (n=29)	p-value
Age (years)				0.172
50 ≤	16 (19.5)	8(9.7)	8 (9.7)	
50 >	66 (80.4)	45 (54.8)	21 (25.6)	
ER status				**<0.001**
Positive	68 (82.9)	52 (63)	16 (20)	
Negative	14 (17.0)	1 (1)	13 (16)	
Comedonecrosis				**<0.001**
Present	43 (52.4)	17 (21)	26 (32)	
Absent	39 (47.5)	36 (44)	3 (4)	
DCIS architecture				**0.003**
Solid pattern	40 (48.7)	23 (28.7)	17 (20.7)	
Cribriform pattern	51 (62.1)	36 (43.9)	15 (18.2)	
papillary pattern	24 (29.2)	22 (26.8)	2 (2.4)	
Micropapillary pattern	19 (23.1)	8 (9.7)	11 (13.4)	
Group categories of DCIS				-
High nuclear grade w/desmoplastic reaction	21 (25.6)	0	21 (25.6)	
Associated benign mass-forming lesion	19 (23)	16 (19.5)	3 (3.6)	
Papillary architecture	18 (22)	17 (20.7)	1 (1.2)	
Radiologically discordant	24 (29.2)	20 (24.3)	4 (4.8)	

Conclusions: The most common mass-forming DCIS lesions were HG DCIS with solid pattern, comedo necrosis, and stromal desmoplasia. In radiological discordant cases, the possibility of an unsampled invasive carcinoma is high (46%). Understanding the histological characteristics of mass-forming DCIS and its correlation with radiology is critical for surgical decision making.

90 A Clinicopathological Study of HER2 Status Changes between Primary Breast Cancer and Subsequent Metastasis in the New Context of HER2-Low Therapy: Are there Clinical or Pathological Characteristics that May Predict Evolution of HER2 Status?

Anthony Bergeron[1], Aurélie Bertaut[2], Françoise Beltjens[2], Céline Charon Barra[2], Alix Amet[2], Clémentine Jankowski[2], Sylvain Ladoire[2], Isabelle Desmoulins[2], Laurent Arnould[2]

[1]Unit of Pathology, Department of Biology and Pathology of the Tumor, Centre Georges-François Leclerc, Dijon, France, [2]Centre Georges-François Leclerc, Dijon, France

Disclosures: Anthony Bergeron: None; Aurélie Bertaut: None; Françoise Beltjens: None; Céline Charon Barra: None; Alix Amet: None; Clémentine Jankowski: None; Sylvain Ladoire: None; Isabelle Desmoulins: None; Laurent Arnould: None

Background: For many years, assessing HER2 status has been essential for the management of breast cancer (BC) patients. HER2 is overexpressed in 20 to 25% of BCs, allowing the patients to benefit from targeted anti-HER2 therapies. However, despite the emergence of new conjugate therapies which may be effective in cases with weak HER2 expression (”HER2-low”), only patients with strong HER2 expression by immunohistochemistry and/or FISH-confirmed amplification are now eligible for these therapies. The objective of this work was to study the HER2 status evolution with disease progression and identify possible clinical and pathologic factors associated with its changes.

Design: We compared the HER2 status between primary and metastatic tumors for all cases with complete HER2 assessment data concordant with the ASCO/CAP guidelines, registered in our database in 1992-2020 (n=279). We also analyzed the clinical, pathological and immunohistochemical characteristics of primary tumors by HER2 status evolution category (stable or variable).

Results: Among primary tumors, 16.9% were HER2-positive at diagnosis, 35.8% were HER2-negative and 47.3% HER2-low. The HER2 status changed at metastasis (either way) in 34.8% of cases, mainly HER2-negative and -low tumors (n=84; 86.6%; Figures 1-2). Clinical, morphological and immunohistochemical characteristics of initially HER2-negative tumors, stratified by HER2 status evolution, are summarized in Table 1. HER2-negative tumors which became HER2-low at recurrence had significantly lower proliferation indexes (*P*=0.042), more frequently expressed hormone receptors (*P*=0.005) and metastasized later (*P*=0.024). Multivariate analysis showed that progression risk was mainly associated with the expression of hormone receptors rather than the timeline of metastasis occurrence (OR=8.60; 95CI: 1.81-40.92; *P*=0.007). No significant differences in any of the analyzed parameters were found for HER2-low tumors which turned negative upon recurrence.

Table 1. Clinical, pathological and immunohistochemical characteristics of breast tumors which were HER2-negative at diagnosis, by the evolution of the HER2 status at recurrence

	Tumors which progressed from HER2-negative to HER2-low (n=39)	**Tumors with stable HER2-negative status (n=58)**	***P-values for comparison between the two groups***
Parameter			
Age at diagnosis (years)			*0.932*
Mean ± Standard Deviation	54.9 ± 10.7	55.1 ± 13.0	
Median [min-max]	55.0 [37.0 - 81.0]	54.0 [26.0 - 87.0]	
Unifocal tumor			*0.510*
Yes	33 (84.6%)	46 (79.3%)	
No	6 (15.4%)	12 (20.7%)	
Histology			*0.936*
Invasive ductal carcinoma	28 (71.8%)	43 (74.1%)	
Invasive lobular carcinoma	8 (20.5%)	12 (20.7%)	
Other	3 (7.7%)	3 (5.2%)	
Tumor Size (cm)			*0.325*
Mean ± Standard Deviation	2.6 ± 1.5	3.1 ± 2.3	
Median [min-max]	2.0 [0.7 - 6.5]	2.5 [0.4 - 10.5]	
Missing data	1	1	
Glandular differentiation			*0.095*
I	0 (0.0%)	1 (1.8%)	
II	14 (36.8%)	11 (19.3%)	
III	24 (63.2%)	45 (78.9%)	
Missing data	1	1	
Nuclear grade			*0.300*
I	1 (2.6%)	2 (3.5%)	
II	30 (78.9%)	37 (64.9%)	
III	7 (18.4%)	18 (31.6%)	
Missing data	1	1	
Mitosis score			*0.263*
I	19 (50.0%)	19 (33.3%)	
II	10 (26.3%)	21 (36.8%)	
III	9 (23.7%)	17 (29.8%)	
Missing data	1	1	
Mitotic index (/mm²)			***0.042***
Mean ± SD	3.7 ± 4.3	8.2 ± 10.5	
Median [min-max]	2.3 [0.4 - 16.0]	4.8 [0.4 - 50.0]	
Missing data	17	18	
Lymph node status			*0.767*
N0	18 (46.2%)	25 (43.1%)	
N+	21 (53.8%)	33 (56.9%)	
Disease stage			*0.265*
I	11 (28.2%)	14 (24.1%)	
II	18 (46.2%)	21 (36.2%)	
III	9 (23.1%)	15 (25.9%)	
IV	1 (2.6%)	8 (13.8%)	
Estrogen receptor expression			***0.005***
Negative	2 (5.1%)	16 (28.1%)	
Positive	37 (94.9%)	41 (71.9%)	
Missing data	0	1	
Progesterone receptor expression			*0.978*
Negative	11 (35.5%)	19 (35.2%)	
Positive	20 (64.5%)	35 (64.8%)	
Missing data	8	4	
Metastasis site			*0.354*
Liver	16 (41.0%)	17 (29.3%)	
Skin and muscle	8 (20.5%)	15 (25.9%)	
Bone	6 (15.4%)	13 (22.4%)	
Lung and pleural	3 (7.7%)	5 (8.6%)	
Gastrointestinal tract	3 (7.7%)	0 (0.0%)	
Gynecological tract	2 (5.1%)	4 (6.9%)	
Other	1 (2.6%)	4 (6.9%)	
Time to recurrence			***0.024***
Mean ± SD	84.6 ± 48.7	64.1 ± 51.3	
Median [min-max]	84.0 [2.0 - 240.0]	48.0 [1.0 - 204.0]	

Figure 1 - 90

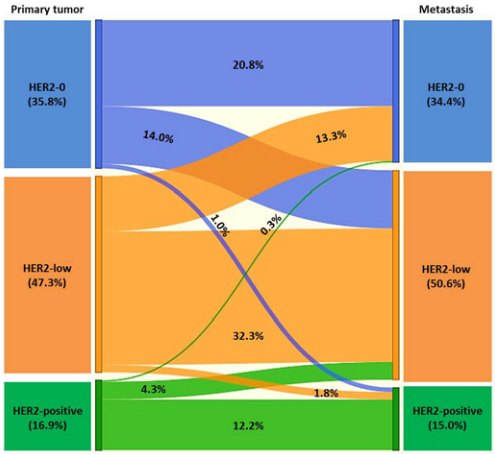

Figure 1. The evolution of the HER2 status between primary breast tumor and metastatic recurrence. Sankey diagram illustrating the HER2 status changes for all cases (n=279), with specific percentages. HER2-0: HER2-negative

Figure 2 - 90

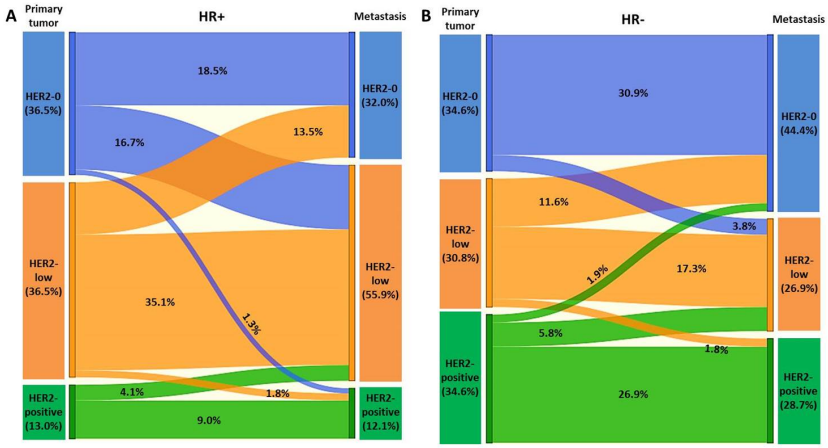

Figure 2. The evolution of the HER2 status between primary breast tumor and metastatic recurrence stratified by the hormone receptor (HR) expression. Sankey diagrams illustrating the HER2 status evolution in HR-positive (HR+) (A) and HR-negative (HR-) (B) primary breast tumors. HER2-0: HER2-negative

Conclusions: We show that the HER2 status varies with BC progression, particularly for HER2-low and -negative tumors, while it is rather stable for HER2-positive tumors. With the emergence of new anti-HER2 therapies effective against HER2-low tumors, it is essential to re-evaluate the HER2 expression in metastases, in particular if the primary tumor had a low proliferation index and hormone receptor expression, and especially if the metastasis occurred late, in order to identify the best candidates for treatment.

91 Leiomyoma of Nipple and Areolar Region: Further Clinicopathological Characterization Based on Review of Twenty-One Cases

Diana Berman[1], Syed Hoda[2]
[1]New York-Presbyterian/Weill Cornell Medical Center, New York, NY, [2]Weill Cornell Medical Center, New York, NY

Disclosures: Diana Berman: None; Syed Hoda: None

Background: Although Leiomyoma of Nipple & Areolar Region (LoNAR) was first reported in 1854 (*Virchow Arch Pathol Anat* 6:525-554), it remains poorly characterized. All known clinicopathological features of LoNAR are based on single case reports & relatively small case series.

Design: Clinical & pathological material from all LoNAR diagnosed in our medical center over a ~20-year period (2001-2021) were reviewed. Clinical follow-up was obtained.

Results: 21 LoNAR were identified. All cases were solitary, unilateral, & presented with a slow-growing (months-years) mass (Fig. 1, with pre-surgical marking). 20 were asymptomatic (1 had nipple discharge: infected lactiferous duct). Both genders (F:17, M:4) & both breasts (R:12, L:9) were affected. 4 had breast carcinoma (ipsilateral: 1, contralateral: 2, unknown: 1; synchronous: 2, metachronous: 2). Mean size of lesion was 1.1 cm (range:0.3-3.3 cm). 12 underwent excision. Others had incisional or multiple core biopsies. Cut section was whorled (Fig. 2). LoNAR were dermal based (n:21, 100%) & characterized by prominent, confluent interlacing variably thick bundles of fusiform cells with elongated nuclei, & perinuclear vacuoles; with minimal intervening fibrous & breast glandular tissue (n:21, 100%). 4 (19%) cases showed marked nuclear atypia (Ki67: <5%, wherein tested); & rare (<1/10 hpf) mitoses were identified in 3 cases. Central degeneration was evident in 1 case. No case showed necrosis, Paget disease or ulceration. All LoNAR blended with native smooth muscle fibers at the perimeter (definitive margin clearance was difficult to evaluate in at least 3 cases). Immunostains (performed in 12 cases) showed LoNAR cells to be positive for actin (HHF & 1A4), desmin, & caldesmon. No case had a history of estrogen-modulating therapy, chemotherapy, radiation, or other significant non-breast disease. In a mean follow-up of 91 (range: 6-240) months, there was no clinically evident recurrence. Note: 1 case in this series was previously reported, *Breast J*. 2020;26:529-530.

Figure 1 - 91

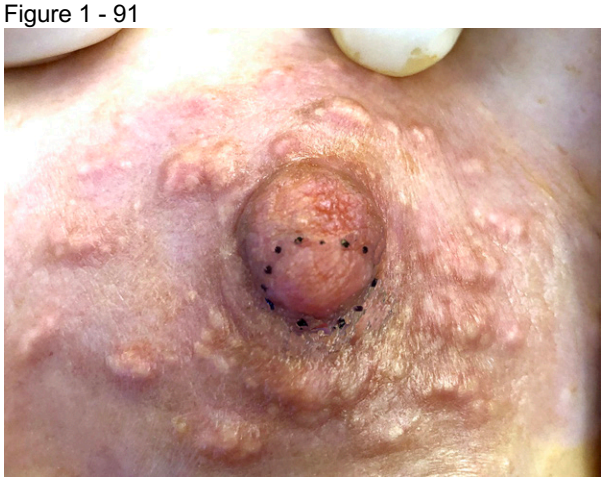

Figure 2 - 91

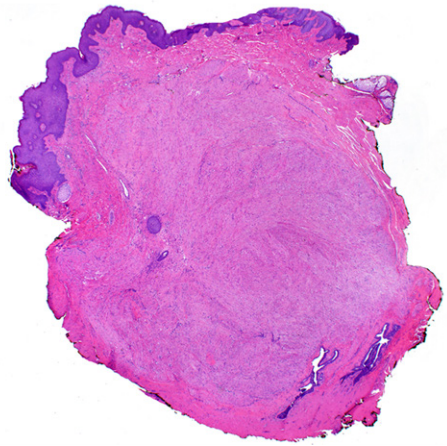

Conclusions: In this retrospective review, the largest to date, LoNAR was an uncommon, typically asymptomatic, unilateral, slow-growing, dermal-based, poorly circumscribed, generally bland, tumor which occurred in adults of both genders. We report that contrary to published literature, pain is not a presenting symptom & marked (symplastic type) nuclear atypia can be encountered. There were no recurrences in this series (the 1 previously reported recurrence developed 9 years s/p excision).

92 Double PIK3CA Mutations are Associated with Distinct Morphological Characteristics in Breast Cancer

Soumar Bouza[1], Tong Sun[2], Malini Harigopal[2], Minghao Zhong[2], Haiying Zhan[3]
[1]Yale School of Medicine, Yale New Haven Hospital, New Haven, CT, [2]Yale School of Medicine, New Haven, CT, [3]Yale New Haven Hospital, Yale School of Medicine, New Haven, CT

Disclosures: Soumar Bouza: None; Tong Sun: None; Malini Harigopal: None; Minghao Zhong: None; Haiying Zhan: None

Background: Activating mutations in *PIK3CA* are frequent in breast cancer, and phosphoinositide 3-kinase alpha (PI3Kα) inhibitors have been shown to prolong progression-free survival. *PIK3CA* mutations can be single-hotspot, double, or multiple-hotspots. Recent studies showed that double *PIK3CA* mutations are associated with increased sensitivity to PI3Kα inhibitors, comparing with single-hotspot mutations. The correlative clinicopathologic features for breast cancer with multiple mutations have not been previously studied. Herein we aim to characterize pathological features of breast cancers harboring double *PIK3CA* mutations in this study.

Design: Breast cancer patients' samples as well as germline control specimens were submitted for molecular profiling using Oncomine Comprehensive Assay v3 (OCP; Thermo Fisher Scientific) to identify alterations in up to 143 cancer related genes by targeted NGS. Additional clinico-pathologic information, including hormone receptor and HER2 status, was retrieved for each individual case.

Results: We retrospectively identified 11 cases with double *PIK3CA* mutations which represent 10-15% of breast cancer. Four of 11 cases (4/11, 36%) showed mixed ductal and lobular carcinoma (IDC/L). Seven cases (7/11, 64%) were invasive ductal carcinoma nonspecific type, and 2 of which showed apocrine differentiation (Table 1). The majority cases (9/11, 82%) were ER-positive and HER2-negative. Two cases (2/11, 18%) demonstrated triple negative breast cancer (TNBC) phenotype (Table 1).

Table 1. Histopathological features of 11 cases of breast cancer with double PIK3CA mutations

Case #	PIK3CA mutations		Additional mutations	Histology Type	Tumor Grade	DCIS	ER	PR	HER2
1	H1047R (49%)	E453K (46%)	CDKN1B, ARID1A, ESR1	Mixed IDC/L	G2	Present	95%, 3+	80%, 3+	Neg
2	E542K (34%)	E726K (26%)	BRCA2, RET, TSC2, SETD2	Mixed IDC/L	G2	N/A	90%, 3+	90%, 3+	Neg
3	E542K (14%)	M1043I (9%)	None	Mixed IDC/L	G2	Present	90%, 3+	60%, 3+	Neg
4	H1047R (41%)	D350G 38%)	None	Mixed IDC/L	G2	Present	95%, 3+	95%, 3+	Neg
5	E453Q (30%)	E545K (27%)	NF1, FANCD2	IDC with LCIS	G1	Present	70%, 2+	neg	Neg
6	H1047R (28%)	R93Q (26%)	NF1	IDC	G1	Present	100%, 3+	90%, 3+	Neg
7	E722Q (31%)	N345K (24%)	None	IDC	G2	Present	95%, 3+	90% 3+	Neg
9	E545K (72%)	E418K (15%)	TP53, BRCA2, RB1, ATM	IDC with apocrine differentiation	G3	Present	100%, 3+	30%, 3+	Neg
10	H1047R (30%)	E545Q (9%)	None	IDC with apocrine differentiation	NA	N/A	Neg	Neg	Neg
11	H1047R (29%)	E542A (26%)	NF1	IDC	G2	N/A	Neg	Neg	Neg

Conclusions: Double *PIK3CA* mutations in breast cancers are associated with unique histopathologic features including a high frequency of mixed ductal and lobular carcinoma, and ER positive HER2 negative immunophenotype. Appropriate recognition of breast cancers with double PIK3CA mutations will help to guide correct clinical management and prognostic evaluation.

93 SMARCA4 Mutated (SMARCA4mut+) Clinically Advanced and Metastatic Breast Cancer (MBC): A Comprehensive Genomic Profiling (CGP) Study

Amy Brady[1], Jeffrey Ross[1], Natalie Danziger[2], Richard Huang[3], Ethan Sokol[2]
[1]SUNY Upstate Medical University, Syracuse, NY, [2]Foundation Medicine, Inc., Cambridge, MA, [3]Foundation Medicine, Inc., Cary, NC

Disclosures: Amy Brady: None; Jeffrey Ross: *Employee*, Foundation Medicine; *Employee*, Foundation Medicine; Natalie Danziger: *Employee*, Foundation Medicine Inc.; *Stock Ownership*, F. Hoffman La Roche Ltd.; Richard Huang: *Employee*, Foundation Medicine; *Employee*, Roche; Ethan Sokol: *Employee*, Foundation Medicine; *Stock Ownership*, Roche

Background: SMARCA4 is a subunit of the SWI/SNF-related matrix-associated actin-dependent regulator of chromatin (SMARC), which is involved in the regulation of chromatin remodeling and gene expression. Inactivating mutations in the *SMARC* genes (*SMARCA4*mut+) play a role in the development of human cancers. In this study, CGP on advanced stage MBC was used to characterize those cancers with *SMARCA4*mut+.

Design: CGP to detect genomic alterations (GA) was performed on 18,297 advanced stage MBC using a hybrid capture-based FDA-approved assay. Tumor mutational burden (TMB) was determined on up to 1.1 Mbp of sequenced DNA and microsatellite instability (MSI) was determined on 114 loci. PD-L1 expression in tumor cells (Dako 22C3) was measured by IHC.

Results: 195 (1.1%) MBC were *SMARCA4*mut+. For the *SMARCA4*mut+ patients, the primary breast tumor was sequenced in 51 cases and a metastatic site in 144 cases (adrenal 1, bone 10, brain 10, liver 39, lymph node 28, lung 11, GI tract 4, body cavities 10, skin and soft tissue 31). Ages were similar. Estrogen receptor (ER) positivity was significantly less frequent TNBC were significantly more frequent in *SMARCA4*mut+ cases (P<.0001). *CDH1* GA (lobular ca genotype) was less frequent in *SMARCA4* wild type (wt) (p=.0004). GA in currently untargetable GA were significantly more frequent in *SMARCA4*mut+ including *ESR1*, *TP53*, *CDKN2A/B*, *KRAS*; and emerging targets *NOTCH1* and *MTAP*. For currently targetable GA, results varied

with *SMARCA4*mut+ MBC featuring more *EGFR*, *NF1* and *KRAS* G12C GA and *SMARCA4*wt featuring more *ERBB2*, *PIK3CA* and *FGFR1* GA. Immunotherapy (IO) biomarkers were more frequent in *SMARCA4*mut+ pts including both efficacy markers (MSI high, TMB, PD-L1 expression) and resistance markers (*STK11*).

	***SMARCA4*mut MBC**	***SMARCA4*wt MBC**	**P Value**
Cases	195	18,102	
Median age (range)	60 (29-89+)	59 (20-89+)	
Mean age	60.0	59	NS
ER+	43.2%	69.3% (1015 cases)	<.0001
TNBC	48.2%	27.0% (1015 cases)	<.0001
GA/tumor	7.6	6.2	
Top Untargetable GA			
ESR1	7.7%	13.4%	=.02
CDH1	5.4%	12.7%	=.004
TP53	64.4%	50.2%	<.0001
CDKN2A	18.6%	7.1%	<.0001
CDKN2B	14.4%	5.1%	<.0001
KRAS	13.4%	3.9%	<.0001
MTAP	10.3%	3.8%	<.0001
MYC	16.0%	18.8%	NS
RAD21	22.2%	20.8%	NS
RB1	9.4%	7.7%	NS
ARID1A	9.3%	6.5%	NS
CCND1	8.9%	18.9%	=.0004
NOTCH1	4.6%	2.2%	=.017
Top Potentially Targetable GA			
EGFR SV mutation	1.5%	0.5%	=.030
ERBB2 Amplification	4.1%	7.3%	NS
ERBB2 SV mutation	2.6%	3.1%	NS
BRAF	3.1%	1.5%	NS
PIK3CA	27.3%	36.6%	=.003
FGFR1	7.2%	14.3%	=.013
PTEN	14.9%	12.8%	NS
KRAS G12C	3.0%	0.2%	<.0001
NF1	11.3%	6.7%	=.027
BRCA1	5.2% (0.5% CN loss)	3.6% (0.3% CN loss)	NS
BRCA2	6.2% (1.5% CN loss)	4.6% (0.4% CN loss)	NS
IO Predictive GA			
PBRM1	0.5%	0.7%	NS
STK11	12.9%	1.5%	<.0001
MDM2	2.6%	4.3%	NS
CD274 amplification	3.1%	1.3%	NS
IO Predictive Biomarkers			
MSI-High	2.6%	0.3%	<.0001
Mean TMB	11.0	4.5	<.0001
Median TMB	5.0	2.5	
TMB≥10 mut/Mb	27.7%	9.1%	<.0001
TMB≥20 mut/Mb	12.3%	2.6%	<.0001
PD-L1 IHC Low Positive	8.0% (88 cases)	3.9% (6863 cases)	NS
PD-L1 IHC High Positive	4.5%	0.7%	=.004

Conclusions: While *SMARCA4*mut+ MBCs are rare, understanding their genetic profile may allow physicians to dictate a more appropriate therapy. *SMARCA4*mut+ MBCs have more untargetable GAs than targetable GAs; however, the IO biomarkers were more frequent, suggesting immunotherapy may have an advantage over other forms of therapy in the treatment of *SMARCA4*mut+ MBCs.

94 Is There a Difference Between Pregnancy-Associated and Non-Pregnancy-Associated Breast Cancer in Females 35 Years or Younger?

Ankica Braun[1], Abdullah Almajnnooni[1], Sindhuja Sivanandham[1], Indu Agarwal[1], Paolo Gattuso[1]
[1]Rush University Medical Center, Chicago, IL

Disclosures: Ankica Braun: None; Abdullah Almajnnooni: None; Sindhuja Sivanandham: None; Indu Agarwal: None; Paolo Gattuso: None

Background: Pregnancy-associated breast cancer (PABC) is not a common clinical presentation; the incidence is approximately 1/3000 pregnancies. Several clinical studies compared PABC to non-pregnancy-associated breast cancer (non-PABC). However, in majority of studies the age matched patients were older than 35 years. We undertook a retrospective study to

address histologic parameters, prognostic markers, and survival in patients with PABC with matched group of non-PABC in patients 35 years or younger.

Design: Our institution's data base was searched for patients with breast cancer 35 years or younger. Subsequently, the patients with secretory changes and the patients within one year postpartum were identified. The PABC and non-PABC patients were compared regarding their clinicopathological features.

Results: The PABC group held 24 patients and the non-PABC group held 226 patients. The mean age was 31.5 in the PABC and 29.8 years in the non-PABC group. Among the PABC, 19 patients had invasive ductal carcinoma (IDC), two metaplastic carcinoma, two ductal carcinoma in situ (DCIS), and one mucinous carcinoma. Among the non-PABC, 186 patients had IDC, 20 patients had DCIS, seven mixed invasive lobular and ductal carcinoma, five invasive lobular carcinoma, four microinvasive carcinoma, two lobular carcinoma in situ, one mucinous, and one metaplastic. In the PABC group 8% were grade 1, 33% grade 2, and 59% grade 3. Regarding the non-PABC, 3% were grade 1, 26% grade 2, and 71% grade 3. ER was positive in 59% of the PABC and 66% of the non-PABC. PR was positive in 45% of the PABC and 54% of the non-PABC. 53% of the PABC and 70% of the non-PABC had proliferative index higher than 20%. HER-2/neu was positive in 16% of the PABC and in 30% of the non-PABC. BRCA1/2 was positive in 19% of PABC and in 20% of the non-PABC. 57% of the PABC and 47% of the non-PABC had lymph node metastasis. 33% of the PABC and 20% of non-PABC received neoadjuvant chemotherapy. In the PABC group, 50% were alive, 13% died of the disease and 37% were lost to follow up. In the non-PABC group, 46% were alive, 12% died of the disease and 42% were lost to follow up.

Conclusions: The PABC had a lower expression of ER, PR and HER-2/neu, however they have a higher rate of lymph node metastasis. There was no survival difference between the two groups of patients. BRCA1/2 was similarly present in the both groups of patients. Invasive ductal carcinoma was the most common malignancy in both groups.

95 Cystic Neutrophilic Granulomatous Mastitis: Clinicopathologic and Morphologic Variables of 49 Cases

Bethany Burns[1], Raza Hoda[2], Gloria Lewis[2], Xiaoyan Cui[2], Sara Abbott[3], Miglena Komforti[2], J. Jordi Rowe[2], Gary Procop[4], Erinn Downs-Kelly[2], Patrick McIntire[2]
[1]Cleveland Clinic Pathology and Laboratory Medicine, Cleveland, OH, [2]Cleveland Clinic, Cleveland, OH, [3]Michigan Medicine, University of Michigan, Ann Arbor, MI, [4]American Board of Pathology, Tampa, FL

Disclosures: Bethany Burns: None; Raza Hoda: None; Gloria Lewis: None; Xiaoyan Cui: None; Sara Abbott: None; Miglena Komforti: None; J. Jordi Rowe: None; Gary Procop: None; Erinn Downs-Kelly: *Advisory Board Member*, Lilly Oncology; Patrick McIntire: None

Background: Cystic Neutrophilic Granulomatous Mastitis (CNGM) is a more recently recognized entity that may cause pain, erythema, mass and fistula formation. The morphologic hallmark of CNGM is identifying cystic spaces that are lined, at least semi-circumferentially, by neutrophils with varying degrees of surrounding granulomatous inflammation. CNGM is presumed to manifest in response to a bacterial infection, most commonly *Corynebacterium* (a gram-positive bacilli), that may be identified within the cystic spaces.

Design: Cases denoted as CNGM diagnosed from 2015-2021 were identified from the surgical pathology files and reviewed by a panel of breast fellowship trained pathologists with the aid of clinical microbiologists, blinded to the clinical outcome and culture results.

Results: A total of 49 biopsies and/or excisions from 34 patients were identified. All patients were female and ranged from 22-60 years of age (average age 37, SD 7.8). The majority of women were parous (28/32, 86%) and previously breastfed (19/24, 79%). Women presented with palpable lesions (32/32, 100%), and local tenderness/erythema (25/32, 78%). Bacterial cultures were frequently ordered (22/32, 68%) and half grew or were consistent with *Corynebacterium* (11/22, 50%). Patients received antibiotics either before (17/32, 53%) or after initial biopsy (25/32, 78%). A majority of cases were regarded as CNGM clinically (18/32, 56%).

Cases consisted of biopsies (35/49, 71%) and excisions/mastectomies (14/49, 29%) with the hallmark cystic spaces being variable (range 1 to > 15 spaces per case). The majority of the cystic spaces were noted within the stroma while a subset (8/49, 16%) had intraductal inflammation with the classic cystic spaces noted intraluminally. Bacteria were frequently identified on H&E (23/47,

49%) and on Gram Stain (23/39, 59%). Please see **Table 1** for a summary of the clinicopathologic and morphologic variables identified.

Table 1: Summary of Clinicopathologic and Morphologic Variables Identified in 49 Cases of CNGM.

Patient Characteristics	**Total (Percent)**	
Age	**Average**: 37 (Range 23-60, SD 7.8)	
Race	**White or Caucasian:** 16/31 (56%)	**Asian:** 6/31 (19%)
	Black or African American: 7/31 (22%)	**American Indian or Alaskan:** 1/31 (3%)
Ethnicity	**Hispanic (All Races):** 4/32 (12%)	**White or Caucasian and Hispanic:** 3/15 (20%)
Travel	**Lived Outside the US:** 5/27 (23%)	**Recent International Travel:** 4/30 (16%)
Medical History	**Endocrinopathy**: 6/32(18%)	**Autoimmune**: 6/30 (20%)
Smoking Status	**Ever Smoker:** 7/32 (21%)	**Current Smoker**: 0/7 (0%)
Parity	**Nulliparous:** 4/32 (13%)	**Parous:** 28/32 (86%)
Gravidity	**Currently Pregnant:** 3/32 (9%)	
Breastfeeding	**Current:** 1/32 (3%)	**Previous:** 19/24 (79%)
Piercing	**Current or Former Nipple Piercing:** 1/30 (3%)	
History of Present Illness	**Palpable Lesion:** 32/32 (100%)	**Incidental on Imaging:** 0/32 (0%)
	Tender/Erythematous Lesion: 25/32 (78%)	**Breast Trauma:** 6/30 (20%)
	Brown/Bloody Nipple Discharge: 3/31 (10%)	
Clinical Microbiology	**Patients with Bacterial Cultures Ordered:** 22/32 (68%)	
Gram Stain	**Gram Positive Bacilli/Diphtheroids**: 4/18 (22%)	
Culture	**Gram Positive Bacilli or *Corynebacterium*:** 11/22 (50%)	***Corynebacterium*:** 8/22 (36%)
Imaging (US)	**Greatest Dimension on Average:** 3.8 cm	**BiRADs:** Average 3.6, Mode 4
Treatment	**Any Treatment**: 27/32 (92%)	**Any Treatment After Bx/Excision:** 26/32 (81%)
	Antibiotics Before Bx: 17/32 (53%)	**Antibiotics After BX/Excision:** 25/32 (78%)
Clinical Diagnosis	**CNGM:** 18/32 (56%)	
Histologic Features	**Total (Percent)**	
Specimen	**Bx:** 35/49 (71%)	**Excision:** 14/49 (29%)
Laterality	**Left**: 15/49 (31%)	**Right**: 34/49 (69%)
Neutrophils	**Present:** 49/49 (100%)	**Throughout:** 23/49 (47%)
	Lining Cystic Space: 49/49 (100%)	**All Spaces Lined by Neutrophils:** 41/47 (87%)
Number of Cystic Spaces	**(1-5):** 31/49 (63%)	**(6-10):** 11/49 (22%)
	(11-15): 4/49 (8%)	**(>15):** 3/49 (6%)
Size of Cystic Spaces	**Consistent:** 9/39 (23%)	**Variable:** 30/39 (77%)
	< Adipocyte: 15/49 (31%)	**= Adipocyte:** 34/49 (69%)
	>Adipocyte: 32/49 (65%)	
Cystic Space Characteristics	**Incipient:** 29/49 (59%)	**Intraductal**: 8/49 (16%)
Adjacent Granulomas	**Present:** 32/49 (65%)	
	Epithelioid: 31/32 (96%)	**Suppurative:** 9/32 (28%)
Histiocytes	**Present:** 48/49 (98%)	
	Epithelioid: 44/48 (92%)	**Spindled:** 15/48 (31%)
Inflammation	**Lymphocytes:** 48/49 (98%)	**Plasma Cells**: 46/49 (94%)
	Eosinophils: 22/49 (45%)	**Giant Cells:** 44/49 (90%)
Background Tissue	**Edema:** 36/49 (73%)	**Fibrosis:** 35/49 (71%)
	Fat Necrosis: 21/48 (44%)	**Benign Breast Epithelium:** 43/4 (88%)
Bacteria Identified	**H&E:** 23/47 (49%)	**Gram Stain:** 23/39 (59%)

Conclusions: CNGM was seen commonly in parous, younger women with a history of previous breastfeeding. The hallmark cystic spaces are highly variable and clinical history along with an inflammatory background should prompt additional levels to more fully evaluate for such findings. The presence of intraductal cystic spaces is a finding not well described previously and raises questions about the possible pathogenesis of this process.

96 Cystic Neutrophilic Granulomatous Mastitis: Treatment Effect and Morphologic Changes Seen in Patients Following Antibiotic Treatment

Bethany Burns[1], Raza Hoda[2], Gloria Lewis[2], Xiaoyan Cui[2], Sara Abbott[3], Miglena Komforti[2], J. Jordi Rowe[2], Gary Procop[4], Erinn Downs-Kelly[2], Patrick McIntire[2]

[1]Cleveland Clinic Pathology and Laboratory Medicine, Cleveland, OH, [2]Cleveland Clinic, Cleveland, OH, [3]Michigan Medicine, University of Michigan, Ann Arbor, MI, [4]American Board of Pathology, Tampa, FL

Disclosures: Bethany Burns: None; Raza Hoda: None; Gloria Lewis: None; Xiaoyan Cui: None; Sara Abbott: None; Miglena Komforti: None; J. Jordi Rowe: None; Gary Procop: None; Erinn Downs-Kelly: *Advisory Board Member*, Lilly Oncology; Patrick McIntire: None

Background: Cystic Neutrophilic Granulomatous Mastitis (CNGM) is classically defined by neutrophils circumferentially lining cystic spaces with coexisting encircling granulomatous inflammation that is induced by infection with *Corynebacterium*. Although the clinical course can be relapsing and remitting, persistent mastitis despite antibiotic therapy may lead to an excision. Excisions may exhibit features similar to a patient's original core needle biopsy (CNB), or have non-classic features. Studying excision specimens may provide insight into whether the pathology of CNGM remains, or if non-specific abscess formation is a driver of complicated and protracted disease.

Design: Paired CNB and excision specimens were compared from six patients. Clinical and histologic characteristics were reviewed by a cohort of breast pathologists with the aid of a clinical microbiologist. Classic features of CNGM were defined as a varying number of neutrophils circumferentially lining cystic spaces with concurrent granulomatous inflammation. CNBs and excisions were reviewed, blinded to culture and clinical outcome, and designated as either classic CNGM (cCNGM), non-classic CNGM (ncCNGM) or both when such patterns were identified in the same specimen.

Results: Patients ranged in age from 32-60 years with the majority of patients presenting with a palpable lesion (6/6) and local pain and erythema (6/6). Most patients had a culture (5/6) with the majority growing either diphtheroid bacilli or *Corynebacterium* (4/5). One patient had 16s sequencing to reaffirm the presence of *Corynebacterium* (1/5)*. The duration between CNB and excision varied from 1-14 months. All patients were treated with antibiotics either before (5/6) and/or during the interim between CNB and excision (5/6). On histologic review, all biopsies were cCNGM. In subsequent excision specimens, patients with short course antibiotics (< 6 months) demonstrated cCNGM (4/4) and patients with prolonged antibiotic therapy (> 6 months) demonstrated ncCNGM morphology (1/2) and both cCNGM and ncCNGM (1/2). Non-classic features included abscess formation and lack of cystic spaces. Disease course ranged between 1-30 month(s) from presentation to resolution of symptoms. A summary of the clinicopathologic findings is provided in Table 1.

Table 1: Clinicopathologic Features of Six Patients Diagnosed with CNGM with Paired Biopsy and Excision Specimens.

	Patient	Presentation (Location)	Antibiotics Prior to CNB (Y/N)	*Corynebacterium* on Culture (Y/N)	Bacteria on CNB (Y/N)	Antibiotics Between CNB and Excision (Y/N)	Time Between CNB and Excision (Months)	Features of CNGM on Excision (Classic/Non-classic)	Outcomes (Resolution of Symptoms (Months))
1	60YF (L)	Palpable mass with erythema and pain (Areola)	Y	NA	N	N	2	C	Resolution of mass (1 month). Follow-up mastectomy for DCIS ipsilateral breast
2	32YF (L)	Palpable mass with erythema and pain (Areola)	Y	Y	N	Y	1	C	Resolution of chronic wound (9 months)
3	37YF (R)	Palpable mass with erythema, pain, swelling and fever (Lateral Breast)	Y	N	Y	Y	10	NC	Resolution of chronic abscess (14 months)
4	44YF (R)	Palpable mass with erythema, pain, swelling, and nipple retraction (Inferior Breast)	Y	Y	Y*	Y	14	NC & C	Resolution of chronic abscess and draining fistula tracts (6 months). Follow-up prophylactic bilateral mastectomy for contralateral breast cancer
5	34YF (R)	Palpable mass with erythema and pain (Areola)	Y	Y	Y	Y	1	C	Resolution of chronic abscess (12 months)
6	50YF (R)	Palpable mass with erythema, pain, nipple retraction and fever (Areola)	N	Y	Y	Y	1	C	Recurrence in bilateral breast with subsequent abscesses (20 months and 30 months with recurrence)

Conclusions: In this series, prolonged antibiotic therapy (> 6 months) demonstrated a diminution or loss of the classic morphologic features of CNGM. This finding highlights the importance of clinical correlation and the need for work-up on CNB early in the disease time course.

97 Breast Nonmass Enhancement and Histologic Findings at Needle Core Biopsy: A Single Institution Experience

Alain Cagaanan[1], Matthew Hanna[1], Sandra Brennan[1], Edi Brogi[1]
[1]Memorial Sloan Kettering Cancer Center, New York, NY

Disclosures: Alain Cagaanan: None; Matthew Hanna: None; Sandra Brennan: None; Edi Brogi: None

Background: Magnetic resonance imaging (MRI) of the breast is a highly sensitive imaging modality for detecting breast cancer. An MRI abnormality may appear as a mass-like or focal enhancement, or as a non-mass enhancement (NME). NME is defined as a region of enhancement distinct from the background breast without a corresponding mass. Needle core biopsy (NCB) may be needed to evaluate NME findings. This study aims to investigate the histopathologic findings at NCB of NME at our institution.

Design: Our pathology database was searched to identify in-house NCBs targeting NMEs performed between January 2020 and July 2021. Indications for breast MRI were classified as extent of disease work-up in patients with concurrent ipsi- or contralateral carcinoma, high risk screening, or evaluation of mammographically or sonographically indeterminate lesions. Radiologic and pathologic diagnoses were reviewed. Pathologic diagnoses were classified into benign, atypical/high risk [e.g. ADH, ALH, LCIS], and malignant (invasive carcinoma and/or DCIS). For each NCB, the highest risk lesion or benign dominant lesion was noted. The findings at follow up (F/U) excision were recorded.

Results: In the study period, there were 617 NCBs of NMEs in 507 women (mean age 50 years, range 22-79). The pathologic findings were benign in 422 NCBs (68%), atypical/high risk in 84 (14%), and malignant in 111 (18%). **Table 1** shows the most common highest risk or benign dominant lesions. In two cases, NCB yielded a low-grade B cell lymphoma and one fibromatosis. **Figure 1** shows the biopsy indications and resulting pathologic diagnoses including follow up excision findings for the atypical/high risk category. NCB of NME had the highest yield of malignancy in patients evaluated for extent of disease (36%).

Table 1

Histologic Finding	N (%)
DCIS	68 (11.0)
PASH	54 (8.8)
Columnar cell changes	50 (8.1)
Sclerosing adenosis	47 (7.6)
ALH+LCIS	42 (6.8)
Usual ductal hyperplasia	41 (6.6)
Ductal Atypia (ADH, CCCA)	40 (6.5)
Invasive Carcinoma	39 (6.3)

ADH- Atypical Ductal Hyperplasia, ALH- Atypical Lobular Hyperplasia, CCCA- Columnar Cell Changes with Atypia, PASH- Pseudoangiomatous Stromal Hyperplasia, DCIS- Ductal Carcinoma in Situ, LCIS- Lobular Carcinoma in Situ

Figure 1

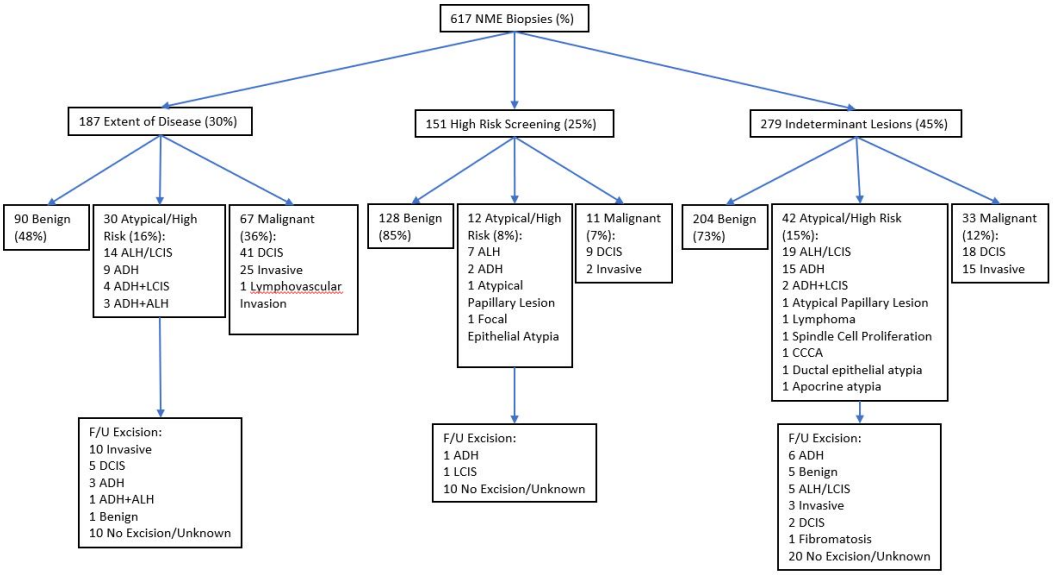

Conclusions: In this cohort, the majority of NME cases yielded benign histologic findings, with PASH representing the most common lesion. NCB of NME detected during extent of disease work-up was associated with the highest rate of malignancy and atypical/high risk findings. DCIS was the most common malignant lesion in all NCBs done for all indications. Evaluation of additional cases is pending. Overall, our findings support the utility of NCB for histologic evaluation of NME regardless of clinical indication. These findings may be further validated in additional larger cohorts.

98 Low Grade Adenosquamous Carcinoma of the Breast: A Clinicopathologic Review of 34 Cases

Lorraine Colon Cartagena[1], Edi Brogi[1], Jorge Reis-Filho[1], Hannah Wen[1]
[1]Memorial Sloan Kettering Cancer Center, New York, NY

Disclosures: Lorraine Colon Cartagena: None; Edi Brogi: None; Jorge Reis-Filho: None; Hannah Wen: None

Background: Low grade adenosquamous carcinoma (LGASC) of the breast is a low-grade variant of metaplastic carcinoma with an indolent behavior. Reports of large series with long-term follow-up are limited due to the rarity of the entity. This study is a comprehensive review of the clinicopathologic features, treatment, and outcome of patients with LGASC treated at our center.

Design: We retrospectively reviewed LGASC diagnosed at our center between 2002-2021. Clinicopathologic data were obtained from the medical record. Available slides were reviewed.

Results: A total of 35 cases from 34 women were identified. Median age was 60 years (29-80). Clinical presentations included palpable mass (10; 28.5%), screen detected mass (13; 37%), nipple discharge (2; 6%), and unknown (10; 28.5%). Median tumor size was 10 mm (1.4- 23). The tumors were composed of infiltrating glandular proliferation with bland cytology and varying degrees of squamous differentiation. LGASC was associated with an intraductal papilloma in 3 cases and with a nipple adenoma in 1 case. Three patients had concurrent ipsilateral invasive ductal carcinoma no special type (IDC NOS), ER/PR+, HER2-, 5 had concurrent ipsilateral DCIS. One of the 21 patients with sentinel lymph node biopsy had isolated tumor cells in one node. This was a 68 years old woman with a 17 mm LGASC and concurrent ipsilateral DCIS. Receptor status was known in 28 cases, of which 24 (86%) were triple negative, 4 (14%) were ER low positive (1-10%), PR/HER2-negative. Molecular study was performed in 1 case which showed somatic mutations in *PIK3CA*, *TERT* and *KEAP1*. Treatment and clinical follow-up data were available for 16 patients, with a median follow-up of 43 months (2 - 115). Surgical treatment was breast conserving surgery (BCS) in 14 (87.5%) patients and mastectomy in 2 (12.5%). Most patients treated with BCS received radiation (12/14; 86%). 8 (50%) patients had no systemic therapy, 8 (50%) had chemotherapy (3 of which had concurrent IDC NOS). One patient developed local recurrence at 98 months

after initial diagnosis. This was a 37-year-old woman with a 6 mm LGASC treated with BCS only with negative margins. No distant metastasis was observed.

Conclusions: Our study confirms that LGASC has an indolent behavior despite triple negative phenotype. Local recurrence may occur, although a rare incidence. No distant metastasis of LGASC in patients with or without adjuvant chemotherapy.

99 The Spectrum of Breast Cancer with TERT Genetic Alterations

Lorraine Colon Cartagena[1], Andrea Gazzo[1], Edaise M. da Silva[1], Fatemeh Derakhshan[1], Antonio Marra[1], Dara Ross[1], Timothy D'Alfonso[1], Hong (Amy) Zhang[1], Hannah Wen[1], Britta Weigelt[1], Edi Brogi[1], Jorge Reis-Filho[1], Fresia Pareja[1]
[1]Memorial Sloan Kettering Cancer Center, New York, NY

Disclosures: Lorraine Colon Cartagena: None; Andrea Gazzo: None; Edaise M. da Silva: None; Fatemeh Derakhshan: None; Antonio Marra: None; Dara Ross: None; Timothy D'Alfonso: None; Hong (Amy) Zhang: None; Hannah Wen: None; Britta Weigelt: None; Edi Brogi: None; Jorge Reis-Filho: None; Fresia Pareja: None

Background: *TERT* promoter mutations and gene amplifications, resulting in increased telomerase activity, constitute one of the most prevalent genetic alterations across cancer types. In breast neoplasms, *TERT* alterations are linked to phyllodes tumors and metaplastic carcinomas. Here, we sought to characterize the histologic spectrum of breast cancers (BCs) with oncogenic *TERT* genetic alterations.

Design: We retrospectively queried 7,582 BCs subjected to clinical targeted massively parallel sequencing to assess for *TERT* promoter mutation/copy number status. We conducted the histologic review of the *TERT*-altered BCs following the WHO criteria. Estrogen receptor (ER) and HER2 status were retrieved from the medical records.

Results: We identified 118 BCs in 106 patients harboring *TERT* gene amplification (n=76; 64%), promoter mutations (n=41; 35%) or both (n=1; 1%) among 7,582 BCs (1.6%); these included 48 primary BCs (pBCs) and 70 metastatic BCs (mBCs). 81% (34/42) of *TERT* promoter mutations were hotspot mutations (C228T,n=24; C250T, n=10). Most *TERT*-altered pBCs were invasive ductal carcinomas (IDCs; 33/48, 69%), followed by metaplastic (10/48; 21%), pleomorphic lobular (pILC; 3/48; 6%), secretory BCs and mucinous BCs (1/48; 2%, each), and were predominantly of histologic grade 3 (38/48; 79%), and ER-/HER2- (21/48, 47%). *TERT*-altered mBCs encompassed IDCs (54/70; 77%), pILCs (6/70; 9%), metaplastic BCs (4/70; 6%), secretory BCs and apocrine BCs (3/70; 4%, each), and were mostly poorly differentiated (65/70; 93%) and ER+/HER2- (34/70; 49%) or ER-/HER2- (27/70; 39%). *TP53* and *PIK3CA* were the most frequently mutated genes in *TERT*-altered pBCs (65% and 35%) and mBCs (66% and 33%). 5/9 *TERT*-altered mBCs with available sequencing data for their matching pBC harbored a *TERT* gene amplification restricted to the mBC and absent in the paired pBC, including HER2+ (n=3) or ER-/HER2- (n=2) poorly differentiated IDCs.

Conclusions: *TERT* genetic alterations, although rare in breast, do occur outside the realm of fibroepithelial lesions. *TERT*-altered BCs are histologically heterogenous; encompassing mostly IDCs followed by metaplastic BCs, and other special histologic subtypes, such as pILCs, secretory BCs and apocrine BCs, and are enriched for high grade features. The presence of *TERT* gene amplification restricted to the metastasis in patients with paired pBC and mBC analyzed suggests that *TERT* genetic alterations might be late events in the evolution and/or progression of a subset of BCs.

100 Artificial Intelligence Grading of Breast Cancer: A Study of Ensemble Learning

Leslie Dalton, Dalton Pathology, West Lake Hills, TX

Disclosures: Leslie Dalton: None

Background: In artificial intelligence (AI) ensemble learning can improve classification. Differences in the training of models can yield differences in predictions. Combining different models (an ensemble) and finding consensus may offer improvement beyond what any single model might provide. Here, ensemble learning was applied to grading breast cancer.

Design: 7162 representative images were taken of 749 TCGA cancers (digitalslidearchive.org). Four AI models were trained. Differences among models was created by respectively dividing images based on ESR1 mRNA expression, MKI67, Nottingham grade and mitotic score. The images were cropped into 125 by 125 pixel tiles and the tiles were submitted for training. Models were programmed in Python using functions from tensorflow/keras. ResNet101V2 was used as pre-trained model. The four AI models

were given an equal weight vote for the prediction of high grade cells within each tile. An independent patient cohort (Cooperative Human Tissue Network [CHTN]) was used as test set. This n=1082 cohort had a single image from each tissue microarray sample. The TMA samples, and corresponding image, approximated the area of a microscopic high power field. Each CHTN cancer image was cropped into 120 tiles. Since each tile had possible votes from zero to 4, each CHTN cancer had a sum vote ranging from 0-480. The sum vote for each cancer was the measure used for analysis of performance.

Results: In CHTN, a random sample of 1000 tiles for each level of voting underwent pathologist review. By simple examination of tile thumbnails, an experienced pathologist would quickly recognize the trend toward high grade which occurred from 0 to 4 votes. Discordance was present in tiles with 1,2, or 3 votes and were 27% of all tiles. With high Nottingham grade as response variable, sum votes corresponded to AUC= 0.82, and Spearman rho of sum votes with Nottingham score= 0.52. AI high grade corresponded to seven-year survival probability of 63.3% (log rank p< 0.00001), while Nottingham high grade had a nearly identical 63.1%. Nottingham grade was superior to AI in low risk stratification. Nottingham low grade had 89% 7yr survival as compared to 82% with AI low grade. For each CHTN cancer, if among 120 tiles, 10 or more tiles had 4 votes (consensus high grade), 50 of 51 cancers had full tissue section microscopic high mitotic score.

Conclusions: Incorporated into the ensemble method was both gene expression and morphology. By doing so, each model had a different learning "experience." This resulted in 27% discordance among predictions. If the models had consensus in the prediction of high grade, significance in prediction of poor patient outcome was reached. Ensemble learning shows potential to exploit discordance (or absence thereof) into an advantage. In this, the machine equals the human.

101 Non-Lobular Invasive Breast Carcinomas with Oncogenic/Likely Oncogenic Cdh1 Somatic Alterations: An Examination of The Morphologic, Genetic and Immunohistochemical Features.

Fatemeh Derakhshan[1], Arnaud Da Cruz Paula[1], Anne Grabenstetter[1], Pier Selenica[1], Andrea Gazzo[1], Edaise M. da Silva[1], Higinio Dopeso[1], Dara Ross[1], Hannah Wen[1], Edi Brogi[1], Hong (Amy) Zhang[1], Fresia Pareja[1], Britta Weigelt[1], Jorge Reis-Filho[1]
[1]Memorial Sloan Kettering Cancer Center, New York, NY

Disclosures: Fatemeh Derakhshan: None; Arnaud Da Cruz Paula: None; Anne Grabenstetter: None; Pier Selenica: None; Andrea Gazzo: None; Edaise M. da Silva: None; Higinio Dopeso: None; Dara Ross: None; Hannah Wen: *Consultant*, AstraZeneca; *Consultant*, Merck; Edi Brogi: None; Hong (Amy) Zhang: *Consultant*, Roche/Genentech; Fresia Pareja: None; Britta Weigelt: *Advisory Board Member*, Repare Therapeutics; Jorge Reis-Filho: *Consultant*, Paige, Repare Therapeutics; *Advisory Board Member*, Roche Tissue Diagnostic, Grupo Oncoclinicas/ Goldman Sachs

Background: Inactivation of E-cadherin (ECAD), encoded by *CDH1*, is the hallmark of invasive lobular carcinoma (ILC) and accounts for its discohesive phenotype. Rarely, *CDH1* alterations may be found in non-lobular breast carcinomas (NL-BCs). Here, we sought to determine the clinicopathologic characteristics and repertoire of genetic alterations of *CDH1*-mutant NL-BC.

Design: A retrospective analysis of 5,842 breast cancers (BCs), subjected to clinical tumor-normal sequencing with an FDA-cleared multi-gene panel, was conducted to identify BCs with *CDH1* oncogenic/likely oncogenic somatic mutations lacking lobular features. A detailed histopathologic review by three pathologists with an interest in breast pathology was conducted and BCs with lobular features were excluded. ECAD expression was assessed by immunohistochemistry (IHC). The genomic features of *CDH1*-mutated NL-BCs were compared to those of ILCs and invasive ductal carcinomas (IDCs), matched by menopausal status, sample type, histologic type, and grade, and estrogen receptor (ER)/HER2 status at a 1:2 and 1:3 ratio, respectively.

Results: Out of 781 CDH1-altered BCs, 772 were excluded based on the diagnosis of invasive mixed ductal/lobular carcinoma (IMC), ILC, or any histological lobular features upon review. Only 9 of the 5,842 (0.15%) BCs harbored *CDH1*-altered and lacked lobular features. Of these, biallelic *CDH1* inactivation was found in 7 BCs (mutation coupled with loss-of-heterozygosity, n=6; homozygous deletion, n=1), and 2/9 harbored a monoallelic splice-site mutation. The clinicopathologic features are outlined in Table 1. The *CDH1*-altered NL-BCs included mucinous carcinoma (n=1), and IDC with focal neuroendocrine (n=3), micropapillary (n=2), or apocrine (n=3) features. ECAD expression was absent (3/7; 43%), aberrant (3/7; 43%) or membranous (1/7; 14%). *CDH1*-altered NLBC displayed recurrent *TP53* (56%, 5/9), *PIK3CA* (44%, 4/9), *FGFR1* (33%, 3/9), *NCOR1*, *BRCA2* and *RB1* (22%, 2/9, each) genetic alterations. As compared to *CDH1*-wildtype IDC, NL-BCs less frequently harbored *GATA3* mutations (0% vs 37%, p=0.03) but no significant differences detected when compared to matched ILCs.

Table 1: Clinicopathologic features of *CDH1*-altered non-lobular breast carcinomas

*ER-low positive (1-10%)

Clinical Feature		N (%)
Median Age		57 years (39-78)
Cancer Site	Primary	7 (78%)
	Metastatic	2 (22%)
Histologic Grade	I	0 (0%)
	II	4 (44%)
	III	5 (56%)
Hormonal Receptor Status	ER+/HER2-	5 (56%)
	ER+/HER2+	1 (11%)*
	ER-/HER2+	0 (0%)
	ER-/HER2-	3 (33%)

Conclusions: NL-BCs harboring *CDH1* alterations are vanishingly rare (0.15% of invasive BCs), and are predominantly IDC with focal special histologic features. The genomic landscape of these cancers are consistent with those of ER-positive invasive BCs.

102 Atypical Epithelial Proliferations in the Male Breast: Upgrade Rates from Core Needle Biopsy

Lauren Duckworth[1], Raza Hoda[2], Miglena Komforti[2], Gloria Lewis[2], Xiaoyan Cui[2], J. Jordi Rowe[2], Erinn Downs-Kelly[2], Patrick McIntire[2]
[1]Cleveland Clinic Foundation, Cleveland, OH, [2]Cleveland Clinic, Cleveland, OH

Disclosures: Lauren Duckworth: None; Raza Hoda: None; Miglena Komforti: None; Gloria Lewis: None; Xiaoyan Cui: None; J. Jordi Rowe: None; Erinn Downs-Kelly: *Advisory Board Member*, Lilly Oncology; Patrick McIntire: None

Background: Atypical intraductal epithelial lesions of the male breast are rare with a reported incidence of <1%, making these uncommon lesions diagnostically challenging on core needle biopsy specimens (CNB). In the female breast, upgrade rates of atypia on CNB to either invasive or in situ carcinoma on excision range in the literature from 10-30%. However, there are insufficient studies exploring these lesions in male patients.

Design: The anatomic pathology database CoPath Plus™ was searched from 1992-2021 for all cases of male breast biopsies with atypia who subsequently underwent surgical excision. Follow-up data was obtained via the medical record.

Results: A total of 19 cases (n=19) from 19 patients with atypia on CNB were identified. There were 15 atypical papillary lesions (APL) and four cases of atypical ductal hyperplasia (ADH). Review of the subsequent resection diagnoses showed that the overall upgrade rate to carcinoma (in situ or invasive) was 68.4% (13/19) with the APL cases having an upgrade rate of 73% (11/15) and the ADH cases having an upgrade rate of 50% (2/4). In the APL cohort, invasive carcinoma was identified in 53% (8/15) and ductal carcinoma in-situ (DCIS) in 20% (3/15). In the ADH cohort, DCIS was identified in 50% (2/4) with no cases of invasion identified. The remainder of the resections that did not upgrade had variable epithelial proliferations ranging from atypical ductal hyperplasia and atypical papillary lesions that were not further classifiable on resection. Of the upgrades to invasive carcinoma, all were estrogen receptor positive, progesterone receptor positive, and HER2 negative. Morphology was consistent with invasive ductal carcinoma, NOS in 63% (5/8), invasive micropapillary carcinoma in 13% (1/8) and invasive papillary in 13% (1/8) with 4/8 (50%) being Nottingham grade 2 and 2/8 (25%) being Nottingham grade 3. Nottingham grades were not provided for 2 cases and slides were not available. All of the invasive carcinomas were pT1 except the invasive papillary carcinoma, which was pT3. Interestingly, the invasive papillary and micropapillary carcinomas had lymph node metastases at the time of resection (pN1a and pN2, respectively). The invasive papillary carcinoma recurred after 38 months and metastasized to the lung, mediastinum, and bone. Despite adjuvant docetaxel and cyclophosphamide chemotherapy and maintenance tamoxifen therapy. No other cases had lymph node metastases, distant metastases, or locoregional recurrence.

Table 1. Resection Specimens of Atypical Epithelial Proliferations Diagnosed on Core Needle Biopsy

			Upgrade (n=13)	No Upgrade (n=6)
Age (median)			63 years	75.5 years
Ethnicity (self-reported)		White	9	6
		Black	3	0
		Asian	1	0
Laterality		Left	5	5
		Right	8	1
Diagnosis on resection	Benign		0	2
	Atypical		0	4
	In-situ	DCIS	3	0
		Encapsulated Papillary Carcinoma	2	0
	Invasive	Low-grade mucoepidermoid carcinoma	1	0
		IDC with papillary features	5	0
		Invasive papillary carcinoma	1	0
		Invasive micropapillary carcinoma	1	0

DCIS= ductal carcinoma in-situ IDC= invasive ductal carcinoma

Conclusions: Atypical intraductal epithelial lesions of the male breast demonstrated a strikingly high rate of in situ and invasive carcinoma upgrade, particularly compared to that of the female breast. This finding was most significantly observed in papillary lesions wherein an upgrade was seen in 73% of cases.

103 Invasive Carcinomas of the Breast in Men

Lauren Duckworth[1], Raza Hoda[2], Miglena Komforti[2], Gloria Lewis[2], Xiaoyan Cui[2], J. Jordi Rowe[2], Erinn Downs-Kelly[2], Patrick McIntire[2]
[1]Cleveland Clinic Foundation, Cleveland, OH, [2]Cleveland Clinic, Cleveland, OH

Disclosures: Lauren Duckworth: None; Raza Hoda: None; Miglena Komforti: None; Gloria Lewis: None; Xiaoyan Cui: None; J. Jordi Rowe: None; Erinn Downs-Kelly: *Advisory Board Member*, Lilly Oncology; Patrick McIntire: None

Background: Male breast cancer (MBC) is a rare entity accounting for approximately 1% of cancers occurring in men. There is exceedingly limited knowledge surrounding male breast cancer, specifically the various subtypes. Herein we report invasive MBC at our institution with clinicopathologic data and clinical outcomes.

Design: The anatomic pathology database CoPath Plus™ was searched from 1992-2021 for all cases of MBC. Cases of MBC were subclassified as invasive ductal carcinoma (IDC)-NOS, IDC with papillary features, invasive papillary carcinoma, and invasive micropapillary carcinoma. Patient follow-up information was obtained via the medical record.

Results: A total of 104 cases of invasive carcinoma were identified (clinicopathologic variables are listed in Table 1). The vast majority of cases were IDC-NOS with IDC with papillary features being the second most common histologic morphology (13%,14/104). The average tumor size across all types was 19.8 mm; 52% were classified as pT1 and 40% were pT2. Nottingham grade overall was 16% grade 1, 49% grade 2 and 35% grade 3. In total, 52% of cases had lymphovascular invasion (LVI). Most were estrogen receptor (ER) and progesterone receptor (PR) positive at 99% and 92%, respectively; 15% were positive for HER2. There were no cases of invasive papillary carcinoma or microinvasive papillary carcinoma that were positive for HER2. One case of IDC was triple negative. Thirteen cases of had locoregional recurrence (LRR) and 14 cases had distant metastases (DM). Of cases with LRR, 62% (8/13) had LVI and surgical margins were positive in only one case. pT stage in these cases were as follows: 1 pT1a, 1 pT1b, 5 pT1c, 4 pT2, 1 pT3, and the case of pT4a. There was no difference between Notthingham grades or biomarker status between cases of LRR and no LRR. Cases with (DM) were predominantly IDC-NOS. All were at Nottingham grade 2 or 3 and 69% (9/14) had LVI. The case of triple negative IDC-NOS metastasized 21 months after diagnosis despite adjuvant chemoradation; the remainder of the cases were all ER positive, 85% (11/13) PR positive, and (8/12) HER2 negative. The most common sites of metastases were bone (9/14), liver (4/14), lung (4/14), brain (3/14), and skin (2/14).

Table 1. Clinicopathologic Characteristics of Men with Invasive Carcinomas of the Breast

		Invasive Ductal Carcinoma (n=83)	Invasive Ductal Carcinoma with Papillary Features (n=14)	Invasive Papillary Carcinoma (n=4)	Invasive Micropapillary (n=3)
Age (median, years)		38-88 (70.5)	48-90 (73)	52-73 (67)	62-72 (62)
BMI (average)		29.2	30.3	28.1	31.0
Ethnicity (self-reported)	White	63	10	3	3
	Black	15	4	1	0
	Other	5	0	0	0
Resection Type	Lumpectomy	14	3	2	0
	Mastectomy	69	11	2	3
Tumor size (average, mm)		19	20	34.5	20
Pathologic Staging	pT1a	7	1	0	0
	pT1b	5	2	1	1
	pT1c	31	4	1	1
	pT2	33	7	1	1
	pT3	1	0	1	0
	pT4a	1	0	0	0
Nottingham Grade	1	9	2	1	1
	2	41	8	2	0
	3	29	4	1	2
DCIS	Present	43	9	4	2
	Absent	40	5	0	1
Lymphovascular Invasion	Present	45	7	0	2
	Absent	38	7	4	1
Biomarkers	ER	78/79	13/13	4/4	3/3
	PR	71/79	13/13	4/4	3/3
	HER2	11/78	4/13	0/4	0/3
Lymph Node Status	Positive	39	4	1	2
	Negative	40	6	2	1
Locoregional Recurrence		12	0	1	0
Distant Metastases		11	1	1	1
BRCA2 Positive		11	1	0	1
Therapy	Tamoxifen	63	11	4	2
	Adjuvant radiation	20	4	1	1
	Neoadjuvant Chemotherapy	0	1	0	0
	Adjuvant Chemotherapy	21	3	1	1

Conclusions: We identified 104 cases of MBC over a 20-year period. The majority of MBC were IDC-NOS. Those that behaved in an aggressively with LRR or DM had higher rates of LVI. All but one case with LRR was pTc or higher. One case of triple negative MBC was identified and had subsequent DM.

104 Oncotype Dx in Men with Invasive Breast Cancer

Lauren Duckworth[1], Raza Hoda[2], Miglena Komforti[2], Gloria Lewis[2], Xiaoyan Cui[2], Daniel Silbiger[1], J. Jordi Rowe[2], Erinn Downs-Kelly[2], Patrick McIntire[2]
[1]Cleveland Clinic Foundation, Cleveland, OH, [2]Cleveland Clinic, Cleveland, OH

Disclosures: Lauren Duckworth: None; Raza Hoda: None; Miglena Komforti: None; Gloria Lewis: None; Xiaoyan Cui: None; Daniel Silbiger: None; J. Jordi Rowe: None; Erinn Downs-Kelly: *Advisory Board Member*, Lilly Oncology; Patrick McIntire: None

Background: Oncotype DX® recurrence score is based on a panel of 21 genes and predicts the likely benefit of chemotherapy and the risk of distant recurrence in early-stage breast cancer. It is used to guide treatment of women diagnosed with invasive stage I, II, or IIIa, estrogen-receptor positive, and HER2 negative breast cancer; however, due to the rare nature of male breast cancer (MBC), there insufficient data regarding the utility of an Oncotype recurrence score in MBC. By convention, scores < 18 are low risk (LR), 18-30 are intermediate risk (IR), and >31 are high risk (HR).

Design: The anatomic pathology database CoPath Plus™ was searched for all cases of MBC cancer from 1992-2021. Patient Oncotype score and follow up information was obtained via the medical record.

Results: A total of 30 cases from 29 male patients with invasive breast cancer were identified (Table 1). One patient in the HR group had bilateral primary breast cancers. All cases were ER positive and HER2 negative. Oncotype scores ranged from 4 to 43. In the LR group, 6/20 cases had positive lymph nodes at time of resection; 1 had received neoadjuvant chemotherapy, 3 received adjuvant chest wall and axillary radiation, and all received tamoxifen. No patients in the LR group developed locoregional recurrence (LRR) or distant metastases (DM). In the IR group, 4 patients had positive lymph nodes at time of resection; 1 received adjuvant chest wall and axillary radiation, 2 received adjuvant radiation and chemotherapy. All patients in this group received tamoxifen therapy. No patients in the IR group had LRR. One patient, node negative at the time of resection, developed metastatic disease to the skin and contralateral axillary lymph nodes 28 months after initial diagnosis. Interestingly, both patients in the HR group did not receive chemotherapy and were only treated with tamoxifen therapy. Both were node negative at time of resection and have not had LRR or DM.

Table 1. Clinicopathologic Characteristics of Men with Oncotype Scores

		Low risk (n=20)	Intermediate Risk (n=7)	High risk (n=3)
Ethnicity (self-reported)	White	17	4	0
	Black	2	3	2
	Multiracial	1	0	0
	Hispanic	0	0	1
Age (years)		35-85 (median = 67)	58-84 (median = 73)	71-83 (median = 77)
Resection type	Lumpectomy	3	1	0
	Mastectomy	16	6	3
Tumor Size (median, mm)		20	20	15
Pathologic Staging	pT1	13	4	2
	pT2	6	3	1
Nottingham Grade	1	3	1	0
	2	13	2	2
	3	3	4	1
DCIS	Present	11	4	2
	Absent	9	3	1
Lymphovascular Invasion	Present	9	5	1
	Absent	11	2	2
Lymph Node Status	Positive	7	4	0
	Negative	13	3	3
Locoregional Recurrence	Yes	0	0	0
	No	20	7	3
Metastases	Yes	0	1	0
	No	20	6	3
Therapy Received	Aromatase Inhibitor	16	7	3
	Radiation	3	3	0
	Adjuvant Chemotherapy	0	2	0
	Neoadjuvant chemotherapy	1	0	0
Follow Up Months		1-170	5-115	9-75

Conclusions: In this data set, the Oncotype recurrence score cutoffs used in female breast cancer did not appear to be equally applicable to MBC as the only case of metastatic disease was in the IR group. There were no cases in the LR or HR group with LRR or DM. Future studies to clarify the optimal Oncotype cut-off points in MBC should be explored as clinicians work to select those who will truly benefit from chemotherapy.

105 ERG Labeling in Malignant Phyllodes Tumors: A Potential Diagnostic Pitfall

Caroline Early[1], Mira Lotfalla[2], Marissa White[3], Eun Yeong Oh[4], Andres Matoso[5], Pete Argani[6], Ashley Cimino-Mathews[3]
[1]Johns Hopkins University, Baltimore, MD, [2]Johns Hopkins Hospital, Baltimore, MD, [3]Johns Hopkins University School of Medicine, Baltimore, MD, [4]Midatlantic Permanente Medical Group, [5]Johns Hopkins Medical Institutions, Baltimore, MD, [6]Johns Hopkins Hospital, Ellicott City, MD

Disclosures: Caroline Early: None; Mira Lotfalla: None; Marissa White: None; Eun Yeong Oh: None; Andres Matoso: None; Pete Argani: None; Ashley Cimino-Mathews: *Grant or Research Support*, Bristol-Myers Squibb

Background: Malignant phyllodes tumors (MPTs) are rare but aggressive fibroepithelial neoplasms that can be difficult to diagnose due to morphologic and immunophenotypic overlap with other malignant spindle cell neoplasms, including metaplastic carcinoma and sarcoma. Immunohistochemistry (IHC) for CD34 labels vascular neoplasms but is also known to label the lesional stromal myofibroblasts of fibroepithelial neoplasms, including MPTs. We encountered a histologically unequivocal MPT that also

demonstrated IHC labeling with ERG, which is an endothelial cell marker thought to be specific for vascular neoplasms such as angiosarcoma. Here, we investigate IHC labeling for the vascular markers ERG and CD31 in a series of MPTs, which could pose a potential diagnostic pitfall.

Design: IHC for ERG, CD31, and CD34 was performed on 19 histologically unequivocal MPTs. IHC was performed on full-face sections for 4 (21%) cases (3 resections and 1 core biopsy). The remaining 15 (79%) cases were evaluated on a previously constructed tissue microarray (TMA), containing five 1.4 mm cores per tumor. The IHC markers were performed either at the time of original diagnosis or as a part of this study.

Results: IHC labeling for ERG was observed in the neoplastic stromal cells in 3 (16%) of 19 malignant phyllodes tumors (Figure 1). The ERG labeling was strong and diffuse in 1 case, strong and focal in 1 case, and weak and focal in 1 case. All 3 cases with ERG labeling were those evaluated on full-face sections. CD34 labeling was observed in 10 (56%) of 18 evaluable MPTs. One MPT displayed labeling for both ERG and CD34. CD31 labeling was not observed in any MPTs. None of the MPTs displayed any morphologic evidence of vascular differentiation.

Figure 1 - 105

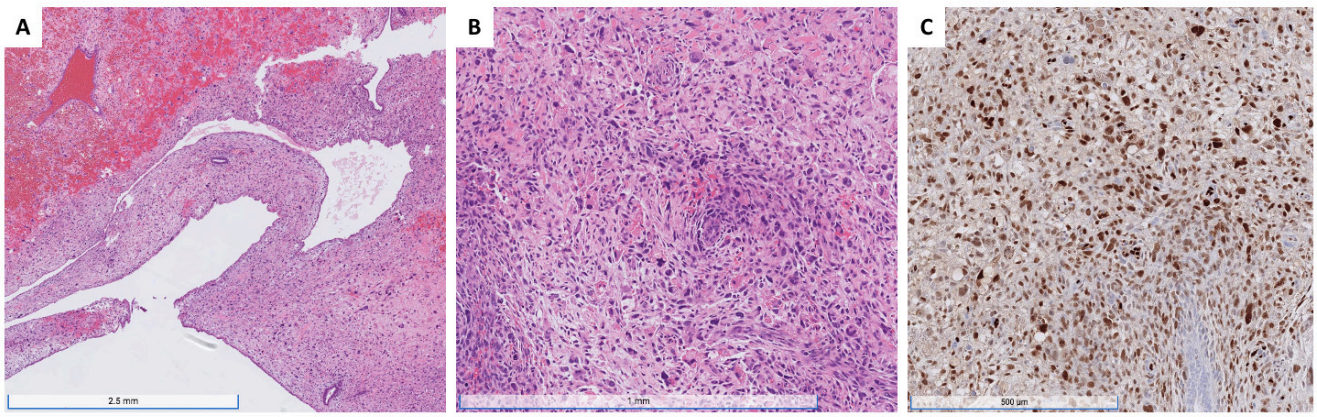

Figure 1: ERG Expression in Malignant Phyllodes Tumors (MPTs). Low power view of a MPT reveals the focal leaf-like architecture helpful for making the diagnosis of MPT (A, H&E). High power view reveals markedly atypical stromal cells on H&E (B) which demonstrate strong, diffuse ERG labeling on IHC (C).

Conclusions: ERG labeling by IHC is seen in a small but notable subset of MPTs, which poses a diagnostic pitfall for a vascular neoplasm. The potential diagnostic pitfall is further pronounced in MPTs with dual ERG and CD34 labeling. The absence of CD31 labeling, as well as lack of histologic evidence of vascular differentiation, underscores the non-specificity of ERG labeling in MPTs. The presence of ERG labeling only in tumors evaluated on full-face sections raises the possibility of false negative results on the tumors evaluated on the TMA, and the rate of ERG positivity may be even higher.

106 Giant Juvenile Fibroadenomas including a Cohort of Lesions with Prominent Pseudoangiomatous Stromal Hyperplasia (PASH): Clinicopathological and Molecular Characteristics

Ayesha Farooq[1], Andrii Puzyrenko[2], Jason Jarzembowski[2], Aye Aye Thike[3], Nur Diyana Md Nasir[3], Cedric Ng[4], Jing Yi Lee[5], Jessica Sook Ting Kok[5], Abner Lim[4], Bin Tean Teh[5], Puay Hoon Tan[3], Julie Jorns[2]

[1]Mayo Clinic, Rochester, MN, [2]Medical College of Wisconsin, Milwaukee, WI, [3]Singapore General Hospital, Singapore, Singapore, [4]Cancer Discovery Hub, National Cancer Center Singapore, Singapore, Singapore, [5]National Cancer Centre Singapore, Singapore, Singapore

Disclosures: Ayesha Farooq: None; Andrii Puzyrenko: None; Jason Jarzembowski: *Grant or Research Support*, Merck, Co.; Aye Aye Thike: None; Nur Diyana Md Nasir: None; Cedric Ng: None; Jing Yi Lee: None; Jessica Sook Ting Kok: None; Abner Lim: None; Bin Tean Teh: None; Puay Hoon Tan: None; Julie Jorns: None

Background: Juvenile fibroadenomas are fibroepithelial lesions (FEL) with stromal and epithelial hypercellularity usually occurring in adolescent females. Giant juvenile fibroadenomas (GJFA) are defined as >5 cm or >500 g and some, like other FEL, exhibit

prominent pseudoangiomatous stromal hyperplasia (PASH). We sought to determine clinicopathological and molecular characteristics of GJFA with and without PASH.

Design: Archives were searched for GJFA. Clinical information was collected via chart review. All cases were reviewed and stained for CD34, progesterone receptor (PR), androgen receptor (AR) and β-catenin. Cases were sequenced using a custom panel of 16 genes – *MED12* (exons 1 and 2), *TERT* promoter (-124C>T and -146C>T), *SETD2*, *KMT2D*, *RARA* (exons 5-9), *FLNA*, *NF1*, *PIK3CA* (exons 10, 11, and 21), *EGFR*, *RB1*, *BCOR*, *TP53*, *PTEN*, *ERBB4*, *IGF1R*, and *MAP3K1*.

Results: 27 GJFA from 21 female patients were found from 1985-2020. Mean age was 13.7 years (range 10.1-25.2). Tumors were from bilateral breasts with no site predominance. Tumor size was up to 21 cm. Six patients had later benign breast disease and two had multiple, bilateral, and later recurrent GJFA.

13 (48%) cases showed prominent PASH. All cases were positive for stromal CD34 and negative for stromal AR, β-catenin and PR. 17 cases (63%), including those from all patients with prominent PASH, showed heterogeneity in CD34 staining owing to regions with abundant loose collagen matrix deposition (Figure 1).

Five cases were not sequenced as the sample failed QC. *MAP3K1* mutations were found in all 22 remaining samples, with *SETD2*, *KMT2D*, *TP53* and *BCOR* aberrations in 18 (82%), 16 (73%), 16 (73%) and 16 (73%) cases respectively, while other alterations were less common. Tumors with PASH had a significantly higher prevalence of *SETD2* (p=0.014) and *TP53* (p=0.029) mutations, while those with absence of PASH had more *RB1* mutations (p=0.043) (Table 1). Cases with multiple synchronous lesions showed similar alterations in all samples.

Table 1. Mutation frequencies for the panel of 16 genes in 22 giant juvenile fibroadenomas.

Gene	No. mutated	Giant juvenile fibroadenomas with PASH (n=12)	Giant juvenile fibroadenomas without PASH (n=10)	p-value
MED12	1 (5%)	0 (0%)	1 (10%)	0.284
TERT (P)	4 (18%)	3 (25%)	1 (10%)	0.388
KMT2D	16 (73%)	10 (83%)	6 (60%)	0.241
RARA	3 (14%)	1 (8%)	2 (20%)	0.451
FLNA	9 (41%)	6 (50%)	3 (30%)	0.366
SETD2	18 (82%)	12 (100%)	6 (60%)	0.014*
TP53	16 (73%)	11 (92%)	5 (50%)	0.029*
RB1	3 (14%)	0 (0%)	3 (30%)	0.043*
NF1	3 (14%)	2 (17%)	1 (10%)	0.668
PTEN	1 (5%)	1 (8%)	0 (0%)	0.374
PIK3CA	1 (5%)	0 (0%)	1 (10%)	0.284
EGFR	9 (41%)	5 (42%)	4 (40%)	0.941
BCOR	16 (73%)	10 (83%)	6 (60%)	0.241
ERBB4	1 (5%)	1 (8%)	0 (0%)	0.374
MAP3K1	22 (100%)	12 (100%)	10 (100%)	N/A
IGF1R	3 (14%)	1 (8%)	2 (20%)	0.451

*Statistically significant with $p < 0.05$.

Figure 1 - 106

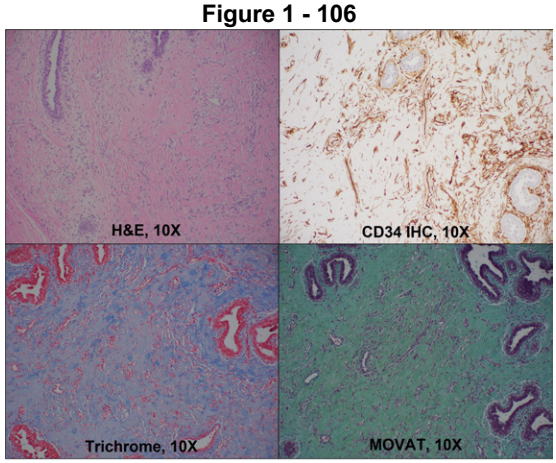

Conclusions: GJFA commonly have *MAP3K1, SETD2*, *KMT2D*, *TP53* and *BCOR* mutations. Tumors with PASH have a significantly higher prevalence of *SETD2* and *TP53* mutations, while those with an absence of PASH have more *RB1* mutations. Low prevalence of *MED12* mutations among GJFA is not surprising as this has been previously reported in JFA. Gene mutations along more advanced phases of the proposed FEL pathogenetic pathway is unusual and may suggest a different mechanism of growth in these tumors.

107 Characterization of Residual TN and HER2 Breast Carcinomas after Neoadjuvant Therapy

Pedro Fernandez[1], Paula Rodríguez-Martínez[2], Mireia Margelí[3], Carolina Sanz[2], Ana M Muñoz-Mármol[1], Aintzane Urbizu[2], Vanesa Quiroga[2], Ana Castillo Gandía[2], Beatriz Cirauqui[4], Iris Teruel[2], Eva Castella[5], Eudald Felip[2], Cecilia Perelló Fabregat[6], Laura Pons[7], Laura Hernández León[2]
[1]Hospital Germans Trias i Pujol, Universidad Autónoma de Barcelona, Barcelona, Spain, [2]Hospital Germans Trias i Pujol, Badalona, Spain, [3]Hospital Germans Trias i Pujol, Bardalona, Spain, [4]Catalan Institute of Oncology (ICO), Badalona, Spain, [5]Hospital Germans Trias i Pujol, Fundació IGTiP, Spain, [6]Hospital Universitari Germans Trias i Pujol, Badalona, Spain, [7]Institute for Health Science Research Germans Trias i Pujol (IGTP), Badalona, Spain

Disclosures: Pedro Fernandez: None; Paula Rodríguez-Martínez: None; Mireia Margelí: None; Carolina Sanz: None; Ana M Muñoz-Mármol: None; Aintzane Urbizu: None; Vanesa Quiroga: None; Ana Castillo Gandía: None; Beatriz Cirauqui: *Speaker*, BMS; *Consultant*, BMS; *Grant or Research Support*, MSD; *Grant or Research Support*, BMS; Iris Teruel: None; Eva Castella: None; Eudald Felip: None; Cecilia Perelló Fabregat: None; Laura Pons: None; Laura Hernández León: None

Background: Neoadjuvant chemotherapy (NAC) is the standard treatment for HER2-positive (HER2+) and triple negative (TN) breast cancer, reaching higher rates of pathological complete response (pCR) than previous treatments. Little is known about the tumor's subclones that survive the NAC. Here, we compare these surviving tumors with their pretreatment counterpart in order to obtain insight on the nature of the NAC resistant cells.

Design: A total of 125 patients diagnosed with HER2+ and TN infiltrative breast cancer who received NAC were recruited from the pathology files of Hospital Germans Trias i Pujol. The surrogate molecular subtype, histological grade, percentage of TILS and Ki67 quantification were compared between pre-treatment biopsies and post-treatment specimens with no pCR.

Results: For HER2+ tumors, pCR was achieved in 44 cases (61.1%) and for TN tumors, pCR was found in 37 cases (69.8%). Thus, we compared the 28 HER2+ and 16 TN residual tumors with their pretreatment sample. Ki67 evaluation showed a decrease in the residual tumor for both subtypes (pre-treated-HER2 $\bar{x}$=34 and treated-HER2 $\bar{x}$=20; pre- treated-TN $\bar{x}$=60,1 and treated-TN $\bar{x}$=20,7). The majority of the HER2 residual tumors showed a lower percentage of TILS than the initial. Interestingly, the vast majority of TN surviving tumor foci had the same or an increased percentage of TILS. We found the same histological grade in the majority of the tumors (HER2+ n=17 (60.7%); TN n=12 (75%)). All TN tumors maintained the same subtype, whereas 7 HER2+ cases (25%) changed their initial surrogate molecular subtype, being the change HR+/HER2+ to HR+/HER2- the most frequent.

Conclusions: Residual HER2+ and TN tumors have a lower residual proliferation Ki67 than pretreatment and this could be explained by a better response to NAC by more proliferative subclones. Inflammatory stromal infiltrate in HER2+ tumors mostly decreased, maybe due to anti-HER2 treatment eliminating more immunogenic tumor cells, suggesting that the residual tumor cells might attract less immune response. On the contrary, this immune response mostly increased or remained the same in TN tumors, perhaps due to its inherent immunogenic nature combined with a less specific NAC. Although the majority of the HER2+ tumors and all of the TN tumors maintained their surrogate subtype, a change in the HER2 subtype can be explained by the anti-HER2 focused treatment.

108 EZH2 Expression and Response to Neoadjuvant Endocrine Therapy in Estrogen Receptor Positive Invasive Breast Cancer

Susan Fineberg[1], Yujun Gan[1]
[1]Montefiore Medical Center, Bronx, NY

Disclosures: Susan Fineberg: *Consultant*, AXDEV CORP; Yujun Gan: None

Background: Neoadjuvant endocrine therapy (NET) is used to treat estrogen receptor (ER) positive invasive breast cancer (IBC). Tumors with Ki67 >10% after 2-4 weeks of NET are considered resistant to endocrine therapy (ET). Although high baseline

Ki67 >30% is associated with higher level of ET resistance, many of these patients will still respond to NET. During the COVID-19 pandemic NET is increasingly being used to defer surgery, hence better and more easily accessible biomarkers are needed to predict likelihood of response to NET. EZH2 is a oncoprotein which can be easily evaluated by immunohistochemistry and overexpression of EZH2 in ER+ IBC has been linked to resistance to ET. We examined the potential utility of EZH2 to predict response to NET .

Design: We identified 34 pts with ER+ IBC of ductal or lobular type who received NET. Ki67 IHC was evaluated on pretherapy biopsies and post-therapy resections and scored according to guidelines of the International Ki67 Working Group with a global weighted score. We quantified EZH2 nuclear expression in pretherapy biopsies using a score which multiplied intensity (0=negative,1=weak,2=moderate,3=strong) by % of cells staining at each intensity X100 . Ki67 post therapy <=10% was considered endocrine responsive. Pretherapy Ki67 was dichotomized into >30% and <=30%.

Results: The pt age range was 48 to 85 yrs (mean 64 yrs and median 65 yrs). All IBCs had ER expression levels >=80% and aromatase inhibitor was the most frequent NET (76%). Duration of NET ranged from 2-24 months (median 6 months and mean 6.5 months). Twenty pts had a pretherapy Ki67 < or =30 % and 14 had a pretherapy Ki67 >30%. Amongst the 20 pts with pretherapy Ki67<=30%, 11 were endocrine responsive and had a mean pretherapy EZH2 of 88 and median of 85 (range 2-150) whereas 9 were resistant with a median pretherapy EZH2 of 108 and a median of 104 (range 42-130). There was no significant difference in mean EZH2 score between groups (t test p=.0.3971). Amongst the 14 pts with pretherapy Ki67>30% 5 were endocrine responsive and had a mean pretherapy EZH2 of 91 and median EZH2 of 93 (range 45-130) whereas 9 were resistant and had a mean pretherapy EZH2 of 186 and median of 178 (range 120-240) There was a significant difference in mean EZH2 score between groups (t test p=.0006). There was a significant association between pretherapy EZH2 score >130 and resistance to NET in pts with Ki67>30% pretherapy (p=.0030).

EZH2 Expression Levels and Response to NET in 14 Patients with KI67>30% Pretherapy

	EZH2>130	EZH2<=130	
Endocrine Responsive(Post NET Ki67<=10%)	0	5	
Endocrine Resistant (Post NET Ki67>10%)	8	1	p=.0030

Conclusions: In our pilot study EZH2 protein expression levels were significantly associated with response to NET in pts with high risk (Ki67>30%) ER+ IBC ; high EZH2 expression (>130) in IDC in pretherapy core biopsies was associated with resistance to NET in these pts. During the Covid-19 Pandemic , or in other situations where surgery might be deferred, our results suggest that EZH2 might be useful to predict tumor response to NET in high risk (Ki67>30%) ER+ IBC.

109 Recurrent ACTB Mutation in Tubular Adenomas of the Breast Detected with Whole Exome Sequencing

Guofeng (George) Gao[1], Aihui Wang[1], Grace Allard[2], Zhicheng Ma[3], Chieh-Yu Lin[4], Gregor Krings[5], Gregory Bean[3]
[1]Stanford University School of Medicine, Stanford, CA, [2]Feinberg School of Medicine/Northwestern University, Chicago, IL, [3]Stanford Medicine/Stanford University, Stanford, CA, [4]Washington University School of Medicine, St. Louis, MO, [5]University of California, San Francisco, San Francisco, CA

Disclosures: Guofeng (George) Gao: None; Aihui Wang: None; Grace Allard: None; Zhicheng Ma: None; Chieh-Yu Lin: *Consultant*, Natera; Gregor Krings: None; Gregory Bean: *Grant or Research Support*, Philips

Background: Tubular adenoma of the breast (TA) is an uncommon benign neoplasm composed of densely packed round tubular epithelial structures with little intervening stroma forming a well-circumscribed mass. TA shows overlapping clinicopathologic and imaging features with fibroadenoma (FA), and the two may be related, with TA sometimes considered a FA variant. However, the pathogenesis and association with FA remains uncertain, with conflicting reports in the literature of *MED12* alterations detected in TA.

Design: 21 cases of breast tubular adenoma were collected from three institutions. Clinical and pathologic data were obtained from electronic medical records. DNA extraction and whole exome sequencing (WES) was performed on 10 cases, with matched normal tissue sequenced from 4 patients. WES results from the remaining cases are pending. Laser capture microdissection is also being performed on select cases to segregate epithelial and stromal components and identify the neoplastic population.

Results: All patients were women; the average age was 30 years old (range 15-54). Median tumor size was 1.6 cm (range 0.8-6.5 cm). TAs arose in all four quadrants of the breast. The majority of cases presented as a palpable mass (70%, 14/20 with available history); a minority was identified on screening mammography (15%, 3/20), incidentally on breast imaging performed for another purpose (10%, 2/20), or within reduction mammoplasty (5%, 1/20). Three patients reported an association with pregnancy/lactation, and two patients noted size variation with their menstrual cycle. One patient had two ipsilateral tumors, and another had two contralateral tumors. Excision was performed in most cases (86%, 18/21). WES identified recurrent missense mutations within the beta-actin (*ACTB*) gene in 6/10 cases, specifically at the c.C283 position in exon 3, resulting in p.R95C (TAs 1 & 8), p.R95L (TA 2), p.R95H (TAs 3 & 4), and p.R95G (TA 5) alterations. No *MED12* exon 2 mutations were detected.

Conclusions: TA is a benign neoplasm with uncertain etiology. A recurrent specific alteration in *ACTB* suggests a pathogenesis distinct from fibroepithelial lesions, as beta-actin mutations have not been reported in WES studies of fibroadenoma and phyllodes tumor.

110 Lobular Neoplasia Involving Intraductal Papilloma Diagnosed on Core Needle Biopsy: Clinicopathologic Features and Upgrade Rates at Excision

Akisha Glasgow[1], Kristen Coffey[1], Edi Brogi[1], Maria Kuba[1]
[1]Memorial Sloan Kettering Cancer Center, New York, NY

Disclosures: Akisha Glasgow: None; Kristen Coffey: None; Edi Brogi: None; Maria Kuba: None

Background: Patients (pts) with intraductal papillomas (IP) of the breast without atypia diagnosed on core needle biopsy (CNB) may be spared excision (EXC) in certain clinical scenarios (i.e. radiologic-pathologic concordant). A similar strategy has been used in pts diagnosed with lobular neoplasia (LN), namely atypical lobular hyperplasia (ALH) and classic lobular carcinoma in situ (LCIS). Evaluation of upgrade rates of IP involved by LN are limited to a few cases in the literature. Our aim was to review the clinicopathologic features and upgrade rate at EXC of LN involving or adjacent to IP diagnosed on CNB.

Design: We searched our pathology database for all in-house CNBs obtained between 1/2000 to 6/2021 with a diagnosis of “ALH” or “LCIS”, and “papilloma”. CNBs with radial scar, ADH, ductal carcinoma in situ (DCIS) and/or invasive carcinoma (IC) were excluded. Pts with ipsilateral breast cancer (BC) but with IP regarded as a separate radiologic lesion were included. Upgrade was defined as (micro)invasive carcinoma or DCIS at EXC. A radiologist reviewed all pertinent imaging studies. The IRB approved the study.

Results: The cohort consisted of 51 cases from 50 women (median age: 60 years, range: 37-76 years); 8 patients had a history of BC. Thirteen CNBs showed LN involving IP. On imaging, 8 patients presented with a mass, 4 with calcifications, and 1 with non-mass enhancement (NME) on MRI. All cases were radiologic-pathologic concordant. Six IPs were excised and none were upgraded. Thirty-eight CNBs showed LN adjacent but not involving the IP; 24 were excised. One case was associated with IC and DCIS. This was a 44 year-old woman with a palpable lesion which on MRI corresponded to a 4 cm area of NME; CNB showed DCIS. A separate area of NME was seen 1.5 cm from the index lesion; CNB showed IP and adjacent LN. The mastectomy had a 0.4 cm well differentiated invasive ductal carcinoma and extensive DCIS, which was extending 0.2 cm from the biopsy site of the IP. There was no residual IP. None of the remaining cases were upgraded. The median follow-up was 48 months (range 2-243 months). One pt developed an ipsilateral IC in a different quadrant from the IP with LN 36 months later.

Conclusions: We found no upgrades at EXC of IP involved by LN. Although our sample size is small, these findings support a non-surgical management of these lesions, if radiologic-pathologic concordant, similar to that of IP and ALH/LCIS diagnosed on CNB.

111 Clinical Significance of Stromal Tumor-Infiltrating Lymphocytes in Triple Negative Breast Cancer

Kanika Goel[1], Gloria Carter[2], Beth Clark[3], Jeffrey Fine[4], Jing Yu[4], Lakshmi Harinath[3], Tatiana Villatoro[2], Rohit Bhargava[3]
[1]Magee-Womens Hospital, University of Pittsburgh Medical Center, Pittsburgh, PA, [2]University of Pittsburgh Medical Center, Pittsburgh, PA, [3]UPMC Magee-Womens Hospital, Pittsburgh, PA, [4]University of Pittsburgh, Pittsburgh, PA

Disclosures: Kanika Goel: None; Gloria Carter: None; Beth Clark: None; Jeffrey Fine: *Stock Ownership*, SpIntellx, Inc.; Jing Yu: None; Lakshmi Harinath: None; Tatiana Villatoro: None; Rohit Bhargava: None

Background: Triple negative breast cancer (TNBC) has an aggressive phenotype with poor clinical outcome compared with other breast cancer subtypes. However, TNBC is a heterogeneous group and efforts are ongoing to identify potential clinical-pathologic prognostic and predictive biomarkers. With the advent of immune checkpoint blockade as an effective anticancer strategy, there is growing interest to study the immune profile of TNBCs, and determine if stromal tumor infiltrating lymphocytes (sTILs) level can be implemented in routine clinical practice to refine prognosis and guide treatment decisions.

Design: We examined the impact of multiple clinical-pathologic variables on prognosis in a well characterized cohort of 139 consecutive TNBCs that were not selected for neoadjuvant chemotherapy (NACT). Recurrence-free survival (RFS) and breast cancer-specific survival (BCSS) were evaluated for individual variables in the overall cohort (detailed results reported in separate abstract). Herein we report RFS and BCSS with respect to increasing levels of sTILs, correlation of sTILs with PD-L1 (clone SP142) % immune cells (IC), and clinical-pathologic features of tumors with prominent sTILs.

Results: Improved recurrence free survival (RFS) was significantly associated with older age, lack of lymphovascular invasion (LVI), lower pT stage, lower AJCC stage, and androgen receptor (AR) positivity, but surprisingly not with sTILs. Improved BCSS was significantly associated with lack of LVI, lower pT stage, lower AJCC stage (detailed results reported in separate abstract).

PD-L1 positivity (%IC >1) was seen in 40% cases. sTILs showed positive linear correlation with PD-L1 % IC (Pearson correlation 0.496, p-value: <0.001, 95% CI: 0.360-0.612). All cases with sTILs greater than 40% were positive for PD-L1 (table 1). Increasing levels of sTILS (analyzed in 10% increments) were not significant for RFS (figure 1) or BCSS, likely due to small case numbers in each group. However, none of the 10 cases with sTILs greater than 60% (lymphocyte predominant TNBC or LP-TNBC) recurred and all were alive with a median follow up of 82 months. Median age of patients with LP-TNBC was 54 years (range 30-64 years), 7 (70%) tumors were stage I and 3 (30%) were stage II, nine (90%) tumors were grade 3, 90% were AR-negative, 90% had Ki-67 proliferation index of 50% or more, and at least 4 (40%) tumors showed medullary features (figure 2). All but one received adjuvant chemotherapy.

sTILs category	N (Column Percent)	PD-L1 positive / total (%)
1 to 10%	46 (33%)	2/46 (4%)
11-20%	36 (26%)	13/36 (33%)
21-30%	22 (16%)	11/22 (50%)
31-40%	13 (9%)	8/13 (62%)
41-50%	6 (4.5%)	6/6 (100%)
51-60%	6 (4.5%)	6/6 (100%)
61-70%	3 (2%)	3/3 (100%)
71-80%	7 (5%)	7/7 (100%)
Total	139 (100%)	55/139 (40%)

Figure 1 - 111

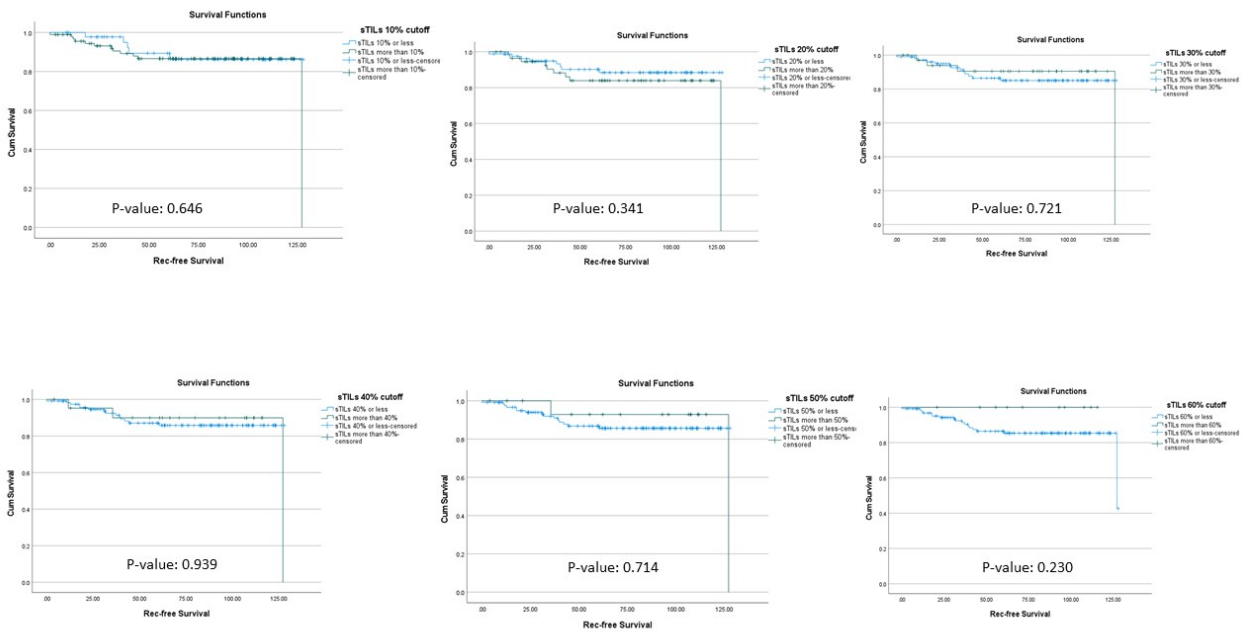

Figure 2 – 111

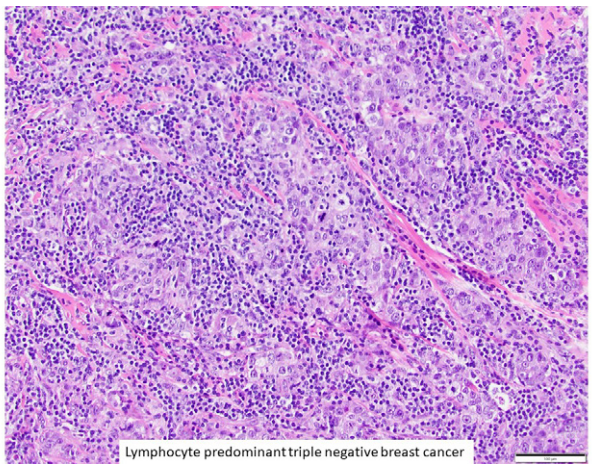

Conclusions: PD-L1 % IC shows linear correlation with sTILs. Neither PD-L1 nor sTILs levels were significantly associated with survival (RFS, BCSS) in this cohort of patients not subjected to NACT; however, LP-TNBC seems to have good prognosis. Approximately one-half of LP-TNBC showed medullary histology. Subsequent investigations are warranted to determine whether systemic adjuvant therapy can be de-escalated in the LP-TNBC patients.

112 Triple Negative Breast Cancers Not Subjected to Neoadjuvant Chemotherapy: What's Prognostic and What's Not?

Kanika Goel[1], Gloria Carter[2], Beth Clark[3], Jeffrey Fine[4], Jing Yu[4], Lakshmi Harinath[3], Tatiana Villatoro[2], Rohit Bhargava[3]
[1]Magee-Womens Hospital, University of Pittsburgh Medical Center, Pittsburgh, PA, [2]University of Pittsburgh Medical Center, Pittsburgh, PA, [3]UPMC Magee-Womens Hospital, Pittsburgh, PA, [4]University of Pittsburgh, Pittsburgh, PA

Disclosures: Kanika Goel: None; Gloria Carter: None; Beth Clark: None; Jeffrey Fine: *Stock Ownership*, SpIntellx, Inc.; Jing Yu: None; Lakshmi Harinath: None; Tatiana Villatoro: None; Rohit Bhargava: None

Background: Molecular classification of triple negative breast cancer (TNBC) has identified distinct subtypes with different gene expression profiles and response to neoadjuvant chemotherapy (NACT) but failed to show differences in recurrence free survival (RFS) between molecular subtypes. TNBCs are heterogeneous and differences in histology, proliferation, molecular features, host immune response, and anatomic stage are all likely responsible for an individual patient outcome and multiple variables may be difficult to capture based on gene expression profiling alone.

Design: We examined the impact of multiple clinical-pathologic variables in a well characterized cohort of 139 consecutive TNBCs that were not selected for neoadjuvant chemotherapy. Tumors were evaluated for androgen receptor (AR). RFS and breast cancer specific survival (BCSS) were evaluated with respect to each variable via Kaplan-Meier (KM) method. Multivariable analysis was also performed. AR positive tumors were compared with AR-negative tumors to identify clinically significant associations.

Results: With a median follow-up of 79.8 months, the RFS was 87.7%, and BCSS of 93.5%. Improved RFS was significantly associated with older age (>60 years), lack of lymphovascular invasion, lower pT stage, lower AJCC stage, and AR positivity. Multiple other clinical-pathologic variables including stromal tumor infiltrating lymphocytes (sTILs), PD-L1 expression (clone SP142-percent immune cells), Ki-67 proliferation index were not significant. On multivariable analysis, only AR positivity showed trend for improved RFS (p-value: 0.066, HR: 6.867, 95% CI: 0.880-53.593). Improved BCSS was associated with lack of lymphovascular invasion, lower pT stage, and lower AJCC stage but not with AR positivity. None of the variables were significant on multivariable analysis. There were distinct differences between AR+ and AR-negative tumors (table 1).

Table 1: AR+ versus AR-negative triple negative breast cancers.			
Variables	AR Negative (n=85)	AR Positive (n=54)	P-value
Age in years Mean Median Range	58 60 27-91	66 65 30-100	0.001*
Histology Apocrine Metaplastic No special type Others	5 (6%) 9 (11%) 68 (80%) 3 (3%)	19 (35%) 1 (2%) 33 (61%) 1 (2%)	<0.001*
Grade I II III	1 (1%) 9 (11%) 75 (88%)	2 (4%) 17 (31%) 35 (65%)	0.004 *
Tumor size in cm Mean Median Range	2 1.7 0.5-8	2 1.6 0.5-10.5	0.979
Lymphovascular inv. No Yes	69 (81%) 16 (19%)	44 (82%) 10 (18%)	1.0
Lymph node status Negative Positive	70 (82%) 15 (18%)	43 (80%) 11 (20%)	0.824
Stage I II III	49 (58%) 30 (35%) 6 (7%)	36 (67%) 14 (30%) 4 (7%)	0.507
Ki-67 index 30% or less 31% to 50% More than 50%	5 (6%) 10 (12%) 70 (82%)	20 (37%) 6 (11%) 28 (52%)	<0.001*
sTILs 10% or less >10% to <50% 50% or more	27 (32%) 41 (48%) 17 (20%)	19 (35%) 30 (56%) 5 (9%)	0.238
PD-L1 Negative Positive	50 (59%) 35 (41%)	34 (63%) 20 (37%)	0.723
Chemotherapy No Yes Unknown	9 (11%) 75 (89%) 1	15 (28%) 38 (72%) 1	0.011*
*Statistically significant. One stage IV patient included with stage III. Apocrine tumors included both pure apocrine carcinomas and carcinomas with some degree of apocrine differentiation.			

Figure 1 - 112

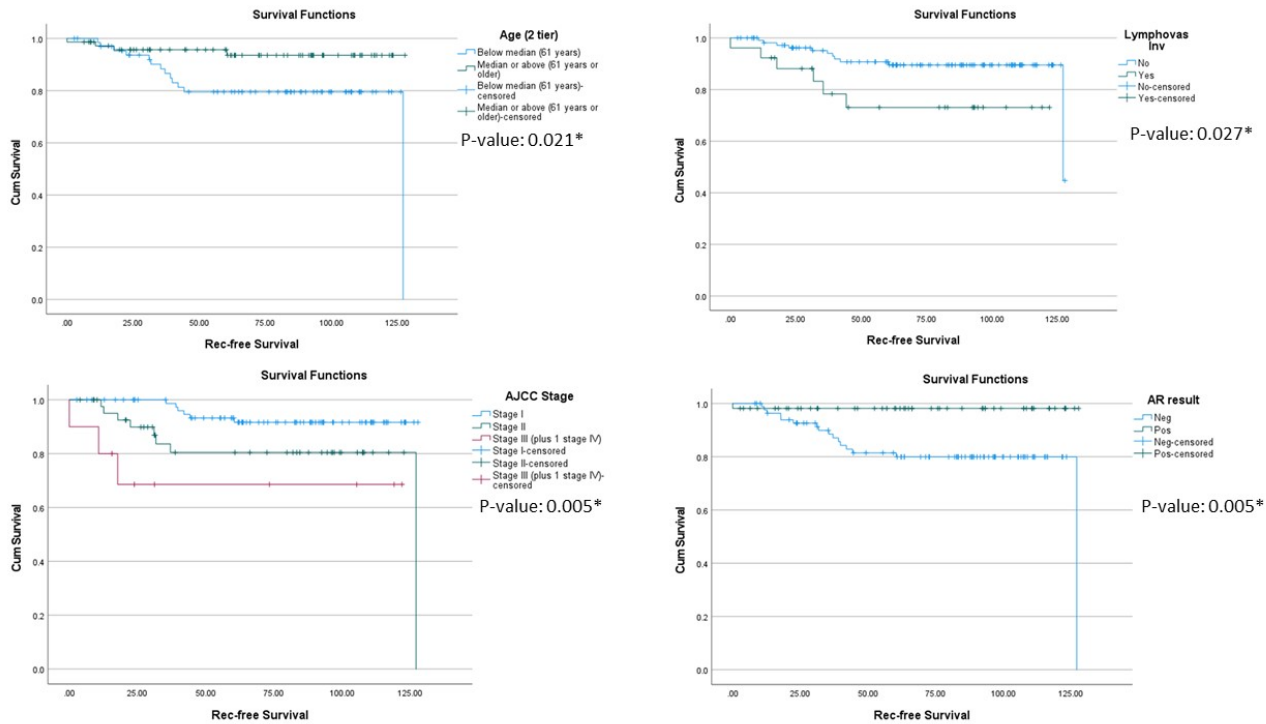

Figure 2 – 112

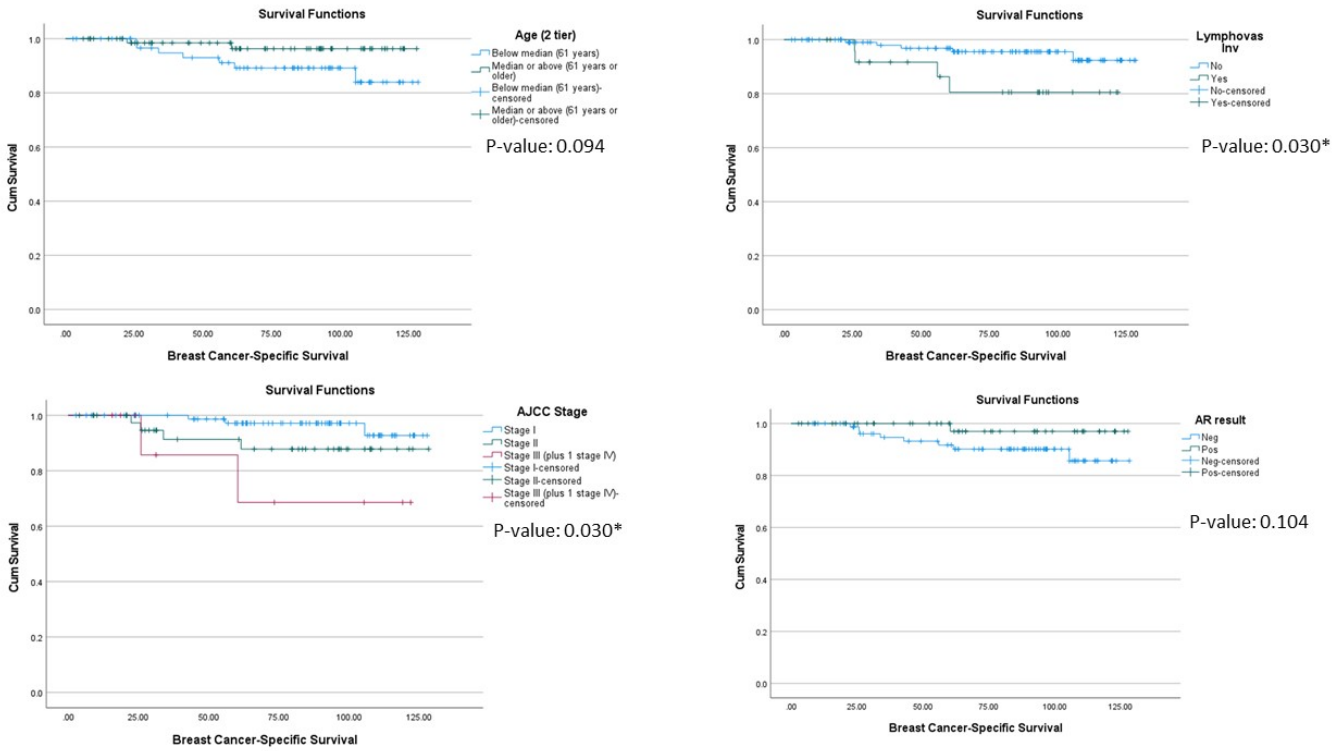

Conclusions: High proportion of AR+ TNBC in our cohort suggests that many of these low-grade/low-proliferation TNBCs are not subjected to NACT. Although AR positivity in TNBC is associated with apocrine differentiation, it can also be seen in tumors without apocrine differentiation. AR positivity and not tumor histology was associated with improved RFS. Histologic typing of TNBC supplemented by AR immunohistochemistry provides useful prognostic information. This information along with tumor stage can be used to de-escalate chemotherapy use in AR+ low-stage, low-proliferation TNBCs.

113 Primary and Secondary Breast Lymphoma: Retrospective Case Series Review of a Single Institution

Mikhail Gorbounov[1], Diana Treaba[2], Evgeny Yakirevich[3], Yihong Wang[1]
[1]Brown University, Rhode Island Hospital, Providence, RI, [2]Brown University Lifespan Academic Medical Center, Providence, RI, [3]Rhode Island Hospital, Providence, RI

Disclosures: Mikhail Gorbounov: None; Diana Treaba: None; Evgeny Yakirevich: None; Yihong Wang: None

Background: Breast lymphoma (BL) is a rare hematologic neoplasm commonly presenting as a mass forming lesion. Primary breast lymphoma (PBL) involves the breast tissue in the absence of extramammary lymphoma and/or widespread disease. Secondary breast lymphoma (SBL) is a relatively common metastasis to the breast (17% of metastatic disease to the breast). The aim of this study is to determine the histological types and features of the lymphomas involving the breast and compare the clinical and pathological differences between PBL and SBL.

Design: BL cases were retrospectively reviewed at our institution from the past 20 years and included 42 needle biopsies and 5 excisional biopsies. Clinical and histological characteristics were analyzed.

Results: Forty-four of the 47 patients (93.6%) were females with mean age of 74 years old (Table 1). Twenty-one (44.6%) cases fulfilled the criteria for PBL, whereas 26 (55.3%) were SBL with either known systemic disease or disease found within months of breast diagnosis. Interestingly, 12 of the 26 (46%) SBL cases were first diagnosed on breast biopsy. No significant age difference was seen in primary vs secondary BLs. The BL mass size average was 2.5cm for PBL and 1.9cm for SBL, respectively. Sixteen (76%) of the PBLs were stage I (breast only), 2 (9.5%) were stage II (breast and axillary lymph node involvement), and 3 (14%) were stage I (breast only) but had a previously diagnosed different type of lymphoma. The most common PBLs were DLBCL

(Diffuse Large B-cell Lymphoma) and MZL (Marginal Zone Lymphoma) (Table 1). FL (Follicular Lymphoma) and SLL (Small Lymphocytic Lymphoma) were more frequently seen when systemic disease involved the breast, with a larger number of high-grade FL cases also seen in the SBL category. A rare B-lymphoblastic leukemia/lymphoma involved the breast at relapse.

Parameter	Primary Breast Lymphoma (PBL)[7]		Secondary Breast Lymphoma (SBL)[8]		Both Groups Combined	
Age (range)	75.7 (58-91)		72.4 (22-94)		73.9 (22-94)	
Female (%)	90.4		96.1		93.6	
Mass Size (range)	2.47 (0.6-5.2)		1.85 (0.4-5.65)		2.13 (0.4-5.65)	
Diagnosis	Count	% of total	Count	% of total	Count	% of total
MZL[1]	7	33.3	6	23.1	13	27.7
FL Low Grade[2]	4	19.0	6	23.1	10	21.3
FL High Grade[3]	1	4.8	3	11.5	4	8.5
CLL/SLL[4]	0	0.0	3	11.5	3	6.4
B-cell Lymphoma, NOS[5]	2	9.5	4	15.4	6	12.8
B-Lymphoblastic Leukemia/Lymphoma	0	0.0	1	3.8	1	2.1
DLBCL, NOS[6]	7	33.3	3	11.5	10	21.3
Total	21	100.0	26	100.0	47	100.0

1. Marginal Zone Lymphoma or with marginal features.

2. Follicular Lymphoma grade 1-2.

3. Follicular Lymphoma grade 3a and 3b.

4. Chronic Lymphocytic Lymphoma/Small Lymphocytic Lymphoma.

5. B-cell Lymphoma, Not Otherwise Specified.

6. Diffuse Large B-cell Lymphoma.

7. PBL (Primary Breast Lymphoma) De novo primary lymphoma in breast +/- involvement of ipsilateral axillary nodes and de novo lymphoma in breast with different lymphoma previously outside of breast.

8. SBL (Secondary Breast Lymphoma) Lymphoma identified in breast in known diffuse disease or diffuse disease found within months of breast biopsy diagnostic pathology.

Conclusions: Of interest, our series identified only B-cell lymphomas involving the breast. Among the B-cell lymphomas, both indolent and aggressive lymphomas were identified with the notable exception of mantle cell lymphoma. MZL and DLBCL were the most common PBLs, while MZL and FL were the most common SBLs. Due to national mammographic screening, increased secondary BLs (46%) were first diagnosed on breast biopsy.

114 Pathologic Measurements Compared with Contrast-Enhanced Mammography Measurements of Invasive Breast Carcinoma

Yaileen Guzman-Arocho[1], Yukun Gao[1], Ted James[1], Jordana Phillips[1], Liza Quintana[1]
[1]Beth Israel Deaconess Medical Center, Boston, MA

Disclosures: Yaileen Guzman-Arocho: None; Yukun Gao: None; Ted James: None; Jordana Phillips: *Grant or Research Support*, GE Healthcare; *Consultant*, Hologic; Liza Quintana: None

Background: The stage of breast cancer has implications for prognosis and management. Contrast-enhanced mammography (CEM) has been associated with greater accuracy measuring breast tumors when compared to other imaging modalities. Here we seek to identify the differences in pathologic versus radiologic measurements by CEM and how these differences may impact tumor staging of invasive breast cancer.

Design: The pathologic measurements of resected invasive breast carcinoma were recorded (microscopic measurement in 44, macroscopic measurement in 13). Two breast radiologists evaluated the size of the tumors by CEM; the average measurement was used for analysis. The staging was assigned according to the eighth edition of the AJCC Cancer Staging Manual (T1 ≤20mm [T1a >1 but ≤5 mm, T1b >5 but ≤10 mm, T1c >10 but ≤ 20 mm], T2 >20 mm but ≤50 mm, T3 >50 mm, and T4 for any size with direct extension to the chest wall and/or to the skin).

Results: A consecutive series of 57 carcinomas that had CEM and underwent surgical excision were included (45 partial mastectomies, 12 mastectomies). The tumors were grade 1 in 19.3% (11), grade 2 in 59.6% (34), and grade 3 in 21.1% (12). Most of the cases were of ductal (47.4%, n=27) or ductal and lobular (35.1%, n=20) histologic subtype. Other subtypes: lobular (8.8%,

n=5), micropapillary (3.5%, n=2), tubular (1.8%, n=1), metaplastic (1.8%, n=1), and mucinous (1.8%, n=1). Significant differences in the measurements by pathology and CEM were observed (Figure 1). Differences in measurements between the pathology and CEM led to differences in staging in 21 (36.8%) cases, causing upstage by CEM in 18 (85.7%) (Figure 2). The tumor characteristics of the cases with differences in staging based on measurement by pathology are shown in Table 1.

Table 1. Characteristics of tumors with differences in staging based on measurement by pathology vs CEM

	N =21 (%)
Grade	
1	5 (23.8%)
2	12 (57.1%)
3	4 (19.0%)
Histologic type	
Ductal	10 (47.6%)
Ductal and lobular	9 (42.9%)
Lobular	1 (4.8%)
Mucinous	1 (4.8%)
Ductal carcinoma in situ	
Yes	17 (81.0%)
No	4 (19.0%)
Extensive intraductal component	
Yes	5 (23.8%)
No	16 (76.2)
Estrogen Receptor	
Positive	18 (85.7%)
Negative	3 (14.3%)
Progesterone Receptor	
Positive	17 (81.0%)
Negative	4 (19.0%)
HER2	
Positive	3 14.3%)
Negative	18 (85.7%)

Figure 1 - 114

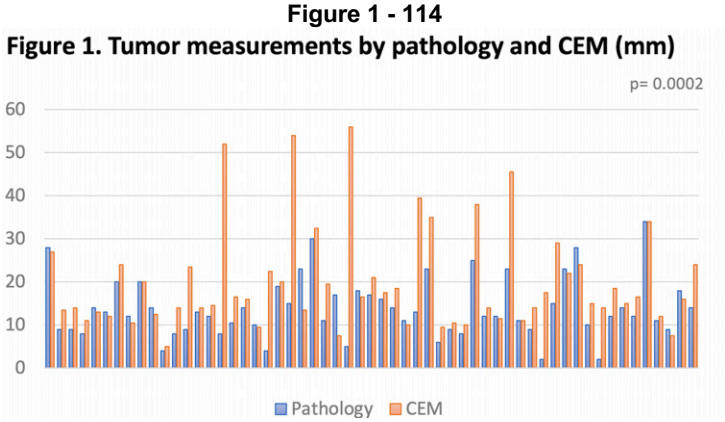

Figure 2 - 114

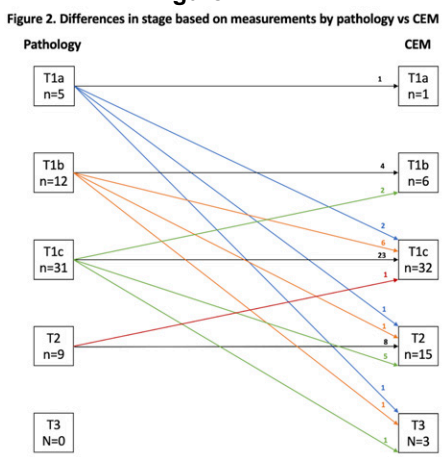

Conclusions: Measurements of invasive breast carcinoma by CEM tend to be larger than the pathologic measurements leading to higher pre-surgical staging and potential changes in clinical decisions. These findings may have clinical implications for the pre-operative assessment using CEM. Further studies are planned to evaluate the specific impact on surgical care.

115 Applied Machine Learning Based on Superpixels and the Tumoral Microenvironment is a Significant Predictor of Neoadjuvant Response in Triple Negative Breast Cancer

Sean Hacking[1], Ayesha Siddique[1], Kamaljeet Singh[2], Ross Taliano[3], Evgeny Yakirevich[4], Yihong Wang[3]
[1]Alpert Medical School of Brown University, Providence, RI, [2]Women and Infants Hospital, Providence, RI, [3]Brown University, Rhode Island Hospital, Providence, RI, [4]Rhode Island Hospital, Providence, RI

Disclosures: Sean Hacking: None; Ayesha Siddique: None; Kamaljeet Singh: None; Ross Taliano: None; Evgeny Yakirevich: None; Yihong Wang: None

Background: Applying applications in machine learning (ML) to the tumoral microenvironment is the next great challenge in pathology. Computational approaches have been developed to quantify and spatially analyze immune cells, proportionate stroma, and detect tumor budding; however, little work has been done to analyze different types of tumor associated stromata both quantitatively and computationally in relation to clinical outcomes.

Design: QuPath (version 0.2) was adopted as an open access source for ML based applications and superpixel image segmentation (SIS) and a random forest (RF) ML based classifier was trained from annotated patches of the tumoral microenvironment on whole slide images (FIG 1). This included segments of myxoid stroma (blue), collagenous stroma (pink), tumor cells (red) and immune cells (purple). Theoretical formulations were developed to calculate myxoid stromal percentage (MSP), myxoid stromal ratio (MSR), collagenous stroma percentage (CSP), proportionated stromal area (PSA), and immune cell percentage (ICP). The predictive value of the computational biomarkers was assessed in relation to neoadjuvant chemotherapy and pathologic response.

Results: The present study evaluated 67 triple negative breast cancer patients with clinical pathological findings represented in Table 1. T test found low CSP (P = 0.02) and low PSA (P = 0.035) to be associated with pathological complete response (pCR) after neoadjuvant treatment. Receiver operator curves (ROC) found high myxoid stromal ratio with an area under the curve of 0.71; 0.586-0.833, P = 0.004 (FIG 2(a)). Low collagenous stromal percentage with an area under the curve of 0.707; CI: 0.580-0.833, P= 0.004 (FIG 2(b)). The following computational biomarkers trended but were not found to be significantly associated with pCR but trended towards significance: low proportionated stroma area with an area under the curve of 0.599; CI: 0.460 – 0.739, P = 0.168 (FIG 2(c)) and high immune cell percentages with an area under the curve of 0.615; CI: 0.480-0.750, P = 0.111 (FIG 2(d)).

Biomarker (Means)	Frequency	MSP	P	CSP	P	MSR	P	PSA	P	ICP	P
Age			0.470		0.177		0.302		0.491		0.147
<45	15 (22%)	28.65		19.56		2.78		2.00		4.58	
>45	52 (78%)	28.33		23.58		3.89		1.90		4.26	
Nodal status			0.439		0.59				0.192		0.197
N0	49 (73%)	12.75		25.61		1.86	0.126	2.10		4.85	
N1-2	18 (27%)	16.36		19.98		5.27		1.69		5.76	
Tumor stage			0.176			0.296			0.278		0.255
I-II	50 (75%)	27.42			4.13			1.96		5.51	
III-IV	17 (25%)	31.28			2.22			1.69		4.79	
Neoadjuvant response			0.299		**0.02**		0.060		**0.035**		0.099
No	39 (58%)	12.94		27.2		1.63		2.22		4.75	
Yes	28 (42%)	16.90		16.3		6.45		1.42		6.13	

Figure 1 - 115

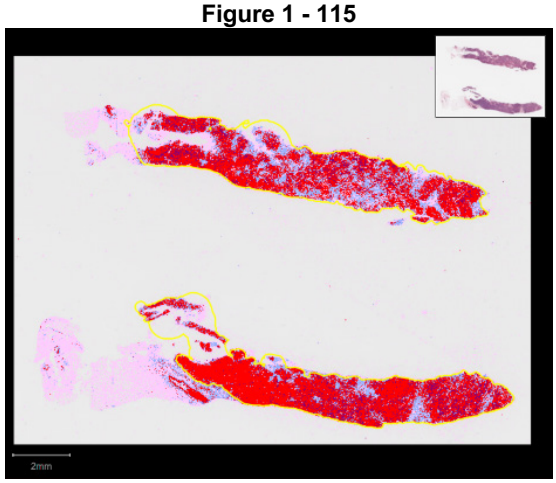

Figure 2 – 115

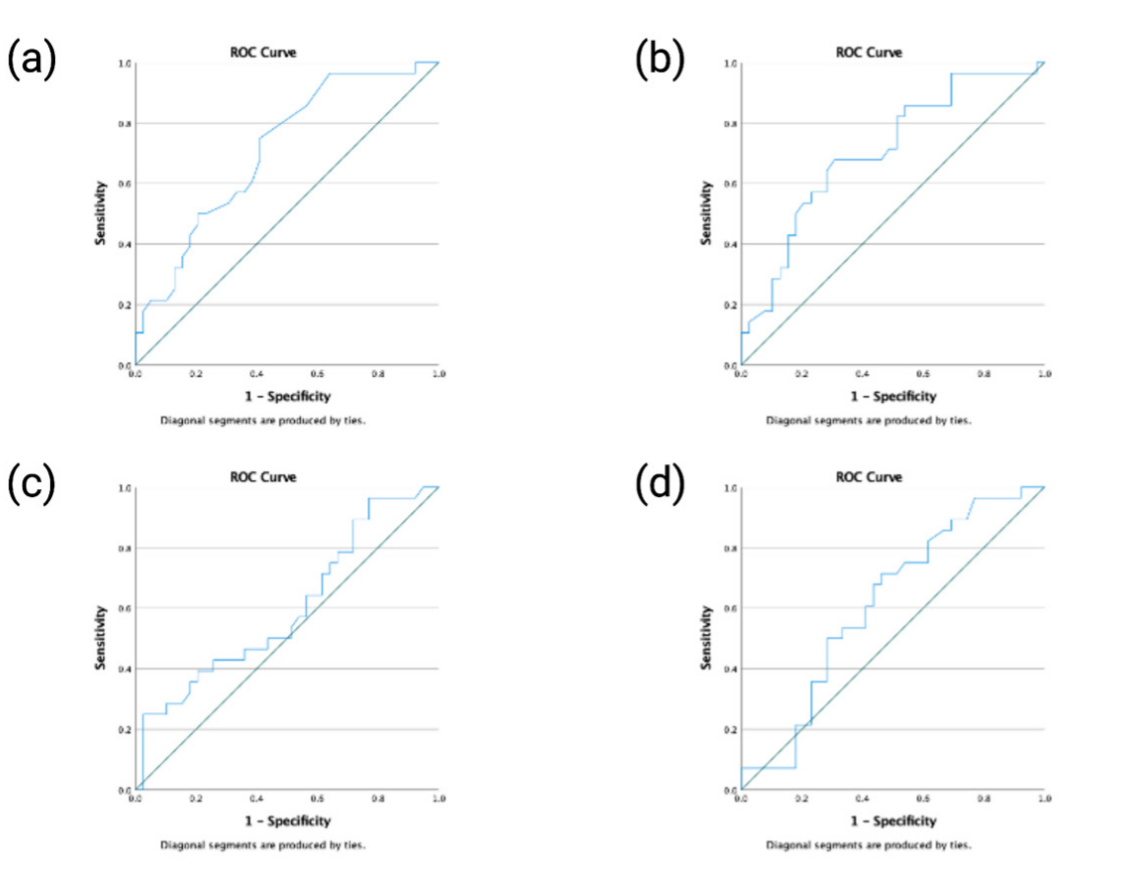

Conclusions: Paradigms in breast cancer are shifting from the tumor to the surrounding tumoral microenvironment and from qualitative to quantitative methods. The techniques demonstrated in this body of work can be performed easily by a surgical pathologist with appropriate quality assurance. Future trials are needed to determine whether ML can improve breast cancer patient outcomes in a true clinical environment.

116 Machine Learning as an Answer to the Mass-Forming DCIS Conundrum: A Pilot Study

Sean Hacking[1], Shaza Ben Khadra[1], Ayesha Siddique[1], Kamaljeet Singh[2], Ross Taliano[3], Evgeny Yakirevich[4], Yihong Wang[3]

[1]Alpert Medical School of Brown University, Providence, RI, [2]Women and Infants Hospital, Providence, RI, [3]Brown University, Rhode Island Hospital, Providence, RI, [4]Rhode Island Hospital, Providence, RI

Disclosures: Sean Hacking: None; Shaza Ben Khadra: None; Ayesha Siddique: None; Kamaljeet Singh: None; Ross Taliano: None; Evgeny Yakirevich: None; Yihong Wang: None

Background: Mass-forming ductal carcinoma in situ (DCIS) detected on core needle biopsy (CNB) is often thought to represent missed invasive carcinoma, although isolated DCIS is often reported. As of now, there is no way to definitively prove which patients diagnosed by biopsy will upgrade to invasive carcinoma following definitive cancer resection. This study applied machine learning (ML) to investigate a series of mass-forming DCIS to assess the tumoral microenvironment and correlated with the outcomes.

Design: CNB specimens were retrieved from the archives from patients with ultrasound guided CNB for mass-forming DCIS. Twenty cases with excision results were included in this study. QuPath (version 0.2) was utilized in this study, an open access solution to ML for whole slide images (WSI). The analysis was based on superpixels, and a random forest (RF) decision tree-based ML classifier was trained from annotated patches of the tumoral microenvironment to identify myxoid stroma, collagenous stroma and DCIS tumor cells. Annotated areas of DCIS were then identified from WSIs (FIG 1).

Results: 44 patients with mass-forming DCIS were retrieved and 20 were found to have invasive carcinoma following definitive excision. The results for receiver operator curves (ROC) for computational biomarkers in relation to upgrade to invasive carcinoma from DCIS are as follows. High myxoid stromal ratio with an area under the curve of 0.923; 0.835-1.000, P = 0.000 (FIG 2a). Low collagenous stroma percentage with an area under the curve of 0.875; CI: 0.762-0.988, P= 0.000 (FIG 2b). High DCIS proportionated area with an area under the curve of 0.681; CI: 0.519-0.844, P = 0.040 (FIG 2c). Low proportionated stromal area with an area under the curve of 0.682; CI: 0.520 – 0.844, P = 0.039 (FIG 2d).

Figure 1 - 116

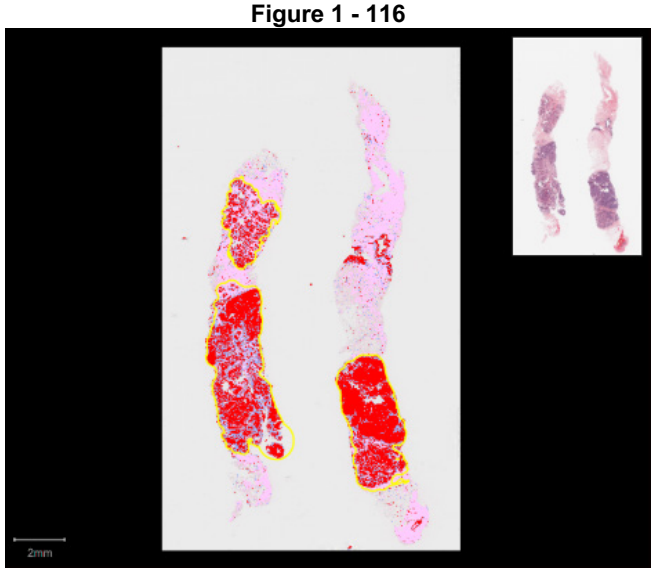

Figure 2 – 116

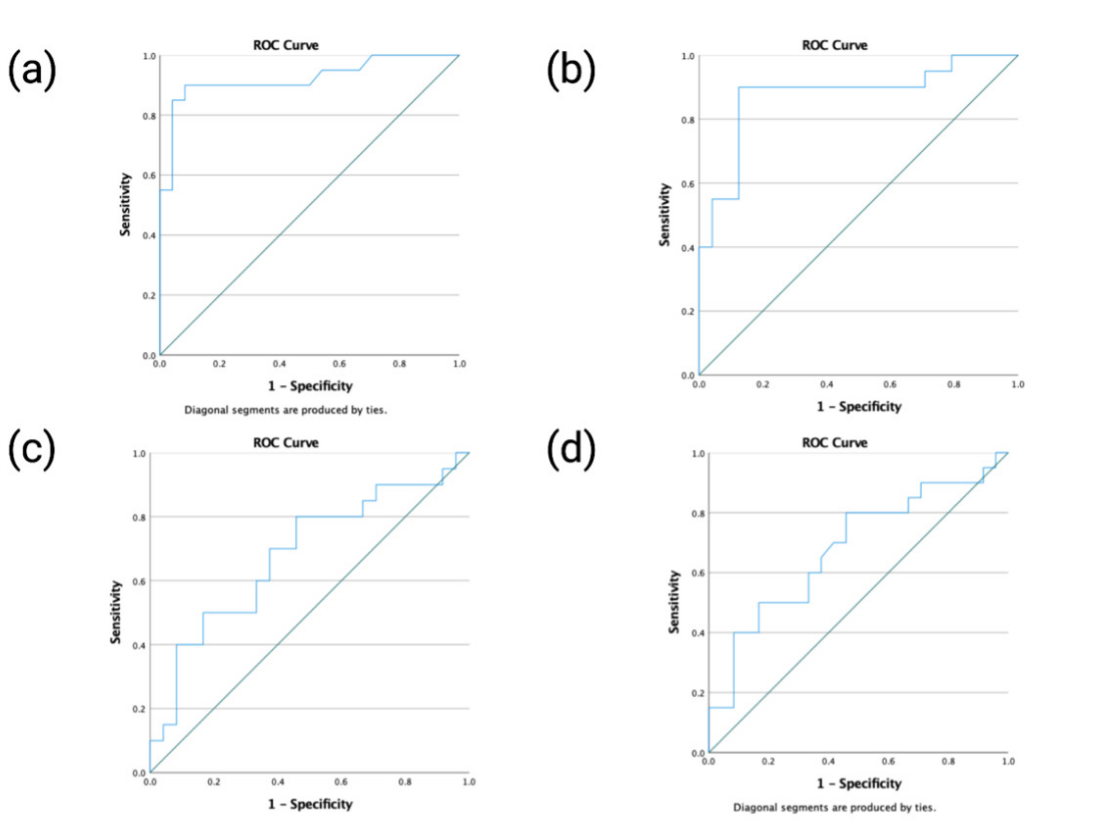

Conclusions: The use of ML in mass-forming DCIS can determine which patients will be upgraded to invasive carcinoma with high sensitivity and specificity. The findings in this study have the potential to change management for patients with mass-forming DCIS on biopsy which can be diagnosed as invasive carcinoma by ML. Larger scale studies on ML in mass-forming DCIS are now needed, although the results from this study suggest the use of ML to be promising.

117 Histologic Patterns of Response after Neoadjuvant Chemotherapy for Breast Cancer: Association with Tumor Phenotypes and Impact on Tumor Size and Pathologic Staging

Dawn Harter[1], Siobhan O'Connor[2], Johann Hertel[1], Benjamin Calhoun[1]
[1]The University of North Carolina at Chapel Hill, Chapel Hill, NC, [2]University of North Carolina School of Medicine, Chapel Hill

Disclosures: Dawn Harter: None; Siobhan O'Connor: None; Johann Hertel: None; Benjamin Calhoun: *Advisory Board Member*, Luminex Corp.

Background: In the 8th Edition of the American Joint Committee on Cancer Staging System (yAJCC), residual tumor size after neoadjuvant chemotherapy (NAC) for invasive breast cancer is based on the largest contiguous focus of tumor cells, excluding treatment-related fibrosis. The goal of this study was to assess the association of histologic patterns of response with tumor phenotypes and estimates of residual tumor size for yAJCC staging.

Design: Breast surgical specimens after NAC from 2016-2020 were identified in the Anatomic Pathology laboratory information system. Cases that were Stage IV, pT4b, pT4d, pCR, neoadjuvant endocrine therapy alone and no response to NAC were excluded from further analysis. Residual tumor size and ypT category were reassessed using current yAJCC criteria. Histologic patterns of response in the breast were categorized as concentric or scattered based on Pastorello et al. Mod Pathol 2021. Review of the breast slides is complete and assessment of the ypN category is ongoing. A median of 30 slides per case were reviewed (range, 9-113).

Results: A total of 188 cases met inclusion criteria with analyzable residual disease, including 56 (30%) TNBCs, 50 (27%) HER2+ and 82 (44%) hormone receptor-positive/HER2-negative (HR+/HER2-). A scattered pattern of response was seen in 36% of TNBC, 66% of HER2+, and 55% of HR+ (p=0.006). The reassessed tumor size and ypT category differed from the original report in 112 (60%) and 106 (56%) cases, respectively (all smaller/lower on review). The 106 cases with lower ypT categories included 39% of TNBCs, 64% of HER2+ and 63% of HR+/HER2- (p=0.009). Residual tumors with a scattered pattern of response accounted for 83/106 (78%) with lower ypT categories. Of the 106 cases with lower ypT categories, the larger size in the original report was based on the gross description in 68 (64%). There were 20 invasive lobular carcinomas (ILC) that included 6 (30%) with no response, 9 (45%) with a scattered pattern and 5 (25%) with a concentric pattern.

Conclusions: Closely following yAJCC criteria resulted smaller size estimates for residual tumor in the breast and lower ypT categories. Tumors with a scattered pattern of response accounted for >75% of cases with lower ypT categories. HR+ and HER2+ tumors were more likely to have a scattered pattern of response than TNBC. Breast cancer phenotypes and histologic patterns of response to NAC may significantly impact post-NAC pathologic staging using the 8th Edition of the AJCC.

118 Clinicopathologic Features and Response to Neoadjuvant Chemotherapy in Metaplastic Breast Carcinoma: A Single Institution Experience

Sherin Hashem[1], Luan Nguyen[2], Farnaz Hasteh[1], Oluwole Fadare[3], Somaye Zare[1]
[1]University of California, San Diego, La Jolla, CA, [2]CellNetix Pathology and Laboratories, Everett, WA, [3]UC San Diego School of Medicine, La Jolla, CA

Disclosures: Sherin Hashem: None; Luan Nguyen: None; Farnaz Hasteh: None; Oluwole Fadare: None; Somaye Zare: None

Background: Metaplastic breast carcinomas (MBC) are rare and aggressive tumors that account for 0.2–1% of all invasive breast cancers (IBC) and are associated with poor outcome. While neoadjuvant chemotherapy (NAC) is an established part of clinical management of many IBC, due to rarity of MBC there is limited data about response to NAC in these tumors. In the current study, we review the clinicopathologic features of MBC treated at our institution and assess their response to NAC.

Design: All the cases of MBC treated at our institution from 2004-2021 were identified. Clinicopathologic characteristics, treatment regimen, and follow up data were reviewed. Treatment responses were evaluated on the excisional specimens using the MD Anderson residual cancer burden (RCB) classification for cases that received NAC and various clinicopathologic variables effect on response to treatment were analyzed.

Results: A total of 98 patients with MBC, with median age of 54.9 were identified. Most patients (53%) had pT2 disease at the time of first presentation and axillary node involvement was detected in 22.4% of patients. 84% of the tumors had a histologic grade of 3 and 87% were triple negative. With an average follow-up of 37 months, 38 patients (38.7%) recurred and 24 patients deceased (24.5%).

49 patients (50%) patients received NAC, of whom 5 (10.2%) achieved pathologic complete response (pCR), 4 (8.1%) RCB-I, 20 (40.8%) RCB-II, and 20 (40.8%) RCB-III. Of these 49 cases, 21 tumors (42.8%) had an associated invasive ductal carcinoma component. Histologic subtypes of MBC included squamous (38.7%), heterologous mesenchymal differentiation-including matrix producing type (30.6%), spindled (16.3%), and mixed and NOS types (16.3%).

Of the 9 cases with substantial response to treatment (pCR and RCB-I), 5 were of mesenchymal differentiation-matrix producing type (2 pCR, 3 RCB-1), 2 were squamous (2 RCB-1) and 2 were spindle cell carcinoma (2 pCR). Matrix-producing histology was associated with better response to treatment (pCR and RCB-1, p= .0473). Other clinicopathologic features did not show significant association with response to treatment.

Conclusions: In the current study, rate of pCR in MBC was 10.2%, and only 18.3% of the patients showed a substantial response to NAC (pCR or RCB-1). In our cohort, patients with Matrix-producing morphology showed better response to treatment. MBC are aggressive and relatively chemorefractory tumors. Response to NAC may vary in different histologic subtypes.

119 Outcome of Non-Invasive Lobular Neoplasia (LN) in Breast Core Needle Biopsies (CNB): A Single Institutional Experience

Elham Hatami[1], Farnaz Hasteh[2], Oluwole Fadare[3], Somaye Zare[2]
[1]University of California, San Diego, San Diego, CA, [2]University of California, San Diego, La Jolla, CA, [3]UC San Diego School of Medicine, La Jolla, CA

Disclosures: Elham Hatami: None; Farnaz Hasteh: None; Oluwole Fadare: None; Somaye Zare: None

Background: The term LN encompasses atypical lobular hyperplasia (ALH) and lobular carcinoma in situ (LCIS). The management of LN diagnosed on CNB has been controversial due to the wide range of reported upgrade rates to carcinoma. We reviewed our experience with cases of LN on CNB to identify the rate and potential risk factors of upgrade to carcinoma in the excision.

Design: Cases of LN diagnosed on CNB between 2010 and 2021 that underwent excision in our institute were identified. All cases were subject to radiological-pathological correlation. Patients with invasive carcinoma (IC), ductal carcinoma in situ (DCIS), or atypical ductal hyperplasia in CNB of the ipsilateral breast were excluded. Upgrade was defined as IC or DCIS upon excision. The clinical, histologic, and imaging features were recorded.

Results: Our study cohort consisted of 87 patients, with mean age of 53.9 yrs (31-77). The imaging findings included 45 calcifications, 24 masses, 10 non-mass enhancements, 8 asymmetry/other abnormalities. CNB diagnoses included 44 ALH, 38 classic LCIS (cLCIS) and 5 pleomorphic LCIS (pLCIS). 25 (29%) patients had a history of contralateral breast cancer (BC).

9 cases were upgraded on excision (6 IC, 3 DCIS), of which the initial CNB showed ALH in 4, pLCIS in 3, and cLCIS in 2. Among the 6 IC, 5 were invasive lobular carcinoma, 1 was of mixed ductal and lobular histotype, and all were stage 1 (4 pT1a and 2 pT1b). 3 of 5 (60%) CNB with pLCIS were associated with IC on the excision.

pLCIS in CNB was significantly associated with upgrade to carcinoma (p=.0001). The patients with carcinoma on the resection were older than the group without upgrade [mean age 61 vs 53.1 (p=.030)] and more likely to have a history of contralateral BC (p=.032). Other clinical and radiologic parameters did not show a significant risk for upgrade (table 1).

	Upgraded to carcinoma	No upgrade	P value
Number	9	78	
Age mean (range)	61 (37-76)	53.1 (31-77)	0.030
Core Needle biopsy findings			
ALH	4	40	Non-significant
Classic LCIS	2	36	Non-significant
Pleomorphic LCIS	3	2	0.0001
History of breast cancer	5	20	0.032
Imaging findings			Non-significant
Calcification	6	39	
Mass lesion	2	22	
Non-mass enhancement (MRI)	1	9	
Asymmetry, cyst, other lesions	0	8	
BIRAD score			Non-significant
<4	1	13	
4	8	75	

Conclusions: Our data showed an overall upgrade rate of 10.3% in LN that was significantly associated with pLCIS variant, older age, and history of contralateral BC. Among the patients with ALH and cLCIS, 6.9% upgraded to carcinoma, of which 66% had a history of contralateral BC. Only 2.5% of the patients with ADH/cLCIS and without a history of BC upgraded on excision. In our study, CNB with pLCIS had a significant risk of IC (60%) on excision. Our findings showed a low rate of upgrade for ADH/cLCIS in patients with concordant radiology-pathology findings and without a history of BC, supporting a non-surgical management and follow-up in this group of patients.

120 Prognostic Impact of Endocrine Treatment on Survival Outcome of Invasive Breast Cancers with Low Estrogen Receptor Expression

Elham Hatami[1], Farnaz Hasteh[2], Oluwole Fadare[3], Somaye Zare[2]
[1]University of California, San Diego, San Diego, CA, [2]University of California, San Diego, La Jolla, CA, [3]UC San Diego School of Medicine, La Jolla, CA

Disclosures: Elham Hatami: None; Farnaz Hasteh: None; Oluwole Fadare: None; Somaye Zare: None

Background: The 2020 American Society of Clinical Oncology/College of American Pathologists (ASCO/CAP) guideline classifies invasive breast carcinomas (IBC) with 1-10% nuclear positivity for estrogen receptor (ER) as “low ER positive” and recommends a comment regarding the limited data on the benefit of endocrine treatment (ET) in these patients. In the current study, we reviewed our experience with low ER+/Her2- cases and compared their survival outcome to high ER+ (>10%)/Her2- and triple negative cancers (TNC).

Design: All cases of low ER+ IBC from 2014-2017 were identified. After excluding Her2+ cancers, 34 patients were included in the study. All the clinicopathologic characteristics, treatment data, and outcomes were recorded and analyzed. Survival outcomes were compared to 2 control groups from TNC and high ER+/Her2- cohort with similar age, stage, and follow up period. Disease-free survival (DFS) and overall survival (OS) were estimated by the Kaplan-Meier method and compared among groups by log-rank test.

Results: Our study cohort consisted of 34 patients with Low ER+/Her2- IBC, with mean age of 57 yrs (30-91). Of these patients, 7 (20.5%) were stage 1, 18 (52.9%) stage 2, 5 (14.7%) stage 3, and 4 (11.7%) stage 4. Axillary nodes were involved in 13 (38.2%) patients. The majority of the tumors were of ductal type (31, 91%), 23 tumors (67.6%) were grade 3, and 11 (32.4%) grade 2. Of these patients, 20 (58.8%) received ET and 14 (61.2%) did not. Median ER staining was 5% with weak expression in most cases. PR was negative in 72% of tumors.

The median follow up time was 42 months (range 2-90). 13 of the low ER+ patients had recurrences, 8 of whom died of disease and 1 died due to other causes. No significant difference in OS (p=.591) and DFS (p=.576) were identified for the patients who received ET and those who did not (Figure 1). There was no statistically significant difference in OS (p=.858) & DFS (p=.665) between low ER+ & TN- IBC, but high ER+ cancers (all received ET) showed a better OS (p=.032) and DFS (p=.029) than low ER+ cases (Figure 2).

Figure 1 - 120

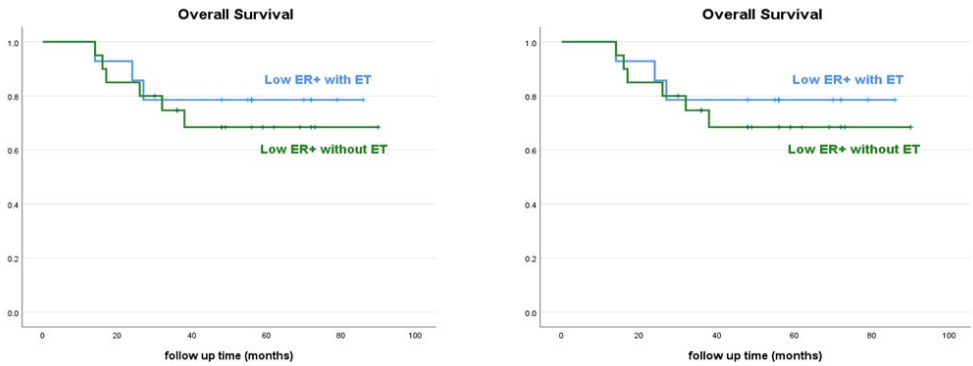

Figure 2 – 120

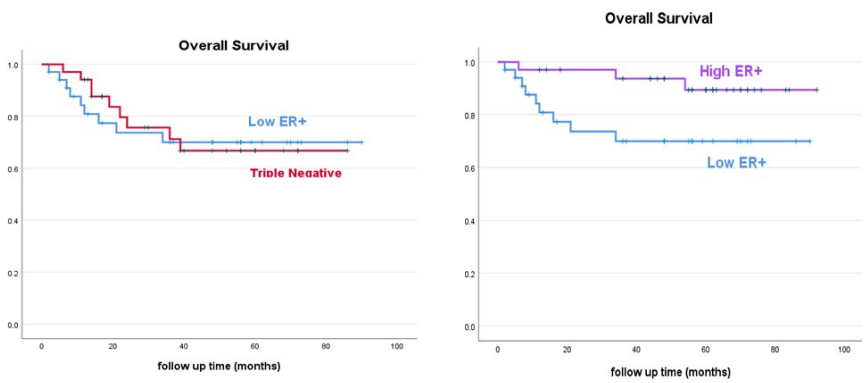

Conclusions: Patients with ER-low/Her2- IBC had similar outcomes as patients with TNC. In this small cohort, patients with low ER+ IBC showed no clearly demonstrable survival advantage from ET. Our results supports the 2020 ASCO/CAP approach of classifying cases with 1-10% ER expression separately as "low ER+". Further studies are needed to validate these findings and to explore the predictive and prognostic factors associated with ER-low/Her2- IBC.

121 Dermatofibrosarcoma Protuberans of the Breast: A Clinicopathological Study of a Rare Cutaneous Low-grade Sarcoma

Romana Idrees[1], Fatima Safdar[2], Abida Sattar[3], Lubna Vohra[2], Naila Kayani[1], Saira Fatima[2], Nasir Ud Din[1]
[1]Aga Khan University Hospital, Karachi, Pakistan, [2]Aga Khan Hospital, Karachi, Pakistan, [3]Aga Khan University Hospital, Karachi City, Pakistan

Disclosures: Romana Idrees: None; Fatima Safdar: None; Abida Sattar: None; Lubna Vohra: None; Naila Kayani: None; Saira Fatima: None; Nasir Ud Din: None

Background: Dermatofibrosarcoma protuberans (DFSP) of breast is a rare entity. It is more commonly seen in trunk and extremities. It is a slow growing neoplasm originating from dermis and involving the subcutaneous tissue. It is an intermediate grade malignancy with a high tendency for recurrence and a low likelihood of metastasis with fibrosarcomatous transformation.

The objective of our study is to present the clinical and histological features of DFSP of breast, which is an uncommon entity of breast.

Design: Patients with histopathologically proven DFSP of the breast, between January 2010 to August 2021 were identified from a prospectively maintained pathology database and their clinical data and histological slides were reviewed by pathologists.

Results: 20 cases of DFSP breast diagnosed from January 2010 to August 2021 were included in the study. Out of 20, 8 were male and 12 were female. The male to female ratio is 2:3. The median age of presentation in females is 37.7 years (range 25 to 54 years) and in males is 38.4 years (range 24 to 49). The average tumor size in females is 5.8cm (range 1.5 to 17cm) and in males is 7.5 (range 1.3 to 20cm). Histologically, 12 cases (60%) showed spindle cells arranged in storiform pattern and 8 cases (40%) showed fibrosarcomatous changes comprising of fasicular pattern along with residual storiform pattern. The mean mitotic count in 12(60%) DFSP cases is 4.3 (range 2 to 8/HPF) and in fibrosarcomatous DFSP is (20.6 range 7 to 72/HPF). On Immunohistochemistry, 12(60%) of DFSP cases showed diffuse strong CD34 positivity while in 7/8 fibrosarcomatous DFSP cases staining was weak in fasicular areas and completely negative in one case. The median follow up period is 4.75 years (range 1 month to 11 years). All patients were alive and healthy at the last follow up. 3/20(15%) patients experienced recurrence after a mean follow up of 4.3 years and were noted to have incompletely excised tumors. In 17/20(85%) patients with complete surgical resection, no recurrence was observed. The three patients with recurrence underwent surgery with margin clearance.

Conclusions: We present the largest series of breast DFSP. The recurrence rate of 15% is similar to DFSP of other common sites. Inadequate surgery with margin involvement remains the main cause of recurrence. Fibrosarcomatous transformation in breast DFSP (40%) is higher as compared to DFSP in other common locations and its long-term clinical behavior cannot be reliably predicted due to lack of long-term follow-up.

122 National Evaluation of Low Estrogen Receptor Positive Breast Cancer: Similarity of Features and Neoadjuvant Therapy Responses to ER Negative Cancers

Bryan Iorgulescu[1], Deborah Dillon[2], Jane Brock[3]
[1]Brigham and Women's Hospital, Boston, MA, [2]Harvard Medical School, Boston, MA, [3]Brigham and Women's Hospital, Harvard Medical School, Boston, MA

Disclosures: Bryan Iorgulescu: None; Deborah Dillon: None; Jane Brock: None

Background: The 2020 ASCO/CAP guidelines recommend reporting low (1-10%+) estrogen receptor (ER)+ breast cancer as a distinct subgroup, given its unpredictable response to endocrine therapy. Therefore, we assessed ER_{low+} features, responses to neoadjuvant therapy, & treatment patterns nationally.

Design: Females presenting in 2018 with invasive breast carcinoma from the U.S. National Cancer Database with ER scoring were stratified by HER2 status. ER_{low+} (ER 1-10%+) cancers' features, OncotypeDX, neoadjuvant therapy responses, & treatment patterns were compared to ER-, ER_{11-50+}, & $ER_{51-100+}$ tumors using X^2 & ANOVA with correction.

Results: Among 154,308 breast carcinoma patients (85% HER2-, 15% HER2+): 2.8% were ER_{low+} (n=4,248; 2.1% of HER2- & 6.2% of HER2+), compared to 16.4% ER-, 2.8% ER_{11-50+}, & 78.1% $ER_{51-100+}$. Among both HER2- & HER2+ cases, ER_{low+} cancers more closely resembled ER- cancers in terms of PR+, histologic grade, AJCC8 stage, age, & race/ethnicity than they did $ER_{51-100+}$ cancers.(**Table**) Additionally, ER_{11-50+} tumors exhibited intermediate features between ER_{low+} & $ER_{51-100+}$ cancers. Among stage I-IIIa HER2- cases with OncotypeDX, ER_{low+} tumors were most likely to have high-risk RS (mean 39.7, SD 19.7, p<.001): 65% had high RS, vs 51% of ER- & 7% of $ER_{51-100+}$.

Whereas 76-78% of ER_{11-50+} & 82-86% of $ER_{51-100\%+}$ cancers received hormonal therapy, only 45-48% of ER_{1-5+} & 61-67% of ER_{6-10+} cancers did. Conversely, like ER- cases, ER_{low+} tumors more likely received chemotherapy than $ER_{51-100+}$ cases. 8,755 HER2- & 5,571 HER2+ stage I-II cases had neoadjuvant therapy – including 27% of HER2-/ER_{low+} & 41% of HER2+/ER_{low+} cases. The PR & CR pathologic response rates in ER_{low+} tumors matched those of ER-.

Nationally, academic programs were least likely to use hormonal therapy for ER_{low+} cases (46-47%) vs 55-57% at community hospitals; whereas academic programs were most likely to use neoadjuvant therapy for ER_{low+} cases (29% of HER2-, 43% of HER2+), vs 19% of HER2- & 38% of HER2+ ER_{low+} cases at community hospitals.

	HER2 negative					HER2 positive				
	n=127,954 (85.2%)					n=22,201 (14.8%)				
ER score	0	1-10	11-50	51-100		0	1-10	11-50	51-100	
% of total	13.9	2.1	2.1	81.9		30.1	6.2	6.2	57.5	
Characteristics of ER low pos, vs other ER groups	0 %	1-10 %	11-50 %	51-100 %	p-val	0 %	1-10 %	11-50 %	51-100 %	p-val
HER2 ISH DP ratio										
mean	0	0	0	0		5.6	6.7	5.6	4.4	
sd	-	-	-	-		7.0	9.6	4.0	5.8	
p-value vs ER low pos	-	-	-	-		0.04	ref	0.15	<.001	
PR+										
% of cases	5	27	41	88	<.001	6	22	34	79	<.001
mean score	16.2	16.8	39.4	71.9		17.2	10.9	29.2	57.5	
sd score	21.4	28.2	31.0	31.4		21.3	19.6	26.4	34.7	
p-value vs ER low pos	1.0	ref	<.001	<.001		0.10	ref	<.001	<.001	
Histologic grade, %					<.001					<.001
Low (3-5)	2	10	16	32		2	3	4	9	
Intermediate (6-7)	19	25	35	53		25	29	37	50	
High (8-9)	80	64	49	14		74	67	59	41	
AJCC stage, %					<.001					<.001
I	36	42	50	80		32	43	49	73	
II	34	35	29	12		40	35	29	15	
III	24	17	13	4		18	13	11	6	
IV	6	6	7	4		9	10	10	6	
Age, yr					<.001					<.001
mean	58.4	58.1	57.4	62.2		57.3	56.6	55.1	57.7	
sd	14.0	14.3	13.8	12.6		13.3	13.0	13.5	13.7	
p-value vs ER low pos	1.0	ref	.001	<.001		0.50	ref	0.02	0.03	
Race/ethnicity, %					<.001					<.001
White, non-Hispanic	65	66	68	78		67	69	67	73	
Black, non-Hispanic	23	20	17	9		16	14	14	12	
Asian/Pacific Islander	4	5	5	4		8	8	8	6	
Hispanic	7	8	7	6		8	8	8	7	
OncotypeDx score (among AJCC8 stage I-IIIa)					<.001					
mean	31.7	39.7	33.9	16.4		Not indicated (<4% had OncotypeDx data)				
sd	22.4	19.7	18.1	9.3						
p-value vs ER low pos	<.001	ref	<.001	<.001						
OncotypeDx risk (among AJCC8 stage I-IIIa), %					<.001					
Low (0-17)	32	20	23	62						
Intermed (18-30)	17	15	27	30						
High (31+)	51	65	50	7						
Received hormonal therapy, %	5	51	78	86	<.001	6	53	76	82	<.001
Received chemotherapy, %	81	72	61	24	<.001	84	85	82	77	<.001
Neoadjuvant therapy (among AJCC8 stage I-II)										
Received neoadj therapy, %	33	27	15	5	<.001	40	41	44	32	<.001
Neoadj path response, %	93	93	91	84	<.001	98	96	99	94	<.001
Among path response, % PR	37	34	43	82	<.001	22	22	22	47	<.001
Among path response, % CR	63	66	57	18		78	78	78	53	
Received hormonal therapy by Hospital type, %										
Community	5	57	73	82		6	55	72	74	
Comprehensive community	5	53	79	85		6	57	72	81	
Academic	4	46	80	88		6	47	79	84	
Integrated network	4	53	78	87		6	46	77	83	
Received neoadjuvant therapy by Hospital type (among AJCC8 stage I-II), %										
Community	22	19	5	4		38	38	42	27	
Comprehensive community	28	21	13	4		36	32	38	26	
Academic/NCI cancer center	33	29	13	5		39	43	42	29	
Integrated network	33	22	15	5		42	41	46	34	

Conclusions: ER_{low+} cancers resemble ER- tumors (both HER2- & HER2+) in features & neoadjuvant therapy responses; & had the highest OncotypeDX RS – supporting separate categorization of ER_{low+} & current concepts that they benefit from management similar to ER- cancers. However, ER_{low+} management varied between academic & community settings. Additionally, ER_{11-50+} cancers exhibit an intermediate disposition between ER_{low+} & $ER_{51-100+}$, together highlighting the value of ER scoring.

123 Immunohistochemical Characterization of RANK/RANKL Signaling in Breast Carcinoma with Osteoclast-Like Giant Cells

K M Islam[1], Wael Ibrahim[2], Muhammad Ahmed[2], Ruhani Sardana[3], Darin Dolezal[4], Marguerite Pinto[5], Paula Ginter[6], Malini Harigopal[4], Kamaljeet Singh[7]

[1]Women & Infants Hospital/Alpert Medical School of Brown University, Providence, RI, [2]Yale New Haven Hospital, New Haven, CT, [3]Advanced Medical Research Institute and Hospital, Bhubaneswar, India, [4]Yale School of Medicine, New Haven, CT, [5]Yale University, New Haven, CT, [6]Weill Cornell Medicine, New York, NY, [7]Women and Infants Hospital, Providence, RI

Disclosures: K M Islam: None; Wael Ibrahim: None; Muhammad Ahmed: None; Ruhani Sardana: None; Darin Dolezal: None; Marguerite Pinto: None; Paula Ginter: None; Malini Harigopal: None; Kamaljeet Singh: None

Background: Osteoclast-like giant cells (OCGC) are a specific type of macrophage polykaryon that rarely populate the stroma of invasive breast carcinoma (IBC). In bone, RANK/RANKL interaction is involved in osteoclast differentiation. A sequencing study on IBC with OCGC has reported upregulation of RANK and RANKL. However, the details of RANK/RANKL expression in the microenvironment of IBC-OCGC are not known. In this study, we assess the immunohistochemical (IHC) expression of RANK and RANKL in IBC with OCGC.

Design: The pathology archives of 2 Institutions were searched for IBC-OCGC. The H&E slides were reviewed to confirm the diagnosis and presence of stromal OCGC. Clinical features including outcome and histological features were recorded. Immunohistochemistry was performed for RANK (ab13918) and RANKL (ab239607) on formalin-fixed paraffin-embedded tissue sections. H-scores (H=intensity score 0-3 x % cells staining=0-300) for RANK and RANKL expression were calculated for tumor cells and stromal components (OCLGC, inflammatory cells & stromal cells). Statistical analysis was performed using SPSS 25.

Results: A total of 26 IBC-OCGC were identified. H&E slides were reviewed on 21 cases and RANK and RANKL IHC were performed on 20 cases. IBC-OCGC were enriched in ER+ (89%), early-stage breast cancers (94%) that showed cellular and hemorrhagic tumor stroma with hemosiderin deposits, variably prominent TILS (mean 30%), and frequent intermediate Oncotype Dx score (mean=16). Highest cytoplasmic RANK expression was identified in stromal inflammatory cells and OCGC (H-score= 156 &155, Fig. 1B & 2A) followed by tumor cells (H-score=111) and stromal cells (H-score=82)(p=.001). Strong RANKL expression was limited to endothelial cells (Fig. 2B), with variably low expression in tumor stroma. Tumor cells were negative for RANKL expression. A significant positive correlation was present between stromal and tumor cell RANK H-score (r=.49;p=.027) and OCGC and stromal inflammatory cells RANKL H score (r=.47, p=.042). A significant negative correlation was present between OCGC RANK and stromal cell RANKL expression (r=-.53, p=.02). No recurrence or tumor-related death was reported in a mean follow-up of 48 months (range=1-242).

Clinicopathological features and RANK and RANKL IHC findings of invasive breast carcinoma with osteoclast-like giant cells

Age (years)	**47 (34-81)**
Histology **Tubular/Cribriform** **IBC, NST** **Mucinous** **Micropapillary** **Mixed**	13 (57%) 5 (22%) 2 ((%) 2 (9%) 1 (4%)
Histologic Grade **1** **2** **3**	8 (32%) 15 (60%) 2(8%)
DCIS **Present** **Absent**	20 (87%) 3 (13%)
Area (%) of tumor with OCGC **Focal (< 5%)** **>10%**	7 (35%) 13 (65%)
ER and PR **Positive** **Negative**	23 (89%) 3 (12%)
HER2 **Positive** **Negative**	1 (4%) 24 (96%)
pT stage **pT1** **pT2**	11 (69%) 4 (25%) 1 (6%)

pT3	
pN stage **pN0** **pN0(i+)** **pN1mi**	16 (89%) 1 (6%) 1 (6%)
Oncotype Dx (mean, range)	16 (3-25)
TILS (mean, range)	31% (5-80%)
Follow up duration (mean, range in months)	48 (1-242)
RANK IHC H score **Tumor cell** **OCGC** **Stromal cell** **Stromal inflammatory cell**	111 (0-300) 155 (30-200) 82 (4-160) 156 (10-270)
RANKL IHC H score **Tumor cell** **OCGC** **Stromal cell** **Stromal inflammatory cell**	0 77 (0-190) 11 (0-100) 3.5 (0-20)

Figure 1 - 123

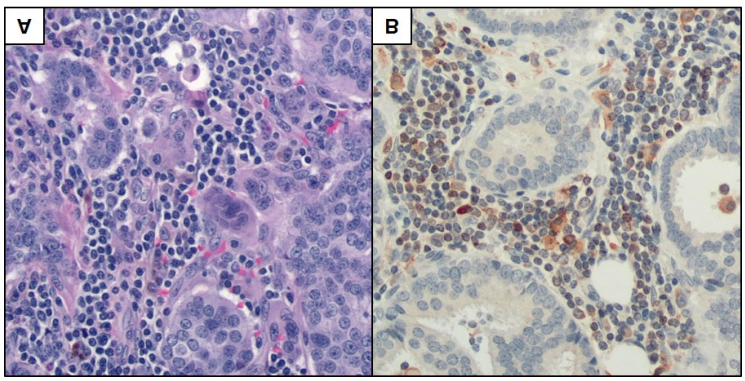

Figure 2 – 123

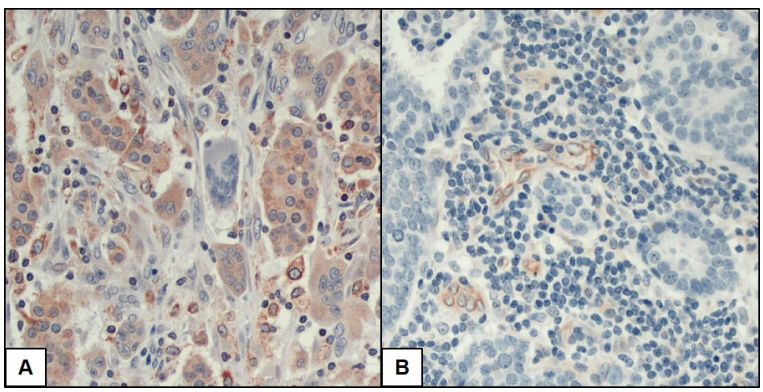

Conclusions: The IBC-OCGC stromal microenvironment is likely influenced by RANK/RANKL signaling. Differential RANK expression is seen in tumor cells and stromal elements of IBC-OCGC. Prominent RANKL expression is limited to tumor capillary endothelium.

124 Oncotype Dx Testing of Multiple Synchronous Tumors of the Breast--Is it necessary?

Cao Jin[1], Shabnam Jaffer[2], Jennifer Zeng[1]
[1]Mount Sinai Hospital Icahn School of Medicine, New York, NY, [2]Mount Sinai Medical Center, New York, NY

Disclosures: Cao Jin: None; Shabnam Jaffer: None; Jennifer Zeng: None

Background: Oncotype DX recurrence score (RS) testing in early stage hormone receptor positive/HER2 negative (HR+/HER2-) breast cancers (BC) help guide adjuvant chemotherapy recommendations. Synchronous ipsilateral HR+/HER- breast cancers may have similar or different histomorphologies and tumor sizes. We examined the RS in women with testing of multiple synchronous tumors to determine if there was a difference in chemotherapy recommendations.

Design: Of 1411 patients who underwent RS testing at our institution from 1/2017 to 7/2021, we identified 38(2.7%) with 79 multiple ipsilateral BCs. Clinicopathologic characteristics were recorded (e.g. patients' age, tumor sizes, histologic subtypes and grades). RS were stratified into 3 risk categories (low RS<15, intermediate RS16-25, and high RS>25), and by age and chemotherapy benefit (age<50, RS>15 and age>50, RS>25). RS for tumor foci were concordant if it conferred the same chemotherapy recommendation and discordant if RS had different recommendations.

Results: Median patient age was 59 years (range 38-79, age<50, n=10; age>50, n=28) with median tumor size =13mm (range 4-50mm). All patients had 2 tumors tested, with the exception of 2 that had 3 tumors, average difference in tumor size was 9.3mm. Tumor classification by grade was low=6(8%), intermediate=57(72%) and high=16(20%). BC types included ductal (n=56), lobular (n=17) and mixed ductal and lobular (n=6). Overall median RS was 14 (range 3-36): low(<10)=17, intermediate(11-25)=59 and high(>26)=3, and average difference between tumors was 3.6. Higher RS correlated with larger tumor size in 22/38 patients (58%)(avg=9.2mm), smaller tumor size in 13 patients (34.2%)(avg=9.5mm), and was identical in both tumors in 3 patients (7.9%). All paired smaller tumors with high RS had same tumor grades except in 1, and subtypes except in 1 case, and neither impacted RS. RS difference between these tumors was 2.3, remained in the same category except for 2 cases that changed from low to high, but didn't impact chemotherapy decision due to patient's age >50. Patients with tumors of the same BC subtypes had same RS except in 13 cases, but only 2 were impactful as far as chemotherapy recommendation.

Conclusions: Oncotype DX testing of the larger tumor is directly related to higher RS in 60% of cases. Tumor grade or subtype was not significant in predicting higher RS in the remaining cases. Due to the higher RS in a subset of smaller tumors, it may be prudent to test multiple ipsilateral synchronous tumors especially given the impact of RS in younger patients.

125 Understanding the Role of Tissue Resident Microbiota in Idiopathic Granulomatous Mastitis Using 16S rRNA Gene Sequencing

Heather Jones[1], Sunati Sahoo[1], Prithvi Raj[1], Matthew Brock[1]
[1]UT Southwestern Medical Center, Dallas, TX

Disclosures: Heather Jones: None; Sunati Sahoo: None; Prithvi Raj: None; Matthew Brock: None

Background: Idiopathic granulomatous mastitis (IGM) is characterized by non-necrotizing granulomas with cystic vacuoles and small aggregates of neutrophils in an inflammatory background that includes histiocytes, giant cells, and lymphoplasmacytic infiltrates. Although IGM has been reported to be associated with *Corynebacterium spp.*, treatment with antibiotics is often ineffective, with recourse to steroids or surgical excision. In this study, we explore the structure of tissue resident microbiome in patients with IGM compared to healthy controls.

Design: This single-center study was approved by institutional review board. DNA was extracted from formalin-fixed paraffin-embedded core biopsies followed by amplification and sequencing of v3-v4 regions of 16S rRNA gene on MiSeqDx Illumina sequencer. Quality pass sequencing reads were compared to GREENGENE, a microbiome reference database, to infer microbial Operational Taxonomic Units (OTUs) in each sample. CLC Bio genomics workbench was used to determine relative abundances of OTUs at various taxonomic levels in each sample. OTUs with >1,000 sequencing reads were considered for analysis.

Results: 16S sequencing analysis revealed significant diversity in microbial community in both control and IGM tissue samples (Figure 1). There were differences in the microbiome of IGM samples compared to controls, notably increased amounts of bacteria from the genus Pseudomonas (5-fold, p = 0.0007, Figure 2), family Rhodospirillaceae (3-fold, p=0.007), and genus Corynebacteria (3-fold, p=0.098).

Figure 1 - 125

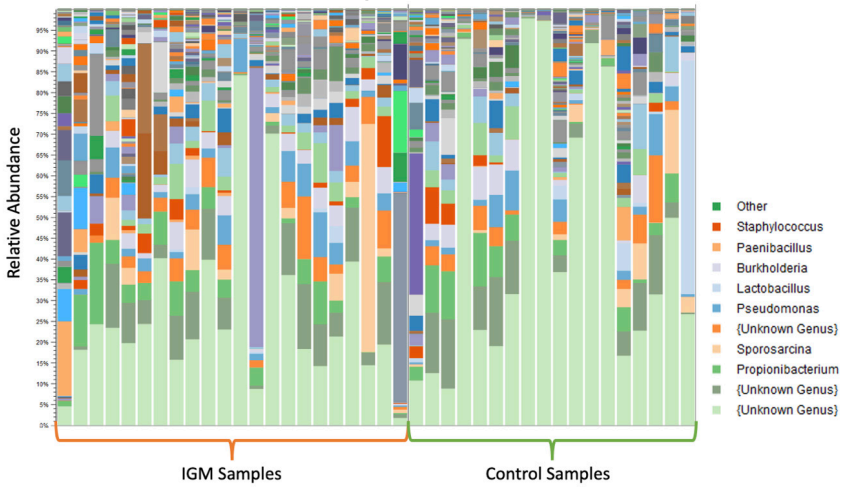

Figure 1. Genus-level OTUs are diverse among samples.

Figure 2 – 125

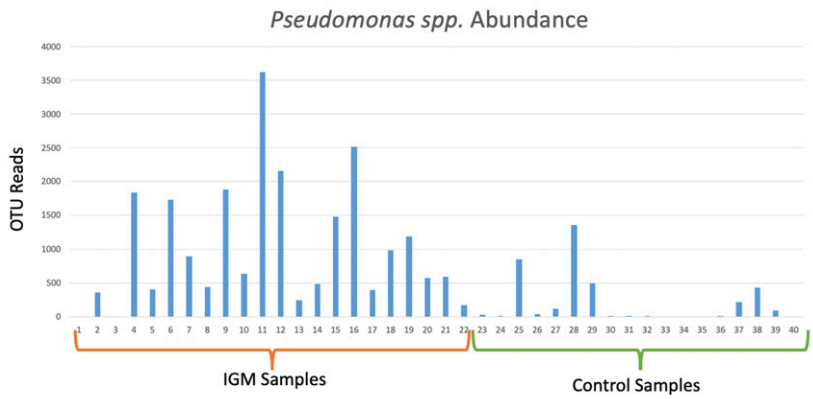

Figure 2. Higher abundance of Pseudomonas in IGM samples than controls.

Conclusions: Existing research supports a resident tissue microbiome unique to the breast. We propose that IGM results from dysbiosis or imbalances in this microbiota composition causing an inappropriate immune response, rather than strictly from infection by a single microbe. Most prior studies investigating IGM have relied on tissue Gram stain or microbiologic cultures for speciation of the "causative agent." Studies supporting *Corynebacteria spp.* as the culprit, however, fail to identify it in a significant proportion of cases, identify a wide variety of other bacteria, or identify no pathogen at all. The lack of consistent evidence regarding a causative microbe and the data presented here support the disease etiology of microbiota imbalance over infection.

126 CDK4/6 Inhibitors for Metastatic HR+/HER2- Breast Cancer: Clinico-Pathological Analysis for Determinants of Response

Vijaya Kadam Maruthi[1], Emily Schultz[2], Erik Knudsen[2], Agnieszka Witkiewicz[3], Deanna Hamilton[2]
[1]University at Buffalo, Buffalo, NY, [2]Roswell Park Comprehensive Cancer Center, Buffalo, NY, [3]Roswell Park Comprehensive Cancer Center

Disclosures: Vijaya Kadam Maruthi: None; Emily Schultz: None; Erik Knudsen: None; Agnieszka Witkiewicz: None; Deanna Hamilton: None

Background: The cyclin D-CDK4/6-RB pathway is a crucial regulator of the G1–S transition of the cell cycle. Consequently, pharmacological CDK4/6 inhibitors can limit cell division in multiple setting. The inclusion of CDK4/6 inhibitors to endocrine

therapy have substantially improved progression-free survival (PFS) in hormone receptor positive and HER2 negative (HR+/HER2-) metastatic breast cancer. However, the duration of PFS is highly variable across patients, emphasizing the need for more rational patient sub-categorization. Here we interrogated clinic-pathological features associated with the real-world of CDK4/6 inhibitors for the treatment of metastatic HR+/HER2- breast cancer.

Design: A total of 222 HR+/HER2- metastatic breast cancers patients who received CDK4/6 inhibitors from 2015 to 2021, were evaluated. 93.69% of patients received palbociclib as the CDK4/6 inhibitor with aromatase inhibitors (AI) or fulvestrant as the predominant endocrine therapies. Clinicopathological determinants were evaluated relative to PFS.

Results: The median progression-free survival with AI (27.6 months) or fulvestrant (17.2 months) groups were comparable to that observed in clinical trials [Table1]. Patients with recurrent disease had shorter PFS relative to those presenting with de novo metastasis (p=0.0024). Presence of visceral metastasis trended toward shorter PFS (p=0.051). The amount of tumor infiltrating lymphocytes were not directly associated with PFS. Similarly, HER2-status was not associated with PFS. However, negative progesterone receptor (PR) status was associated with shorter PFS (p=0.0014) [Fig 1].

Table 1. Comparison of Progression Free Survival in Our Study with Published Literature

Study	Treatment	Patient Selection	Months PFS	HR	*P*
Our study	**CDK4/6i+ A I**	**ER+/HER2-** **Metastatic or LR**	27.6		
PALOMA-2	Palbociclib + Letrozole vs Letrozole	ER+/HER2- Postmenopausal	22.1 Vs 14.5	0.58	<0.001
MONALEESA-2	Ribociclib + Letrozole vs Placebo + Letrozole	HR+/HER2- Postmenopausal Recurrent / Metastatic No prior ET ECOG 0/1	25. 3 vs 16	0.56	3.29x10-6
MONARCH-3	Abemaciclib + LeVAnast vs Placebo + LeVAnast	HR+/HER2- Postmenopausal LR not amenable to surgery or Metastatic without prior **ET** ECOG 0/1	28.2 vs 14.8	0.54	0.000002
Our Study	**CDK4/6i+ Fulvestrant**	**ER+/HER2-** **Metastatic or LR**	**17.2**		
PALOMA-3	Palbociclib + Fulvestrant vs Placebo + Futvestrant	HR+/HER2- Postmenopausal Progressed on previous ET	9.5 vs 4.6	0.43	<0.0001
MONARCH-2	Abemaciclib + Fulvestrant vs Placebo + Futvestrant	HR+/HER2- Postmenopausal Progressed on previous ET 12 months since ET or during 1st-line **ET** for metastatic ECOG 0/1	16.4 vs 9.3	0.553	<0.001
MONALEESA-3	Ribociclib + Fulvestrant vs Placebo + Futvestrant	HR+/HER2- Postmenopausal Advanced cancer No prior treatment with Futvestrant	20.5 vs 12.8	0.593	<0.001

Figure 1 - 126

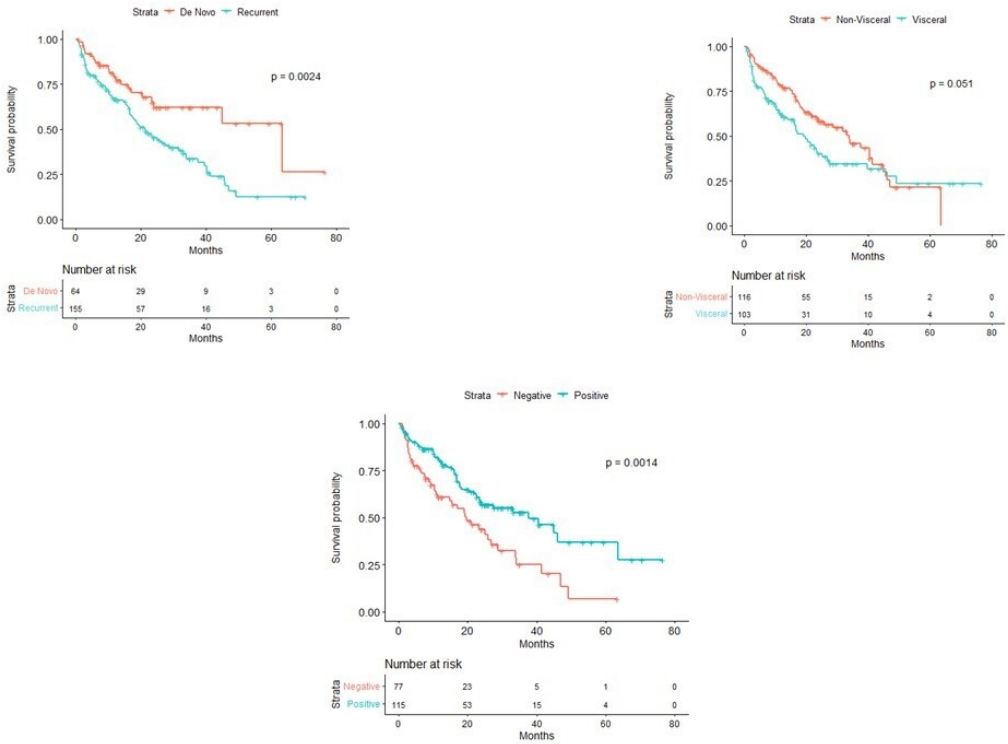

Conclusions: A significantly shorter PFS was identified in patients with recurrent disease, metastasis to viscera, and with PR-negative status. Our findings suggest that sub-categorization of patients based on standard clinicopathological determinants could be utilized to predict PFS with CDK4/6 inhibitor-based therapies for the treatment of HR+/HER2- metastatic breast cancer. This also lays the groundwork for investigating additional biomarkers which may be predictive of clinical outcomes.

127 Synchronous or Metachronous Breast Carcinoma with Divergent Grade or Biomarker Status: Correlation with Germline Mutation Status

Aysenur Keske[1], Paul Weisman[2], Kelcy Smith-Simmer[1], Anna Zakas[1], Jin Xu[3]
[1]University of Wisconsin-Madison Hospital and Clinics, Madison, WI, [2]University of Wisconsin-Madison, Madison, WI, [3]University of Wisconsin, Madison, WI

Disclosures: Aysenur Keske: None; Paul Weisman: None; Kelcy Smith-Simmer: None; Anna Zakas: None; Jin Xu: None

Background: Multiple tumors in the same patient, whether synchronous or metachronous, complicate patient management, but never more than when they have divergent grade and/or biomarker profiles. Following 4 index cases of germline mutation carriers with multiple divergent breast cancers (MDBC) in *MUTYH* (2 cases), *ATM* (1 case) and *BRCA2* (1 case), we set out to determine the frequency of MDBC in both *BRCA* and non-*BRCA* germline mutation carriers.

Design: In collaboration with our genetic counseling department, we retrospectively identified patients from a prospectively created log of breast cancer patients referred to genetic counseling between 2017- 2020 that tested positive for a pathogenic germline mutation in the following
genes: *ATM*, *BARD1*, *BRCA1*, *BRCA2*, *BRIP1*, *CDH1*, *CHEK2*, *MSH6*, *MUTYH*, *NBN*, *NF1*, *PALB2*, *PTEN*, *STK11* and *TP53*. Divergent grade/biomarker status was defined as a difference between 2 tumors in a single patient of either 2 tumor grades (i.e. grade 1 vs. grade 3) and/or a difference of biomarker status (i.e. hormone receptor (HR) + vs. HR -; HER2+ vs. HER2-; triple-negative vs. non- triple-negative).

Results: A total of 72 invasive breast cancer patients with a pathogenic germline mutation in one of the above genes, as well as known breast cancer histology, were identified. The frequency of germline mutations was as follows (in descending

order): *CHEK2* (16/72, 22%), *BRCA1* (16/72, 22%), *MUTYH* (14/72, 19%), *BRCA2* (8/72, 11%), *PALB2* (6/72, 8%), *BRIP1* (4/72, 5%), *ATM* (3/72, 4%), *MSH6* & *TP53* (each 2/72, 3%) and *BARD1* (1/72, 1%). From these patients, a total of 4 patients had MDBC as follows: *MUTYH* (1/4, 25%), *ATM* (1/4, 25%), *CHEK2* (1/4, 25%) and *PALB2* (1/4, 25%). If our 4 index cases are added back into this cohort, we have the following frequency of MDBC: *MUTYH* (3/8, 38%), *ATM* (2/8, 25%), *CHEK2* (1/8, 12%), *PALB2* (1/8, 12%) and *BRCA2* (1/8, 12%). A single additional case of *MUTYH* germline mutation carrier had bilateral DCIS with divergent histology (one with high-grade DCIS and HR- status, the other with intermediate grade DCIS with HR+ status).

Conclusions: *CHEK2, BRCA1* and *MUTYH* mutations were most common in our cohort. However, *MUTYH* mutation was most commonly associated with MDBC, though our numbers are admittedly small. A detailed morphologic analysis of all of the *MUTYH* cases (including those without MDBC) is forthcoming and will be reported as part of our poster.

128 Clinicopathologic Predictors of Clinical Outcomes in Mammary Adenoid Cystic Carcinoma: A Multi-Institutional Study

Thaer Khoury[1], Marilin Rosa[2], Anupma Nayak[3], Rouzan Karabakhtsian[4], Oluwole Fadare[5], Zaibo Li[6], Bradley Turner[7], Yisheng Fang[8], Asangi Kumarapeli[9], Xiaoxian Li[10], Tatiana Villatoro[11], Numbereye Numbere[7], Jigang Wang[12], Saed Rahmat Sadeghi[13], Li Yan[1], Wanqing Tian[1], Rohit Bhargava[14]

[1]Roswell Park Comprehensive Cancer Center, Buffalo, NY, [2]H. Lee Moffitt Cancer Center & Research Institute, Tampa, FL, [3]Perelman School of Medicine at the University of Pennsylvania, Philadelphia, PA, [4]Montefiore Medical Center - Einstein Campus, NY, [5]UC San Diego School of Medicine, La Jolla, CA, [6]The Ohio State University Wexner Medical Center, Columbus, OH, [7]University of Rochester Medical Center, Rochester, NY, [8]UT Southwestern Medical Center, Dallas, TX, [9]Summa Health, Akron, OH, [10]Emory University, Atlanta, GA, [11]University of Pittsburgh Medical Center, Pittsburgh, PA, [12]The Affiliated Hospital of Qingdao University, Qingdao, China, [13]Albert Einstein College of Medicine, Montefiore Medical Center, Irvine, CA, [14]UPMC Magee-Womens Hospital, Pittsburgh, PA

Disclosures: Thaer Khoury: None; Marilin Rosa: None; Anupma Nayak: None; Rouzan Karabakhtsian: None; Oluwole Fadare: None; Zaibo Li: None; Bradley Turner: None; Yisheng Fang: None; Asangi Kumarapeli: None; Xiaoxian Li: None; Tatiana Villatoro: None; Numbereye Numbere: None; Jigang Wang: None; Saed Rahmat Sadeghi: None; Li Yan: None; Wanqing Tian: None; Rohit Bhargava: None

Background: Adenoid cystic carcinoma (ACC) is an uncommon type of invasive breast carcinoma. Our aim was to collect a relatively large number of cases across multiple institutions to evaluate clinicopathological variables and correlate with disease free survival (DFS).

Design: Seventy-six ACC cases were collected from 11 institutions and reviewed by the breast pathologist in each respective institution. The following variables were recorded, patient's age, race, treatment modality (type of surgery, chemotherapy, and radiation therapy), way of detection (incidental, palpable mass, or screening mammography), imaging findings (mass, calcifications, asymmetry/density), and AJCC stage. The following histologic features were recorded including, Nottingham grade, percentages of various growth patterns (solid, cribriform, trabecular/tubular), percentage of basaloid component, tumor borders (pushing, infiltrative), perineural invasion, lymphovascular invasion, necrosis, distance from the margin, ER, PR and KI-67. DFS was defined as interval between time of diagnosis to first recurrence (local and/or distant) or last follow-up (in absence of recurrence). Associations between these variables and DFS were analyzed.

Results: Nineteen (25%) patients developed local and/or distant recurrence. Median and range of time of follow-up was 52.5 (3, 300) months. Time to recur was 45 (5, 160) months. Two patients presented with stage IV disease. Six of 58 (10.3%) had axillary node involvement. Basaloid component (≥10% of tumor) was identified in 24 (31.6%), solid component (>40% of tumor) in 22 (28.9%), and cribriform component (>15%) in 52 (68%) cases. Univariate and multivariate analysis results correlating with DFS are listed in Table 1. Kaplan Meier curves showing the association of basaloid, solid, and cribriform type with DFS are represented in figures 1 and 2.

Table 1: Clinicopathologic variables association with DFS (univariate and multivariate analyses)

Param

Parameter	Reference	Hazard ratio (95% CI)	P value	Hazard ratio (95% CI)	P value
		Univariate	Univariate	Multivariate	Multivariate
Cribriform (>15%)	Non-Cribriform	0.24 (0.095, 0.59)	.002	0.11 (0.03, 0.43)	.001
Solid (>40%)	Non-Solid	4.54 (1.79, 11.54)	<.001	0.16 (0.02, 1.29)	.085
Basaloid (≥10%)	Non-Basaloid	3.57 (1.43, 8.9)	.006	2.24 (0.42, 11.96)	.35
Nottingham grade-2	1	2.27 (0.76, 6.74)	.14	3.78 (0.96, 14.8)	.057
Nottingham grade-3	1	4.17 (1.21, 14.34)	.024	5.35 (0.91, 31.28)	.063
Necrosis-Yes	No	4.77 (1.69, 13.49)	.003	18.48 (4.05, 84.31)	<.001
Perineural invasion-Yes	No	2.96 (1.19, 7.39)	.02	1.27 (0.38, 4.23)	.69
Lymphovascular invasion-Yes	No	7.31 (1.97, 27.03)	.003	18.36 (2.79, 120.75)	.002

Figure 1 - 128

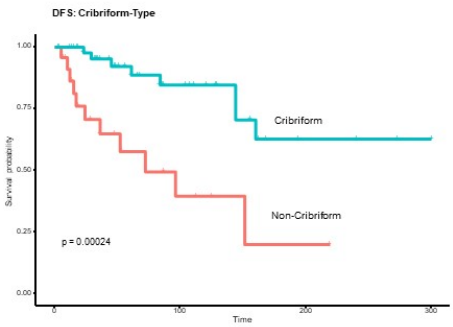

Figure 2 - 128

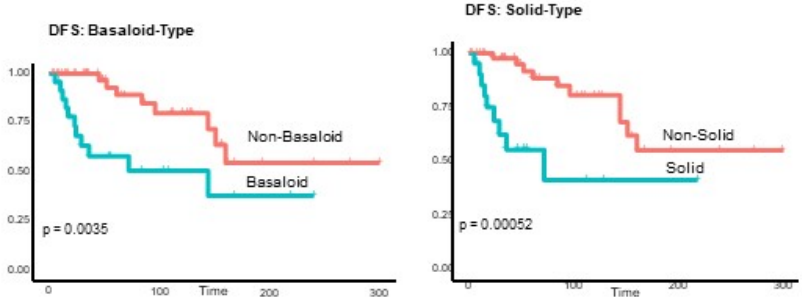

Conclusions: Histologic features including histologic patterns (basaloid, solid, and cribriform), lymphovascular invasion, Nottingham grade, and tumor necrosis may predict tumor recurrence. A grading system incorporating these variables is required to better predict tumor recurrence. Therefore, a study with a larger group of cases is warranted to achieve this goal.

129 Genomic and Protein Expression of TERT, MED12, and RARA in Malignant Phyllodes Tumours of the Breast

Valerie Koh[1], Nur Diyana Md Nasir[1], Cedric Ng[2], Vikneswari Rajasegaran[3], Jing Yi Lee[3], Peiyong Guan[3], Wen Chen[1], Huihua Li[4], Xiaoyang Chen[1], Rachel Gan Lin Rong[1], Aye Aye Thike[1], Mihir Gudi[5], Kenneth Chang[6], George Yip[7], Boon Bay[7], Bin Tean Teh[3], Puay Hoon Tan[1]

[1]Singapore General Hospital, Singapore, Singapore, [2]Cancer Discovery Hub, National Cancer Center Singapore, Singapore, [3]National Cancer Centre Singapore, Singapore, [4]Singapore, [5]KK Women's and Children's Hospital, Singapore, [6]KKH, Singapore, [7]Yong Loo Lin School of Medicine, National University of Singapore, Singapore

Disclosures: Valerie Koh: None; Nur Diyana Md Nasir: None; Cedric Ng: None; Vikneswari Rajasegaran: None; Jing Yi Lee: None; Peiyong Guan: None; Wen Chen: None; Huihua Li: None; Xiaoyang Chen: None; Rachel Gan Lin Rong: None; Aye Aye Thike: None; Mihir Gudi: None; Kenneth Chang: *Advisory Board Member*, Bayer South-East Asia; *Speaker*, European Society of Medical Oncology; *Grant or Research Support*, Bayer South-East Asia; George Yip: None; Boon Bay: None; Bin Tean Teh: None; Puay Hoon Tan: None

Background: Breast phyllodes tumours (PTs) are a rare subset of fibroepithelial tumours classified as benign, borderline or malignant. Although the majority are benign, malignant PTs can be clinically aggressive by metastasizing, leading to poor prognosis and eventually death. This study aims to investigate the mutation status and protein expression of TERT, MED12 and RARA and correlate them with clinicopathological data and survival outcomes.

Design: Comprising 83 cases of malignant PTs diagnosed at our institution from Jan 1992 to Oct 2017, targeted sequencing using a 16-gene panel was performed on a subset of 18 cases, and an additional 10 malignant cases from another local institution (total 28 cases). Immunohistochemistry was conducted on all 83 cases from our institution using tissue microarrays.

Results: The top 2 mutations were *TERT* (57.1%) and MED12 (50.0%), with *RARA* disclosing a mutation rate of 17.9%. *MED12* and *RARA* mutations significantly correlated with each other (p=0.041). High protein expression of stromal nuclear TERT was associated with younger patient age (p=0.008), absence of stromal overgrowth (p=0.032) and lower mitotic activity (p=0.006). High stromal cytoplasmic TERT expression also correlated with lower mitotic activity (p=0.011). High expression of stromal nuclear RARA showed significant association with absence of stromal overgrowth (p=0.013) and presence of malignant heterologous elements (p=0.015). High stromal cytoplasmic RARA expression also correlated with absence of stromal overgrowth (p=0.016).

On Kaplan-Meier analysis, high cytoplasmic expression of stromal TERT disclosed poorer metastasis-free survival (MFS) (p=0.015) and disease-specific survival (DSS) (p=0.044), while high stromal nuclear TERT showed better MFS (p=0.039). On multivariate analysis, stromal cytoplasmic TERT expression remained a significant indicator for poorer DSS (HR 8.521, 95% CI 1.393 to 52.129, p=0.020) and MFS (HR 5.220, 95% CI 1.128 to 24.166, p=0.035). MED12 was not significantly associated with any clinicopathological data or survival outcomes. There was no correlation of mutation status of all 3 genes with protein expression.

Conclusions: Our findings affirm the presence of *TERT* and *MED12* mutations in malignant PTs, the strong relationship between *MED12* and *RARA*, and provide insights to protein expression of TERT, MED12 and RARA in malignant PTs. Further investigations are warranted for deeper comprehension of the mechanisms of PT progression.

130 The Utility of Ki67 Quantification to Triage OncotypeDX Testing in Breast Cancer

Melissa Krystel-Whittemore[1], Hannah Wen[1], Dilip Giri[1], Maria Kuba[1], Edi Brogi[1], Matthew Hanna[1]
[1]Memorial Sloan Kettering Cancer Center, New York, NY

Disclosures: Melissa Krystel-Whittemore: None; Hannah Wen: None; Dilip Giri: None; Maria Kuba: None; Edi Brogi: None; Matthew Hanna: *Consultant*, Paige, PathPresenter

Background: The International Ki67 in Breast Cancer Working Group (IKWG) provided guidelines for Ki67 assessment and recommended T1-2 N0-1 ER+/HER2- breast cancer with Ki67 ≤5% or ≥30% did not need gene expression assay testing, as these patients would likely have low or high RS, respectively. Additionally, tumors with Magee Score (MS), of <18, 18-25 with low mitotic score, or >31 can safely forego gene expression assays. The aim of this study was to compare the risk stratifications by Ki67 assessment, MS, and ODx testing in early stage ER+/HER2- breast cancer.

Design: The study cohort consisted of 57 consecutive invasive breast carcinomas with ODx testing performed. Ki67 IHC was performed on whole tissue sections of surgical resection specimens using two antibody clones (MIB and 30-9). A 400x Ki67 hotspot was captured. 3 pathologists and 3 image analysis tools independently quantified Ki67 proliferation index. Ki67 index and subsequent calculations were performed using the means of the above assessments. MS was calculated using Ki67 quantification and clinicopathology data. Triage based on Ki67 index according to the IKWG guidelines and MS were compared. Sensitivity and specificity of using MS and Ki67 value compared to ODx as a reference standard were calculated.

Results: 57 consecutive T1-2 N0-1 ER+/HER2- invasive breast carcinomas were identified with clinical metadata (Table 1). Median Ki67 MIB and 30-9 clones were 15% (range 14-18) and 26% (range 25-30%), respectively. Using the respective Ki67 IKWG guidelines and Magee criteria to triage genomic profiling, 51% and 75% of cases in this cohort would not be recommended for ODx testing. Sensitivity and specificity of Ki67 index and MS for triaging ODx testing are shown in Figure 1. Of note, biopsy site changes were present in 58% of discordant cases (7/12) compared to 31% of concordant cases (14/45).

Table 1. Clinicopathologic characteristics

Patients (n)	57
Invasive carcinoma type	
IDC NOS	38 (67%)
ILC	10 (17%)
Classic	6 (10%)
Pleomorphic	4 (7%)
Mammary	1 (2%)
Special types	8 (14%)
Mucinous	4 (7%)
Apocrine	1 (2%)
Micropapillary	2 (3%)
Cribriform	1 (2%)
Nottingham Grade 1 (n) %	12 (21%)
Nottingham Grade 2 (n) %	37 (65%)
Nottingham Grade 3 (n) %	8 (14%)
Median tumor size, mm (range)	16 (11-42)
Lymph node stage	
Nx	1 (2%)
N0	44 (77%)
N0 (i+)	4 (7%)
N1mi	5 (9%)
N1a	3 (5%)
Estrogen receptor (%)	
<1	0 (0%)
1-10	1 (2%)
11-50	4 (7%)
>50	52 (91%)
Progesterone receptor (%)	
<1	8 (14%)
1-10	14 (25%)
11-50	4 (7%)
>50	31 (54%)
OncotypeDX RS	
Median RS (range)	19 (0-46)
<=25	41 (72%)
>25	16 (28%)

IDC, invasive ductal carcinoma; ILC, invasive lobular carcinoma; RS, Recurrence score

Figure 1 - 130

Figure 1. Input values for sensitivity and specificity calculation (A and B); Average sensitivity and specificity of calculated Magee and IKWG Ki67 guidelines predicting OncotypeDX recurrence risk for all pathologists and IA tools (C)

A

Ki67 clone	IKWG	ODx RS >25	ODx RS ≤25
30-9	Ki67 ≥30%*	4	12
30-9	Ki67 ≤5%+	1	3
MIB	Ki67 ≥30%*	4	6
MIB	Ki67 ≤5%+	3	5

B

Ki67 clone	Magee	ODx RS >25	ODx RS ≤25
30-9	Magee >31*	3	0
30-9	Magee <18 or 18-25 with mitosis score = 1+	1	53
MIB	Magee >31*	3	0
MIB	Magee <18 or 18-25 with mitosis score = 1+	1	53

C

Ki67 Clone	Magee sensitivity	Magee specificity	IKWG sensitivity	IKWG specificity
30-9	75%	100%	80%	20%
MIB	75%	100%	57%	45%

ODx RS, OncotypeDX Recurrence Score
*Expected OncotypeDX Recurrence Score >25
+Expected OncotypeDX Recurrence Score ≤25

IKWG, International Ki67 Working Group

Conclusions: Ki67 30-9 clone shows higher Ki67 expression than MIB. Sensitivity and specificity were significantly higher for MS compared to IKWG guidelines with hotspot Ki67 assessment. Tumors with Ki67 ≤5% with 30-9 clone did well predicting low ODx RS, however, there is a high false positive rate using Ki67>30% to predict high risk ODx RS with both clones. Low specificity of IKWG guidelines could be a result of using hotspot Ki67 quantification instead of global evaluation. Further comparison of hotspot and global Ki67 evaluation may provide additional insights to use Ki67 for ODx testing triage.

131 Ductal or Lobular: A Correlation Study of Histomorphology and E-cadherin/p120 Immunoprofile in Mixed Ductal and Lobular Carcinoma of Breast

Hae-Sun La[1], Thing Rinda Soong[2], Beth Clark[3], Gloria Carter[1], Jeffrey Fine[2], Lakshmi Harinath[3], Tatiana Villatoro[1], Rohit Bhargava[3], Jing Yu[2]
[1]University of Pittsburgh Medical Center, Pittsburgh, PA, [2]University of Pittsburgh, Pittsburgh, PA, [3]UPMC Magee-Womens Hospital, Pittsburgh, PA

Disclosures: Hae-Sun La: None; Thing Rinda Soong: None; Beth Clark: None; Gloria Carter: None; Jeffrey Fine: *Stock Ownership*, SpIntellx, Inc.; Lakshmi Harinath: None; Tatiana Villatoro: None; Rohit Bhargava: None; Jing Yu: None

Background: With the availability of p120 immunohistochemical (IHC) stain in the past decade, retained yet abnormal E-cadherin (Ecad) patterns have been increasingly recognized. We re-evaluated previously diagnosed mixed ductal and lobular carcinoma (MDLC) cases in order to (i) define abnormal Ecad staining patterns with reference to p120 expression, (ii) correlate tumor morphology with E-cad/p120 immunophenotypes, and to (iii) evaluate whether the prior MDLC diagnoses may be revisited based on our current understanding of Ecad/p120 patterns in breast carcinoma.

Design: A 10-year (2006-2015) archive search identified 69 MDLCs with Ecad and p120 immunostains previously performed. Tumor morphologic patterns, percentage of each morphologic component and corresponding Ecad/p120 IHC patterns were documented. Sharp, intense, complete membranous staining similar to the pattern seen in native benign ducts for both Ecad and p120 was considered intact expression compatible with ductal phenotype.

Results: Overall, 1/3 of the previously diagnosed MDLC cases were reclassified. Distinct double Ecad/p120 membranous staining was observed with various proportions in 49 (71%) tumors, including 5 (7%) showing lobular-like growth pattern with 100% double membranous staining. Complete lack of double membranous staining was found in 20 (29%) tumors, with all such tumors revealing

cytoplasmic p120 and abnormal Ecad staining patterns including partial membranous, beaded membranous, cytoplasmic, or cytoplasmic with membranous accentuation (Figure 1). Tubular component was present in 33 tumors, with 28 of them displaying similar Ecad/p120 pattern as the non-tubular component in the same tumor, including 8 with complete absent or abnormal Ecad staining (Table 1, Figure 2).

Comparison of Ecad/p120 Immunoprofile in Tubular and Non-Tubular Components		
Tumor Type	**Percentage of Tubular Component**	**Cases with Similar Ecad/p120 Profile in Tubular and Non-tubular components**
ILC	3-10%	8/8 (100%)
MDLC, Intermixed Type	10-50%	9/11 (82%)
MDLC, Collision Type	10-70%	11/14 (79%)

Figure 1 - 131

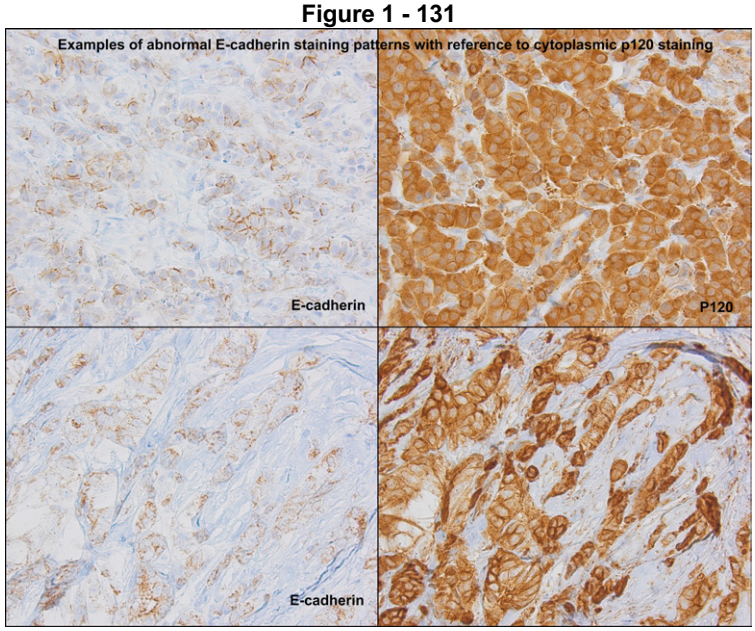

Figure 2 – 131

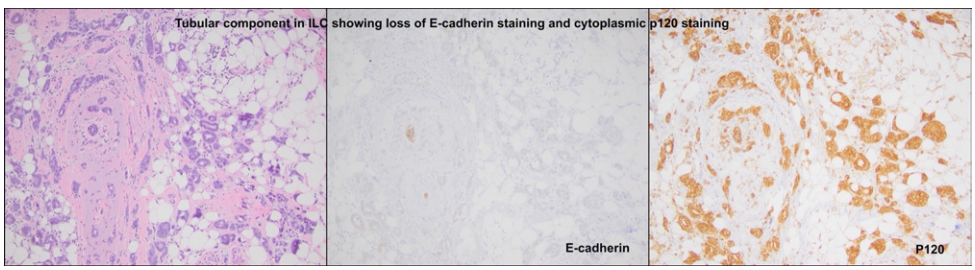

Conclusions: Recognition of abnormal Ecad staining patterns may provide further clue to understanding the nature of ductal versus lobular phenotypes in equivocal cases. Comparing with the staining pattern of internal benign ducts or using concurrent p120 stain can help resolve misinterpretation. Tubular component in the majority of invasive breast carcinomas in this cohort showed an Ecad/p120 immunophenotype similar to the non-tubular components in the same tumor, including abnormal patterns suggestive of E-cadherin mutation and thus likely the same underlying biologic process. Classifying a portion or the entire tumor as ductal solely based on tubule-forming structures may not capture the full biologic profile of these tumors.

132 Correlation of Axillary Nodal Metastasis with Tubular Morphology in Invasive Breast Carcinoma

Mamoor Latef[1], Ankica Braun[1], Lei Yan[1], Xinhai Zhang[2], Vijaya Reddy[1], Paolo Gattuso[1], Indu Agarwal[1]
[1]Rush University Medical Center, Chicago, IL, [2]Rush University, Chicago, IL

Disclosures: Mamoor Latef: None; Ankica Braun: None; Lei Yan: None; Xinhai Zhang: None; Vijaya Reddy: None; Paolo Gattuso: None; Indu Agarwal: None

Background: Currently, there are no guidelines for axillary lymph node staging according to the morphologic subtype of breast carcinoma. We retrospectively assessed the incidence of lymph node metastasis (LNM) in invasive tubular carcinoma and invasive ductal carcinoma, no special type (IDC, NST), grade 1 to see if tubular morphology is associated with a lower incidence of LNM. Additionally, we investigated tumor stage and prognostic markers as possible predictors of LNM in these cases.

Design: We selected invasive tubular carcinomas which underwent excision at our institute from 01/2000 to 08/2021. We then stratified these into PITC (pure invasive tubular carcinoma) and invasive ductal carcinomas with tubular features (IDCTF, tubular morphology <90%). We further selected another patient group of same age range with IDC, NST, grade 1. Prognostic markers: Estrogen receptor (ER), progesterone receptor (PR), HER-2/neu, and Ki-67 were also recorded.

Results: Among group 1, 12.9% cases showed LNM including 5 macrometastasis (MM), 2 micrometastasis (MIC) and 1 isolated tumor cells (ITC). When correlating with size, none of the pT1a tumors had LNM, 18.5% of pT1b, 11.1% of pT1c, and 100% of pT2 tumors showed LNM. All the 8 cases had a favorable Ki-67, were ER+.

In group 2, 23.9% had LNM (7 MM, 2 MIC, 2 ITC). 5.8% of pT1a, 7.6% of pT1b, 44.4% of pT1c, and 71.4% of pT2 tumors showed LNM. Of these 11 cases, 90.9% were ER+ and 25% had either intermediate or unfavorable Ki-67.

In group 3, 19.4% showed LNM (13 MM and 1 MIC). 0% of pT1a, 7.6% of pT1b, 40% of pT1c, and 50% of pT2 tumors had LNM. 100% of these were ER+ and 21.4% had intermediate or unfavorable Ki-67.

All cases were HER-2/neu-.

Group 1 had lower rates of LNM but not statistically significant (Group 1 vs Groups 2+3, p=0.22 and Group 1+2 vs Group 3, p=0.84). Groups 2 and 3 showed significant higher LNM in tumors >5 mm than tumors 5 mm but slightly short of statistical significance (p=0.09). See figure 1 , 2 and Table.

	Group 1: PITC	Group 2: IDCTF	Group 3: IDC, NST, grade 1
Total cases	101	70	101
Sentinal lymph nodes examined	52/101 (51.4%)	37/70 (52.8%)	63/101 (72.3%)
Axillary lymph node dissection	10/101 (9.9%)	9/70 (12.8%)	9/101 (15%)
Both sentinal and axillary dissection	1/101 (1%)	2/70 (2.8%)	3/101(2.9%)
Nodal metastatses	8/62 (12.9%)	11/46 (23.9%)	14/72 (19.4%)
pT1a lesions with nodal metastatsis	0/16 (0%)	1/17 (5.8%)	0/19 (0%)
pT1b lesions with nodal metastasis	5/27 (18.5%)	1/13 (7.6%)	2/25 (7.6%)
pT1c lesions with nodal metastasis	2/18 (11.1%)	4/9 (44.4%)	8/20 (40%)
pT2 lesions with nodal metastasis	1/1(100%)	5/7(71.4%)	4/8(50%)
ER positive	98/99(98.9%)	64/65(98.4%)	101/101(100%)
PR positive	87/98(88.7%)	52/65(80%)	84/101(83.2%)
Her-2 positive	0/97(0%)	0/65(0%)	0/98(0%)
Ki-67: Low (<10%)	91/99(91.9%)	52/65(80%)	86/98(87.8)
Ki-67: Intermediate (10-20%)	6/99(6%)	8/65(12.3%)	10/98(10.2%)
Ki-67: High (>20%)	2/99(2%)	5/65(7.6%)	2/98(2%)
Age	37-84 (median 60)	34-88 (median 57)	37-84 (median 62)

Figure 1 - 132
Correlation of size of tumor with lymph node metastases

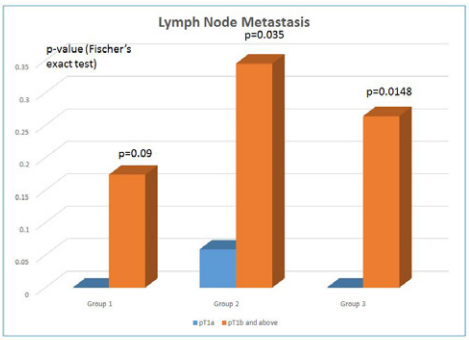

Figure 2 - 132
Correlation of intermediate or unfavorable Ki67 with lymph node metastases

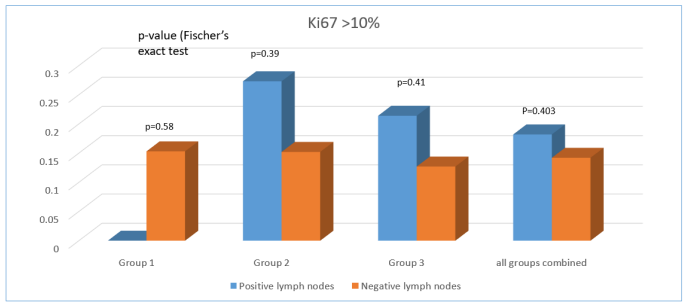

Conclusions: PITC had the lowest rate of LNM, compared to IDCTF and IDC, NST, but not statistically significant. The most important factor influencing LNM was tumor stage with higher LNM in tumors >5 mm. Prognostic markers including Ki67 did not correlate with LNM. Decision of adjuvant chemotherapy depends on nodal status in PITC and since LNM was not statistically lower in this group, lymph node examination remains crucial. Omission of nodal staging can be considered by in pT1a tumors on a case to case basis.

133 Trichorhinophalangeal Syndrome Type 1 (TRPS1) Expression in Male Breast Cancer

Timothy Law[1], Qingqing Ding[1], Matthew Piotrowski[1], Jing Ning[1], Xinyang Jiang[1], Aysegul Sahin[1]
[1]The University of Texas MD Anderson Cancer Center, Houston, TX

Disclosures: Timothy Law: None; Qingqing Ding: None; Matthew Piotrowski: None; Jing Ning: None; Xinyang Jiang: None; Aysegul Sahin: None

Background: Invasive carcinoma of the male breast is a rare malignant neoplasm that accounts for <1% of all breast cancers. It is clinically important to distinguish between primary and metastatic carcinoma in the breast, but the reliability of differentiating these two entities is not optimal. From a histologic standpoint, primary breast carcinoma can resemble carcinoma from other organ systems and can become exceedingly difficult when the tumor exhibits high-grade morphology. Unfortunately, there is no readily available immunohistochemical stain that offers optimal sensitivity and specificity in the detection of a breast primary. While GATA3 is the most used marker to determine breast origin, it has a low sensitivity in detecting triple negative (negative ER, PR, and HER2) breast carcinomas (TNBC). Recently, trichorhinophalangeal syndrome type 1 (TRPS1) was described as a highly sensitive and specific marker for female breast carcinoma. In this study, we investigated the expression profile of TRPS1, GATA3, and AR in cases of primary male breast carcinoma.

Design: We selected 70 cases of primary male breast carcinoma from our institutional database collected from 2010-2020. Case information including ER, PR, and HER2 status were recorded. A representative block of each case containing tumor was selected and stained with TRPS1, GATA3, and AR. Only nuclear staining was counted as positive. The immunoreactivity scores were calculated semi-quantitatively and categorized as negative (<1%), low positive (1-10%), intermediate positive (11-50%), and high positive (>50%).

Results: A total of 64 cases of male breast carcinoma were ER and/or PR+ and HER2-. 97% of these cases showed intermediate-to-high positive staining for TRPS1 or GATA3. 94% of these cases showed intermediate or high positive staining for AR. A total of five cases were HER2+. 100% of these cases showed intermediate or high positive staining for TRPS1, GATA3, and AR. In the only one TNBC case, TRPS1 was high positive, GATA3 was negative, and AR was intermediate positive (Table 1). Figure 1 shows representative cases of male breast carcinoma with TRPS1, GATA3, and AR staining.

Table 1. TRPS1, GATA3, and AR Expression in Male Breast Cancer

		Negative	Positive			Total
			Low	Intermediate	High	
TRPS1						
	ER/PR+	1 (1.5%)	1 (1.5%)	3 (5%)	59 (92%)	64
	HER2+	0	0	1 (20%)	4 (80%)	5
	TNBC	0	0	0	1 (100%)	1
GATA3						
	ER/PR+	2 (3%)	0	0	62 (97%)	64
	HER2+	0	0	0	5 (100%)	5
	TNBC	1 (100%)	0	0	0	1
AR						
	ER/PR+	0	4 (6%)	11 (17%)	49 (77%)	64
	HER2+	0	0	1 (20%)	4 (80%)	5
	TNBC	0	0	1 (100%)	0	1

Figure 1 - 133

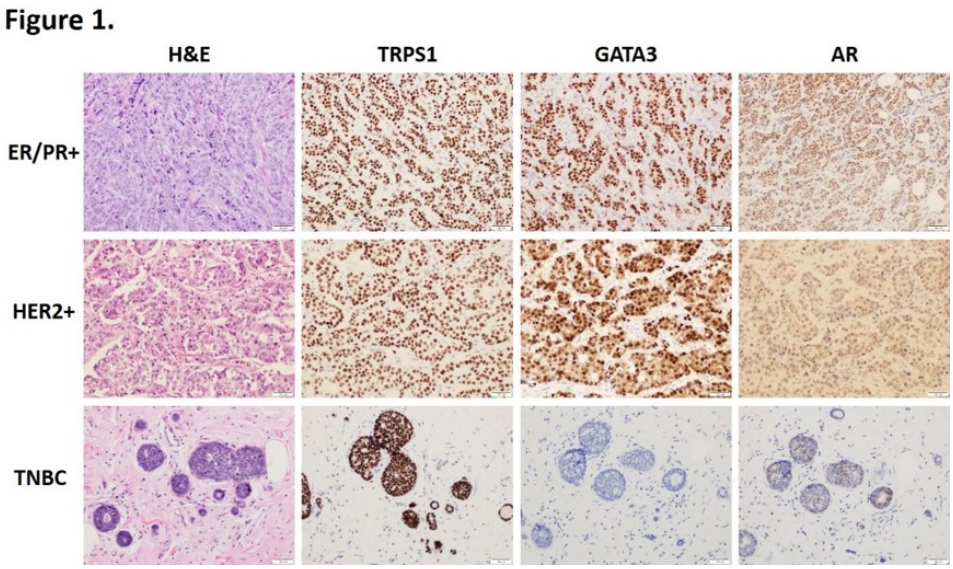

Conclusions: The results show that TRPS1 and GATA3 can be utilized as complementary markers in the identification of primary male breast carcinoma. Additionally, TRPS1 offers greater potential in the diagnosis of triple negative male breast cancer.

134 Automatic Histological Grading of Breast Cancer Resection Tissue

Geongyu Lee[1], Chung-Yeul Kim[2], Tae-Yeong Kwak[3], Sun Woo Kim[1], Hyeyoon Chang[1]
[1]Deep Bio Inc., Seoul, South Korea, [2]Korea University, Guro-gu, South Korea, [3]Deep Bio Inc., Guro-gu, South Korea

Disclosures: Geongyu Lee: *Employee*, Deep Bio Inc.; Chung-Yeul Kim: None; Tae-Yeong Kwak: *Employee*, Deep Bio Inc.; Sun Woo Kim: *Stock Ownership*, Deep Bio Inc.; Hyeyoon Chang: *Employee*, Deep Bio Inc.

Background: Histology grade of breast cancer including tubular formations, nuclear grade, and mitotic activity, is an important prognostic factor. However, the interobserver variability between the pathologists is of clinical concern. In this study, we introduced a generalized model which produces consistent results by learning from the grading of a specialist for hormone-positive, HER2-negative, and node-negative patients using deep learning.

Design: In this study, we used 125 hematoxylin and eosin (H&E) stained whole slide images (WSIs). The histology grading and the region level annotations of invasive tumors were provided by an experienced pathologist. Each WSI is divided into 512x512 patches on the model and we split the whole dataset into 8:2 (293,637: 69,634) patches for training, and the test If the patch is an invasive tumor, then our model defines the histology grade for each patch.

Results: Table 1 shows the confusion matrix of histology grade and shows the value that is calculated by the confusion matrix of histology. The column shows the actual histology grade, while the row shows the predicted histology grade from the model. Figure 1 shows how individual patches were classified by the algorithm. From left to right, each column shows the grade 1, grade 2, and grade 3 patches. Figure 2 is a Class Activation Map (CAM) that shows which part of the image the deep learning model watched and classified into the corresponding class.

		Histology grade			
		Benign	1	2	3
Prediction	Benign	50192	348	608	126
	1	756	3576	708	85
	2	362	1028	5744	1212
	3	139	0	1493	3257
Accuracy		0.966	0.958	0.922	0.956
Sensitivity		0.976	0.722	0.672	0.696
Specificity		0.941	0.976	0.957	0.975
PPV		0.979	0.698	0.688	0.666

Figure 1 - 134

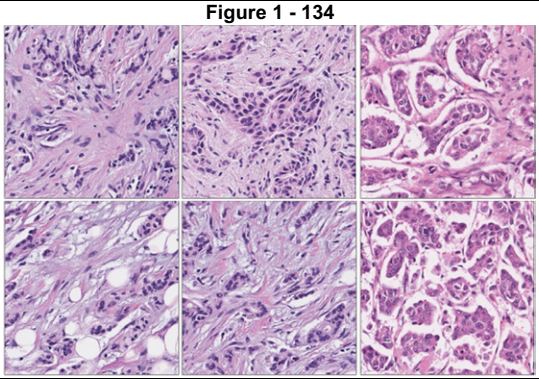

Figure 2 - 134

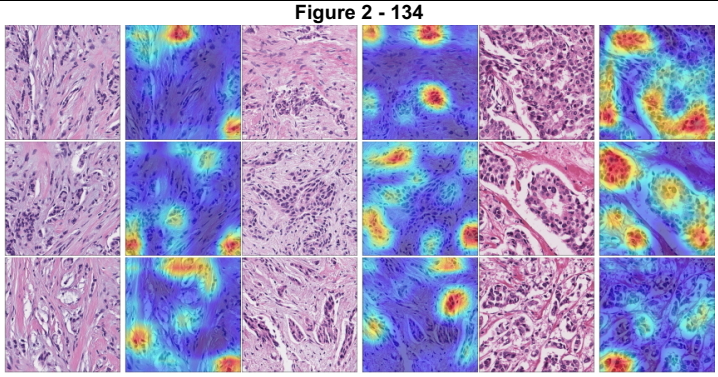

Conclusions: In this study, we introduced an automatic histology grading system of breast cancer to reduce interobserver variability and make a consistent diagnosis using deep learning. Further studies using larger numbers of data and establishing strong reference standards are needed for evaluating the model's performance.

135 Breast Cancer Survival Analysis through the Extracted Feature from the Prostate Diagnosis Model

Joonho Lee[1], Geongyu Lee[1], Tae-Yeong Kwak[2], Sun Woo Kim[1], Hyeyoon Chang[1]
[1]Deep Bio Inc., Seoul, South Korea, [2]Deep Bio Inc., Guro-gu, South Korea

Disclosures: Joonho Lee: *Employee*, Deep Bio Inc.; Geongyu Lee: *Employee*, Deep Bio Inc.; Tae-Yeong Kwak: *Employee*, Deep Bio Inc.; Sun Woo Kim: *Stock Ownership*, DeepBio; Hyeyoon Chang: *Employee*, Deep Bio Inc.

Background: Breast cancer is a common disease in women and one of the leading causes of death. To analyze how the histomorphological features of cancer lesions are related to the survival of patients, we developed a deep learning model that predicts death risk by analyzing hematoxylin and eosin stained whole slide images(WSIs) of breast cancer. To get better pathological features we used the pre-trained prostate diagnosis model rather than the other general models that are pre-trained based on the general images.

Design: The data analyzed in this study was from The Cancer Genome Atlas's breast cancer data set (TCGA-BRCA). There were 1000 WSIs labeled with survival events and periods, among which randomly sampled 640 WSI's tumor regions were annotated by an experienced pathologist and used. There existed 63 uncensored data, and we split the whole dataset into 6:2:2 for training, validation, and testing. Each WSI was divided in to 256*256 size patches. After random sampling of patches, morphological features were extracted using the prostate cancer diagnosis model and clustered based on their similarities to constitute cluster-wise feature tensors. Then the attention-based multi-instance learning was applied to train the survival model. The trained model returned a risk score for each patient.

Results: The C-index for the test set was 0.628. Figure 1 shows the Kaplan-Meir curves that compares the top 30% of the risk group and low 70% of the risk group. The p-value was 0.0143 for the log-rank test.

Figure 2 shows the patches that affect the most to classify certain patients as high-risk groups or low-risk. Patches above show the high-risk patients' patches, and the patches below show the low-risk patient's patches.

Figure 1 - 135

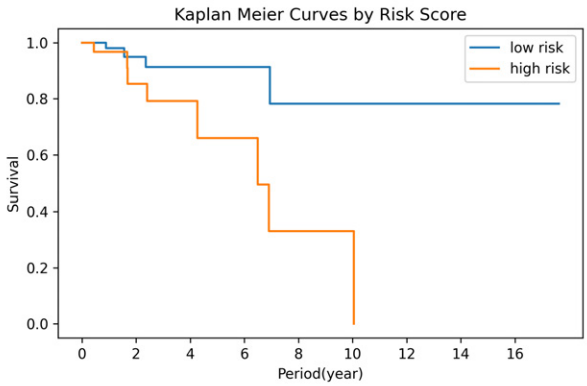

Figure 2 - 135

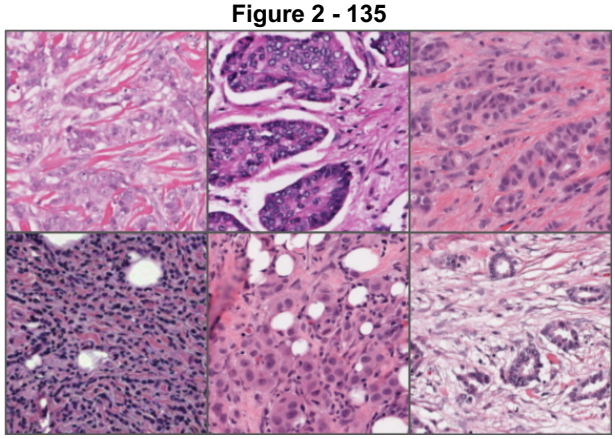

Conclusions: We conducted an experiment to evaluate if the results of analyzing the histomorphological features of breast cancer using a diagnostic model learned from prostate cancer WSI can be applied to the survival analysis of breast cancer.

Through this study, we found that the analysis of the model that learned the features of prostate morphology had some correlation with breast survival prediction, and we could see the possibility of transferability of histomorphological knowledge trained from prostate cancer grading.

136 Artificial Intelligence Assisted to Evaluate the Immunotherapy Microenvironment of Breast Cancer

Jinze Li[1], Hui Xing[1], Yueping Liu[1]
[1]*The Fourth Hospital of Hebei Medical University, Shijiazhuang, China*

Disclosures: Jinze Li: None; Hui Xing: None; Yueping Liu: None

Background: Tumor infiltrating lymphocytes (TILs) in the tumor microenvironment (TME) play a key role in immune surveillance and immune tolerance. The PD-1/PD-L1 pathway is an important mechanism of immunosuppression in the tumor microenvironment. However, current breast pathologists lack accuracy and repeatability in the visual quantitative assessment of TILs and PD-L1 (DAKO 22C3) CPS scores. Based on this, this study aims to compare visual assessment (VA) and artificial intelligence(AI) microscope-assisted interpretation of the difference and consistency of TILs and PD-L1 (DAKO 22C3) CPS scores, to explore whether artificial intelligence microscopes can improve interpretation consistency between pathologists.

Design: This study included 100 patients diagnosed with invasive breast cancer without neoadjuvant treatment and undergoing surgical resection. Nine pathologists of different levels used VA and AI to assist in the evaluation of TILs and PD-L1 in TNBC patients. In this study, SPSS 26.0, Friedman M and Bonferroni correction were used for statistical analysis and difference analysis, and intra-group correlation coefficients and Bland-Altman scatter plots were used for consistency research.

Results: Both in TILs and PD-L1, there were significant differences in the interpretation results of the 9 pathologists in the VA group ($P<0.001$). After the assistance of artificial intelligence microscopes, there was no significant difference in the interpretation results. Through the consistency test analysis, it can be seen that the ICC between the interpretation results of TILs and PD-L1 of TNBC patients by intermediate and senior pathologists is greater than 0.8, which has good consistency; the ICC between primary pathologists is less than 0.7, and the consistency is poor. All pathologists in the AI-assisted group had an ICC between the interpretation results of TILs and PD-L1 and the gold standard higher than 0.9, all with excellent repeatability.

Figure 1 - 136

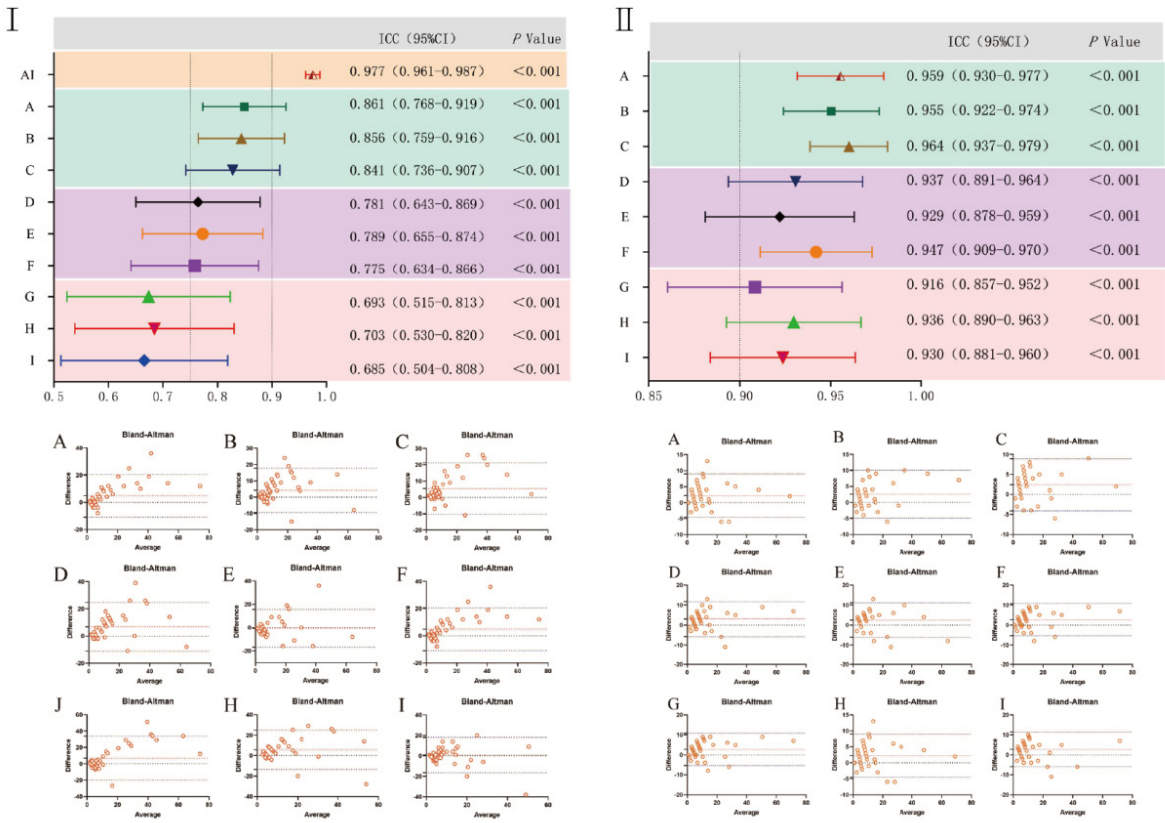

Figure 2 – 136

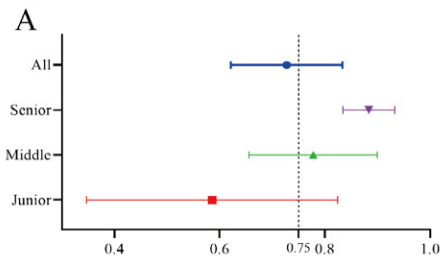

	ICC (95%CI)	*P value*
All	0.736 (0.617-0.829)	*P*<0.001
Senior	0.889 (0.832-0.930)	*P<0.001*
Middle	0.800 (0.646-0.887)	*P*<0.001
Junior	0.631 (0.327-0.798)	*P*<0.001

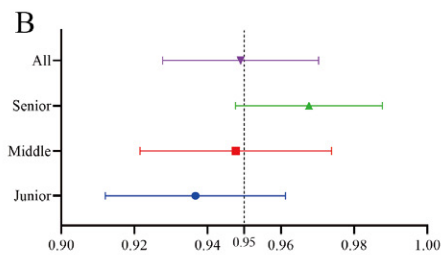

	ICC (95%CI)	*P value*
All	0.953 (0.926-0.968)	*P*<0.001
Senior	0.975 (0.945-0.983)	*P*<0.001
Middle	0.951 (0.920-0.972)	*P*<0.001
Junior	0.937 (0.909-0.964)	*P*<0.001

Conclusions: Using artificial intelligence microscope to assist the interpretation of TILs and PD-L1 (DAKO 22C3) CPS score improves the consistency of the interpretation results of pathologists at different levels, and improves the repeatability and accuracy of the interpretation results of pathologists at different levels. AI-assisted interpretation of TILs and PD-L1 of TNBC patients can help improve the accuracy of interpretation results of pathologists at all levels and reduce the gap in interpretation results.

137 Characterization of Estrogen Receptor Low Positive/Human Epidermal Growth Factor Receptor 2 Negative Breast Cancer

Ming Li[1], Hong Lv[1], Ruohong Shui[1], Hongfen Lu[1], Wentao Yang[1]
[1]*Fudan University Shanghai Cancer Center, Shanghai, China*

Disclosures: Ming Li: None; Hong Lv: None; Ruohong Shui: None; Hongfen Lu: None; Wentao Yang: None

Background: Invasive breast cancers with 1% to 10% estrogen receptor (ER) positive cells are termed as “ER Low Positive” according to the ASCO/CAP updated guideline. Forkhead box transcription factor C1 (FOXC1) expression has been identified as a specific biomarker for triple-negative breast cancer (TNBC). This study aimed to evaluate the clinicopathologic characteristics of patients with ER low positive/HER2-negative expression and investigate the diagnostic utility of FOXC1 expression in assisting their molecular subtyping.

Design: Clinicopathological data of 4328 patients diagnosed with primary invasive breast cancer from Fudan University Shanghai Cancer Center during 2019 to 2020 were collected. The clinicopathologic features of ER low positive/ HER2-negative breast cancers were characterized and compared with ER>10%/ HER2-negative and TNBC tumors. In ER low positive/HER2-negative tumors, FOXC1 expression was evaluated using immunohistochemistry and correlated with clinicopathological parameters and other markers.

Results: Among 4328 breast cancer patients, the percentage of ER>10%/ HER2-negative, ER low positive/ HER2-negative, and TNBC cases were 59.96% (2595), 1.25% (54), and13.54% (586), respectively. ER low positive/ HER2-negative tumors showed similar clinicopathologic characteristics to TNBC tumors, but significantly higher histological grade and Ki-67 index than ER>10%/ HER2-negative tumors. In the cohort of ER low positive/ HER2-negative patients, 42 cases demonstrated positive FOXC1 expression (scores≥1%), of which 32 cases showed strong staining (scores more than 40%),2 cases with moderate staining（ >10%, <40%), and 8 cases with weak staining (≤10%). FOXC1 expression was significantly associated with aggressive phenotypes: higher histological grade (p=0.01) and Ki-67 index (p<0.001). Furthermore, FOXC1 expression was significantly associated with the expression of basal markers, CK14(p=0.004) and CK5/6 (p<0.001).

Characteristics		ER low positive/HER2 negative		ER ＞10%/HER2 negative		TNBC		P value		
								ER ＞10%	ER low positive	ER ＞ 10%
		n	%	n	%	n	%	vs. ER low positive	vs. TNBC	vs. TNBC
All patients		54		2595		586				
Gender								1	1	0.234
Female	3224	54	100.00	2584	99.58	586	100.00			
Male	11	0	0.00	11	0.42	0	0.00			
Age								0.141	0.142	0.889
＜50	1416	29	53.70	1133	43.66	254	43.34			
≥50	1819	25	46.30	1462	56.34	332	56.66			
Histological grade								＜0.001	0.77	＜0.001
G1, G2	2097	11	20.37	1957	75.41	129	22.01			
G3	1132	43	79.63	634	24.43	455	77.65			
unavailable	6	0	0.00	4	0.15	2	0.34			
Tumor Size								0.484	0.845	＜0.001
≤2	1590	24	44.44	1335	51.45	231	39.42			
2–5	1525	29	53.70	1160	44.70	336	57.34			
>5	101	1	1.85	84	3.24	16	2.73			
unavailable	18	0	0.00	15	0.58	3	0.51			
Lymph node status								0.786	0.315	0.023
pN0	1543	24	44.44	1220	47.01	299	51.02			
N1-3	1372	24	44.44	1127	43.43	221	37.71			
unavailable	320	6	11.11	248	9.56	66	11.26			
Ki 67								＜0.001	0.37	＜0.001
low	1736	6	11.11	1638	63.12	92	15.70			
high	1498	48	88.89	956	36.84	494	84.30			
unavailable	1	0	0.00	1	0.04	0	0.00			

Conclusions: Primary breast cancer patients with ER low positive/HER2-negative manifest poorer clinicopathological characteristics compared with those with ER>10%/HER2 negative, while similar to TNBC. FOXC1, a TNBC specific marker, has a higher positive rate in ER low positive/HER2-negative patients. Thus, incorporation of FOXC1 testing might help to identify the intrinsic molecular subtype and may act as a complement to ER testing in the decision-making of endocrine therapy for the category of patients with ER low positive/HER2-negative expression.

138 Gene Expression Profile of Cellular Fibroadenomas and Phyllodes Tumor of the Breast

Xiaomo Li[1], Armando Giuliano[2], Eric Vail[1], Horacio Maluf[1], Farnaz Dadmanesh[1]
[1]Cedars-Sinai Medical Center, Los Angeles, CA, [2]Cedars-Sinai Medical Center, West Hollywood, CA

Disclosures: Xiaomo Li: None; Armando Giuliano: None; Eric Vail: None; Horacio Maluf: None; Farnaz Dadmanesh: None

Background: Breast fibroepithelial lesions (FELs) are a heterogeneous group ranging from benign fibroadenomas (FA) to malignant phyllodes tumors (PT). Despite published criteria for distinguishing cellular FA from PT, diagnostic challenges remain. A variety of mutations (eg, MED12 and RARA) have been found in FA and PT; however, the landscape of genetic alterations remains unclear. The molecular profiles of cellular FA, benign PTs, and borderline PTs were examined to gain further understanding of these lesions.

Design: 32 cases of FELs were selected from our files between 2017 and 2021, which included 4 FA, 9 cellular FA, 8 benign PT, 7 borderline PT, and 4 malignant PT. Slides from all cases were reviewed by two breast pathologists applying WHO guidelines to confirm the diagnosis. Total RNA was extracted from paraffin-fixed specimens. The expression of 750 tumor-related genes was measured using the nCounter platform. Rosalind platform was used for principal component and differential expression analyses. Statistical significance was defined as P less than or equal to 0.05.

Results: In gene set analysis, matrix remodeling, cell proliferation, hypoxia, angiogenesis, and PI3K-Akt pathway-related genes are found highly expressed in malignant PTs and less expressed in borderline, benign PTs, and FAs. The genetic profile of benign PTs, cellular FAs, and FA are very similar. A slight difference was observed between benign and borderline PTs. The macrophage cell abundance scores and CCL5 are significantly higher in malignant phyllodes tumors compared with all other groups.

Figure 1 - 138

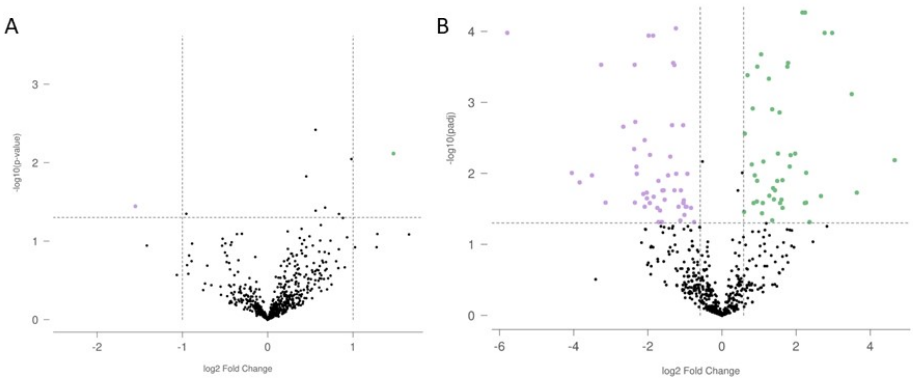

Figure 1. Volcano plots show similar gene expression level when comparing cellular fibroadenoma with benign phyllodes tumors (A), distinctive gene expression level when comparing benign phyllodes tumors with malignant phyllodes tumors (B). X axis represents log2 of the gene expression level difference between two groups; Y axis represents the p value; dot line is at p=0.05.

Figure 2 – 138

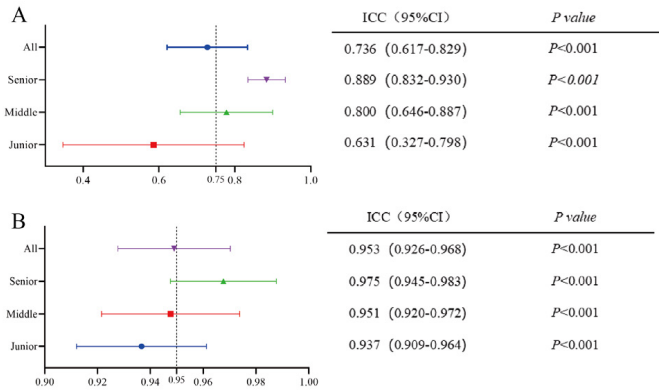

Conclusions: The overall gene expression profile of benign PTs, cellular FAs, and FAs was very similar. While there was a slight difference in genomic profiling of borderline versus benign PTs, a more significant difference was observed in relation to malignant PTs. The increased macrophage abundance score and CCL5 seen in malignant PT may provide insights into the carcinogenesis of this lesion. These results suggest that gene expression profiling may improve understanding of the pathogenesis and classification of breast fibroepithelial lesions which could lead to more appropriate clinical management.

139 Cystic Neutrophilic Granulomatous Mastitis: Further Characterizing Clinicopathological Features, Large Cohort in a Single Institute

Yuanxin Liang[1], Haiying Zhan[2], Tong Sun[1]
[1]Yale School of Medicine, New Haven, CT, [2]Yale New Haven Hospital, Yale School of Medicine, New Haven, CT

Disclosures: Yuanxin Liang: None; Haiying Zhan: None; Tong Sun: None

Background: Cystic Neutrophilic Granulomatous Mastitis (CNGM) is a rare subtype of mastitis with highly distinct histological pattern which has been correlated to *Coreynebacterium* species. Though the diagnostic criteria have been proposed, clinical and demographic risk factors associated with CNGM remain largely unknown due to rarity of the disease. In current study, we performed a case-control study to determine clinicopathological characteristics of CNGM.

Design: This study was conducted under an IRB-approved protocol. A search of surgical pathology archives over 8-year period was performed for breast biopsy or resection specimens with term “granulomatous mastitis” or “granulomatous inflammation” in final diagnosis. Histologic slides were revied by 2 breast pathologists. Only cases showing CNGM histological classic features were included in cases group (n =31). The cases showing granulomatous inflammation without any CNGM morphological features were included in control group (n = 30). Correlative demographic, clinical, radiological, pathological, management, and outcome information were scrutinized and summarized in Table 1. Statistical analysis was performed using Graphpad Prism 8. Two-tailed t-test and chi-square analysis were employed to compare between two groups.

Results: Comparing to nonspecific granulomatous mastitis, patients with CNGM tend to be younger (38 y vs 43 y, p=0.03), have a larger size of breast mass by imaging study (4.6 cm versus 1.9 cm, p <0.001). The detection rate for Corynebacterium and other reported associated bacteria was significantly higher in patients with CNGM (p<0.001). The clinical resolving time for patients with CNGM was much prolonged comparing to control group. Interestingly, our data for the first time showed that CNGM was not associated with smoking history. Additionally different from previous studies, CNGM was not found to be associated with lactation status, recent pregnancy or Hispanic ethnicity (P values all > 0.05) in our study.

Table 1. Comparison of Demographic and Clinicopathological Characteristics Between Cystic Neutrophilic Granulomatous Mastitis (CNGM) and Other non-CNGM Granulomatous Mastitis

Characteristic		CNGM	Other non-CNGM Granulomatous Mastitis	*P* value
Total (N)		31	30	
Demographic and clinical characteristics				
Age (median, range) years		38 (24 - 71)	43 (24 - 73)	0.03
Self-reported ethnicity	Caucasian	12 (39 %)	8 (27%)	0.65
	American African	6 (19 %)	10 (33 %)	
	Hispanic or Latino	10 (32 %)	10 (33 %)	
	Asian	3 (10 %)	2 (7 %)	
	Other	0 (0 %)	1 (3 %)	
BMI (median, range)		31 (19 - 54)	30 (22 - 49)	0.64
Ever Smoker		3 (9 %)	12 (40 %)	< 0.01
Current or recent nursing, N (%)		0 (0 %)	3 (10 %)	0.13
Nulliparous		2 (6%)	4 (13 %)	0.68
Time since last birth (median, range) years		7 (0 -35)*	6 (0.1 -38)	0.84
Prior procedure at same side breast, N (%)		3 (10 %)	5 (17 %)	0.47
Painful lesion		30 (97 %)	23 (77 %)	0.03
Laterality	Left	19 (61 %)	12 (40 %)	0.24
	Right	11 (36 %)	16 (53 %)	
	Bilateral	1 (3 %)	2 (7 %)	
Radiological findings				
Mass like lesion		28 (90 %)	24 (80 %)	0.30
Size by imaging (median, range) cm		4.6 (1.5-12)	1.9 (0.8-4.8)	< 0.001
BI-RADS score	<= 3	6 (19 %)	14 (47 %)	0.03
	4 or 5	25 (81 %)	16 (53 %)	
Pathological findings				
Bacteria present at H&E		13 (42 %)	0 (0 %)	< 0.001
Special stain positive for any bacteria		14 (45 %)	1 (3 %)	< 0.001
Culture	Positive for Corynebacterium	11 (36 %)	0 (0 %)	< 0.001
	Positive for other bacteria	3 (10 %)	6 (20 %)	
	Negative	14 (45 %)	20 (67 %)	
Treatment	Antibiotics	29 (94 %)	24 (80 %)	Not done
	Steroid	2 (6 %)	1 (3 %)	
	Drainage	8 (26 %)	8 (27 %)	
	Resection	4 (13 %)	3 (3 %)	
Resolving time (median, range) months		12 (4-54)	6 (3 -11)	< 0.001

*Including 2 pregnant patients

Figure 1. Representative Histopathologic Findings. (A-C). An Example of Cystic Neutrophilic Granulomatous Mastitis (A, low power; B, high power and C, GMS stain). (D-E). Other Types of Granulomatous Mastitis. An Example of Granulomatous Mastitis Due to Cyst Rupture. (D, low power and E, high power with multinucleated giant cells)

Figure 1 - 139

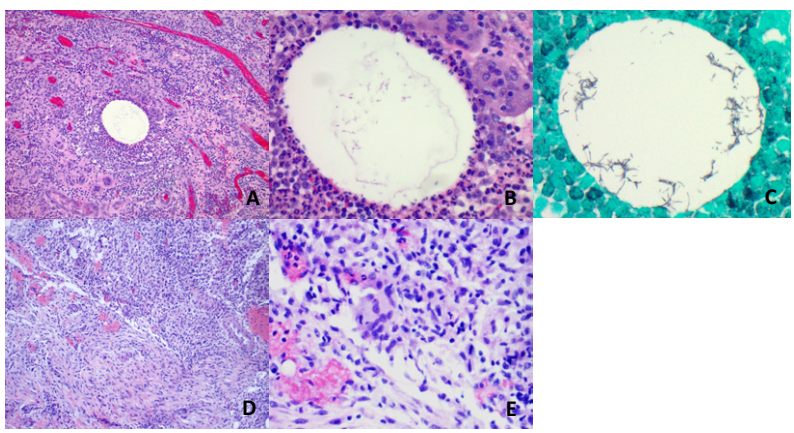

Conclusions: Our data demonstrated CNGM as a unique infectious disease with specific clinical and radiological features. Recognizing these features would help accuracy of pathological diagnosis and guidance better treatment.

140 Semi-Automated Analysis of HER2 Immunohistochemistry in Invasive Breast Carcinoma using Whole Slide Images: Utility for Training, Interpretation and Treatment

Chiu-Hsiang Liao[1], Emine Cesmecioglu[1], Kareem Ibrahim[1], Matthew Hanna[1], Fresia Pareja[1], Hannah Wen[1], Timothy D'Alfonso[1], Edi Brogi[1], Yukako Yagi[1], Dara Ross[1]
[1]Memorial Sloan Kettering Cancer Center, New York, NY

Disclosures: Chiu-Hsiang Liao: None; Emine Cesmecioglu: None; Kareem Ibrahim: None; Matthew Hanna: *Consultant*, Paige, PathPresenter; Fresia Pareja: None; Hannah Wen: *Consultant*, AstraZeneca, Merck; Timothy D'Alfonso: None; Edi Brogi: None; Yukako Yagi: None; Dara Ross: None

Background: Human epidermal growth factor receptor 2 (HER2) overexpression is a strong prognostic and predictive biomarker in invasive breast cancer (IBC), tested by immunohistochemistry (IHC) and/or in situ hybridization (ISH) per ASCO/CAP. HER2 IHC interpretation is subjective, with training needed for accurate reporting. The HER2 IHC scoring algorithm includes percentage, completeness, intensity and uniformity of membrane staining in IBC, with scores 0 or 1+ (negative), 2+ (equivocal) and 3+ (positive). Anti-HER2 monoclonal antibodies have revolutionized treatment of HER2-positive IBC and evolution of antibody-drug conjugates for HER2 low-expressing IBC (IHC 2+/ISH-, IHC 1+/ISH-) makes distinction between IHC 0 to 2+ crucial. The project aim was to validate a semi-automated computational model to assist in HER2 IHC interpretation using QuantCenter (QC) software developed by 3DHISTECH Ltd. (Budapest, Hungary).

Design: A calibration dataset with HER2 IHC scores 0 to 3+ and fluorescence ISH (FISH) was used. H&E and IHC whole slide images (WSI) with 0.5-0.26/pixel resolution were scanned by Leica AT2 or GT450 for diagnostic use; images were downloaded and converted into 3DHISTECH format. IBC regions of interest were manually annotated and IHC scores were generated by QC. H-scores [(3x%IHC3+)+(2x%IHC2+)+(1x%IHC1+)] were calculated for microscopic (Mx) (glass slides) and automated (WSI) analysis (Table 1). Primary endpoint was comparing HER2 IHC Mx scoring with semi-automated scoring by QC.

Results: 32 cases were analyzed, including 14 HER2 FISH+, 18 HER2 FISH- (Table 1). All (9) Mx IHC 3+ IBC were scored 3+ by QC. For Mx IHC 2+/FISH+ IBC (5), QC scored 4 as 2+ and 1 as 3+; the QC 3+ IBC had Mx H-score 200 (5% 3+, 90% 2+, 5% 1+), QC H-score 181 (23% 3+, 37% 2+, 38% 1+, 2% 0). For IHC 2+/FISH- IBC (8), QC scored 7 as 2+ and 1 as 1+; the QC 1+ IBC had Mx H-score 120 (0% 3+, 30% 2+, 60% 1+, 10% 0), QC H-score 45 (0.01% 3+, 9.9% 2+, 25% 1+, 65% 0). For Mx IHC 1+/FISH- (4), QC scored all as 1+. For Mx IHC 0/FISH- (6), QC scored 3 as 0 and 3 as 1+. Figure 1 displays IHC/QC images.

Table 1: Comparison of HER2 IHC scores by microscopic and semi-automated analysis.

FISH	Microscopic HER2 IHC Score				3DHISTECH HER2 IHC Score			
	0	1+	2+	3+	0	1+	2+	3+
AMPLIFIED, N (%)	0 (0%)	0 (0%)	5 (16%)	9 (28%)	0 (0%)	0 (0%)	4 (13%)	10 (31%)
H-SCORE, Median (range)	N/A	N/A	183 (130-200)	260 (180-280)	N/A	N/A	127.5 (99-185)	174 (88-190)
NON-AMPLIFIED, N (%)	6 (19%)	4 (12%)	8 (25%)	0 (0%)	3 (9%)	8 (25%)	7 (22%)	0 (0%)
H-SCORE, Median (range)	0 (0-5)	75 (60-80)	135 (110-200)	N/A	0 (0-0)	42.5 (18-80)	117 (62-156)	N/A

Figure 1 - 140

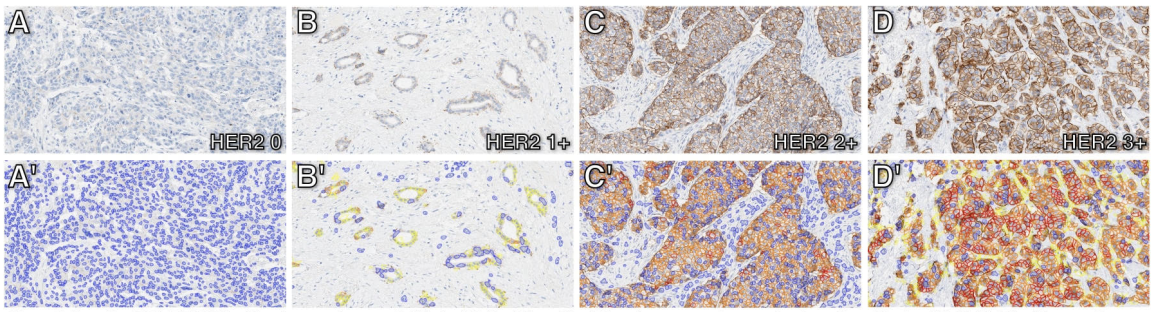

Figure 1: Invasive BC HER2 IHC with microscopic score 0 (A), 1+ (B), 2+ (C) and 3+ (D) and corresponding overlay from QuantCenter (A', B', C', D') with score 3 highlighted by red, score 2 orange, score 1 yellow and score 0 blue.

Conclusions: Semi-automated analysis using WSI and microscopic assessment yield similar HER2 IHC scores, particularly for 2+ and 3+, showing utility of this tool for training, interpretation and accurate treatment. Distinguishing HER2 IHC 0 from 1+ remains challenging, even with computational tools, highlighting the limitations of existing HER2 assays in detecting HER2 low IBC. Further studies for IHC scores 0 and 1+ are needed.

141 Utility of Exhaustive Search for Microcalcification in Breast Biopsies

Chiu-Hsiang Liao[1], Sandra Brennan[1], Edi Brogi[1], Hannah Wen[1]
[1]*Memorial Sloan Kettering Cancer Center, New York, NY*

Disclosures: Chiu-Hsiang Liao: None; Sandra Brennan: None; Edi Brogi: None; Hannah Wen: *Consultant*, AstraZeneca, Merck

Background: Mammography detected calcification (Ca++) is a frequent biopsy target. Ca++ can be associated with benign or malignant lesions. It is standard practice in breast pathology to identify microscopic Ca++ corresponding to radiographic findings and comment on lesions associated with Ca++. At our institution, three initial H&E slides are routinely examined. If the initial examination does not reveal Ca++, or the microscopic Ca++ does not account for the radiographic Ca++, the pathologists have the option to send the tissue blocks for specimen radiograph and multiple levels are obtained accordingly. The goal of this study is to investigate the yield of such exhaustive search of Ca++.

Design: 109 consecutive core biopsies (97 patients) for mammographic Ca++ that required radiographic examination of the tissue blocks were identified. Patient demographics, mammographic findings and pathological diagnosis were obtained from medical records. The highest risk diagnosis and the histological findings associated with the targeted Ca++ were documented.

Results: Between 10/2018 and 06/2021, 3804 stereotactic core biopsies were performed. Of which, 109 biopsies from 97 patients had tissue blocks sent for specimen radiograph. Median patient age was 52 (30-85). 48% and 24% patients had history of ipsilateral and contralateral carcinoma respectively. The median size of targeted Ca++ on mammography was 0.8 cm (0.1-9.2 cm). A total of 291 blocks from 109 biopsies (97 patients) were sent for radiographical examination and 120 blocks from 78 biopsies (70 patients) were found to have Ca++. Additional 1255 H&E levels were performed on 154 blocks (median 8 (range 3-28) levels per block). Most biopsies had benign diagnosis (83%, 90/109). The highest risk diagnoses included invasive carcinoma (IC, 1.8%; 2/109, one of which is microinvasive), ductal carcinoma in situ (DCIS, 4.6%; 5/109), atypical ductal hyperplasia (ADH, 3.6%; 4/109), lobular neoplasia in situ (ALH/LCIS, classic 6.4%; 7/109, pleomorphic 1%, 1/109) (Table 1). Additional pathological findings that changed clinical management were detected only in 2 cases (1 DCIS and 1 ADH) after radiographic localization of the Ca++ and additional levels.

Table 1: Highest risk diagnoses in biopsies and the histological findings associated with the targeted calcifications.

	Total N (%)	Calcifications in invasive carcinoma	Calcifications in DCIS	Calcifications in benign high-risk lesions	Calcifications in benign	No calcification seen
Invasive carcinoma	2 (1.8%)	1/2 with IC and DCIS		-	-	1/2
DCIS	5 (4.6%)	-	1/5	-	3/5	1/5
ADH	4 (3.7%)	-	-	2/4	-	2/4
LCIS, pleomorphic	1 (1%)	-	-	-	1/1	-
ALH/classic LCIS	7 (6.4%)	-	-		5/7	2/7
FEA	0 (0%)	-	-	-	-	-
Radial scar	0 (0%)	-	-	-	-	-
Papilloma	0 (0%)	-	-	-	-	-
Benign	90 (83%)	-	-	-	60/90 (67%)	30/90 (33%)

Conclusions: Most of the cases in this study had a benign diagnosis. In cases with high risk-lesions, majority of Ca++ were associated with a benign process (79%, 15/19). Additional pathological findings that changed clinical management were only detected in 1.8% (2/109) of the biopsies after exhaustive search of Ca++.

142 Comparative Analysis of PD-L1 Expression and Tumor-Infiltrating Lymphocytes in Metaplastic Breast Carcinoma and Gynecologic Carcinosarcoma: A Single-Institution Retrospective Study

Michelle Lin[1], Paloma Monroig-Bosque[2], Donna Coffey[1], Susan Haley[1], Ekene Okoye[1], Michael Deavers[1], Mary Schwartz[1], Suzanne Crumley[1]

[1]Houston Methodist Hospital, Houston, TX, [2]Houston Methodist Hospital, Pearland, TX

Disclosures: Michelle Lin: None; Paloma Monroig-Bosque: None; Donna Coffey: None; Susan Haley: None; Ekene Okoye: None; Michael Deavers: None; Mary Schwartz: None; Suzanne Crumley: None

Background: Metaplastic breast carcinoma (MBC) and gynecologic carcinosarcoma (GCS) are both characterized by differentiation of neoplastic epithelium to mesenchymal or sarcomatoid elements. Due to their rarity, heterogeneity, and typically aggressive behavior, treatment can be challenging and the potential role of immunotherapy has recently been considered. The goal of this study was to investigate PD-L1 expression and tumor-infiltrating lymphocytes (TILs) in MBC and GCS.

Design: 55 cases of MBC and GCS from 2015-2021 were identified from our institutional database. Clinicopathologic parameters including age, tumor size, stage, and histologic subtype(s) were recorded. If not already done, immunohistochemical staining for PD-L1 (clone SP142) was performed. Positive staining for PD-L1 was defined as ≥ 1% expression in tumor cells (TcPD-L1) or tumor-infiltrating immune cells (IcPD-L1). TILs were evaluated and cases were grouped as follows: 1 (0-10%), 2 (11-40%), or 3 (41-100%).

Results: PD-L1 expression was seen in 50% (14/28) of MBC (Fig. 1) and 51.9% (14/27) of GCS (Fig. 2). TcPD-L1 was significantly higher in MBC than GCS (p = 0.034); IcPD-L1 was similar in both (Table 1). For MBC and GCS, there was higher PD-L1 expression in epithelial components than in mesenchymal components (p = 0.0005). MBC with squamous differentiation had the highest rate of PD-L1 expression (61.1%, 11/18), while MBC with chondroid/osseous elements had the lowest rate (0%, 0/8). GCS with chondroid elements also had lower PD-L1 expression (0%, 0/6) than those with other sarcomatous components (18.5%, 5/27). Most cases demonstrated ≤ 10% TILs; cases with > 10% TILs had significantly higher PD-L1 expression than those with ≤ 10% TILs (p = 0.0005).

Table 1. Comparison of PD-L1 expression and tumor-infiltrating lymphocytes in metaplastic breast carcinoma and gynecologic carcinosarcoma.

	MBC*	GCS
TcPD-L1 vs. IcPD-L1		
TcPD-L1		
Any PD-L1 positivity (≥ 1%)	46.2% (12/26)	11.1% (3/27)
PD-L1 positivity ≥ 10%	26.9% (7/26)	0% (0/27)
IcPD-L1		
Any PD-L1 positivity (≥ 1%)	44.4% (12/27)	51.9% (14/27)
PD-L1 positivity ≥ 10%	14.8% (4/27)	14.8% (4/27)
PD-L1 in epithelial vs. mesenchymal component		
PD-L1 positivity in epithelial component	57.1% (12/21)	40.7% (11/27)
PD-L1 positivity in mesenchymal component	0% (0/8)	18.5% (5/27)
TILs		
Group 1: 0-10%	53.8% (14/26)	70.4% (19/27)
Group 2: 11-40%	34.6% (9/26)	18.5% (5/27)
Group 3: 41-100%	11.5% (3/26)	11.1% (3/27)
PD-L1 positivity by % TILs		
PD-L1 positivity in Group 1	28.6% (4/14)	36.8% (7/19)
PD-L1 positivity in Group 2	77.8% (7/9)	80% (4/5)
PD-L1 positivity in Group 3	100% (3/3)	100% (3/3)

MBC – metaplastic breast carcinoma; GCS – gynecologic carcinosarcoma; TcPD-L1 – PD-L1 expression in tumor cells; IcPD-L1 – PD-L1 expression in tumor-infiltrating immune cells, TILs – tumor-infiltrating lymphocytes.

* TcPD-L1 and TILs were not able to be evaluated in 2 MBC cases; IcPD-L1 was not able to be evaluated in 1 MBC case.

Figure 1 - 142

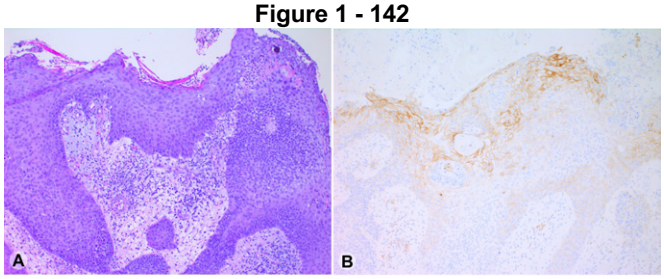

Figure 1. Metaplastic breast carcinoma with squamous differentiation (A) showing positive tumor cell staining for PD-L1 (B) (all images at 100x magnification).

Figure 2 - 142

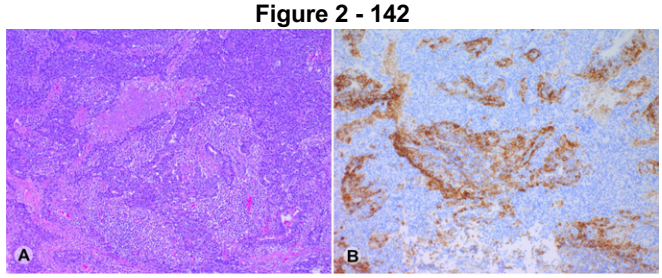

Figure 2. Carcinomatous component of gynecologic carcinosarcoma (A) showing PD-L1 staining in associated immune cells (B) (all images at 100x magnification).

Conclusions: We demonstrated a high rate of TcPD-L1 expression in MBC, in contrast to GCS; therefore, reporting TcPD-1 in addition to IcPD-L1 may be important in evaluation of MBC. In addition, we observed higher PD-L1 expression in epithelial compared to mesenchymal (particularly chondroid) elements in both MBC and GCS, indicating that sarcomatous components may be less immunogenic than carcinomatous components, which may also have further implications in the prognosis and management of these tumors. While TILs generally correlated with PD-L1 expression, there were still several cases with low TILs that demonstrated PD-L1 staining, suggesting that sole assessment of TILs may not always be predictive of PD-L1 positivity for these tumors.

143 Immunohistochemistry for Markers of Prostate and Breast Origin in Male Breast Carcinoma

Mira Lotfalla[1], Rebecca Asch-Kendrick[2], Marissa White[3], Andres Matoso[4], Pete Argani[5], Ashley Cimino-Mathews[3]
[1]Johns Hopkins Hospital, Baltimore, MD, [2]Midwest Medical Examiner's Office, MN, [3]Johns Hopkins University School of Medicine, Baltimore, MD, [4]Johns Hopkins Medical Institutions, Baltimore, MD, [5]Johns Hopkins Hospital, Ellicott City, MD

Disclosures: Mira Lotfalla: None; Rebecca Asch-Kendrick: None; Marissa White: None; Andres Matoso: None; Pete Argani: None; Ashley Cimino-Mathews: *Grant or Research Support*, Bristol-Myers Squibb

Background: Invasive ductal carcinomas in male patients (“male IDC”), although uncommon, share histologic and immunophenotypic features with invasive ductal carcinomas in female patients (“female IDC”). The differential diagnosis of male breast cancer includes metastatic prostatic adenocarcinoma to the breast. NKX3.1 is an androgen-regulated tumor suppression gene, and NKX3.1 immunohistochemistry (IHC) is largely specific for primary and metastatic prostate cancer. However, we and others have reported NKX3.1 labeling in a small percentage of female breast cancers, particularly cancers with estrogen receptor (ER) positivity, androgen receptor (AR) positivity, and lobular phenotype. Here, we evaluate the expression of NKX3.1 in male IDC, along with the expression of additional IHC markers that support prostatic or breast origin.

Design: IHC for markers that support prostatic origin (NKX3.1, PSA, P501S, AR) and breast origin (GATA3, GCDFP, mammaglobin [MMGB]) were performed on tissue microarrays (TMAs) containing 27 male IDC and 15 female IDC. All IDC were ER+. Tumors were sampled on the TMAs with five 1.4 mm cores per tumor, to include adjacent normal breast tissue.

Results: Eight (29%) of the male patients also carried a diagnosis of prostate cancer. IHC for markers of prostatic origin labeled a greater proportion of male IDC than female IDC. All cases of male and female IDC with NKX3.1 labeling were positive for GATA3 and either GCDFP or MMGB or both. The one male IDC with P501S labeling was also positive for NKX3.1, GATA3, GCDFP, and MMGB.

Table 1: Immunohistochemistry for markers of prostatic and breast origin in invasive ductal carcinomas in male and female

	ER+ n (%)	AR+ n (%)	NKX3.1+ n (%)	PSA+ n (%)	P501S+ n (%)	GCDFP-15+ n (%)	MMGB+ n (%)	GATA3+ n (%)
Male IDC (n = 27)	27 (100%)	27 (100%)	7 (26%)	0	1 (4%)	23 (85%)	14 (52%)	27 (100%)
Female IDC (n = 15)	15 (100%)	13 (86%)	1 (7%)	0	0	9 (60%)	12 (80%)	15 (100%)

Conclusions: To our knowledge, this is the first study to evaluate NKX3.1 labeling in male breast cancers. NKX3.1 labels a small but significant proportion (26%) of male IDC, which poses a potential diagnostic pitfall with metastatic prostate cancer to the breast, both of which have strong AR expression by IHC. This potential pitfall is further highlighted by the history of prostate cancer in nearly one third (29%) of male patients in this series. Labeling for both NKX3.1 and AR is more common in male IDC than female IDC, which raises the possibility of differential impact of androgen-related signaling in male and female IDC. An immunopanel to distinguish metastatic prostate cancer from primary male IDC should not be limited to markers of prostatic origin, but should also include markers of breast origin such as GATA3 and GCDFP or MMGB.

144 Correlations between PD-L1 Expression and Tumor Infiltrating Lymphocytes and Molecular Subtype in Triple-Negative Breast Cancer

Xiaoxi Ma, Chen Chen[1], Wentao Yang[1], Ruohong Shui[1]
[1]Fudan University Shanghai Cancer Center, Shanghai, China

Disclosures: Xiaoxi Ma: None; Chen Chen: None; Wentao Yang: None; Ruohong Shui: None

Background: To analyze the expression of programmed cell death 1 ligand 1 (PD-L1) in immune cells (IC)and tumor cells (TC) in triple-negative breast cancer (TNBC), and the correlation between PD-L1 expression and tumor-infiltrating lymphocytes (TILs). To explore the correlation between IC PD-L1 expression and molecular subtypes in TNBC.

Design: 430 cases of TNBC between 2008 and 2014 were extracted from Fudan University Shanghai Cancer Center. In each case, a representative tumor tissue block was selected, and the PD-L1 (Ventana SP142) antibody was used for immunohistochemical staining to detect the PD-L1 expression in IC and TC. PD-L1 positive cells accounted for more than 1% of the invasive tumor area was judged as PD-L1 positive. TILs, including intratumoral TILs (iTILs) and stromal TILs (sTILs), was scored. TNBC subtypes based on multi-omics data in this study comes from the results of a 2019 study conducted by Fudan University Shanghai Cancer Center (FUSCC), including luminal androgen receptor (LAR), immunomodulatory (IM), basal-like immune-suppressed (BLIS), and mesenchymal-like (MES). Statistical methods were used to analyze the correlation of PD-L1 expression and TILs, as well as the correlation between IC PD-L1 expression and molecular subtypes of TNBC.

Results: (1) There were 161 cases (37.4%) with positive PD-L1 expression in IC, and 93 cases (21.6%) with positive PD-L1 expression in TC. (2) PD-L1 expression in IC was significantly correlated with sTILs and iTILs (P <0.001, P <0.001). Spearman correlation analysis showed the higher the level of sTILs (r = 0.502, P <0.001) and iTILs (r = 0.410, P <0.001), the higher the expression level of PD-L1 in immune cells. The ROC curve showed that the area under the curve (AUC) of sTILs was 0.763 (95% CI 0.712-0.815, P <0.001), and the optimal threshold for sTILs to predict PD-L1 was 15%. The AUC of iTILs is 0.676 (95% CI 0.618-0.734, P <0.001), and the optimal threshold for predicting PD-L1 is 5%. (3) The expression of PD-L1 in IC was correlated with molecular subtypes of TNBC (P <0.05), and the positive expression of PD-L1 was significantly correlated with IM subtype (P <0.001).(1) There were 161 cases (37.4%) with positive PD-L1 expression in IC, and 93 cases (21.6%) with positive PD-L1 expression in TC. (2) PD-L1 expression in IC was significantly correlated with sTILs and iTILs (P <0.001, P <0.001). Spearman correlation analysis showed the higher the level of sTILs (r = 0.502, P <0.001) and iTILs (r = 0.410, P <0.001), the higher the

expression level of PD-L1 in immune cells. The ROC curve showed that the area under the curve (AUC) of sTILs was 0.763 (95% CI 0.712-0.815, P <0.001), and the optimal threshold for sTILs to predict PD-L1 was 15%. The AUC of iTILs is 0.676 (95% CI 0.618-0.734, P <0.001), and the optimal threshold for predicting PD-L1 is 5%. (3) The expression of PD-L1 in IC was correlated with molecular subtypes of TNBC (P <0.05), and the positive expression of PD-L1 was significantly correlated with IM subtype (P <0.001).(1) There were 161 cases (37.4%) with positive PD-L1 expression in IC, and 93 cases (21.6%) with positive PD-L1 expression in TC. (2) PD-L1 expression in IC was significantly correlated with sTILs and iTILs (P <0.001, P <0.001). Spearman correlation analysis showed the higher the level of sTILs (r = 0.502, P <0.001) and iTILs (r = 0.410, P <0.001), the higher the expression level of PD-L1 in immune cells. The ROC curve showed that the area under the curve (AUC) of sTILs was 0.763 (95% CI 0.712-0.815, P <0.001), and the optimal threshold for sTILs to predict PD-L1 was 15%. The AUC of iTILs is 0.676 (95% CI 0.618-0.734, P <0.001), and the optimal threshold for predicting PD-L1 is 5%. (3) The expression of PD-L1 in IC was correlated with molecular subtypes of TNBC (P <0.05), and the positive expression of PD-L1 was significantly correlated with IM subtype (P <0.001).(1) There were 161 cases (37.4%) with positive PD-L1 expression in IC, and 93 cases (21.6%) with positive PD-L1 expression in TC. (2) PD-L1 expression in IC was significantly correlated with sTILs and iTILs (P <0.001, P <0.001). Spearman correlation analysis showed the higher the level of sTILs (r = 0.502, P <0.001) and iTILs (r = 0.410, P <0.001), the higher the expression level of PD-L1 in immune cells. The ROC curve showed that the area under the curve (AUC) of sTILs was 0.763 (95% CI 0.712-0.815, P <0.001), and the optimal threshold for sTILs to predict PD-L1 was 15%. The AUC of iTILs is 0.676 (95% CI 0.618-0.734, P <0.001), and the optimal threshold for predicting PD-L1 is 5%. (3) The expression of PD-L1 in IC was correlated with molecular subtypes of TNBC (P <0.05), and the positive expression of PD-L1 was significantly correlated with IM subtype (P <0.001).

Conclusions: The expression level of PD-L1 in TNBC is positively correlated with the level of sTILs and iTILs. TILs score may be used to predict the expression of PD-L1. The positive expression of PD-L1 in IC is significantly correlated with IM subtype in TNBC, which may be related to the high expression of TILs in IM subtypes, indicating that patients with IM subtypes in TNBC may be benefited from anti-PD-1 /PDL1 immunotherapy.

145 MHC Class I and PD-L1 Expression May Predict Treatment Response to Anti-PD-1/PD-L1 Therapy in Breast Cancer Patients

Joseph Maniaci[1], Anne Mills[1], Patrick Dillon[1], Elizabeth Gaughan[2], Taylor Jenkins[2]
[1]University of Virginia, Charlottesville, VA, [2]University of Virginia Health System, Charlottesville, VA

Disclosures: Joseph Maniaci: None; Anne Mills: None; Patrick Dillon: *Primary Investigator*, Merck, Radius Pharmaceuticals, Seattle Genetics, Syndax Pharmaceuticals, Oncolytics, Daichi Sankyo, Bayer; Elizabeth Gaughan: None; Taylor Jenkins: None

Background: Although immune checkpoint inhibition has proven to be efficacious in a subset of breast cancer patients, there remains a disparity in clinical responses. Major histocompatibility complex class I (MHC I) expression has been touted as a possible predictor of response to immune checkpoint inhibition given its role in the adaptive immune system. Loss of tumoral MHC I expression in breast cancer as a potential barrier to immune checkpoint inhibition has been described; however, treatment outcome data is limited. We herein evaluate the relationship between PD-L1 and MHC I expression and response to PD-1/PD-L1 inhibitors in a cohort of treated breast cancer patients.

Design: Best treatment response was assessed in 19 breast cancer patients treated with anti-PD-1/PD-L1 immune checkpoint inhibition with or without chemotherapy. Primary and metastatic tumors were evaluated by immunohistochemistry for expression of PD-L1 and MHC I. PD-L1 was scored via the combined positive score (CPS) and tumor infiltrating cell score (TICS). MHC I was evaluated for retention, partial loss (≥10%), or complete loss within the tumor cells. Models using logistic ordinal regression were constructed to determine the ability of PD-L1 and MHC I to predict treatment response.

Results: 1 patient (5%) had complete response (CR), 1 patient (5%) had partial response (PR), 6 patients (32%) had stable disease without progression (SD), and 11 patients (58%) experienced progressive disease (PD). The patient with CR had a high PD-L1 score (CPS 80, TICS 40%) and retained MHC I. The patient with PR had a high PD-L1 score (CPS 60, TICS 50%) and partial MHC I loss. Of the patients with SD, 2 of 6 had high PD-L1 scores (CPS >80, TICS ≥60%) while the remaining 4 had low PD-L1 scores (CPS <5, TICS <10%). All patients with PD had PD-L1 scores (CPS and TICS) ≤25, 9 of which (82%) were ≤5. Of the patients with SD and PD, 50% and 55%, respectively, demonstrated partial or complete MHC I loss. Higher PD-L1 scores (≥50) are linked to treatment response (TICS: p=0.0261, CPS: p=0.0071). Models including MHC I and PD-L1 scores as independent variables strengthened the association between PD-L1 score and treatment response (TICS: p=0.0156, CPS: p=0.0041).

Conclusions: Higher PD-L1 expression is associated with a higher probability of treatment response in our cohort of breast cancer patients. Loss of tumoral MHC I expression is more frequently seen in patients with SD or PD, despite most of these tumors having some PD-L1 expression (CPS ≥1). Additional studies evaluating MHC I loss as a potential barrier to successful immune checkpoint inhibition are needed to ascertain the potential use of MHC I as a predictive biomarker in combination with PD-L1.

146 Metaplastic Breast Carcinoma: Clinicopathologic Features, Recurrence Score Results from Population Based Database

Valarie McMurtry[1], Allison Cleary[2], Ana Ruano[2], H. Evin Gulbahce[1]
[1]The University of Utah, Salt Lake City, UT, [2]The University of Utah/ARUP Laboratories, Salt Lake City, UT

Disclosures: Valarie McMurtry: None; Allison Cleary: None; Ana Ruano: None; H. Evin Gulbahce: None

Background: Metaplastic breast carcinoma (MBC) is a rare, heterogenous type of cancer that is frequently triple negative (TN). The goal of this study is to assess the clinicopathological features and outcome of MBC identified in surveillance, epidemiology, and results (SEER) database.

Design: ICD-O-3 codes (8032, 8033, 8070, 8071, 8072, 8074, 8560, 8570, 8571, 8572, 8575, 8980) were selected in SEER to identify MBC from 2004-2015. Bivariate analyses compared MBC and invasive ductal carcinoma (IDC) on clinicopathological characteristics, recurrence score (RS) testing, and treatment received. Hazards Ratios (HR) were estimated using Cox proportional hazards model. Kaplan-Meier survival plot was generated using log-rank test. Patients with unknown status in any category were removed from comparative analysis.

Results: 3,888 patients with MBC were identified. Age, tumor size, lymph nodes (LN) status, stage, grade, hormone receptor (HormRec), HER2 status, tumor subtype, and RS were significantly different between MBC and IDC (Table 1). 48.9% of MBC did not have tumor subtype determined because HER2 status is reliably collected only after 2010 in SEER. When HormRec and HER2 status were tested, 69.9% of MBC were TN, 24.4% HormRec+/HER2-, and 5.8% HER2+. Breast cancer specific death (BCSD) was significantly different between MBC and IDC in all cases, TN and HormRec+/HER2- subtypes (p<0.001). In multivariate analysis, MBC was independently associated with increased BCSD in all cases (HR: 1.87; CI: 1.73-2.3), TN (HR: 1.36; CI: 1.17-1.57) and HormRec+/HER2- (HR: 2.37; CI: 1.86-3.02) subtypes. Grade was not associated with outcome.

Table 1. Clinical and pathologic characteristics of metaplastic and invasive ductal carcinomas, NOS, diagnosed in 2004-2015, SEER registries.

	Metaplastic Carcinoma			Invasive Ductal Carcinoma, NOS		
	N= 3,888	% *		N= 510,358	% *	P
Age Group						<0.001
<50	700	18.0		115,950	22.7	
50-64	1,349	34.7		192,979	37.8	
≥65	1,839	47.3		201,429	39.5	
Race						<0.001
Non-Hispanic White	2,618	67.3		354,540	69.5	
Black	621	16.0		55,973	11.0	
Others	638	16.4		97,417	19.1	
Unknown***	11	0.3		2,428	0.5	
Tumor Size						<0.001
Tis	12	0.3		494	0.1	
T1 (≤2cm)	931	24.0		304,764	59.7	
T2 (2-≤5 cm)	1,644	42.3		59.72	28.1	
T3 (>5 cm)	597	15.4		23,426	4.6	
T4	372	9.6		20,745	4.1	
Unknown***	332	8.5		17,764	3.5	
Lymph Node Status						<0.001
N0	2,742	70.5		337,249	66.1	
N1 (1-3 positive nodes)	579	14.9		117,153	23.0	
N2 (4-9 positive nodes)	165	4.2		28,399	5.6	
N3 (≥10 positive nodes)	87	2.2		15,761	3.1	
Unknown***	315	8.1		11,796	2.3	
Stage						<0.001
0	0	0.0		26	0.0	
I	817	21.0		244,217	47.9	
II	1,963	50.5		168,686	33.1	
III	505	13.0		53,323	10.5	

IV	242	6.2		23,526	4.6		
Unknown***	361	9.3		20,580	4.0		
Grade						<0.001	
1	182	4.7		96,503	18.9		
2	483	12.4		202,891	39.8		
3	2,637	67.8		188,631	37.0		
Unknown***	586	15.1		22,333	4.4		
Hormone Receptor						<0.001	
Positive	869	22.4		390,009	76.4		
Negative	2,688	69.1		99,436	19.5		
Unknown	331	8.5		20,913	4.1		
HER2 Status **						<0.001	
Negative	1,883	48.4		211,178	41.4		
Positive	114	2.9		44,530	8.7		
Borderline	26	0.7		6,335	1.2		
Unknown or Diagnosed before 2010**	1,865	48.0		248,315	48.7		
Tumor Subtype						<0.001	
Hormone Receptor+/HER2-	484	12.5		178,103	34.9		
Hormone Receptor+/HER2+	45	1.2		30,547	6.0		
Hormone Receptor-/HER2+	69	1.8		13,878	2.7		
Triple Negative	1,389	35.7		32,769	6.4		
Unknown***	1,901	48.9		255,061	50.0		
Chemotherapy						<0.001	
No/Unknown	1,714	44.1		296,227	58.0		
Yes	2,174	55.9		214,131	42.0		
Recurrence Score Risk Group #	N=29	%*		N= 80,921	%*	<0.001	
Low (RS<11)	2	6.9		16,837	20.8		
Intermediate (RS 11-25)	8	27.6		50,457	62.4		
High (RS>25)	19	65.5		13,627	16.8		

*Percentages may not add to 100 due to rounding; ** HER2 status is collected after 2010 by SEER; ***Unknown patients are excluded from comparative analysis ; # Includes only cases tested for Recurrence Score.

Conclusions: MBC is more common among older women, more likely to have larger tumor size and higher stage but less likely to be LN+ compared to IDC. The majority of MBC are TN. When HormRec+ and tested for RS, MBC is more likely to have high-risk RS. MBC of all subtypes, including HormRec+, have worse prognosis after adjusting for age, tumor size, LN status and grade.

147 Multi-gene Sequencing Reveals Mutational Heterogeneity Between Phyllodes Tumours Harbouring Mutant and Wild-type PIK3CA

Nur Diyana Md Nasir[1], Cedric Ng[2], Sandy Lim[3], Abner Lim[2], Jingxian Zhang[4], Vikneswari Rajasegaran[5], Jing Yi Lee[5], Jessica Sook Ting Kok[5], Aye Aye Thike[1], Johnathan Xiande Lim[1], Ruifen Weng[4], Sidney Yee[4], Min-Han Tan[6], Bin Tean Teh[5], Puay Hoon Tan[1]

*[1]Singapore General Hospital, Singapore, [2]Cancer Discovery Hub, National Cancer Center Singapore, Singapore, [3]Diagnostics Development Hub (DxD Hub), Agency for Science, Technology and Research (A*STAR), Singapore, [4]Diagnostics Development Hub (DxD Hub), Agency for Science, Technology and Research (A*STAR), Singapore, [5]National Cancer Centre Singapore, Singapore, [6]Lucence Diagnostics Pte Ltd, Singapore*

Disclosures: Nur Diyana Md Nasir: None; Cedric Ng: None; Sandy Lim: None; Abner Lim: None; Jingxian Zhang: None; Vikneswari Rajasegaran: None; Jing Yi Lee: None; Jessica Sook Ting Kok: None; Aye Aye Thike: None; Johnathan Xiande Lim: None; Ruifen Weng: None; Sidney Yee: None; Min-Han Tan: *Employee*, Lucence Diagnostics; *Stock Ownership*, Lucence Diagnostics; Bin Tean Teh: None; Puay Hoon Tan: None

Background: Breast phyllodes tumours (PT) are characterized by proliferation of both epithelial and stromal components, and are graded into benign, borderline and malignant categories based on multiple histological criteria. They are uncommon and potentially aggressive, and grade progression is possible. The higher grades have a greater likelihood of recurrence, while occasional metastases may occur for malignant PTs. We aim to investigate the genomic alterations in PTs, to better understand their pathogenesis and mutations related to FDA-approved therapies, since such actionable mutations may confer higher sensitivity to therapy. These include *PIK3CA* (for Alpelisib), *BRCA1/2* (for Olaparib, Talazoparib), and *ERBB2* (for Lapatinib, Trastuzumab).

Design: Our study cohort comprised 20 PTs (6 benign, 9 borderline and 5 malignant) from an Asian cohort. We extracted genomic DNA and RNA from eight sections of formalin-fixed paraffin-embedded (FFPE) tissues per tumour block. A nucleic acid capture

based sequencing assay was utilized to profile the tumours with a median depth of approximately 1053x, consisting of a DNA panel of 572 genes and RNA panel of 91 genes.

Results: PTs were found to harbour a high rate of *MED12* (75%), *KMT2D* (70%), *TERT* promoter (55%), *FLNA* (50%), *NF1* (50%) and *ERBB4* (50%) mutations. There were 9 cases (45%) with *PIK3CA* mutations, exhibiting recurrent p.R108S, p.R770L, p.L92I, p.W1051L and other variants. These were mainly borderline (6/9, 67%) and malignant PTs (2/9, 22%). PTs with mutant *PIK3CA* were significantly more likely to have a higher number of mutations (p-value <0.001), *BRCA1* (89% vs 0%, p-value <0.001), *BRCA2* (78% vs 9%, p-value=0.001), *ERBB2* (78% vs 27%, p-value=0.024), *EGFR* (67% vs 0%, p-value <0.001), and *MTOR* (89% vs 9%, p-value <0.001) alterations than those with wild-type *PIK3CA*. We did not detect a significant correlation between *PIK3CA* mutations with age (p-value=0.069), tumour size (p-value=0.220) and mitotic activity (p-value=0.587). RNA fusions and marked microsatellite instability were not observed in all samples.

Conclusions: Targeted sequencing revealed genetic heterogeneity in PTs, and demonstrated the multitude of signalling pathways potentially involved in pathogenesis. Further studies are needed in establishing the impact of somatic mutations on tumour morphology and behaviour, and their suitability as candidate markers for approved therapies.

148 Multiple Breast Fibroepithelial Lesions in Paediatric Patients

Nur Diyana Md Nasir[1], Fan Foon Cheo[1], Kuick Hong[2], Amos Hong Pheng Loh[2], Cedric Ng[3], Jing Yi Lee[4], Jessica Sook Ting Kok[4], Abner Lim[3], Peiyong Guan[4], Aye Aye Thike[1], Timothy Tay[1], Kenneth Chang[5], Bin Tean Teh[4], Puay Hoon Tan[1]
[1]Singapore General Hospital, Singapore, Singapore, [2]KK Women's and Children's Hospital, Singapore, Singapore, [3]Cancer Discovery Hub, National Cancer Center Singapore, Singapore, Singapore, [4]National Cancer Centre Singapore, Singapore, Singapore, [5]KKH, Singapore, Singapore

Disclosures: Nur Diyana Md Nasir: None; Fan Foon Cheo: None; Kuick Hong: None; Amos Hong Pheng Loh: None; Cedric Ng: None; Jing Yi Lee: None; Jessica Sook Ting Kok: None; Abner Lim: None; Peiyong Guan: None; Aye Aye Thike: None; Timothy Tay: None; Kenneth Chang: *Advisory Board Member*, Bayer South-East Asia; *Grant or Research Support*, Bayer South-East Asia; Bin Tean Teh: None; Puay Hoon Tan: None

Background: Fibroepithelial lesions (FELs) of the breast consist of fibroadenomas (FAs) and the rarer phyllodes tumours (PTs) which are graded into benign, borderline and malignant. Multiple FELs occur in some paediatric patients either synchronously or metachronously. We aim to review the histomorphology and genomic alterations of multiple FELs, to shed light on their occurrence and provide possible insights into clinical management.

Design: A total of 18 FELs from 8 patients was included in the study. 14 (78%) were conventional FAs, 3 (17%) were juvenile FAs and 1 (5%) was a benign PT. Genomic DNA was extracted from eight sections of a formalin-fixed paraffin-embedded (FFPE) block per lesion. 12 samples were sequenced with a 50-gene panel, and 6 samples were profiled with a 16-gene panel.

Results: The number of nodules per patient ranged from 2 to 4 (mean 2.25; median 2). 7 (87.5%) patients had metachronous lesions while 1 patient (12.5%) presented with 2 synchronous lesions. The size of each nodule measured from 1.2cm to 5.5cm (mean 2.73cm, median 2.6cm). All lesions were well circumscribed with smooth borders, with up to 2 stromal mitotic figures in most lesions, without atypical mitotic figures.

We detected *MED12* (50%), *RARA* (17%), *FLNA* (11%), *KMT2D* (11%), *KMT2C* (6%), *EGFR* (6%) and *STAT3* (6%) alterations. 5 of 6 patients with non-recurrent metachronous lesions had either different mutations, or mutations occurring at a different codon of the same *MED12* gene. In our sole patient with recurrent FEL, both the initial and recurrent lesions harboured identical *MED12* missense mutation (c130G>A), and an additional *RARA* stop-gain mutation (c940C>T) in the latter. One FA was found to have *KMT2C* mutation, and it occurred a year after a juvenile FA with *STAT3* mutation was excised at a similar location. Each of 2 synchronous lesions had both *MED12* and *RARA* mutations. We did not observe a significant correlation between *MED12* mutations with stromal cellularity (p=0.346), stromal atypia (p=0.229), and intracanalicular patterns (p=0.825).

Conclusions: Mutations in *MED12* play a pivotal role in the tumourigenesis of FELs in the paediatric population. There are no distinctive molecular characteristics which are unique to multiple FELs, and a study of larger scale is needed especially focused on recurrent FELs.

149 Differential Distribution of Actual and Surrogate Oncotype DX Recurrence Scores by Age, Race, and Body Mass Index

Anas Mohamed[1], Aisha Kousar[2], Joseph Geradts[1]
[1]Vidant Medical Center/East Carolina University, Greenville, NC, [2]East Carolina University, Greenville, NC

Disclosures: Anas Mohamed: None; Aisha Kousar: None; Joseph Geradts: None

Background: Various epidemiologic parameters have been known to impact breast cancer outcome. The Oncotype DX Recurrence Score (RS) is widely used as an objective tool to predict recurrence risk in estrogen receptor-positive breast cancer patients. Multiple surrogate models that include tumor grade and breast cancer biomarker expression can predict RS with good accuracy. In this study we aimed to determine whether the RS and two surrogate indices, as measures of tumor aggressiveness, were differentially distributed by important epidemiologic variables including age, race, and body mass index (BMI).

Design: 418 breast cancer patients with available Oncotype DX RS were retrieved from our institutional files. Age, race, BMI, tumor size, grade, and breast cancer biomarker status were abstracted. Breast Cancer Prognostic Score (BCPS) and Magee Equation 2 were used to calculate surrogate RS. Patients were stratified into different groups based on age, race, BMI, or a combination of parameters. Mean, standard deviation, and median of actual and calculated RS were calculated for each group.

Results: The median age in our patient cohort was 63 years. It included 263 Caucasian (C) and 155 African American (AA) women. Patients < 63 years old had a mean RS that was 2 points higher than that in patients ≥ 63 (p=0.026), and the difference was more pronounced (3.5 points) in AA patients. BMI ≥30 was associated with lower RS, especially in AA patients and patients older than 63 (mean difference 4.1 and 3.2, respectively). While no statistically significant difference in RS was seen between C and AA patients overall (p=0.29), younger AA had higher RS than older C (mean difference 3.4, p < 0.02). Some of these observations were recapitulated by the two surrogate models. Both BCPS and Magee 2 scores were higher in non-obese older (but not younger) women and in younger AA versus older C patients.

	Oncotype DX Recurrence Score (RS)								
	<11	11-17	18-25	26-30	>30	Median	Mean	SD	P value
Age									
< 63 (204)	49 (24)	85 (42)	41 (20)	10 (5)	19 (10)	15	16.9	10	0.026
≥ 63 (214)	66 (31)	81 (38)	41 (19)	13 (6)	13 (6)	14	14.9	8.9	
Youngest 25% (<55+2m) (105)	24 (23)	43 (41)	23 (22)	2 (2)	13 (12)	16	17.7	11	0.06
Oldest 25% (>69+3m) (105)	31 (30)	42 (40)	17 (16)	6 (6)	9 (9)	14	14.8	8.9	
BMI									
< 30 (188)	41 (22)	78 (41)	43 (23)	13 (7)	13 (7)	15	16.8	9.1	0.06
≥ 30 (230)	74 (32)	90 (39)	39 (17)	9 (4)	18 (8)	13	15.1	9.8	
Lowest 25% BMI (≤26) (105)	16 (15)	46 (44)	28 (27)	7 (7)	8 (8)	16	17.9	8.5	0.19
Highest 25% BMI (>37.4)(105)	30 (29)	42 (40)	15 (14)	5 (5)	13 (12)	14	16.1	11.1	
Race									
C (263)	73 (28)	107 (41)	52 (20)	11 (4)	20 (8)	14	15.5	9.3	0.29
AA (155)	41 (26)	59 (38)	30 (19)	12 (8)	13 (8)	14	16.5	9.8	
C, < 63 (127)	33 (26)	55 (43)	26 (20)	2 (2)	11 (8)	14	16.1	9.4	0.3
C, ≥ 63 (136)	40 (29)	52 (38)	26 (19)	9 (7)	9 (7)	14	14.9	9.2	
AA, < 63 (77)	15 (19)	30 (39)	15 (19)	8 (10)	9 (12)	16	18.3	10.9	0.03
AA, ≥ 63 (78)	26 (33)	29 (37)	15 (19)	4 (5)	4 (5)	13	14.8	8.4	
C, ≥ 63 (136)	40 (29)	52 (38)	26 (19)	9 (7)	9 (7)	14	14.9	9.2	0.017
AA, < 63 (77)	15 (19)	30 (39)	15 (19)	8 (10)	9 (12)	16	18.3	10.9	
C, BMI < 30 (145)	37 (26)	60 (41)	31 (21)	7 (5)	10 (7)	15	16	9	0.30
C, BMI ≥ 30 (118)	36 (31)	47 (40)	21 (18)	4 (3)	10 (8)	13.5	14.9	9.6	
AA, BMI < 30 (43)	4 (9)	17 (40)	11 (26)	7 (16)	4 (9)	18	19.5	8.9	0.02
AA, BMI ≥ 30 (112)	37 (33)	42 (38)	18 (16)	6 (5)	9 (8)	13	15.4	10	
< 63, BMI < 30 (95)	21 (22)	41 (43)	20 (21)	5 (5)	8 (8)	16	17	9.3	0.98
< 63, BMI ≥ 30 (109)	27 (25)	44 (40)	21 (19)	5 (5)	12 (11)	14	16.9	10.6	
≥ 63, BMI < 30 (93)	20 (22)	36 (39)	23 (25)	8 (9)	6 (6)	15	16.7	8.9	0.01
≥ 63, BMI ≥ 30 (121)	46 (38)	45 (37)	18 (15)	5 (4)	7 (6)	12	13.5	8.6	
SD = Standard Deviation; BMI = Body Mass Index; C = Caucasians; AA = African Americans									

Conclusions: Oncotype DX RS were higher in patients below the median age, especially among AA, and in non-obese women, especially among AA and older patients, suggesting more aggressive disease in these groups of breast cancer patients. Similar observations held true for two surrogate models, BCPS and Magee 2, suggesting that they may have utility in epidemiologic

studies that do not rely on the Oncotype DX RS. Overall there was no statistically significant difference in RS distribution between C and AA women in this study, which has a higher proportion of AA patients than many other cohorts.

150 Pathological and Clinical Features Associated with Invasive Breast Cancer ISH Group 3 Classified According to the 2018 CAP/ASCO HER2 Guidelines: A Retrospective Analysis

Nada Mohamed[1], Jaya Asirvatham[1]
[1]Baylor Scott & White Health/Texas A & M Health Science Center College of Medicine, Temple, TX

Disclosures: Nada Mohamed: None; Jaya Asirvatham: None

Background: About 15% of breast cancer (BC) are positive for Human epidermal growth factor receptor 2 (HER2) and can benefit from HER2-targeted therapy (HTT). Either immunohistochemistry (IHC) or in situ hybridization (ISH) can determine HER2 status. In 2013, ASCO/CAP guidelines recommended interpreting tumors with average HER2 signals/cell ≥ 6.0 with a HER2/CEP17 ratio of <2.0 as HER2 positive and eligible for HTT. In 2018, ASCO/CAP guidelines reclassified these as Group3, requiring interpretation along with IHC. Group3 represented 0.4% and 0.5% of cases in the HERA and BCIRG trials, respectively.

Design: At our institution, HER2 was evaluated with ISH & IHC or ISH with reflex to IHC. Demographic, clinical and pathological data (including CISH and IHC slides) if available from patients with invasive, recurrent or metastatic BC from 1/1/10 to 8/31/21 were reviewed. Differences between patients who received and did not receive HTT were assessed using Fisher exact test or Student t-test.

Results: Thirty-one samples from 31 patients met criteria for Group 3 (0.73% of BC). Average age was 58 years. Average tumor size was 2.6 cm. Nearly 60% were clinical stage I. 47% were stage pT1. The majority were invasive carcinoma of no special type (88%). The HER2/CEP17 ratio varied from 0.6 to 1.9. Average HER2 signals/ nucleus varied from 6.0 to 16.6.

4/31 patients had a separate sample (1 concurrent) that was HER2 positive. 24 (20 primary, 4 other) were identified prior to the adoption of 2013 guidelines. HER2 IHC was 3+, 2+ or negative (0-1+) in 4, 6 and 14 cases. 21/24 were hormone receptor (HR) positive. 3/17 patients (IHC 3+ or negative) received HTT (1 neoadjuvant with pCR, IHC 0). 9 samples (8 primary) were identified after the adoption of 2013 guidelines. HER2 IHC was 3+, 2+ or negative in (1, 2 and 2) samples. 7/9 were HR-positive. 6/7 patients received HTT (3 neoadjuvant). All downstaged, but none achieved pCR. No cases were identified after adoption of 2018 guidelines. Median follow-up was 7 years. 20/28 are alive (19 with no evidence of disease). 4 died of BC, and 4 died of other causes. HTT treated patients (n=9) had a smaller tumor size compared to patients without HTT (p=0.02). There was no significant difference in clinical outcomes between the two groups.

Table1. Clinical and pathologic features of ISH group 3 breast cancer results (HER2/CEP17 ratio < 2.0 and average HER2 copy number ≥ 6 copies.

	Group 3 patients with anti-HER2 treatment (n = 9)	**Group 3 patients without anti-HER2 treatment (n = 17)**	***P value***
Age at diagnosis (years) Mean ± SD, Median	57 ±14 57	61 ±12 62	0.45
HER2/CEP17 ratio Mean ± SD Median	1.63 ±0.24 1.60	1.53 ±0.33 1.70	0.37
HER2 copy number Mean ± SD Median	 7.34 ±1.35 7.10	7.24 ±1.31 6.80	0.86
Tumor size (cm) Mean ± SD Median	1.39 ±0.74 1.30	2.56 ±1.62 1.75	**0.02**
Clinical stage, No. (%)			0.69
Stage I Stage II Stage III Data unavailable	6 (67%) 2 (22%) 1 (9%) 0	9 (56%) 6 (38%) 1 (6 %) 1	
Pathologic tumor stage (AJCC), No. (%)			0.4
T0 (pCR) T1 T2 T3 or T4 Data not available	1 (11%) 7 (78%) 1 (11%) 0 0	1 (6%) 8 (50%) 5 (31%) 2 (13%) 1	
Lymph node involvement, No. (%)			1
Yes No Data not available	6 (67%) 3 (33%) 0	11 (73%) 4 (27%) 2	
Tumor histology, No. (%)			1.0

Invasive carcinoma of no special type Invasive lobular carcinoma Invasive papillary carcinoma	9 (100%) 0 0	15 (88%) 1 (6%) 1 (6%)	
Nottingham overall grade, No. (%)			0.35
Grade 1 Grade 2 Grade 3	1 (11%) 2 (22%) 6 (67%)	0 6 (35%) 11 (65%)	
HER2 IHC result, No. (%)			0.2
Negative (0 or 1+) Equivocal (2+) Positive (3+) Not performed	2 (40%) 1 (20%) 2 (40%) 4	10 (59%) 5 (29%) 2 (12%) 0	
Hormone receptor status, No. (%)			1.0
Hormone receptor positive Hormone receptor negative	8 (89%) 1 (11%)	14 (82%) 3 (18%)	
Neoadjuvant Chemotherapy, No. (%)			0.13
Received Did not receive Data not available	4 (50%) 4 (50%) 1	6 (14%) 16 (86%) 3	
Adjuvant Radiation therapy, No. (%)			0.2
Received Did not receive Data not available	7 (78%) 2 (22%) 0	7 (47%) 8 (53%) 2	
Adjuvant Chemotherapy, No. (%)			1.0
Received Did not receive Data not available	6 (67%) 3 (33%) 0	9 (60%) 6 (40%) 2	
Endocrine therapy, No. (%)			0.6
Received Did not receive Data not available	8 (56%) 1 (38%) 0	3 (56%) 11 (38%) 3	
Clinical outcome, No. (%)			0.76
No evidence of disease Alive with recurrent and/or metastatic disease Deceased Data not available	8 (89%) 0 1 (11%)	11 (69%) 1 (6%) 4 (25%) 1	
Clinical follow-up (months) Mean ± SD	70 ±29.6	104.8 ±40.3	
Abbreviations: HER2, human epidermal growth factor receptor 2; ISH, in-situ hybridization; SD, standard deviation; IHC, immunohistochemistry.			

Conclusions: In this small retrospective study, there were similar clinical outcomes in patients who received and did not receive HTT. Analysis of a larger data set and prospective trials may help optimize therapy in this group of patients.

151 Contemporary Evaluation of Estrogen Receptor and Progesterone Receptor Expression in Tumor-Associated Stromal Cells

Gustavo Moreno[1], Mariel Molina[2], Julie Jorns[1]
[1]Medical College of Wisconsin, Milwaukee, WI, [2]Froedtert and the Medical College of Wisconsin, Milwaukee, WI

Disclosures: Gustavo Moreno: None; Mariel Molina: None; Julie Jorns: None

Background: There is growing interest in the role of the stromal microenvironment in progression to breast cancer. Although nuclear ER/PR expression in invasive breast cancer has been extensively studied, stromal expression of these markers, and influence in tumor growth/progression is poorly understood. The aim of this study was to investigate stromal ER/PR patterns and associations with other clinicopathologic features.

Design: Retrospective database search (1/2017-12/2020) identified breast core biopsies with invasive carcinoma from 3 hospitals that comprise our enterprise. Staining was done at a single testing site. Nuclear ER/PR IHC expression in invasive carcinoma and peritumoral stromal cells was categorized visually as positive (>10%), low positive (1-10%) or negative (<1%). Smooth muscle staining (e.g. blood vessel, superficial muscle bundle) was excluded. (Figure)

Tumors were divided into 4 subtypes by IHC: triple negative (TNBC), HER2 enriched (HER2), luminal HER2 positive (LUMHER2) and luminal (LUM). ER/PR low positive tumors were considered negative (i.e. TNBC or HER2 depending on HER2 status).

Results: Of 1512 biopsies with invasive carcinoma, 1278 tumors from 1241 patients had accessible IHC, with breakdown by subtype as follows: 76.5% (977/1278) LUM, 11.7% (149/1278) TNBC, 7.7% (99/1278) LUMHER2 and 4.1% (53/1278) HER2. 9.4% had low positive and 1% had positive peritumoral stromal PR expression. Stromal ER was more frequent, with 33.9% and 21.8% showing low positive and positive expression, respectively.

IHC staining utilized two platforms: Ventana (781/1278; 61.1%) and Leica (497/1278; 38.9%). When comparing platforms, there was a significantly lower frequency of tumors with positive stromal ER in the Leica platform (p=.03). The Leica patient population also had more academic site biopsies and higher-grade tumors (p<.01) but was otherwise like the group tested via the Ventana platform. (Table)

Stromal ER was seen among all tumor subtypes but with significant differences in frequency, with low positive or positive staining in 57.6% (333/977) LUM, 44.3% (66/149) TNBC, 53.5% (53/99) LUMHER2 and 54.7% (29/53) HER2 (p=.02). This difference was also significant when divided by low positive and positive expression (p=.01).

	All Cases	Ventana	Leica
Site of biopsy (N, %)*			
Academic center	798 (62.4)	461 (59)	337 (67.8)
Community hospital	480 (37.6)	320 (41)	160 (32.2)
Age (mean, range)	63.8 (27.2-97)	63.6 (27.2-95.7)	64.2 (27.6-97)
Sex (N, %)			
Female	1228 (99)	744 (99.1)	484 (98.8)
Male	13 (1)	7 (0.9)	6 (1.2)
Race (N, %)			
White	1082 (87.2)	658 (87.6)	424 (86.6)
Black	126 (10.1)	70 (9.3)	56 (11.4)
Hispanic	16 (1.3)	11 (1.5)	5 (1)
Asian/pacific islander	11 (0.9)	9 (1.2)	2 (0.4)
Other	6 (0.5)	3 (0.4)	3 (0.6)
BMI (N, %)			
<18.5	9 (0.7)	8 (1.1)	1 (0.2)
18.5-24.9	269 (21.7)	157 (20.9)	112 (22.9)
25-29.9	406 (32.7)	250 (33.3)	156 (31.8)
>=30	529 (42.6)	320 (42.6)	209 (42.7)
Not available	28 (2.3)	16 (2.1)	12 (2.4)
Menopausal status (N,%)			
Pre-menopausal	342 (27.6)	214 (28.5)	128 (26.1)
Post-menopausal	885 (71.3)	530 (70.6)	355 (72.5)
N/A (male)	14 (1.1)	7 (0.9)	7 (1.4)
Parity (N,%)			
0	235 (19)	137 (18.2)	98 (20)
>=1	989 (79.7)	603 (80.3)	386 (78.8)
N/A (male)	13 (1)	7 (1)	6 (1.2)
Not available	4 (0.3)	4 (0.5)	0 (0)
Laterality (N, %)			
Right	658 (51.5)	394 (50.4)	264 (53.1)
Left	620 (48.5)	387 (49.6)	233 (46.9)
Biopsy type (N, %)			
Stereotactic	214 (16.8)	132 (16.9)	82 (16.5)
Ultrasound	1011 (79.1)	619 (79.3)	392 (78.9)
MRI	41 (3.2)	23 (2.9)	18 (3.6)
Other	12 (0.9)	7 (0.9)	5 (1)
Diagnosis (N, %)			
Invasive ductal	1014 (79.4)	621 (79.5)	393 (79.1)
Invasive lobular	215 (16.8)	132 (16.9)	83 (16.7)
Other invasive	49 (3.8)	28 (3.6)	21 (4.2)
mBR Grade (N, %)*			
1	473 (37)	320 (41)	153 (30.8)
2	520 (40.7)	299 (38.3)	221 (44.5)
3	285 (22.3)	162 (20.7)	123 (24.7)
Subtype (N, %)			
Luminal	977 (76.5)	600 (76.8))	377 (75.9)
Luminal HER2	99 (7.7)	66 (8.5)	33 (6.6)
HER2	53 (4.1)	29 (3.7)	24 (4.8)
Triple Negative	149 (11.7)	86 (11)	63 (12.7)
Stromal ER (N, %)*			
Negative (<1%)	567 (44.4)	326 (41.7)	241 (48.5)
Low positive (1-10%)	433 (33.9)	271 (34.7)	162 (32.6)
Positive (>10%)	278 (21.7)	184 (23.6)	94 (18.9)

Clinicopathologic features (N=1278 tumors from 1241 patients) with comparison of those tested via the Ventana (N=781 tumors from 751 patients) and Leica (N=497 tumors from 490 patients) platforms. *Statistically significant (p<.05)

Figure 1 - 151

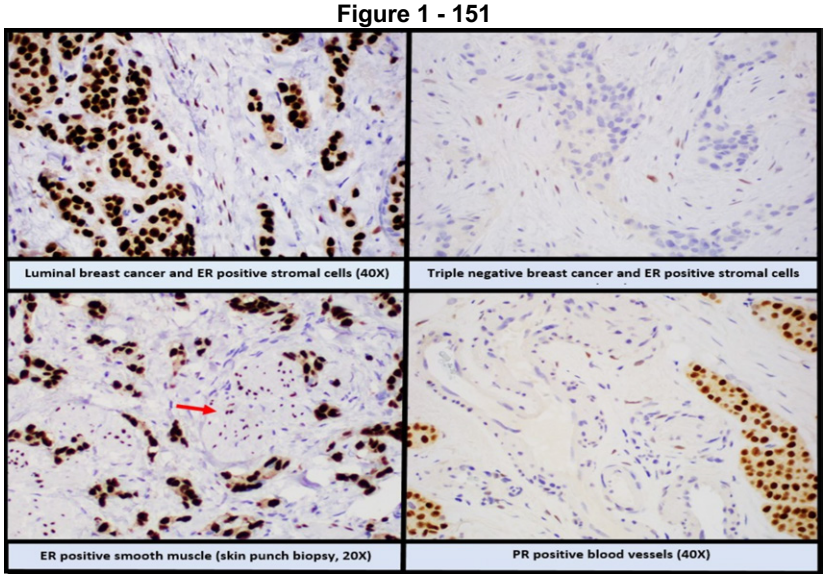

Conclusions: Stromal ER expression was lowest amongst TNBC, with additional differences when comparing platforms, suggesting both biologic and analytic variation.

152 Impact of HER2 Overexpression and Coexpression of Hormonal Receptors on Pathological Response after Neoadjuvant Chemotherapy in HER2-Positive Breast Cancer

Louis Moscoso[1], Guadalupe Ruiz-Merino[2], Lourdes Salazar Huayna[1], Emma Iborra-Lacal[2], Santiago Escrivá de Romaní[3], Maria Jiménez-Lucas[2], Christian Sisó Raber[1], Juan Cabezas-Herrera[2], Vicente Peg[1], Santiago Ramon Y Cajal[4], Antonio Piñero-Madrona[2]

[1]Hospital Universitari Vall d'Hebron, Barcelona, Spain, [2]Murcia, Spain, [3]Vall d'Hebron Institute of Oncology, Vall d'Hebron University Hospital, Barcelona, [4]Vall d'Hebron University Hospital, Barcelona, Spain

Disclosures: Louis Moscoso: None; Guadalupe Ruiz-Merino: None; Lourdes Salazar Huayna: None; Emma Iborra-Lacal: None; Santiago Escrivá de Romaní: None; Maria Jiménez-Lucas: None; Christian Sisó Raber: None; Juan Cabezas-Herrera: None; Vicente Peg: *Advisory Board Member*, Roche; *Speaker*, MSD; *Advisory Board Member*, Sysmex; *Advisory Board Member*, Bayern; *Advisory Board Member*, Astra Zeneca; *Advisory Board Member*, Exact Sciences; Santiago Ramon Y Cajal: None; Antonio Piñero-Madrona: None

Background: HER2 overexpression in breast carcinomas (BC) has been associated with poorer prognosis and higher aggressiveness. The development of targeted therapies has changed the behavior of this disease. Targeted therapies became the optimal neoadjuvant chemotherapy (NAC), achieving high rates of complete pathologic response (pCR). The ASCO/CAP guidelines classify HER2 positive tumors either by immunohistochemistry (3+) and/or in situ hybridization (HER2 amplification), but no correlation with response is addressed. In this study, we asked whether all HER2-positive cases (IHC 2+/ISH+ vs. IHC 3+) show the same response to NAC aiming at pCR rates, and whether this can be influenced hormone receptors co-expression.

Design: A retrospective series of 207 HER2-positive BC treated with NAC at two institutions between 2011 and 2017 was reviewed. Age, histologic type, TNM staging, treatment received, and pathological response were evaluated. HER2 and hormone receptor assessment was performed according to ASCO/CAP guidelines. Bivariate comparative analysis for the categorized qualitative and quantitative variables and multivariate analysis using logistic regression were performed.

Results: Mean age was 53.9 years. pCR was observed in 116 cases (56%). 94,2% were carcinomas of no special type, 72 cases were non-luminal HER2 (34.8%) and 135 cases were Luminal B-HER2 positive (65 %). Tumors with IHC 3+ presented a pCR rate of 60% compared to 29.6% of the IHC 2+/ ISH+ group (p = 0.003), and the risk of achieving a pCR was three times higher in this first group (OR: 3.07 (1.24-7.59), p = 0.015) (Table 1). Furthermore, non-luminal HER2 tumors presented 75% pCR (54/72) compared to 45.9% of luminal HER2-positive tumors (62/135) (p = 0.0001). No differences in pCR rates were observed depending on Ki67 (p = 0.179) or type of surgery or anti-HER2 treatment received (p = 0.503).

n=207	NO pCR	pCR	p	p - OR (IC95%)
Age	55.08 ± 14.23	52.91 ± 11.95	0.234	
Histological subtype Carcinoma NST (n=195) ILC (n=6) Others (n=6)	83 (42.6%) 4 (66.7%) 4 (66.7%)	112 (57.4%) 2 (33.3%) 2 (33.3%)	0.264	
cT 1 (n=20) 2 (n=131) 3 (n=33) 4 (n=23)	8 (40%) 58 (44.3%) 15 (45.5%) 10 (43.5%)	12 (60%) 73 (55.7%) 18 (54.5%) 13 (56.5%)	0.983	
cN 0 (n=73) 1 (n=107) 2 (n=27)	35 (47.9%) 48 (44.8%) 9 (33.3%)	38 (52.0%) 59 (55.1%) 18 (66.6%)	0.575	
Type of surgery Conservative (n=109) Radical (n=96)	45 (41.3%) 44 (45.8%)	64 (58.7%) 52 (54.2%)	0.512	
Her2neu 2+ (n=27) 3+ (n=180)	**19 (70.4%)** 72 (40.0%)	8(29.6%) **108 (60.0%)**	**0.003**	0.01 OR: 3.07 (1.24-7.59)
IHC profile HER2 positive (no Luminal) (n=72) Luminal B-HER2 positive (n=135)	18 (25.0%) **73 (54.1%)**	**54 (75.0%)** 62 (45.9%)	**0.0001**	0.0001 OR: 0.30 (0.16-0.57)
ER <1% (n=67) ≥1% (n=140)	18 (26.9%) **73 (52.1%)**	**49 (73.1%)** 67 (47.9%)	**0.001**	
PR <1% (n=115) ≥1% (n=92)	37 (32.2%) **54 (58.7%)**	**78 (67.8%)** 38 (41.3%)	**0.0001**	
Hormone receptors Negative (n=65) Positive (n=142)	18 (27.7%) **73 (51.4%)**	**47 (72.3%)** 69 (48.6%)	**0.001**	
Ki67 <20% (n=33) ≥20% (n=172)	18 (54.5%) 72 (41.9%)	15 (45.5%) 100 (58.1%)	0.179	
Chemotherapy T+P (n=119) T (n=70) T+L (n=13) T+N (n=5)	48 (40.3%) 35 (50.0%) 5 (38.5%) 3 (60.0%)	71 (59.7%) 35 (50.0%) 8 (61.5%) 2 (40.0%)	0.503	

Conclusions: Overall, not all tumors classified as "HER2 positive" respond equally to NAC. pCR rates after NAC were higher in tumors with complete immunohistochemical overexpression (IHC 3+) and without hormone receptor co-expression (HER2 positive (non-Luminal). In addition, progesterone receptor co-expression was associated with lower pCR.

153 Retrospective Review and Reclassification of Borderline and Malignant Phyllodes Tumors Based on the 5th Edition of the World Health Organization: Need for Further Refinement

Miralem Mrkonjic[1], Gulisa Turashvili[1]
[1]Mount Sinai Hospital, University of Toronto, Toronto, Canada

Disclosures: Miralem Mrkonjic: None; Gulisa Turashvili: None

Background: According to the most recent 5th edition of the World Health Organization (WHO) Classification of Breast Tumors, malignant phyllodes tumors (MPT) are diagnosed when all of the following features are present: infiltrative borders, diffuse stromal cellularity, stromal overgrowth, marked stromal nuclear pleomorphism and >10 mitoses per 10 high power fields (HPF). Borderline phyllodes tumors (BoPT) are diagnosed when some, but not all, of the features are present. In addition, liposarcomatous malignant heterologous elements (MHEs) no longer warrant diagnosis of MPT. We set out to evaluate the impact of these guidelines in a retrospective cohort of MPT and BoPT.

Design: All BoPTs and MPTs diagnosed at our institution between 2000-2021 were identified. Clinical and pathologic features were collected when available and slides were pulled and reviewed for all ambiguous diagnoses.

Results: A total of 152 phyllodes tumors (PTs) were identified during the study period, including 79 BoPTs and 73 MPTs. The 79 BoPTs had a mean size of 4.9 cm, with a mitotic count of <5, 5-9 and >10 per 10 HPF in 15 (19%), 37 (46.8%) and 27 (34.2%) cases, respectively. Stromal overgrowth was seen in 21 (26.6%) cases and MHEs in 3 (3.8%) cases, while 42 (53.2%) had negative margins on initial resection. All 17 patients with available outcome data (mean follow-up 36.9 months) were free of disease. Of 73 MPTs, 12 (16.4%) were reclassified as BoPTs due to lack of all required features. The 12 reclassified BoPTs had a mean size of 3.9 cm, with <5 mitoses in 3 (25%), 5-9 mitoses in 2 (16.7%), and >10 mitoses in 7 (58.3%) as well as stromal overgrowth in 3 (25%), MHEs in 6 (50%) and negative margins at initial resection in 4 (33.3%) patients. Of these 12 BoPTs, outcome data (mean follow-up 88.3 months) was available for 3 patients, and one 1 (33.3%) patient whose PT only had one required feature (>10 mitoses per 10 HPF) developed distant metastasis. The remaining 61 MPTs had a mean size of 8.5 cm, with a mitotic count of 5-9 and >10 per 10 HPF in 1 (1.6%) and 60 (98.4%) cases, respectively, stromal overgrowth in 54 (88.5%), MHEs in 23 (37.7%) and negative margins in 42 (68.9%) cases. Of 11 MPTs with available outcome data (mean follow-up 28.8 months), 3 (27.3%) had distant metastases and 1 (9.1%) had local recurrence.

Conclusions: While the new WHO guidelines clarify histologic criteria for MPT and BoPT, the absence of some malignant features does not exclude aggressive behavior in a subset of PTs warranting further investigations and validation to refine diagnostic criteria.

154 Upregulated mRNA Expression of Alpha-Methylacyl-CoA Racemase (AMACR) in Breast Carcinoma with Apocrine Differentiation

Harumi Nakamura, Osaka International Cancer Institute, Osaka, Osaka, Japan

Disclosures: Harumi Nakamura: None

Background: My colleagues and I previously have reported that most of breast carcinomas with apocrine differentiation are positive for anti-AMACR antibodies. This time, I used real-time polymerase chain reaction (real-time PCR) to investigate whether *AMACR* gene is upregulated at the gene level in breast carcinomas with apocrine differentiation compared to non-apocrine carcinomas.

Design: Formalin-fixed paraffin-embedded specimens of apocrine-differentiated carcinoma (including apocrine ductal carcinoma in situ) and non-apocrine carcinoma tissues obtained by surgery or biopsy were used. Total RNA was extracted using a nucleic acid extraction kit. Following reverse transcription reaction, real-time PCR was performed using primers for *AMACR* gene and for *Tributyl phosphate (TBP)* gene, which is one of housekeeping genes for comparison, to detect and quantify *AMACR* gene expression compared to *TBP* gene in each case (Figure 1).

Results: The results showed in Figure 1. The comparison value of *AMACR* gene expression with TBP gene was significantly higher in carcinomas with apocrine differentiation (median 4.19) than in non-apocrine carcinomas (median 1.16) ($p<0.001$). There were scattered cases with high expression of *AMACR* gene in non-apocrine carcinoma (non A 70, 74, 83, and 198 in Figure 1). All of them were cases in which AMACR protein expression was observed locally. Some (non A 70 and 74) of them showed human epidermal growth factor receptor 2 (HER2) protein expression.

Figure 1 Comparison value of *AMACR* gene expression with *TBP*. Abbreviations: A, Carcinoma with apocrine differentiation; ADCIS, DCIS with apocrine differentiation; non A, non-apocrine carcinoma.

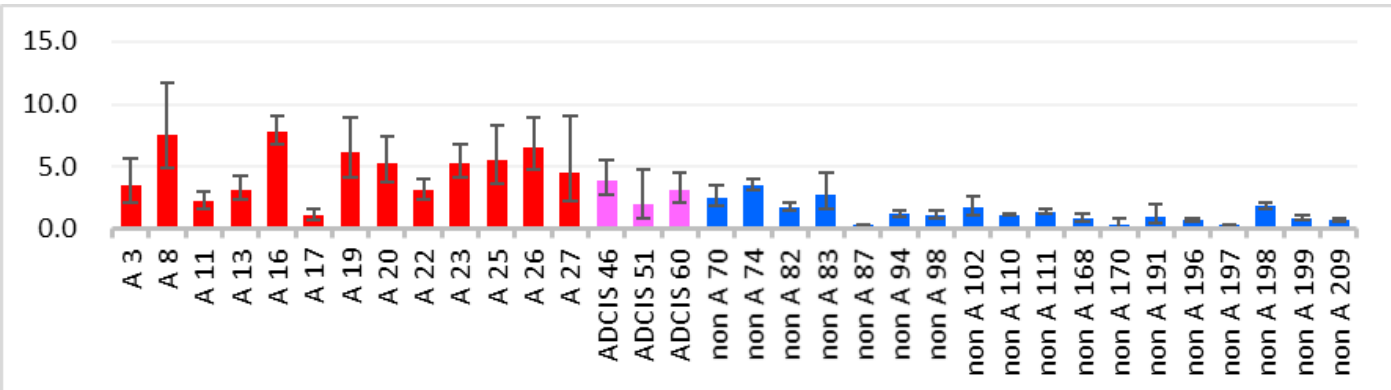

Figure 1 Comparison value of *AMACR* gene expression with *TBP*. Abbreviations: A, Carcinoma with apocrine differentiation; ADCIS, DCIS with apocrine differentiation; non A, non-apocrine carcinoma.

Conclusions: *AMACR* gene expression is found to be upregulated in breast carcinoma with apocrine differentiation. AMACR inhibitors may have therapeutic applications.

155 Development and Validation of an Artificial Intelligence Model for Predicting the Status of ER-Low-Positive Breast Cancer

Shuyao Niu[1], Zhanli Jia[1], Yueping Liu[1]
[1]*The Fourth Hospital of Hebei Medical University, Shijiazhuang, China*

Disclosures: Shuyao Niu: None; Zhanli Jia: None; Yueping Liu: None

Background: To establish a model for predicting the expression state of ER based on the Naive Bayes classification algorithm, by using artificial intelligence to extract the morphological characteristics of infiltrating cancer cells and combining the clinicopathological characteristics of patients. And the model will be used to identify patients with ER-low-positive breast cancer whose clinicopathological characteristics are similar to ER-negative patients. It will provide a reference for the treatment decisions for these patients.

Design: A retrospective study of breast cancer patients who had undergone surgery at the Fourth Hospital of Hebei Medical University. The training cohort included 139 (30.89%) ER-negative (＜1%) patients and 311 (69.11%) ER-positive (＞10%) patients in 2012. The H&E stained section of tumor tissue was passed through the Unic digital scanner to obtain whole slide images. Then use image processing technology to extract the morphological characteristics of each cell, and combine the clinicopathological characteristics of the patient to construct a model to predict the expression state of ER based on the Naive Bayes classification algorithm. The predictive performance of the model is verified by 5-fold cross-validation. And the subgroups prediction of 260 ER-low-positive breast cancer from 2012 to 2018 was made.

Results: The model has a good degree of discrimination for the expression state of ER. By drawing the ROC curve, its AUC is 0.91 (95%CI±0.03). The subgroups prediction were performed on 260 ER-low-positive patients, of which 206 (79.23%) patients were predicted to be negative, and 54 (20.77%) patients were predicted to be positive. By comparing the two groups, it was found that in ER-low-positive breast cancer, patients with high histological grade and Ki67 high expression are more likely to have negative predicted results, and they have lower expression of ESR1 mRNA, cannot benefit from endocrine therapy and have a poor prognosis.

Figure 1 - 155

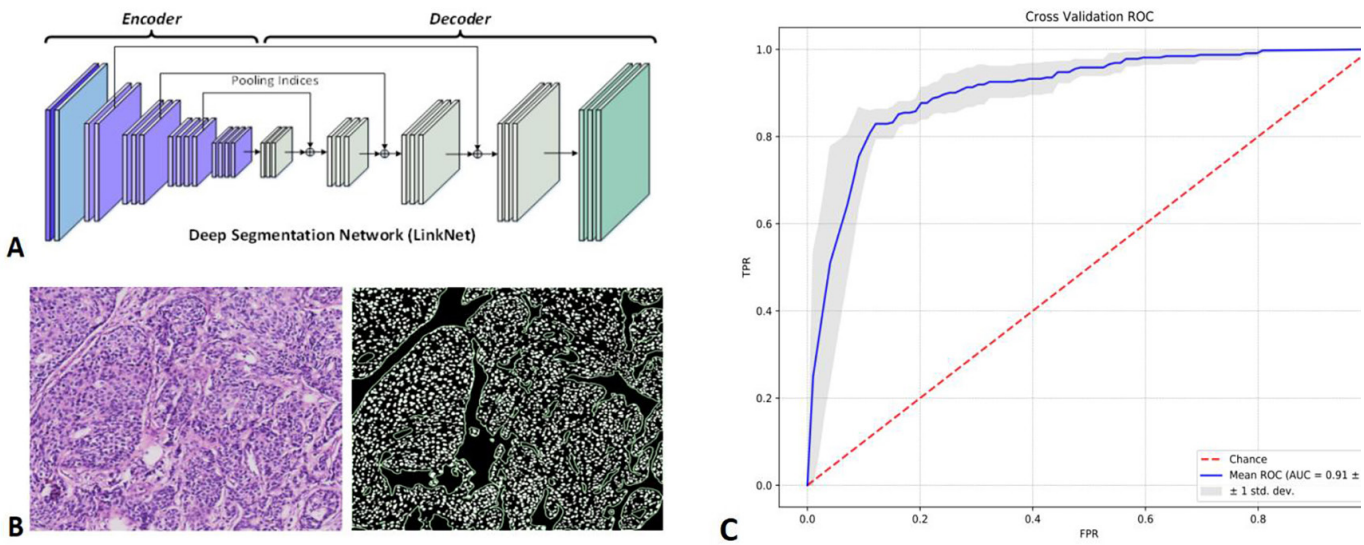

Figure 2 – 155

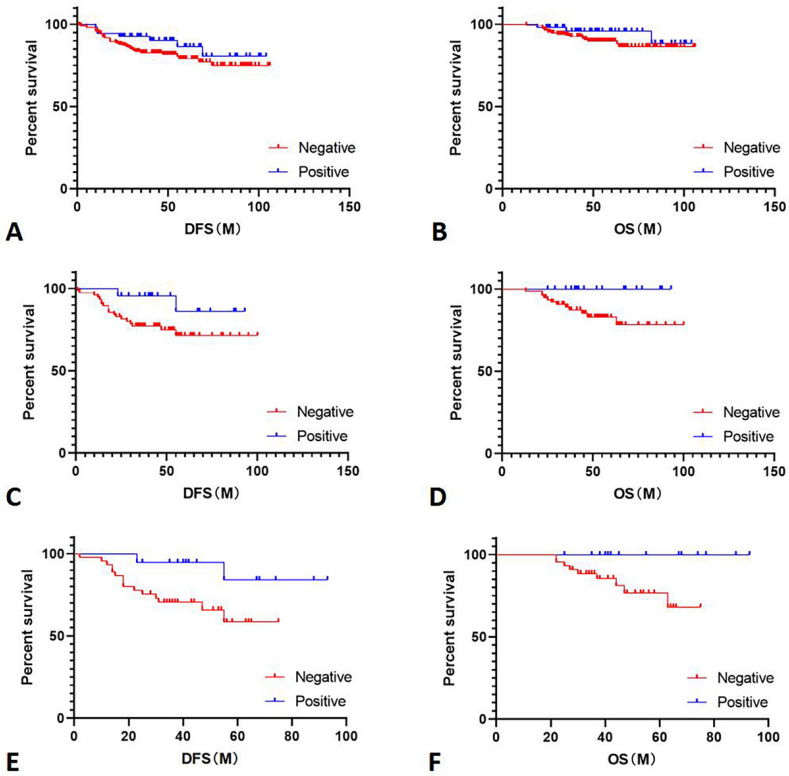

Conclusions: Based on the Naive Bayes classification algorithm, we use artificial intelligence to extract the morphological characteristics of infiltrating cancer cells and combine the clinicopathological characteristics of the patient to develop a model to predicts the ER expression state. It can identify patients with ER-low-positive breast cancer who cannot benefit from endocrine therapy and have a poor prognosis.

156 The Rochester Modified Magee Algorithm (RoMMA): A Strategy for Clinical Risk-Assessment and Risk-Stratification in ER Positive, HER2 Negative Breast Cancer Patients Being Considered for Multigene Assay Testing

Numbereye Numbere[1], Ioana Moisini[2], Hani Katerji[1], Huina Zhang[1], Xi Wang[3], David Hicks[1], Bradley Turner[1]
[1]University of Rochester Medical Center, Rochester, NY, [2]Burnsville, MN, [3]University of Rochester, Rochester, NY

Disclosures: Numbereye Numbere: None; Ioana Moisini: None; Hani Katerji: None; Huina Zhang: None; Xi Wang: None; David Hicks: *Advisory Board Member*, AstraZeneca; Bradley Turner: None

Background: In 2015, we published a modification of the new Magee equations, originally published in 2013 by Klein et al. Based on this modification, we presented an algorithmic approach using an average Modified Magee score, suggesting that Oncotype DX (ODX) testing might only be needed in certain subsets of patients. We subsequently published a validation of this algorithmic approach in 2019, the Rochester Modified Magee Algorithm (RoMMA), with outcome data, suggesting that ER positive breast cancer patients with an average Modified Magee score of ≤ 12 had a low risk of breast cancer recurrence. There has been limited published outcome data on the Magee equation since that 2019 study. We present additional outcome data in 416 ER positive breast cancer patients, with considerations of the results for risk-stratification discussed in the TAILORx study.

Design: 416 patients with an ODX recurrence score who had at least five years of follow-up data or a breast cancer recurrence were included in the final outcome analysis (2008-2017). All patients received either Tamoxifen or an aromatase inhibitor. None of the patients received adjuvant systemic chemotherapy. The average Modified Magee score was calculated and patients were

stratified into three risk-stratification categories: **1)** very low, **2)** low, and **4)** high. We compared these three risk-stratification categories, with outcomes, between the average Modified Magee score and the ODX recurrence score.

Results: 27/416 (6.5%) patients had a recurrence of breast cancer. When comparing outcomes from similar risk category groups, there was no significant difference between the average Modified Magee score and the ODX recurrence score (Table 1).

TABLE 1: Risk stratification categories and outcome	**RECURRNCE (N, %)**	**NO RECURENCE (N, %)**	**p-value**
VERY LOW (N)			
Average Modified Magee score ≤ 12 (76)	**1** (1.3)	**75** (98.7)	0.65
Oncotype DX < 11 (108)	**4** (3.7)	**104** (96.3)	
LOW (N)			
Average Modified Magee score > 12, ≤ 18 (203)	**11** (5.4)	**192** (94.6)	0.56
Oncotype DX 11 - 25 (246)*	**17** (6.9)	**229** (93.1)	
HIGH (N)			
Average Modified Magee score >18 (137)	**15** (10.9)	**122** (89.1)	1.0
Oncotype DX ≥16 - 25 (33)** and Oncotype DX >25 (29)***	**6** (9.6)	**56** (90.4)	

* Does not include patients ≤ 50 years of age with an Oncotype DX score of ≥16 – 25
**Patients ≤ 50 years of age with an Oncotype DX score of ≥16 – 25
*** All patients with an Oncotype DX of >25

Conclusions: Our study further reinforces that breast cancer patients can be confidently stratified into very low, low, and high-risk recurrence groups using the average Modified Magee score, reflecting similar outcomes compared to similar risk-stratification categories defined by ODX, with considerations for the risk-stratification results discussed in the TAILORx study. The average Modified Magee score can be helpful for clinical risk-assessment and risk-stratification, particularly in lower risk patients, when considering the clinical utility of multigene assay testing. The average Modified Magee score offers breast cancer patients increased access to clinical risk-assessment and risk-stratification, with a potential for a significant cost savings for health care systems, both domestically and internationally.

157 Clinicopathological characteristics of Breast Cancer with MET Exon 14 Skipping Alterations in Japan

Hiroko Onagi[1], Keita Sasa[1], Miyu Ichida[1], Yumiko Ishizuka[1], Yoshiya Horimoto[2], Takuo Hayashi[3], Atsushi Arakawa[1], Takashi Yao[4], Tsuyoshi Saito[5], Sou Okano[1]
[1]Juntendo University, Bunkyo-ku, Japan, [2]Juntendo University, Bunkyoku, Japan, [3]Juntendo University Graduate School of Medicine, Tokyo, Japan, [4]Juntendo University, Tokyo, Japan, [5]Juntendo University, School of Medicine, Tokyo, Japan

Disclosures: Hiroko Onagi: None; Keita Sasa: None; Miyu Ichida: None; Yumiko Ishizuka: None; Yoshiya Horimoto: None; Takuo Hayashi: None; Atsushi Arakawa: None; Takashi Yao: None; Tsuyoshi Saito: None; Sou Okano: None

Background: Mesenchymal-epithelial transition factor gene (*MET*) has been recognized as a novel therapeutic target in non-small-cell lung cancer (NSCLC). Activating mutations and genomic amplifications in *MET* have been implicated to promote the proliferation, invasion and migration of carcinoma cells. *MET* exon 14 alterations have been detected in NSCLC, pulmonary sarcomatoid carcinoma, gastric cancer and colorectal cancer. In breast cancer (BC), the frequency of *MET* gene amplification and MET genetic variant is reported 4.7% and 9%, however, its frequency in Japan remains unknown. In this study, we examined MET expression by immunohistochemistry (IHC) and *MET* exon 14 skipping alterations in Japanese BC patients.

Design: We performed c-MET staining by IHC on tissue microarrays (TMAs) containing 1000 cases of surgically resected BCs and evaluated the clinicopathological characteristics of MET-positive BC cases. Furthermore, we examined *MET* exon 14 skipping alterations by reverse transcription-polymerase chain reaction (RT-PCR) for c-MET positive cases.

Results: Totally, 91 BC cases showed cytoplasmic and/or membrane staining for c-MET, and *MET* exon 14 skipping alterations were detected in 20 out of 91 cases. Clinicopathologically, 20 patients with *MET* genetic alterations had a median age of 57.35 years. The histological subtypes were 3 invasive ductal carcinoma (IDC), 1 apocrine carcinoma and 16 ductal carcinoma in situ (DCIS). Four invasive breast carcinomas were classified as low and moderate grade. Fourteen out of 20 cases were positive for estrogen and progesterone receptors. Triple negative BC was observed in 2 out of 20 cases with MET exon14 skipping and 1 of which had lymph node metastasis. One patient experienced metastasis to liver and bones 24 months after surgery and died after another 14 months. Other patients have survived with no recurrence and metastasis. There was no difference between *MET* exon14 skipping status and histological grade/metastatic state.

Conclusions: This is the first report regarding the frequency of *MET* exon14 skipping alterations in Japanese BC. Debora et al reported that *MET* alterations in BC were associated with higher pathological grade tumors, lower positive rate for estrogen and progesterone receptors and frequent metastases compared to BC without MET alterations. However, our results seemed not to be in line with these previous findings and the ethnic difference may have been affected.

158 Significance of Lobular Features in Inflammatory Breast Carcinoma

Allison Onken[1], Allison Cleary[2], Faina Nakhlis[3], Jennifer Bellon[3], Beth Overmoyer[4], Filipa Lynce[4], Beth Harrison[3]
[1]Brigham and Women's Hospital, Harvard Medical School, Boston, MA, [2]The University of Utah/ARUP Laboratories, Salt Lake City, UT, [3]Brigham and Women's Hospital, Boston, MA, [4]Dana-Farber Cancer Institute, Boston, MA

Disclosures: Allison Onken: None; Allison Cleary: None; Faina Nakhlis: None; Jennifer Bellon: None; Beth Overmoyer: None; Filipa Lynce: None; Beth Harrison: None

Background: Inflammatory Breast Carcinoma (IBC) is an aggressive form of breast cancer (BC) defined by erythema and edema involving ≥ 1/3 of the breast, with skin changes due to dermal lymphatic obstruction by tumor emboli. Although the pathophysiology of IBC is not well defined, it has been associated with over-expression of e-cadherin. IBC is enriched for HER2 positive and triple negative BC with a ductal phenotype; however, little is known about IBC with lobular features (IBC-LF). We aimed to further characterize its clinico-pathologic features.

Design: This was a retrospective study of patients (pts) enrolled in the IBC registry at the Dana-Farber Cancer Institute between 2000 and 2019, which includes data on clinical presentation, radiologic and pathologic findings, treatment course, and outcomes. IBC-LF, defined as cases of invasive lobular carcinoma (ILC) or invasive carcinoma with ductal and lobular features (IDLC), was compared to cases of pure invasive ductal carcinoma (IDC) using $\chi 2$ or Fisher exact test to compare ratios, t test to compare means, and Kaplan-Meier curves to compare overall survival (OS). All cases of IBC-LF were reviewed by pathologists at our institution.

Results: 521 patients with IBC were included, with diagnoses of IDC (n=447), ILC (n=19), or IDLC (n=55). Demographic data were similar between subtypes. Consistent with clinical diagnosis of IBC, most pts regardless of histologic subtype presented with breast erythema and edema, with rapid symptom onset (≤6 months). IBC-LF were significantly more likely to present as a palpable mass (p=0.0007) and with nipple retraction (p=0.05). IBC-LF were less likely to be grade 3 (p=0.04) and more likely PR-positive (p=0.03) and HER2-negative (p=0.04). Both subtypes were frequently associated with dermal lymphovascular invasion (LVI); however, IBC-LF trended towards greater likelihood of direct dermal invasion (p=0.12). Following neoadjuvant chemotherapy, pts with IBC-LF were significantly more likely to have a Residual Cancer Burden (RCB) score 3 (p<0.00001). Among stage 3 disease, IBC-LF had a significantly shorter OS than IDC (median, 55.4 vs 114.7 mos; Log-rank p=0.0158). No significant differences were seen among other factors analyzed. See Table 1 and Figure 1.

		IBC-LF	IBC-IDC	
		n=74	*n*=447	*p*
Demographics				
	Mean age (+/- SD)(yrs)	50.7 (+/-10.5)	50.8 (+/-11.6)	0.94
	Menopausal status			0.37
	Pre- or perimenopausal, % (n)[1]	43.8 (73)	49.5 (426)	
	Postmenopausal, % (n)	56.2 (73)	50.5 (426)	
Presentation				
	Symptom Onset ≤6 months, % (n)	91.7 (72)	94.7 (418)	0.30
	Skin erythema, % (n)	88.6 (70)	91.9 (420)	0.36
	Skin edema, % (n)	89.7 (68)	83.9 (409)	0.22
	Diffuse breast enlargement, % (n)	50.0 (70)	61.4 (409)	0.07
	Palpable mass, % (n)	77.3 (66)	59.8 (398)	**0.007**
	Radiologically evident mass, % (n)	83.3 (66)	87.3 (394)	0.38
	Nipple retraction, % (n)	57.6 (66)	47.6 (397)	**0.05**
	Skin ulceration, % (n)	5.5 (73)	4.2 (430)	0.62
	Palpable lymph nodes, % (n)	63.1 (65)	73.7 (388)	0.08
	Lymph node metastasis on presentation, % (n)	20.3 (74)	16.8 (447)	0.46
	Distant metastasis on presentation, % (n)	25.7 (74)	24.2 (447)	0.81
Pathologic findings				
	Grade 3 (vs lower grade), % (n)	47.1 (34)	66.0 (188)	**0.04**
	ER positive, % (n)	55.4 (74)	44.4 (444)	0.08
	PR positive, % (n)	47.3 (74)	34.0 (444)	**0.03**
	Her2/Neu positive, % (n)	31.1 (74)	44.1 (444)	**0.04**

	Direct dermal invasion, % (n)	54.9 (51)	43.0 (263)	0.12
	Dermal lymphovascular invasion, % (n)	65.5 (58)	58.9 (331)	0.34
	Any lymphovascular invasion, % (n)	76.4 (72)	69.7 (429)	0.25
	RCB 0 (vs nonzero) , % (n)	18.2 (33)	33.3 (204)	0.08
	RCB III (vs RCB 0-II) , % (n)	66.7 (33)	27.5 (204)	**<0.00001**

[11](n) is number of patients with available data.

Figure 1 - 158

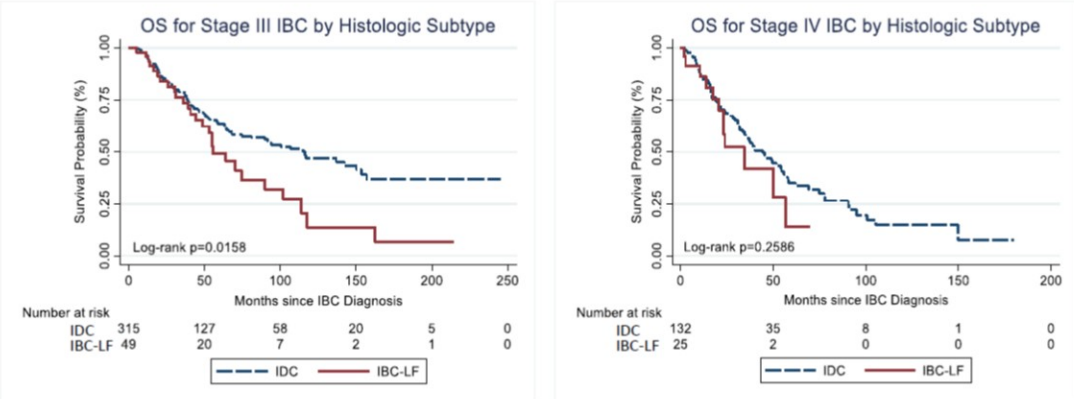

Conclusions: IBC-LF demonstrates the defining clinico-pathologic features of IBC, including skin changes, rapid symptom onset, and dermal LVI; however, direct dermal invasion is frequently present and may contribute to skin changes. It responds poorly to neoadjuvant chemotherapy and has worse overall survival than does IDC.

159 Heterogeneity of HER2 Positive Invasive Breast Cancer; A Comparative Analysis of Clinical Subtypes and Correlation with Response to Neoadjuvant Anti-HER2 Therapy (NAHT) and Clinical Outcome

David Pacheco[1], Tricia Rood[2], Yulun Liu[2], Yisheng Fang[2], Sunati Sahoo[2], Yan Peng[2], Helena Hwang[1], Prasad Koduru[2], Venetia Sarode[2]
[1]University of Texas Southwestern Medical Center, Dallas, TX, [2]UT Southwestern Medical Center, Dallas, TX

Disclosures: David Pacheco: None; Tricia Rood: None; Yulun Liu: None; Yisheng Fang: None; Sunati Sahoo: None; Yan Peng: None; Helena Hwang: None; Prasad Koduru: None; Venetia Sarode: None

Background: The heterogeneity of HER2 positive breast cancer has been recently elucidated by gene expression analysis. Some of the heterogeneity results from co-expression of estrogen receptor (ER) and or progesterone receptor (PR). Bidirectional cross-talk between ER and HER2 pathways has been demonstrated *in vivo* and ER status is a predictive marker of response to anti-HER2 therapy. The upregulation of ER expression can function as an escape mechanism leading to resistance to therapy.

We aim to further elucidate the HER2+ subtypes based on ER, PR expression, HER2 gene amplification levels and ki67 labeling index in patients treated with NAHT. To determine if there are differences in clinical-pathologic characteristics including pathologic response to NAHT and survival outcome among the HER2+ subtypes.

Design: This retrospective study was approved by the institutional review board. Data was obtained from the electronic medical records and laboratory information system such as age, menopausal status, BMI, procedure date, tumor size, lymph node status. Reflex testing for ER, PR, HER2, Ki67 was performed prior to pre-surgical therapy according to standard protocol and scoring was performed according to CAP/ASCO guidelines. HER2 gene amplification was assessed using the PathVysion Kit (Abbott Molecular, Abbot Park, IL) according to the manufacturer's specifications.

Tumor response to pre-surgical therapy was calculated based on-line MD Anderson Residual Cancer Burden® (RCB) with final pathologic staging according to the AJCC® staging. Pathologic complete response (pCR) was defined as absence residual

invasive cancer in the breast and axillary lymph nodes (ypT0/is pN0). The HER2 subtypes were classified as: HER2 enriched (ER-/PR-), HER2-luminal (ER+/ PR+) and HER2-luminal (ER+/PR-). Clinical follow-up (disease recurrence and metastasis) and survival was obtained from the electronic medical records.

Results: See table

Comparison of the clinical and pathological characteristics among Her2 subtype (n = 232)				
Variables	HER2+/ER-/PR- (n = 104)	HER2+/ER+/PR+ (n = 90)	ER+/PR- (n = 35)	*P* value
Age				
Mean ± SD Median [IQR]	51.66 ± 11.37 51.0 [44.0, 59.0]	48.50 ± 11.37 46.5 [41.0, 56.8]	53.26 ± 10.72 53.0 [47.0, 60.5]	0.056
BMI				
< 29	53 (51.0%)	49/89 (55.1%)	17 (48.6%)	0.764
≥ 29	51 (49.0%)	40/89 (44.9%)	18 (51.4%)	
Menopausal				
Pre	41/97 (42.3%)	49/88 (55.7%)	11 (31.4%)	0.032*
Post	56/97 (57.7%)	39/88 (44.3%)	24 (68.6%)	
Imaging size, cm				
Mean ± SD Median[IQR]	3.70 ± 2.80 3.1 [1.8, 4.9]	3.92 ± 3.13 3.0 [2.2, 4.2]	4.09 ± 2.41 3.8 [2.5, 5.6]	0.369
Nodal status				
Negative	15/71 (21.1%)	7/56 (12.5%)	6/27 (22.2%)	0.367
Positive	56/71 (78.9%)	49/56 (87.5%)	21/27 (77.8%)	
Tumor grade				
1 or 2	25/103 (24.3%)	37/86 (43.0%)	12 (34.3%)	0.024*
3	78/103 (75.7%)	49/86 (57.0%)	23 (65.7%)	
HER2 copy				
Mean ± SD Median [IQR]	16.70 ± 9.03 17.4 [10.8, 22.2]	15.02 ± 7.53 15.8 [7.6, 20.3]	15.69± 6.04 14.7 [10.5, 20.9]	0.700
HER2 ratio				
Mean ± SD Median [IQR]	6.93 ± 3.57 6.9 [4.1, 9.0]	6.37 ± 3.33 6.1 [2.9, 9.2]	6.50 ± 2.92 5.8 [4.7, 8.2]	0.681
ER				
Percent positive Mean ± SD Median [IQR]	NA	79.16 ± 25.05 90.0 [70.0, 98.0]	44.43 ± 41.23 40.0 [2.5, 89.5]	<0.001*
PR				
Percent positive Mean ± SD Median [IQR]	NA	41.27 ± 34.23 35.0 [9.0, 70.0]	NA	NA
Ki67				
Percent positive Mean ± SD Median [IRQ]	54.75 ± 21.48 52.5 [40.0, 70.0]	42.86 ± 22.11 40.0 [30.0, 55.0]	52.59 ± 20.94 48.5 [40.0, 67.0]	<0.001*
Neoadjuvant therapy				
Herceptin	34 (32.7%)	26 (28.9%)	12 (34.3%)	0.787
Herceptin + Pertuzumab	70 (67.3%)	64 (71.1%)	23 (65.7%)	
pCR				
No	51 (49.0%)	65 (72.2%)	19 (54.3%)	0.004*
Yes	53 (51.0%)	25 (27.8%)	16 (45.7%)	
RCB score				
0	53 (51.0%)	25 (27.8%)	16 (45.7%)	0.012*
1	20 (19.2%)	15 (16.7%)	7 (20.0%)	
2	23 (22.1%)	35 (38.8%)	10 (28.6%)	
3	8 (7.7%)	15 (16.7%)	2 (5.7%)	
Overall survival				
Alive	95 (91.3%)	86 (95.6%)	32 (91.4%)	0.439
Dead	9 (8.7%)	4 (4.4%)	3 (8.6%)	
Recurrence				
No	81 (77.9%)	80 (88.9%)	29 (82.9%)	0.118
Yes	23 (22.1%)	10 (11.1%)	6 (17.1%)	

Figure 1 - 159

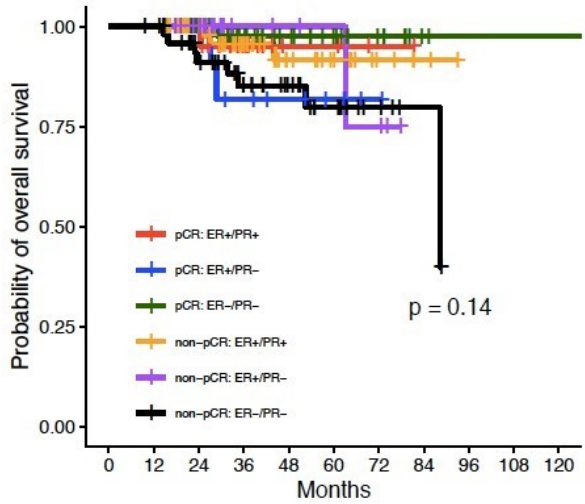

Figure 2 - 159

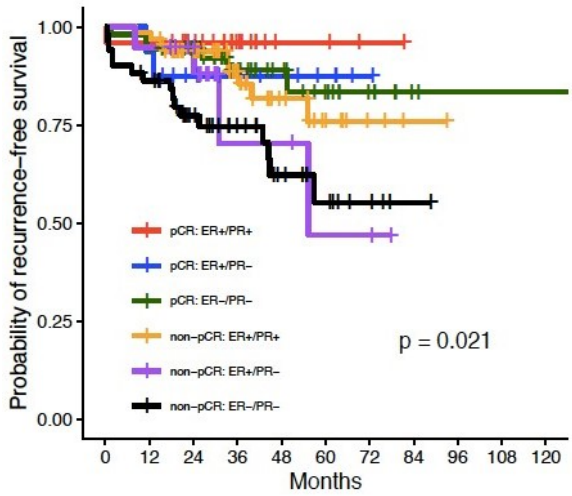

Conclusions: HER2 positive breast cancer subtypes are clinically distinct with significant differences in age, menopausal status, tumor grade, ki67 and pathologic response. The stratification based on ER and PR expression is clinically relevant with different sensitivities to NAHT. We demonstrated significant difference in recurrence free survival in those who achieved pCR versus non-pCR group based on ER and PR status.

Dual inhibition targeting both ER and HER2 pathways simultaneously may help to achieve best anti-tumor activity in this subtype of breast cancer.

160 Correlation of PD-L1 (22C3) and p53 Immunohistochemical Expression Patterns in Paired Primary and Metastatic Breast Carcinoma

Carlos Prieto Granada[1], Jingyun Yang[2], John Pickens[1], Lei Huo[3], Aysegul Sahin[3], Shuojun Chen[4], Shi Wei[5], Rati Chkheidze[1], Xiao Huang[1]

[1]The University of Alabama at Birmingham, Birmingham, AL, [2]Rush University Medical Center, Chicago, IL, [3]The University of Texas MD Anderson Cancer Center, Houston, TX, [4]East Carolina University, School of Medicine, Greenville, NC, [5]The University of Kansas School of Medicine, Birmingham, AL

Disclosures: Carlos Prieto Granada: None; Jingyun Yang: None; John Pickens: None; Lei Huo: None; Aysegul Sahin: None; Shuojun Chen: None; Shi Wei: None; Rati Chkheidze: None; Xiao Huang: None

Background: Overexpression of p53 by IHC in breast carcinomas has been correlated with both triple negative (TN) status and worse clinical behavior. The recently FDA-approved 22C3 PD-L1 IHC can give access to TN breast carcinoma patients to another immune check-point inhibitor (ICI) therapy. Herein, we describe the correlation between p53 and 22C3 PD-L1 IHC expression to pathological features and clinical outcome in breast carcinoma patients from out institution.

Design: Primary and paired metastatic tumors from 33 patients diagnosed and treated between 2003 and 2021 were reviewed and their Nottingham grade (NG), receptor status and clinical outcome were recorded. sTIL were assessed following the International sTIL working group's recommendations. Using p53 IHC (Bp53-11 Clone), p53 mutant pattern (p53 mut-p) was defined as either consistently strong and diffuse staining of at least 80% of tumor cells or as complete loss of expression in lesional cells with positive internal control. p53 wild-type pattern (p53 wt-p) was defined as variable nuclear staining signal in the tumor cells. 22C3 PD-L1 expression was assessed separately in tumor-infiltrating immune cells (IC) and in tumor cells (TC) as well as combining both cell types as combined positive score (CPS). A ³ 1% was used as the cutoff for PD-L1 positivity on IC, TC and 1 for CPS. Statistical correlation between these parameters was performed using Krushal-Wallis and Fisher exact studies.

Results: Results were shown in table 1, figure 1 and 2. All the paired primary-metastatic lesions (31/31, 100%) showed identical p53 status. p53 mut-p was significantly correlated with TN status, NG 3 and worse overall survival in primary tumors, and significantly correlated with TN status in metastatic lesions. In primary tumors, p53 mut-p showed higher sTIL (p=0.0169) and PD-

L1 TC (p=0.0018) when compared to lesions with p53 wt-p. In metastatic tumors, p53 mut-p did not show significant correlations with high sTIL, PD-L1 IC, TC or CPS positivity (Figure 2A-2D).

	Primary (n=32)				Metastasis (n=28)*		
	p53 mut-p (n=10)	p53 wt-p (n=22)	p-value		p53 mut-p (n=8)	p53 wt-p (n=20)	p-value
**TN(n=6)	6 (60%)	0 (0%)	0.0002	**TN(n=12)	7 (88%)	5 (25%)	0.0042
Non-TN(n=26)	4 (40%)	22 (100%)		Non-TN(n=16)	1 (12%)	15 (75%)	
**NG3 (n=13)	8 (80%)	5 (23%)	0.0051	N/A	N/A	N/A	N/A
Non-NG3(n=19)	2 (20%)	17 (77%)		N/A	N/A	N/A	N/A
Overall survival, month, average (range)	37 (8-92)	81 (28-170)	0.0032	N/A	N/A	N/A	N/A

**TN: Triple negative; NG3: Nottingham grade 3

* Twenty of thirty two metastatic tumors have available hormonal receptor studies for analysis.

Figure 1 - 160

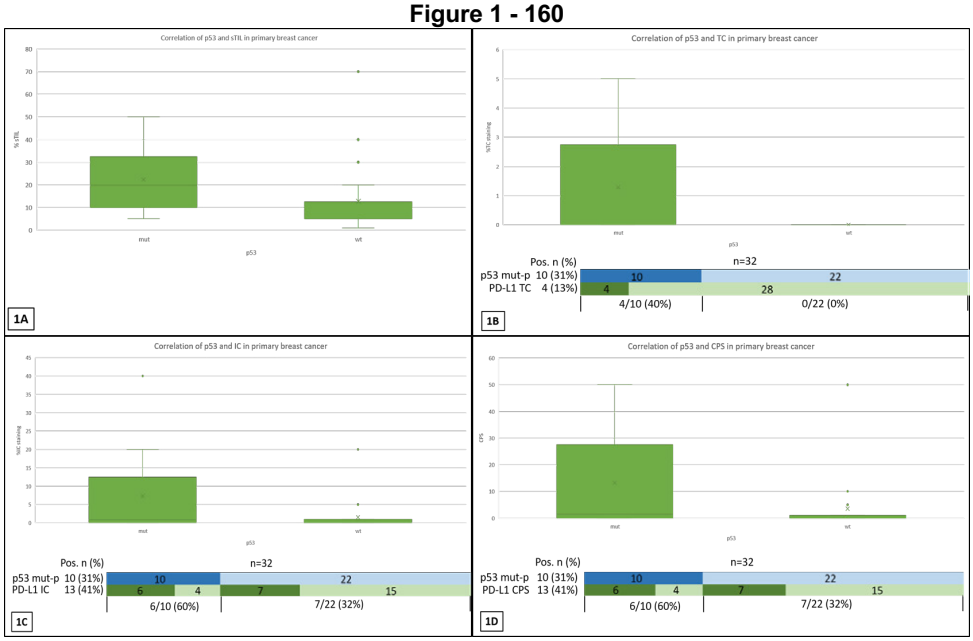

Figure 2 – 160

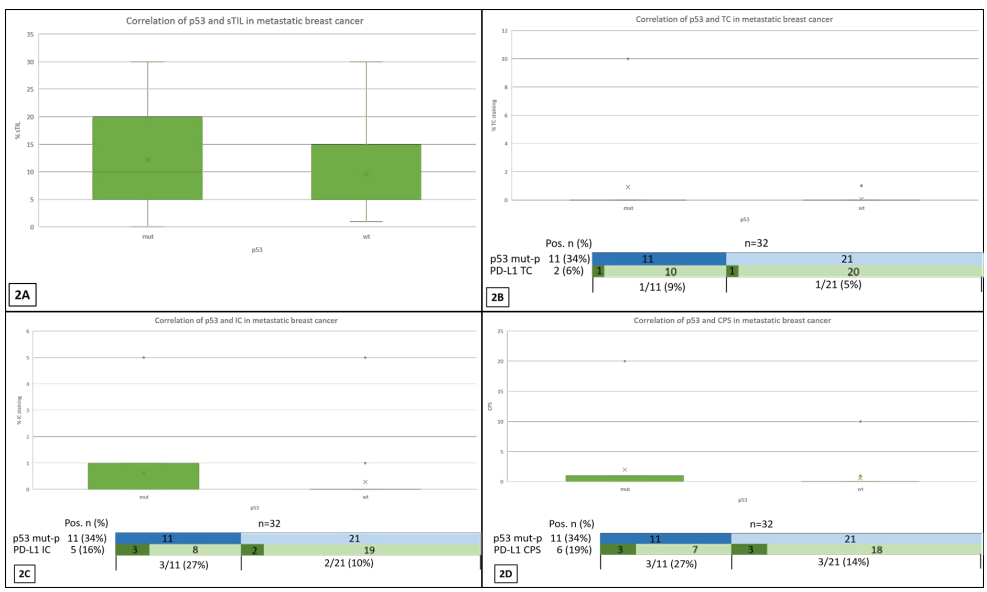

Conclusions: Our study shows clinicopathological significance of p53 IHC in breast carcinomas with p53 mut-p lesions being associated with higher grade, TN, increased sTIL and PD-L1 expression in the tumor cells, and have worse prognosis than p53 wt-p lesions.

161 Association of KISS1/ KISS1R Expression in Breast Cancer Subtypes in African American Women

Fareed Rajack[1], Luisel Ricks-Santi[2], Tammey Naab[3], Mustafa Qasim[4], Yasmine Kanaan[1]
[1]Howard University Hospital, Washington, DC, [2]Hampton University, Hampton, VA, [3]Washington, VA, [4]Howard University, Washington, DC

Disclosures: Fareed Rajack: None; Luisel Ricks-Santi: None; Tammey Naab: None; Mustafa Qasim: None; Yasmine Kanaan: None

Background: The kisspeptin (KISS) gene, located at 1q32, encodes a precursor polypeptide, which, after proteolysis, forms kisspeptin-10 (KISS1). KISS1 retains maximum physiological activity when binding to its receptor, KISS1R, acts as a metastasis suppressor in melanoma and carcinomas and is down regulated in metastases due to absent antimetastatic KISS1 function. KISS1 action is mediated by the G-protein coupled receptor 54, KISS1R, due to suppression of cell migration from the primary tumor site. Deletion of the partial estrogen response element (ERE), located in the KISS1R promoter sequence, could have a transcriptional suppressor effect on KISS1R expression. The study objective was to correlate immunohistochemical expression of KISS1 and KISS1R in subtypes of breast carcinoma in 214 African American (AA) women with grade, stage, disease-free, and overall survival.

Design: Expression of polyclonal rabbit anti-human antibodies, KISS1 and KISS1R (US Biological) was evaluated using duplicate cores on tissue microarray slides from 214 AA women. H-scores were determined based on multiplying intensity (0 to 3+) and the % of cells showing immunochemical expression, cytoplasmic for KISS1 and membranous for KISS1R.Final H-score was the average of the duplicate cores. Bivariate analysis was done via $\chi 2$ analysis and survivability data was calculated via the generation of Kaplan-Meier curves (SPSS v19). Statistical significance was assumed if $P < 0.05$.

Results: ANOVA analysis showed an association between PR and KISS1R with a P value of 0.035, but not KISS1 expression. No association was found between ER or HER2 with KISS1 or KISS1R expression. ANOVA analysis also showed an association of KISS1 with TBC and tumor size ($p<0.001$, $P<0.07$; respectively); and an association of KISS1R with TNBC, age of diagnosis, recurrence, and disease-free survival ($P<0.001$, $P<0.064$, $P=0.001$, $P=0.01$; respectively).

Conclusions: This initial investigation potentially implicates a role for KISS1/KISS1R in the pathogenesis of TNBC in AA women due to a role in suppression of metastasis. The association of KISS1/KISS1R recurrence and disease free survival in triple negative breast cancer in AA needs to be verified by larger studies including comparison with different ethnic populations.

162 SOX10 Can Help Distinguish Triple Negative Breast Cancers from Gynecologic Carcinomas

Rayan Rammal[1], Gloria Carter[1], Beth Clark[2], Esther Elishaev[2], Jeffrey Fine[3], Lakshmi Harinath[2], Mirka Jones[3], Thing Rinda Soong[3], Tatiana Villatoro[1], Jing Yu[3], Chengquan Zhao[4], Rohit Bhargava[2]
[1]University of Pittsburgh Medical Center, Pittsburgh, PA, [2]UPMC Magee-Womens Hospital, Pittsburgh, PA, [3]University of Pittsburgh, Pittsburgh, PA, [4]Magee-Womens Hospital, University of Pittsburgh Medical Center, Pittsburgh, PA

Disclosures: Rayan Rammal: None; Gloria Carter: None; Beth Clark: None; Esther Elishaev: None; Jeffrey Fine: *Stock Ownership*, SpIntellx, Inc.; Lakshmi Harinath: None; Mirka Jones: None; Thing Rinda Soong: None; Tatiana Villatoro: None; Jing Yu: None; Chengquan Zhao: None; Rohit Bhargava: None

Background: A high-grade invasive carcinoma in the breast that is negative for hormone receptors and HER2 without an accompanying in-situ carcinoma often requires additional workup to confirm breast origin. A panel comprised of breast-specific markers (GATA3, GCDFP15, Mammaglobin) along with TTF1 and PAX8 is often sufficient for confirmation. However, occasionally, the tumor is negative for all breast-specific markers and shows weak/moderate expression for PAX8 creating some confusion about the site of origin. Since SOX10 has been reported to be a sensitive marker of triple negative breast carcinomas (TNBCs), we investigated if SOX10 could be a useful marker in distinguishing TNBCs from gynecologic cancers.

Design: Consecutive breast carcinomas (n=146), TNBCs (n=139), TNBCs with low Ki-67 proliferation index (triple negative low proliferation or TNLP tumors, n=50), and various subtypes of gynecologic carcinomas (n=157) were evaluated with SOX10 immunohistochemistry using tissue microarrays (TMAs). The tissue TMAs of gynecological carcinomas were enriched for serous carcinoma. The TNLP tumors are automatically enriched for luminal androgen receptor or LAR-type tumors. An H-score of 1 was considered a positive result for SOX10.

Results: A total of 492 tumors were tested for SOX10 staining (see table).

TMA type and tumors	SOX10 +ve/total (%)	Comment
Consecutive breast cancers (n=146) ER+/HER2-neg HER2+ ER-neg/HER2-neg	7/103 (7%) 2/20 (10%) 16/23 (70%)	The ER-neg/HER2-neg tumors showed moderate to strong nuclear staining, while the ER+ and HER2+ tumors showed only scattered weak staining with median H-score of 10 in positive cases.
TNBC-all types (n=139)	92/139 (66%)	SOX10 mostly positive in basal-like and matrix producing (median H-score 205 in positive cases), but apocrine tumors were negative
TNLP only (n=50)	11/50 (22%)	TMA enriched for apocrine tumors, which were negative for SOX10
Ovarian carcinomas (n=92) Serous Clear cell Endometrioid	0/61 (0%) 0/26 (0%) 0/5 (0%)	
Endometrial carcinomas (n=45) Endometrioid Serous Clear cell Undifferentiated Carcinosarcoma	0/31 (0%) 0/7 (0%) 0/3 (0%) 0/3 (0%) 0/1 (0%)	
Endocervical carcinomas (n=20) Typical and endometrioid Others	0/16 (0%) 0/4 (0%)	

TMA: Tissue microarray; TNBC: Triple negative breast cancer; TNLP: Triple negative low proliferation (TNBCs with 30% or less Ki-67 proliferation index)

Figure 1 - 162

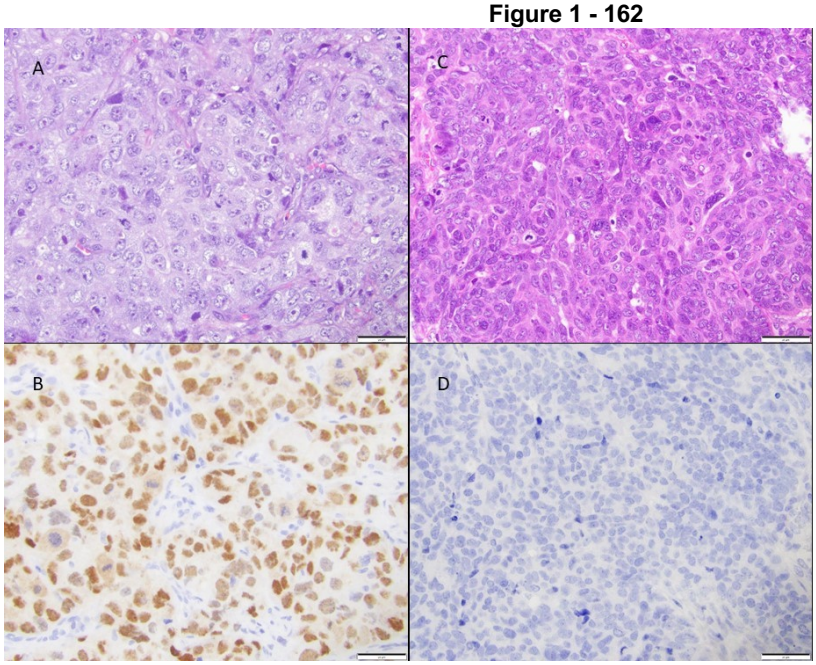

A: Triple negative breast carcinoma

B: Tumor in A positive for SOX10

C: Ovarian serous carcinoma

D: Tumor in B negative for SOX10

Conclusions: SOX10 is positive in 65-70% of TNBCs (mostly positive in basal-like but negative in LAR-type) and is negative in gynecologic carcinomas (all subtypes tested negative in our cohort). When breast-specific markers are negative in a breast tumor and the differential diagnosis includes a metastatic tumor from the gynecologic tract, SOX10 immunoreactivity supports mammary origin and one can confidently exclude a gynecologic primary.

163 Utility of SOX10 in Distinguishing Atypical Ductal Hyperplasia and DCIS from Usual Ductal Hyperplasia

Rayan Rammal[1], Gloria Carter[1], Beth Clark[2], Jeffrey Fine[3], Lakshmi Harinath[2], Tatiana Villatoro[1], Jing Yu[3], Rohit Bhargava[2]
[1]University of Pittsburgh Medical Center, Pittsburgh, PA, [2]UPMC Magee-Womens Hospital, Pittsburgh, PA, [3]University of Pittsburgh, Pittsburgh, PA

Disclosures: Rayan Rammal: None; Gloria Carter: None; Beth Clark: None; Jeffrey Fine: *Stock Ownership*, SpIntellx, Inc.; Lakshmi Harinath: None; Tatiana Villatoro: None; Jing Yu: None; Rohit Bhargava: None

Background: Atypical ductal hyperplasia (ADH) of the breast increases the risk of subsequent invasive carcinoma by 3.5 fold. With an upgrade rate (to in-situ or invasive carcinoma) of around 10-15%, often resulting in diagnostic excision procedure, an accurate diagnosis of ADH on core biopsy has significant clinical implications. Morphologic criteria are often sufficient to make a diagnosis of ADH but in cases with equivocal findings, lack of CK5 (a basal marker) staining of intra-ductal proliferative epithelium is utilized to make the diagnosis of ADH. In contrast, a mosaic pattern of staining with CK5 is expected in usual ductal hyperplasia (UDH). Staining for ER is less helpful in making the distinction between ADH and UDH. Other basal markers have not been extensively examined in making this distinction. SOX10 has been shown to stain 70% of triple negative (TN) breast cancers and described to stain breast myoepithelial cells. Our own experience suggests SOX10 to be a robust basal-like marker. Therefore, we hypothesized that SOX10 can be used to distinguish ADH from UDH.

Design: 34 cases of ADH (for which CK5 was utilized to confirm the diagnosis), 50 cases of UDH and 29 cases of DCIS (19 ER+ and 10 ER-negative) were stained for SOX10.

Results: All 34 ADH cases lacked SOX10 staining. All 50 UDH cases showed patchy mosaic nuclear reactivity within intra-ductal proliferative epithelium. These included 36 cases of UDH in which CK5 was performed and showed reactivity within UDH. SOX10 was negative in all 19 ER+ DCIS cases. Of the 10 ER-negative DCIS cases, 8 were SOX10 negative and 2 were SOX10 positive. The two SOX10+ DCIS cases had co-existing invasive carcinoma which were TN and SOX10+. 2 DCIS cases also contained solid papillary carcinoma (SPC) and showed lack of SOX10 staining within and around SPC. SOX10 consistently stained myoepithelium around normal ducts/lobules, ADH and UDH, however, SOX10 staining of myoepithelium around DCIS was somewhat attenuated in 9 of 29 cases (31%).

Figure 1 - 163

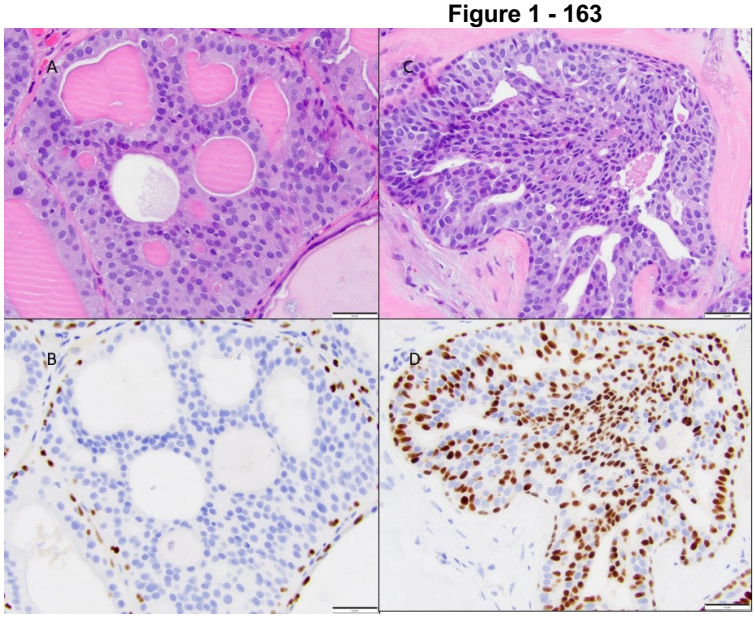

A: Atypical ductal hyperplasia (ADH)

B: ADH negative for SOX10

C: Usual ductal hyperplasia (UDH)

D: UDH mosaic positive for SOX10

Conclusions: Similar to CK5, SOX10 is negative within ADH and ER+ DCIS, but shows patchy/mosaic staining within UDH, thus SOX10 can be used in place of or along with CK5 in distinguishing ADH from UDH. SOX10 more reliably stains myoepithelial cells compared to CK5 within normal breast tissue, but SOX10 expression around DCIS can be somewhat attenuated and should be used with caution in diagnosing invasion. One should continue using the usual myoepithelial markers (such as p63, myosin heavy chain) for diagnosing invasion.

164 Using Machine Learning to Predict Final HER2 Status in Invasive Breast Cancer Cases that are Equivocal (2+) by Immunohistochemistry

Sean Rasmussen[1], Valerie Taylor[2], Alexi Surette[3], Penny Barnes[1], Gillian Bethune[1]
[1]Queen Elizabeth II Health Sciences Centre and Dalhousie University, Halifax, Canada, [2]Dalhousie University, Halifax, Canada, [3]Vitalite Health Network, Moncton, Canada

Disclosures: Sean Rasmussen: None; Valerie Taylor: None; Alexi Surette: None; Penny Barnes: None; Gillian Bethune: None

Background: Cases of invasive breast carcinoma are routinely tested for HER2 using immunohistochemistry (IHC), with reflex in situ hybridization (ISH) for those scored as equivocal (2+). ISH testing is expensive, time-consuming, and not universally available. In this study, we trained a machine learning algorithm to directly predict HER2 gene amplification status from IHC slides scored as equivocal.

Design: Data included 115 consecutive cases of invasive breast carcinoma scored as equivocal (2+) by IHC that had follow-up ISH testing to determine HER2 status. All IHC slides were digitized and divided into training (80%) and test (20%) sets using a 5-fold cross-validation approach. From each digitized slide, representative regions containing invasive carcinoma were extracted and divided into small patches (256x256 pixels). A convolutional neural network with EfficientNetB0 architecture was trained using a transfer learning approach, whereby the base model was pre-trained on ImageNet data and only the final layers were trained on the 256x256 pixel patches from HER2 IHC slides. To generate HER2 predictions for slides in the test set, 101 small patches extracted from regions of invasive cancer were analyzed, and the results were aggregated according to the percentage of patches classified as positive.

Results: On small image patches, the trained model achieved a receiver operating characteristic area under the curve (AUC) of 0.72. Aggregating patch predictions to generate a slide-level prediction resulted in an AUC of 0.83. This equated to an overall accuracy of 79.4% (sensitivity = 0.70, specificity = 0.82).

Conclusions: Using only IHC slides scored as equivocal (2+), this model is capable of correctly predicting HER2 amplification status in 79.4% of cases. Although the sensitivity and specificity are not high enough to negate the need for reflexive ISH testing entirely, this approach may be useful for triaging cases and initiating treatment planning in centers where HER2 ISH testing is not readily available.

165 Myofibroepithelial Nodules: Expanding the Spectrum of Myofibroblastic Proliferations of the Breast

Edward Richardson[1], Stuart Schnitt[2]
[1]Brigham and Women's Hospital, Harvard Medical School, Boston, MA, [2]Brigham and Women's Hospital, Dana-Farber Cancer Institute, Harvard Medical School, Boston, MA

Disclosures: Edward Richardson: None; Stuart Schnitt: None

Background: Fibroepithelial lesions (FEL), such as fibroadenomas (FA) and phyllodes tumors (PT), are the prototypical combined stromal-epithelial lesions of the breast. We have encountered a series of combined stromal-epithelial nodules in breast core needle biopsies (CNB) that superficially resemble FEL but with the stromal areas showing myofibroblastic features, lesions we term myofibroepithelial nodules (MFN).

Design: Between 1/2021 and 9/2021, 10 cases of MFN on CNB were identified in consultation material (n=6) or in house CNB (n=4). To identify additional cases, we searched our pathology archive between 1/2019 and 8/2021 for "cellular FEL" and "FEL with increased cellularity." 37 cases were identified; histologic review revealed 1 MFN and 36 FEL. For each case, we reviewed clinical and radiologic features and performed CD34, smooth muscle actin (SMA) and desmin immunohistochemical stains.

Results: Among the 11 MFN cases, the median patient age was 43 years (range 22-58) and all were female. 9 patients had available clinical and radiologic details; all had masses on imaging studies and 2 were palpable. On imaging, the median lesion size was 1.2 cm (range 0.6-2.7); the border was circumscribed in 2 cases and non-circumscribed in 7. MFN were composed of a variably cellular proliferation of spindle cells with ovoid nuclei, arranged in short fascicles, with admixed dense collagen. The epithelial component consisted of round to ovoid, open glands composed of columnar cells with ovoid nuclei and apical snouts. Where present, the lesion edge was circumscribed to focally irregular with entrapped adipocytes. Pseudoangiomatous stromal hyperplasia (PASH) was seen in the adjacent breast tissue in 6 cases and within the lesion in 3. The stromal cells of all 11 MFN

showed uniform, strong SMA staining, variable CD34 staining, and focal desmin staining. While most FEL showed some staining for SMA, none had the same extent and intensity as the MFN.

Conclusions: MFN are combined stromal-epithelial lesions in which the stromal component is composed of myofibroblasts. While the histologic appearance resembles cellular FEL, MFN are distinguished by diffuse staining for SMA and lack of an intracanalicular pattern. While MFN could be considered a variant of fascicular PASH, the admixed glandular component and nodular configuration are more suggestive of a distinct hyperplastic stromal-epithelial lesion with myofibroblastic differentiation. Further studies are needed to address the pathogenesis of these lesions.

166 Mammary Adenomyoepithelioma and Malignant Adenomyoepithelioma: Clinical, Histologic and Immunophenotypic Characteristics of 34 cases

Prih Rohra[1], Nour Sneige[1], Constance Albarracin[1]
[1]The University of Texas MD Anderson Cancer Center, Houston, TX

Disclosures: Prih Rohra: None; Nour Sneige: None; Constance Albarracin: None

Background: Adenomyoepithelioma (AME) of the breast is a rare neoplasm characterized by a biphasic proliferation of epithelial (EC) and myoepithelial cells (MEC) in varying proportions and with different morphologies. Although majority of AMEs are benign with good prognosis, some may show malignant transformation, local recurrence or distant metastasis. There is no established reference to differentiate between benign and malignant AMEs. The primary objective of this study is to identify specific histologic and immunophenotypic features that may assist in the diagnosis and predict clinical behavior.

Design: 41 cases of breast AME between 2010-2021 were identified and evaluated for histopathologic and immunohistochemical features along with radiologic findings.

Results: 41 cases were evaluated by 2 breast pathologists blinded to the original diagnosis. Excluded were 7 papillomas with myoepithelial proliferation or involvement by lobular carcinoma in-situ mimicking myoepithelial cells and metaplastic tumors. Radiologic findings available in 19 cases, included asymmetry in 4,mass in 13 and calcifications in 3. Histologically, 7 cases were categorized as malignant and 27 as benign. Of the malignant cases (Table),4 had infiltrative borders,2 were circumscribed, and 1 was multinodular associated with a satellite nodule . Histologically, 5 were tubular and 2 had both spindle and tubular patterns. All these cases had >4 mitosis/10hpf and nuclear grade 2-3 atypia. Necrosis was noted in 1 case. All 7cases were positive for SMA, 2/7 showed loss of SMM expression however P63 was variable, showing antigenic variability. 27/34 cases were categorized as benign, 1 of which had infiltrative borders, and 26 were circumscribed. Histologically, 22 were tubular and 2 had tubular and spindled mixed features. 4 cases had multinodularity. Mitosis were <4/10hpf in all cases.3/27 cases showed mild nuclear pleomorphism.

Case#	Capsule	Tumor borders	Configuration	MEC pattern of growth	MEC%	MEC atypia	MEC mitosis per 10HPF	Epithelial atypia	Specific Epithelial features	Stroma characteristics	Necrosis%	Compressed /dilated ducts	Metaplastic change	Calcification within the lesion	Satellite nodules	Hyaline degeneration in center	Thick fibrous septa	Background lesion
1	No	Circumscribed	Tubular	nests	>50	G3	>4	G2	luminal apical snouts	No	No	No	No	No	Yes	No	No	Intraductal papilloma
2	No	Infiltrative	spindle	sheets	70	G2	>8	G2	cytically dilated with intraluminal papillary projections	No	No	No	No	No	No	No	Yes	No
3	No	Infiltrative	Tubular	Sheets	>50	G2	>5	G2-G3	No	Fibromyxoid stroma	Yes	No	No	No	No	Yes	Yes	No
4	Yes	Multinodular	Tubular	nests	50	G3	>10	G2	No	Hyalinized stroma	No			Yes	Yes	Yes	Yes	Collagenous spherulosis, Intraductal papilloma
5	No	Infiltrative	Tubular and spindle	nests	50	Malignant spindle cells, G3	>4	No	No	No	No	No	No	No	No	No	No	Sclerosing adenosis
6	No	Circumscribed	Tubular	sheets	70	G2	>4	G3,	Luminal secretions	No	No	No	No	No	No	No	No	Radial sclerosing lesion
7	No	Infiltrative	Tubular	nests and sheets	60	G2-3	>4	G2-3	Luminal secretions	no	No	No	no	no	no	Yes	yes	No

Conclusions: Histologic features favoring malignancy included high grade atypia often involving both components, extensive necrosis, and >4 mitosis/10hpf.Most consistent EC marker was Ck8/18 highlighting all EC component diffusely and strongly in all cases and was very helpful especially where MEC proliferation was pronounced. For MECs SMA was most consistent marker which was consistently positive in 100% of the cases. CK 5/6 and E-cadherin were variable and least helpful MEC markers. The above histologic features coupled with SMA and CK8/18 panel are highly recommended in the evaluation of these lesions.

167 Diagnostic Utility of TRPS1 Immunohistochemistry in Primary and Metastatic Breast Carcinoma with Special Emphasis on Spindle Cell Neoplasms of the Breast

Sudarshana Roychoudhury[1], Hassan Sheikh[2], Silvat Sheikh-Fayyaz[1]
[1]Donald and Barbara Zucker School of Medicine at Hofstra/Northwell, New York, NY, [2]Hofstra Northwell School of Medicine

Disclosures: Sudarshana Roychoudhury: None; Hassan Sheikh: None; Silvat Sheikh-Fayyaz: None

Background: Trichorhinophalangeal syndrome type 1 (TRPS1) has recently been recommended as a sensitive and specific marker for triple negative breast carcinoma (TNBC) and in supporting breast origin in metastatic carcinomas of unknown origin. However, TRPS1 expression by immunohistochemical (IHC) staining has not been evaluated in other spindle cell neoplasms of breast which are differential diagnosis of metaplastic carcinoma. We aim to evaluate the role of TRPS1 in TNBC and metastatic breast carcinomas with special emphasis on TRPS1 IHC expression in spindle cell neoplasms of breast.

Design: Primary poorly differentiated breast carcinomas and metastatic carcinomas of unknown origin collected during January – July 2021 were analyzed. Only those metastatic carcinomas with subsequent clinical confirmation of breast origin were included. TRPS1 and GATA3 IHC were assessed (intensity and percentage of nuclear positivity in tumor cells) by 2 breast pathologists. Numerical values were assigned to percentage of positive cells (0:< 1%, 1: 1-50%, 2 > 50%) and intensity of staining (0: negative, 1: weak, 2: moderate, 3: strong). A composite score was calculated by multiplying the two numerical scores and then divided into 3 groups (1: low, 2,3: Moderate, 4,6: High).

Results: 14 TNBC, 13 spindle cells neoplasms of breast and 14 metastatic breast carcinoma (MBC) cases were analyzed. TRPS1 and GATA3 had comparable positive expression in ER/PR positive, HER 2 positive and MBC cases. TRPS1 expression in TNBC, was significantly higher than GATA3 (p-value .043047; Chi-Square) along with intensity of expression (p-value .000648; t-test). However, TRPS1 was positive in 46% of non-metaplastic spindle cell neoplasms of breast (composite staining score intermediate/high) compared to 0 % with GATA -3 (p-value .000048; ANOVA analysis).

Table 1: TRPS1 and GATA-3 immunohistochemical (IHC) expression in primary and metastatic breast carcinoma

			Negative Cases	Positive cases			Total Cases
Composite staining score				Low	Moderate	High	
TRPS1							
	Primary breast carcinoma						
	ER/PR+				1 (100%)		1
	HER2 +				1 (100%)		1
	TNBC						
		Metaplastic breast carcinoma	2 (20%)		1(10%)	7(70%)	10
		Non-metaplastic breast carcinoma				4(100%)	4
	Other spindle cell neoplasms of breast						
			2(15%)	5(38.5%)	5(38.5%)	1(8%)	13
GATA -3							
	Primary breast carcinoma						
	ER/PR+					1(100%)	1
	HER2 +					1(100%	1
	TNBC						
		Metaplastic		5(50%)	4(40%)	1(10%)	10
		Non-metaplastic breast carcinoma	2(50%)			2(50%)	4
	Other spindle cell neoplasms of breast						
			10(77%)	3(23%)			13
Metastatic breast carcinoma							
TRPS1							
	ER/PR+					7(100%)	7
	HER 2+					1(100%)	1
	TNBC		1(17%)		1(17%)	4(66%)	6
GATA-3							
	ER/PR+					7(100%)	7
	HER2+					1(100%)	1
	TNBC		1(17%)			5(83%)	6

Metaplastic carcinoma: 4 spindle cell metaplastic; 2 squamous; 4 heterologous (3 chondroid, 1 osteoid).
Spindle cell neoplasms: myofibroblastoma (5), fibromatosis (2); angiosarcoma (2); malignant phyllodes (2); DFSP (1); synovial sarcoma (1)
Metastatic sites: Brain (4); lymph node (3); spinal cord (2); bone (2); liver (2); pancreas(1)

Figure 1 - 167

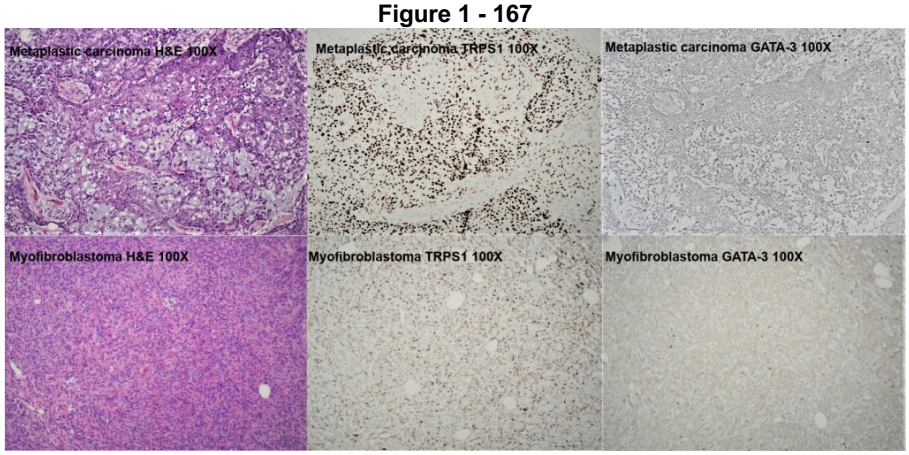

Conclusions: TRPS1 is a sensitive new diagnostic marker for TNBC compared to GATA3. However, TRPS1 can be positive in other spindle cell neoplasms of breast which are differential diagnosis of metaplastic carcinoma. It is important to be aware of this while interpreting spindle cell lesions of the breast. This was a pilot study in our institution and we are performing further studies to investigate the expression of TRPS1 in non metaplastic spindle cell neoplasms of breast.

168 Upgrade Rates of Radial Scar/Complex Sclerosing Lesions Diagnosed on Breast Core Needle Biopsies with Radiologic-Pathologic Concordance

Thomas Sabljic[1], Rachel Han[1], Emily Boulos[2], Vivianne Freitas[3], Elzbieta Slodkowska[4], Anna Marie Mulligan[5], Gulisa Turashvili[6]

[1]University of Toronto, Toronto, Canada, [2]University Health Network, Toronto, Canada, [3]Princess Margaret Hospital, Toronto, Canada, [4]Sunnybrook Health Sciences Centre, University of Toronto, Toronto, Canada, [5]University Health Network, University of Toronto, Toronto, Canada, [6]Mount Sinai Hospital, University of Toronto, Toronto, Canada

Disclosures: Thomas Sabljic: None; Rachel Han: None; Emily Boulos: None; Vivianne Freitas: None; Elzbieta Slodkowska: None; Anna Marie Mulligan: None; Gulisa Turashvili: None

Background: Radial scar/complex sclerosing lesions (RS/CSL) of the breast are benign entities characterized by central fibroelastosis with entrapped glandular structures. Due to variability in reported upgrade rates in the literature (0-41%), optimal management of RS/CSL without atypia diagnosed on core needle biopsies (CNB) remains controversial. We set out to evaluate whether excision is warranted in cases where RS/CSL is diagnosed as the highest risk lesion on CNB in the context of radiologic-pathologic concordance.

Design: Electronic database searches for RS/CSL without atypia diagnosed on CNB between 2000 and 2018 with paired excisions were performed at three academic institutions. Clinical, pathologic and radiologic features were recorded. Radiologic-pathologic concordance was reassessed for each case. Cases with coexisting atypia or malignancy or with radiologic-pathologic discordance were excluded. Upgrade was defined by the presence of ductal carcinoma in situ (DCIS) or invasive carcinoma on excision.

Results: The cohort consists of 98 patients with RS/CSL lacking atypia diagnosed on CNB with subsequent excisions. Eleven cases with radiologic-pathologic discordance were excluded, none of which was associated with upgrade. The median patient age was 47 years (20-75). Residual RS/CSL was identified in 74/98 (76%) excisions. The overall upgrade rate was 6% (6/98), including DCIS in 5 cases (5%) and invasive carcinoma (tubular carcinoma) arising within a RS/CSL in 1 case (1%) (Table 1).

Table 1. Summary of Upgrade Cases

Case	**1**	**2**	**3**	**4**	**5**	**6**
Age	45	47	50	53	57	63
BI-RADS Score	5	4	4	4	4	4
Concordance	Yes	Yes	Yes	Yes	Yes	Yes
Upgrade Diagnosis	DCIS	DCIS	DCIS	DCIS	Tubular carcinoma	DCIS

Conclusions: This study demonstrates that a finding of RS/CSL without atypia on CNB with radiologic-pathologic concordance is associated with a modest overall upgrade rate of 6%. The upgrade rate to invasive carcinoma of 1% is similar to the findings of recent studies incorporating radiologic-pathologic concordance. The findings provide further evidence to support conservative management of RS/CSL without atypia diagnosed on CNB when radiologic-pathologic concordance is achieved.

169 Effect of Tumor Cell-Derived Interferon Beta-1 on Immune Environment of Basal-Like Carcinomas of Breast

Qandeel Sadiq[1], FNU Alnoor[1], Twisha Oza[1], Meiyun Fan[1]
[1]The University of Tennessee Health Science Center, Memphis, TN

Disclosures: Qandeel Sadiq: None; FNU Alnoor: None; Twisha Oza: None; Meiyun Fan: None

Background: Breast cancer constitutes a varied spectrum of tumors with different degrees of immunogenicity. Basal-like carcinoma (BLC) is known to be a more immunogenic subtype that is characterized by the presence of high levels of tumor-infiltrating lymphocytes (TILs) and tertiary lymphoid structures (TLS). This study is aimed to examine whether tumor cell-derived IFNB1, a key regulatory cytokine of immune responses to foreign and self-antigens, plays a role in modulating the immune environment of BLC.

Design: The H&E images, gene expression, and DNA methylation data of BLC in the TCGA database were used to examine the association of IFNB1 expression in tumor cells with the presence of TLS and expression of signatures of various subtypes of TILs. Formalin-fixed, paraffin-embedded (FFPE) tissues were subjected to H&E staining, RNAscope 2.5 LS in situ hybridization, IHC, and qPCR assays to validate key findings from the TCGA data analysis. In addition, Single-cell RNAseq data of breast cancer in the Gene Expression Omnibus (GEO) GSE114725, GSE161529, and GSE158399 were analyzed to identify immune cells primarily targeted by tumor cell-derived IFNB1.

Results: IFNB1 expression, coupled with high expression of CDKN2A and demethylation of a CpG island cg14069088 was detected in 24% (42/172 cases) of BLC in the TCGA database. TLS was observed in 23.8% (41/172 cases). No association between tumor cell-derived IFNB1 and the presence of TLS was observed. Correlation analysis revealed that IFNB1 expression was positively associated with expression of signatures of IFN type I (i.e., CXCL10, IFI44L, USP18, ISG15, and CMPK2), myeloid-derived immune-tolerant dendritic cells (i.e. CD163, MS4A4A, IDO1, CCL8, and IL10), and regulatory T cells (i.e., FOXP3, CTLA4, TIGIT, PDCD1). By using RNAscope 2.5 LS ISH assay and patient FFPE tissues, we confirmed that 25% of BLC tissues contain tumor cells that coexpress IFNB1 and CDKN2A. IHC analysis showed that CD3+T cells and CD79+B cells were primarily located in TLS, while myeloid-derived cells (CD68 positive) were in tumor islets to form direct contact with tumor cells. Single-cell RNAseq data of breast cancer in the GEO database confirmed the presence of the myeloid-derived immune-tolerant dendritic cells that express genes induced by IFNB1 such as CXCL10.

Conclusions: Although tumor cell-derived IFNB1 in BLC is not a crucial factor for the formation and maintenance of TLS, it promotes the generation of immune tolerant dendritic cells and regulatory T cells.

170 Invasive Breast Carcinoma Associated with Microglandular Adenosis: A Tertiary Care Cancer Institute Experience of a Rare Entity

Ayushi Sahay[1], Asawari Patil[2], Tanuja Shet[1], Sangeeta Desai[3]
[1]Tata Memorial Hospital, Mumbai, India, [2]ACTREC-Tata Memorial Centre, Thane, India, [3]Tata Memorial Centre, Mumbai, India

Disclosures: Ayushi Sahay: None; Asawari Patil: None; Tanuja Shet: None; Sangeeta Desai: None

Background: Microglandular adenosis (MGA) forms a rare exception to the presence of myoepithelial cells (MEC) around benign ducts and is extremely rare. The transition of MGA to atypical MGA to ductal carcinoma in situ (DCIS) and finally invasive breast carcinoma (IBC) (MGA-CA) has been described suggesting a role as IBC precursor. Due to rarity, there is a marked paucity of data on the clinicopathological spectrum of MGA-CA. We studied clinicopathological features of IBC developing in MGA.

Design: We retrospectively analyzed clinicopathological features of all MGA-CA diagnosed at our tertiary care oncology center from 2005-2021. All available slides were reviewed. Clinical findings were obtained from electronic medical records.

Results: Nineteen patients of MGA-CA (with 21 tumors) formed <0.1% of all IBC diagnosed in the specified duration. All were females with an age range 33-60 years (median 46). Family history (FH) of cancer was noted in 5/10 patients (3 uterine/ovarian, 1 breast & prostate, 1 hematological), and one without FH showed BRCA1 mutation. Two tumors were bilateral, one (BRCA+) showed synchronous tumors, while the other was metachronous, and MGA was unilateral in both. Breast conservation surgery (BSC) was done for 10, mastectomy for 7, and BCS followed by revision (wide excision or mastectomy) in 4 for the initial margin involved by tumor/MGA. Core biopsies were done in 9 cases for primary diagnosis, 4 of them showed only IBC, 3 showed IBC with MGA, while 2 only atypical MGA. On histology, 19 tumors were grade III, 2 were grade II. The majority were IBC, no special type (NST)(16/21), 1 metaplastic, 2 each with focal acinic/clear cell morphology. The transition from typical MGA to atypical to DCIS and IBC was noted. All were triple negative (TNBC), except one PR low positive and one contralateral tumor ER positive. MGA areas showed lack of MEC markers while reticulin stain highlighted intact basement membrane, which was disrupted in areas of invasion. S100 was diffusely positive in all MGA but variable in invasive tumor. P53 showed diffuse strong positivity in both MGA and invasive tumor (5/11 cases). Details of therapy and follow-up were available in 11 cases- neaoadjuvant chemotherapy followed by surgery and adjuvant (adj) CT &/or RT (3 cases); Adj CT+RT (5), only adj CT (1) and no adj (2). No local recurrence was noted in cases that underwent resection with clear margins. Three patients progressed (3/11, 27%), with widespread metastasis, one developed contralateral tumor after 17 months, and one Ca endometrium 5 years later. Clinical remission was seen in 6 patients after therapy (duration 1-71 months, median 31).

Conclusions: MGA-CA, usually TNBC, NST, are exceedingly rare and may be associated with FH of cancer and/or BRCA and/or p53 overexpression. Core biopsy may show areas of MGA associated with IBC. Wide excision with margins clear of tumor and MGA can be planned to prevent local recurrence if MGA is detected on core biopsy.

171 Explainable Deep Learning Predicts Molecular Subtypes and Improves Risk of Relapse Assessment from Invasive Breast Cancer Histological Slides

Charlie Saillard[1], Ingrid Garberis[2], Damien Drubay[2], Valentin Gaury[1], Victor Aubert[1], Benoît Schmauch[1], Alexandre Jaeger[2], Loïc Herpin[1], Kevin Elgui[1], Julia Linhart[1], Aurélie Kamoun[1], Fabrice Andre[2], Magali Lacroix-Triki[3]

[1]Owkin, Paris, France, [2]Gustave Roussy, Cancer Campus, Grand Paris, Villejuif, France, [3]Gustave Roussy, Cancer Campus, Grand Paris, Villeurbanne, France

Disclosures: Charlie Saillard: *Employee*, Owkin; Ingrid Garberis: None; Damien Drubay: None; Valentin Gaury: None; Victor Aubert: *Employee*, Owkin; Benoît Schmauch: *Employee*, Owkin; Alexandre Jaeger: *Consultant*, Calypse Consulting; Loïc Herpin: None; Kevin Elgui: *Employee*, Owkin; Julia Linhart: *Employee*, Owkin; Aurélie Kamoun: *Employee*, Owkin; Fabrice Andre: *Grant or Research Support*, Roche; *Grant or Research Support*, Novartis, Astra Zeneca, Lilly, Pfizer, Daiichi Sankyo; Magali Lacroix-Triki: *Consultant*, Owkin, Myriad Genetics; *Speaker*, Genomic Health; *Consultant*, Roche, Roche Diagnostics; *Speaker*, AstraZeneca; *Speaker*, MSD; *Advisory Board Member*, MyPI

Background: Breast cancer (BC) is a heterogeneous disease with regards to subtype classification, and associated to a wide range of prognosis related to the tumor molecular phenotypes, defined by surrogate biomarkers, including estrogen receptor (ER), progesterone receptor (PR), HER2 and Ki67. The aims of our study were to develop explainable Deep Learning (DL) models able to i) predict the phenotype from tumor, hematoxylin-eosin (HE)-stained, whole slide images (WSI), and ii) predict the distant relapse from tumor HE-stained WSI combined with clinical data.

Design: We included 1802 patients diagnosed with early BC (1429 ER+/HER2-, 110 ER+/HER2+, 70 ER-/HER2+, 193 ER-/HER2-) between 2005 and 2013, with available digitized HE tumor slides. Several DL models were trained to predict from the WSi i) the molecular phenotype, and ii) the 5-year metastasis free interval (MFI). Models performance was evaluated using cross-validation with i) the area under ROC (AUROC), and ii) the Uno's AUC (UAUC). Cox models were used to assess the additional predictive value of our AI-based model compared to clinico-pathological factors. Histology regions (tiles) predictive of high/low risk of relapse were reviewed by two pathologists blinded to the predicted outcome.

Results: DL models were able to predict phenotype with an AUROC of 0.90 for ER, 0.76 for PR, 0.89 for HER2, 0.85 for Ki67 and 0.90 for identification of ER-/HER2- BC. In ER+/HER2- subgroup, the prediction of 5-year MFI based solely on standard risk factors (age, pT, pN, tumor size, number of tumors, type of surgery) yielded an UAUC of 0.77. Combining our AI model with the standard risk factors, performance was further improved with an UAUC of 0.82 (p=0.03). Interestingly, our model was able to predict the risk of relapse in the histological grade 2 subgroup (UAUC=0,7) suggesting that our model goes beyond the existing histology classification. High relapse risk tiles identified by the model displayed high tumor cell content, strong nuclear atypia and massive architecture, whilst the most contributive tiles of low risk corresponded to fibrotic stroma with a few low-grade tumor cells.

Conclusions: DL models based on a single HE tumor WSI shows promising performance for biomarker status and molecular subgroup prediction. In addition, the use of an AI-based score combined with existing clinico-pathological factors improved identification of patients at high risk of relapse. External validation on large independent cohorts is in progress.

172 Tubulopapillary Carcinoma of the Breast: A Distinct Morphologic Entity with Molecular and Immunohistochemical Analysis

Abeer Salama[1], Christopher Schwartz[2], Kelsey Zhu[1], Varshini Vasudevaraja[3], Jonathan Serrano[4], George Jour[4], Kyung Park[5], Matija Snuderl[4], Paolo Cotzia[1], Farbod Darvishian[3]

[1]NYU Langone Medical Center, New York, NY, [2]University of California San Francisco, San Francisco, CA, [3]New York University Medical Center, New York, NY, [4]New York University, New York, NY, [5]NYU Langone Health, New York, NY

Disclosures: Abeer Salama: None; Christopher Schwartz: None; Kelsey Zhu: None; Varshini Vasudevaraja: None; Jonathan Serrano: None; George Jour: None; Kyung Park: None; Matija Snuderl: None; Paolo Cotzia: None; Farbod Darvishian: None

Background: Tubulopapillary carcinomas (TPC) of the breast are rare tumors with a distinct morphology reminiscent of serous carcinomas of Mullerian origin. However, it is unclear whether TPCs are distinct at the immunohistochemical (IHC) and molecular levels. The aim of this study is to define this entity using IHC and molecular analysis.

Design: We identified 9 cases of TPC with distinct serous-like morphology. Clinicopathologic review, IHC stains (PAX-8, GATA-3, P53 and Ki-67), breast biomarkers and next generation sequencing (NGS) analysis of 580 cancer-related genes were performed.

Results: All nine TPC cases were from female patients with a median age of 61. Mean tumor size was 14.78 ± 6.2 mm. Histologically, all cases showed infiltrating gaping tubules with intra tubular papillary and micropapillary projections in at least 50% of the tumor (Figure 1). The majority of cases had high nuclear grade (grade 2 in 2 cases; grade 3 in 7 cases). All cases were positive for GATA-3 and negative for PAX-8, excluding a metastatic serous carcinoma of Mullerian origin. Ki-67 proliferation index was high (>15%) in 7 cases (78%). P53 was aberrant in 5 (56%) cases (4 strong-diffuse, 1 null-type). The biomarker profile included: 4 triple negative (TN), 3 HER2-positive and 2 hormone receptors positive cases. Clinicopathological features are shown in table1.

All nine cases were sequenced. The most common genomic alterations were TP53 mutations (n=5; 56%), followed by ATRX and FGFR1 mutations (n=3; 33%) (Figure 2). Of the 5 cases with TP53 mutation, 3 were TN and 2 were HER2-positive. P53 IHC results showed a prefect correlation (r =1, P-value <0.05) with TP53 molecular findings. Mean follow-up period was 71 months; seven patients showed no evidence of disease (one with axillary lymph node metastasis), one died of disease, and another is alive with recurrence of disease.

Table 1. Summary of Clinicopathologic Features of Breast Tubulopapillary Carcinoma

	n (%)
Age, median	61
Tumor size	
≤20 mm	7 (78%)
>20 mm	2 (22%)
Nuclear grade	
1	0 (0%)
2-3	9 (100%)
Ki-67	
Low ≤ 15%	2 (22%)
High >15%	7 (78%)
Tumor focality	
Unifocal	8 (89%)
Multicentric	1 (11%)
Clinical T staging	
T1/T2	9 (100%)
T3/T4	0 (0%)
AJCC Nodal staging	
N0	8 (89%)
N+	1 (11%)
Procedure	
Mastectomy	4 (44%)
Lumpectomy	5 (56%)
Status	
Dead of disease	1 (11%)
Alive with disease	1 (11%)
No evidence of disease	7 (78%)

Figure 1 - 172

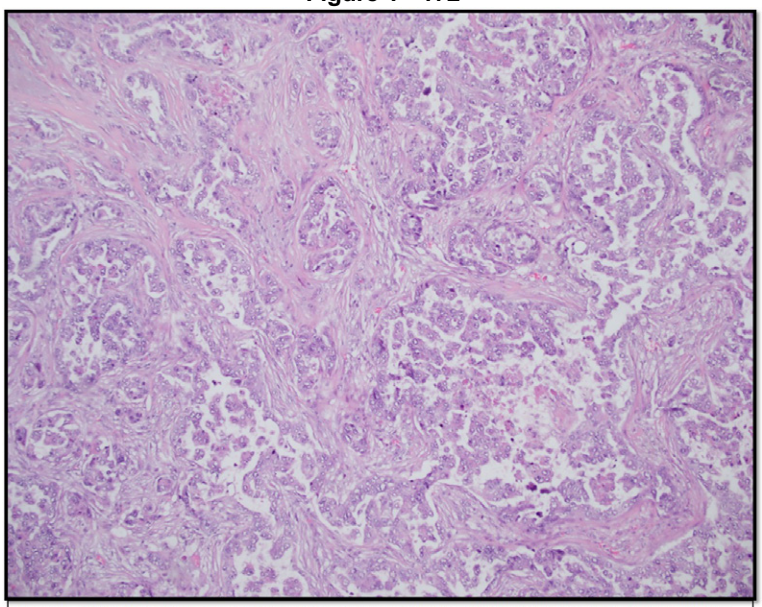

Figure 1 – Histopathologic features of tubulopapillary carcinoma of the breast- Distinct infiltrating gaping tubules with intra tubular papillary and micropapillary projections lined by cells with typically grade 3 nuclei

Figure 2 - 172

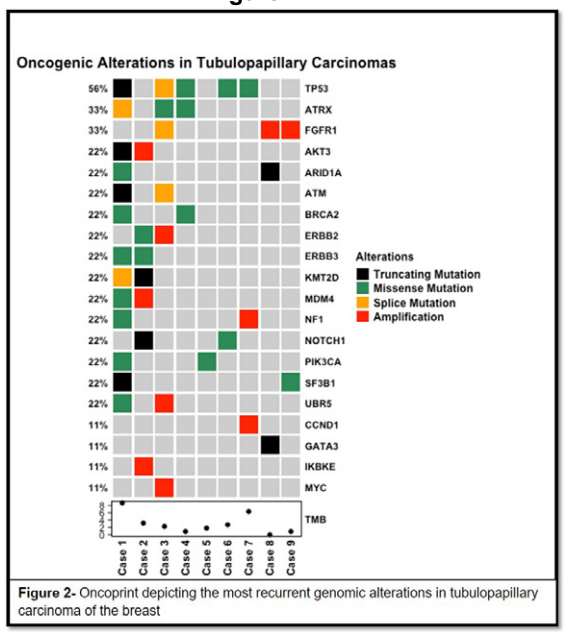

Figure 2- Oncoprint depicting the most recurrent genomic alterations in tubulopapillary carcinoma of the breast

Conclusions: TPC is a rare and morphologically distinct tumor reminiscent of serous carcinomas of Mullerian origin. Similar to the latter, *TP53* alterations appear to be the most common mutational event. Overall, the biomarker profile of TPCs is heterogeneous in line with their mutational landscape

173 TRPS1 and GATA3 Expression in Adenoid Cystic Carcinoma of the Breast

Alireza Salem[1], Yun Wu[1], Constance Albarracin[1], Hongxia Sun[2], Aysegul Sahin[1], Qingqing Ding[1]
[1]The University of Texas MD Anderson Cancer Center, Houston, TX, [2]The University of Texas Health Science Center at Houston, Houston, TX

Disclosures: Alireza Salem: None; Yun Wu: None; Constance Albarracin: None; Hongxia Sun: None; Aysegul Sahin: None; Qingqing Ding: None

Background: Adenoid cystic carcinoma (AdCC) of the breast is a rare subtype of triple negative (negative ER, PR and HER2) breast carcinoma (TNBC) characterized by the proliferation of two cell types, the luminal and myoepithelial cells, which are commonly arranged in either the cribriform or solid growth pattern. Whereas the cribriform pattern usually exhibits an indolent clinical behavior with excellent prognosis, the solid pattern generally presents high-grade tumors with an aggressive clinical course. Additionally, the solid variant of AdCC may be difficult to morphologically differentiate from basaloid TNBC. Most AdCCs harbor a characteristic chromosomal translocation resulting in an MYB-NFIB fusion gene and the overexpression of MYB, which can be used for differential diagnoses. While GATA3 is the most widely used breast marker, its utility is limited in diagnosing TNBC. In this study, we have investigated the expression of a new breast marker, TRPS1, in identifying breast AdCC and basaloid TNBC, and compared its utility to GATA3.

Design: We collected 26 cases of breast AdCC (including 5 pure cribriform, 9 mixed cribriform and solid, and 12 pure solid types), and 13 cases of basaloid TNBC diagnosed at our institution from 2015-2020. Immunohistochemical staining for TRPS1 and GATA3 were performed. Only nuclear staining was considered as positive. The immunoreactivity scores were calculated semi-quantitively and categorized as negative (<1%), low positive (1-10%), intermediate positive (11-50%), and high positive (>50%).

Results: TRPS1 was positive (intermediate or high) in all cases (100%) of basaloid TNBC, high positive in 84% of solid AdCC, low to high positive in 100% of mixed AdCC, but negative in 60% of cribriform AdCC. On the contrary, GATA3 is negative in most AdCC (22/26, with 1 low positive in the 5 cribriform group, 2 low positives in the 9 mixed group, and 1 intermediate positive in the

12 pure solid group), and negative in most basaloid TNBC (11/13, with only 1 low positive and 1 intermediate positive) (Table 1). Figure 1 shows representative cases of AdCC and basaloid TNBC with TRPS1 and GATA3 immunostain.

Table 1 TRPS1 and GATA3 expression in AdCC

		Negative	Positive			Total
			Low	Intermediate	High	
TRPS1						
	Cribriform AdCC	3(60%)	1(20%)	1(20%)	0	5
	Mix AdCC	0	2(22%)	5(56%)	2(22%)	9
	Solid AdCC	1(8%)	1(8%)	0	10(84%)	12
	Basaloid TNBC	0	0	4(31%)	9(69%)	13
GATA3						
	Cribriform AdCC	4(80%)	1(20%)	0	0	5
	Mix AdCC	7(78%)	2(22%)	0	0	9
	Solid AdCC	11(92%)	0	1(8%)	0	12
	Basaloid TNBC	11(84%)	1(8%)	1(8%)	0	13

Figure 1 - 173

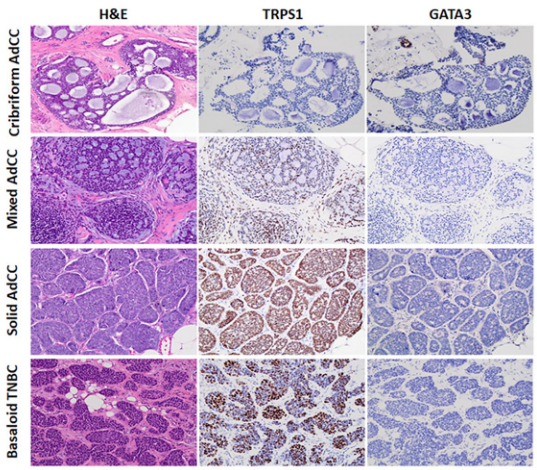

Conclusions: TRPS1 is an excellent marker to identify solid pattern AdCC and basaloid TNBC. Due to the increased sensitivity of TRPS1 when compared to GATA3, TRSP1 offers a more robust diagnostic tool for the identification of solid pattern AdCC. However, the lack of both TRPS1 and GATA3 in pure cribriform AdCC should not exclude breast origin.

174 Aberrant E-cadherin Expression in Pleomorphic (PLCIS) and Florid (FLCIS) Lobular Carcinoma in Situ (LCIS) and Comparison to CDH1 Mutation Type

Christopher Schwartz[1], Eliah Shamir[2], Yunn-Yi Chen[2], Gregor Krings[2]
[1]University of California San Francisco, San Francisco, CA, [2]University of California, San Francisco, San Francisco, CA

Disclosures: Christopher Schwartz: None; Eliah Shamir: *Employee*, Genentech; Yunn-Yi Chen: None; Gregor Krings: None

Background: PLCIS and FLCIS are rare LCIS subtypes considered to be more aggressive than classic LCIS. PLCIS and FLCIS should be distinguished from ductal carcinoma in situ (DCIS), and this can impact clinical decisions, including margin assessment and radiation use. 15% of invasive lobular carcinomas (ILC) have retained but aberrant E-cadherin (E-cad) expression by immunohistochemistry (IHC), a pitfall in distinction from invasive ductal carcinoma (IDC). Although E-cad IHC is often used to distinguish PLCIS and FLCIS from DCIS, aberrant staining patterns may lead to misdiagnosis but have not been systematically described.

Design: 87 cases with LCIS variants (39 PLCIS, 9 apocrine PLCIS [A-PLCIS], 30 FLCIS, 9 mixed PLCIS/FLCIS) were identified and clinicopathologic data was collected. IHC was performed for E-cad (n=87) and p120 (n=39) and evaluated in LCIS and a subset of associated invasive carcinomas. Aberrant E-cad IHC in LCIS/ILC was defined as any membranous and/or cytoplasmic staining. For 15 LCIS (10 PLCIS, 5 FLCIS), capture-based next generation sequencing (NGS) was performed targeting exons of 480 cancer-related genes, including *CDH1*. NGS of remaining cases with aberrant E-cad staining is ongoing.

Results: 69% LCIS (69% PLCIS/A-PLCIS, 63% FLCIS, 90% mixed PLCIS/FLCIS) were associated with invasive carcinoma (92% ILC, 5% mixed ductal/lobular, 3% IDC), and 20% LCIS (27% PLCIS/A-PLCIS, 10% FLCIS, 11% mixed PLCIS/FLCIS) were associated with DCIS. Aberrant E-cad was identified in 14/87 (16%) LCIS (15% PLCIS, 11% A-PLCIS, 13% FLCIS, 33% mixed PLCIS/FLCIS), including membrane staining in 8 (57%), membrane plus cytoplasmic staining in 1 (7%), and cytoplasmic staining only in 5 (36%). E-cad staining pattern in invasive carcinoma was concordant with LCIS in all analyzed cases (n=37). P120 expression was cytoplasmic in 38/39 (97%) LCIS, with 1 PLCIS being negative. *CDH1* mutations were identified in 14/15 (93%) LCIS: 11 nonsense/frameshift (NS/FS) and 3 missense (MS). Of the 11 LCIS with NS/FS *CDH1*, 7 (64%) were E-cad negative and 4 (all of which were PLCIS/A-PLCIS) were aberrant: 2 incomplete membrane and 2 weak cytoplasmic. All 3 LCIS with MS *CDH1* and 1 *CDH1*-wildtype PLCIS were E-cad negative.

Table 1: E-cadherin staining patterns across LCIS variants

	PLCIS (n=39)	A-PLCIS (n=9)	FLCIS (n=30)	Mixed PLCIS/FLCIS (n=9)
Negative	33/39 (85%)	8/9 (88%)	26/30 (87%)	6/9 (67%)
Aberrant	6/39 (15%)	1/9 (11%)	4/30 (13%)	3/9 (33%)
Aberrant Pattern				
Membrane, incomplete, weak	2/6 (33%)	1/1 (100%)	3/4 (75%)	1/3 (33%)
Membrane, strong	0	0	0	1/3 (33%)
Cytoplasm, weak granular +/- incomplete membrane	2/6 (33%)	0	1/4 (25%)	1/3(33%)
Cytoplasm, moderate-strong	2/6 (33%)	0	0	0

Conclusions: PLCIS and FLCIS show aberrant E-cad expression by IHC at comparable frequency to ILC, which can be a pitfall in distinction from DCIS. P120 IHC can help resolve the diagnostic dilemma. E-cad staining pattern does not clearly correlate with type of *CDH1* mutation.

175 The Diagnostic Utility of TRPS-1 and SOX10 in Triple-Negative Breast Cancers

Sharlene See[1], Suzanne Iwaz[1], Taylor Zak[1], Carissa LaBoy[1], Jorge Novo[1], Kalliopi Siziopikou[2], Luis Blanco[1]
[1]Northwestern University Feinberg School of Medicine, Chicago, IL, [2]Northwestern University, Chicago, IL

Disclosures: Sharlene See: None; Suzanne Iwaz: None; Taylor Zak: None; Carissa LaBoy: None; Jorge Novo: None; Kalliopi Siziopikou: None; Luis Blanco: None

Background: Triple negative breast cancers (TNBCs) are often very poorly differentiated such that a highly sensitive and specific marker is needed to ascertain breast origin in metastatic cases. In current practice, the most used marker is GATA3 with sensitivity of 15-60%, while mammaglobin and GCDFP-15 have lower sensitivities of 10-30%. SOX-10 has recently emerged as a useful marker of TNBC especially in GATA3-negative cases with sensitivity ranging from 62.3 to 85.7%. Of interest, a new marker, TRPS-1, was cited to be a highly sensitive and specific marker for all types of breast cancer, including TNBCs (86%) with very low positivity for melanoma (2%). Our study aims to compare the expression of TRPS1 and SOX10 in TNBCs.

Design: This is a retrospective cohort study of TNBC patients diagnosed at our institution. Nuclear staining of TRPS-1 and SOX10 was assessed using the following scoring: percentage of reactive cells (0: <1%; 1: 1–10%; 2: 11–50%; 3: 51–100%) x staining intensity (0: negative; 1: weak; 2: moderate; and 3: strong). Final immunoreactivity scores were considered negative (0–1), low (2), intermediate (3–4), or high (6 and 9). Only intermediate to high scores were considered positive.

Results: Our cohort consisted of 62 whole-slide cases, and 39 tissue microarray (TMA) cases, amounting to a total of 101 cases. Our preliminary results show that of these 101 TNBCs, 64% were positive for SOX10 while 92% were positive for TRPS-1 ($P<0.001$). Thirty-two cases were positive for TRPS-1 but negative for SOX10, while 4 cases were negative for TRPS1 but positive for SOX10, and 4 cases were negative for both. Specificities will be computed subsequently using negative controls.

Conclusions: Our preliminary results show that TRPS-1 is expressed in a higher percentage of TNBCs compared to SOX10. TRPS-1 can prove to be very useful in supporting breast origin in limited specimens such as small core biopsy specimens, cytology preparations, and metastatic lesions.

176 The Role of PRAME and NY-ESO-1 as Potential Therapeutic and Prognostic Biomarkers in Triple-Negative Breast Carcinomas

Sharlene See[1], Brian Finkelman[2], Carissa LaBoy[1], Jorge Novo[1], Kalliopi Siziopikou[3], Luis Blanco[1]
[1]Northwestern University Feinberg School of Medicine, Chicago, IL, [2]The Johns Hopkins Medical Institutions, Baltimore, MD, [3]Northwestern University, Chicago, IL

Disclosures: Sharlene See: None; Brian Finkelman: None; Carissa LaBoy: None; Jorge Novo: None; Kalliopi Siziopikou: None; Luis Blanco: None

Background: Given the limited therapeutic options for triple-negative breast cancers (TNBCs), there is a critical need for potential prognostic and therapeutic biomarkers. PRAME and NY-ESO-1 are cancer-testis antigens reported to be highly enriched in TNBCs and vaccines are currently being developed against these antigens. Our study aims to determine the prevalence of PRAME and NY-ESO-1 expression in our cohort of TNBC patients and correlate expression with clinical outcomes.

Design: This is a retrospective cohort study of TNBC patients who underwent neoadjuvant chemotherapy. PRAME and NY-ESO-1 expression was assessed on pre-therapy biopsy material as an H-score (percentage x intensity) with intensity subdivided as: 0 = absent; 1 = weak; 2 = moderate; and 3 = strong. The final H-score was subclassified as: 0 = score 0; 1-100 = score 1; 101-200 = score 2; and 201-300 = score 3. Scores 2-3 were considered positive. Association between markers and pathologic complete response (pCR) and metastatic disease was assessed via logistic regression, while association with RCB category was assessed via ordinal logistic regression. Cox proportional hazards models were used to assess association with progression-free survival. P-values of < 0.05 were considered statistically significant.

Results: Out of 76 TNBC patients, 63% were positive for PRAME (score 2-3). In contrast, NY-ESO1 was positive in only 5% of cases, with majority (89%) having score 0. Biopsy-proven metastatic disease either prior to or at the time of surgery was seen in 35 (46%) cases. Local recurrence/distant metastasis following surgery occurred in 28 cases and 14 deaths were noted. Median follow-up was 3 years and progression-free survival at 3 years was 66%. Positivity for PRAME was significantly associated with a lower likelihood of early metastatic disease (OR = 0.24, 95% CI 0.08-0.62; P = 0.005). However, it was not significantly associated with pCR, RCB category, or progression-free survival. NY-ESO1 score was not significantly associated with early metastatic disease, pCR, RCB category, or progression-free survival.

Conclusions: Our results suggest that positivity for PRAME may be associated with a lower risk of early metastasis in TNBCs, but not with response to neoadjuvant chemotherapy or progression-free survival. The high expression of PRAME in TNBCs makes it a potential therapeutic target while NY-ESO1 appears to be a less useful marker. However, further research into the usefulness of these markers in this aggressive breast cancer subtype is still warranted.

177 PD-L1 (SP142) Immunohistochemistry in Clinical Metastatic Breast Carcinomas and its Association with Survival

Saba Shafi[1], Bindu Challa[1], Anil Parwani[2], Zaibo Li[1]
[1]The Ohio State University Wexner Medical Center, Columbus, OH, [2]The Ohio State University, Columbus, OH

Disclosures: Saba Shafi: None; Bindu Challa: None; Anil Parwani: None; Zaibo Li: None

Background: The discovery of new immune checkpoint molecules has led to the emergence of new treatment modalities in various cancer types including breast carcinoma. While the expression of PD-L1 in non-metastatic TNBCs has been elucidated, very little has been published regarding PD-L1 in metastatic breast cancers. In the present study, we focused on the expression of PD-L1 in metastatic breast cancers and its correlation with clinicopathologic features.

Design: Eighty-two clinically metastatic/locally recurrent breast cancer cases (biopsy= 77, resections=5) with SP142 immunohistochemistry (IHC) testing results were included. Expression in immune cells was assessed as the proportion of tumor area occupied by PD-L1-positive IC of any intensity. The scoring algorithm used for classification was as follows: negative (IC <1)

and positive (IC ≥1). Representative SP142 staining images were shown in Figure 1. Other clinicopathological features were also collected.

Results: Clinicopathologic characteristics was summarized in the table. (Table 1). SP142 was positive in 23.2% (19/82) of cases. No significant difference in metastatic locations, estrogen receptor expression, progesterone receptor expression, androgen receptor, and HER2 status was noted. Mismatch repair (MMR) protein IHC results were available for 64 cases and all had intact MMR proteins. Nine (11%) patients received PD-L1 immunotherapy (SP142 positive: 8; SP142 negative: 1). Survival data showed a trend of increased survival rate in SP142 positive patients (73.7%) comparing to SP142 negative patients (55.6%), but with no statistical significance (p=0.08).

Table 1. Clinicopathological characteristics of our study set.

Characteristics		Total cases (n=82)	PD-L1 (SP142) positive (n=19)	PD-L1 (SP142) negative (n=63)
Age		57 (27, 89)	56 (27, 76)	58 (30, 89)
Specimen type	Biopsy	77 (93.9)	17 (89.5)	60 (95.2)
	Resection	5 (6.1)	2 (10.5)	3 (4.7)
Location/Site	Breast	3 (3.6)	1 (5.3)	2 (3.2)
	Bone	13 (15.8)	1 (5.3)	12 (19.0)
	Lung	10 (12.2)	3 (15.8)	7 (11.1)
	Brain	6 (7.3)	3 (15.8)	3 (4.7)
	Liver	28 (34.1)	3 (15.8)	25 (39.7)
	Lymph node	10 (12.2)	4 (21.0)	6 (9.5)
	Other	12 (14.6)	4 (21.0)	8 (12.7)
Distant metastases	Yes	79 (96.3)	18 (94.7)	61 (96.8)
	No	3 (3.6)	1 (5.3)	2 (3.2)
Local recurrence	Yes	5 (6.1)	1 (5.3)	4 (6.3)
	No	77 (93.9)	18 (94.7)	59 (93.6)
Estrogen Receptor (ER)	Positive	10 (12.2)	3 (15.8)	7 (11.1)
	Negative	72 (87.8)	16 (84.2)	56 (88.9)
Progesterone Receptor (PR)	Positive	3 (3.6)	0 (0.00)	3 (4.7)
	Negative	79 (96.3)	19 (15.8)	60 (95.3)
Androgen receptor (AR)	Positive	34 (41.5)	5 (26.3)	29 (46.1)
	Negative	39 (47.5)	11 (57.9)	28 (44.4)
	NA	9 (11.0)	3 (15.8)	6 (9.5)
Overall HER 2 status	Negative	81 (98.7)	19 (100.0)	62(98.4)
	Positive	1 (1.2)	0 (0.0)	1 (1.6)
Mismatch Repair (MMR) Gene	Intact	64 (78.0)	15 (78.9)	49 (77.8)
	Loss	0 (0.0)	0 (0.0)	0 (0.0)
	NA	18 (22)	4 (21.1)	14 (22.2)
PD-L1 targeted therapy	Yes	9 (11.0)	8 (42.1)	1 (1.6)
	No	73 (89.0)	11 (57.9)	62 (98.4)
Survival data	Dead	33 (40.2)	5 (26.3)	28 (44.4)
	Alive	49 (59.8)	14 (73.7)	35 (55.6)

Figure 1. PD-L1 (SP142) staining in breast carcinoma. A) One case with negative SP142 staining (0%); B) One case with positive SP142 staining (1%); C) One case with positive SP142 staining (2%); D) One case with positive SP142 staining (40%).

Figure 1 - 177

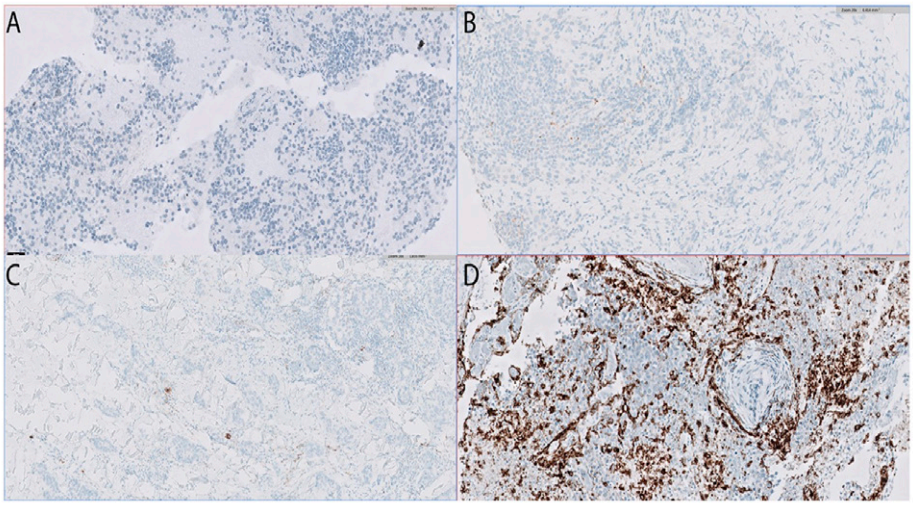

Conclusions: This is one of first exploratory studies analyzing SP142 expression in metastatic breast cancers in a clinical setting. PD-L1 (SP142) positive patients showed a trend of increased survival rate, however, a statistical significance was not reached due to small sample size.

178 Pathological Assessment of Post Chemotherapy Locally Advanced Breast Cancers - Comparison and Feasibility of Grading Systems: A Single Tertiary Oncology Center Experience from India

Prarthna Shah[1], Trupti Pai[2], Tanuja Shet[1], Sangeeta Desai[3]
[1]Tata Memorial Hospital, Mumbai, India, [2]Vashi, India, [3]Tata Memorial Centre, Mumbai, India

Disclosures: Prarthna Shah: None; Trupti Pai: None; Tanuja Shet: None; Sangeeta Desai: None

Background: Pathological evaluation is the gold standard for determining tumor sensitivity to neoadjuvant chemotherapy (NACT) in locally advanced breast cancer (LABC). Although the Residual Cancer Burden (RCB) score, as proposed by MD Anderson Cancer Center, has been validated as an independent prognostic marker, it requires tumor bed localization prior to chemotherapy which may not be always possible in low and middle income countries (LMIC). The present study aimed at evaluating and comparing various grading systems for its effective adoption in a standardized way for routine clinical practice in the low economy settings and in predicting survival in LABC post NACT patients.

Design: In this study, 200 post chemotherapy LABC specimens were studied. The largest cross sectional area of tumor bed was submitted in the form of a grid without the need for tumor bed localization with clip prior to NACT. Tumor response was assessed by 4 grading systems [Miller Payne system (MPS), Residual Cancer Burden (RCB), Sataloff system and Residual Disease in Breast and Nodes (RDBN)]. Its impact on overall survival (OS) and event free survival (EFS) was assessed using Kaplan-Meier and Cox regression analysis with median follow up of 36 months. p value of <0.05 was considered as statistically significant. Harrell's C index was used to calculate predictive accuracy of systems. Level of agreement of various systems with RCB was done by kappa analysis. Pathological complete response (pCR) was defined as no residual invasive tumor in the breast and/or lymph nodes.

Results: A pCR rate of 29.5% was observed. It was maximum in patients with HER2/neu positive tumors (52.5%, 21/40 cases) followed by TNBC (35.6%, 21/59 cases). Patients having pCR had a better OS (p=0.011) and EFS (p=0.016). All the 4 grading systems assessed, significantly predicted OS (Figure 1) and EFS (Figure 2). Harrell's C index was >0.5 for both OS and EFS for all the systems. Considering RCB as gold standard, RDBN showed the best agreement (kappa=0.742) as compared to other systems (Table 1). Also, both RCB and RDBN could significantly differentiate between the OS and EFS estimates of classes with complete, partial and no regression.

Table 1: Distribution of patients according to various grading systems and respective kappa values.								
			RCB system (n=200)					Kappa value
			RCB-0	RCB-I	RCB-II	RCB-III	Total	
Other systems	Miller Payne system	Grade 5	59	3	6	0	68	0.478
		Grade 4	0	9	18	1	28	
		Grade 3	0	0	26	40	66	
		Grade 2	0	0	7	25	32	
		Grade 1	0	0	1	5	6	
	Sataloff Tumour	T-A	59	12	17	0	88	0.231
		T-B	0	0	23	25	48	
		T-C	0	0	18	40	58	
		T-D	0	0	0	6	6	
	Sataloff Nodes	N-A	27	5	5	0	37	0.218
		N-B	32	5	28	1	66	
		N-C	0	2	20	43	65	
		N-D	0	0	5	27	32	
	RDBN	Class 1	59	0	0	0	59	**0.742**
		Class 2	0	1	1	0	2	
		Class 3	0	8	36	2	46	
		Class 4	0	3	21	69	93	
RCB- Residual Cancer Burden; RDBN- Residual Disease in Breast and Nodes.								

Figure 1 - 178

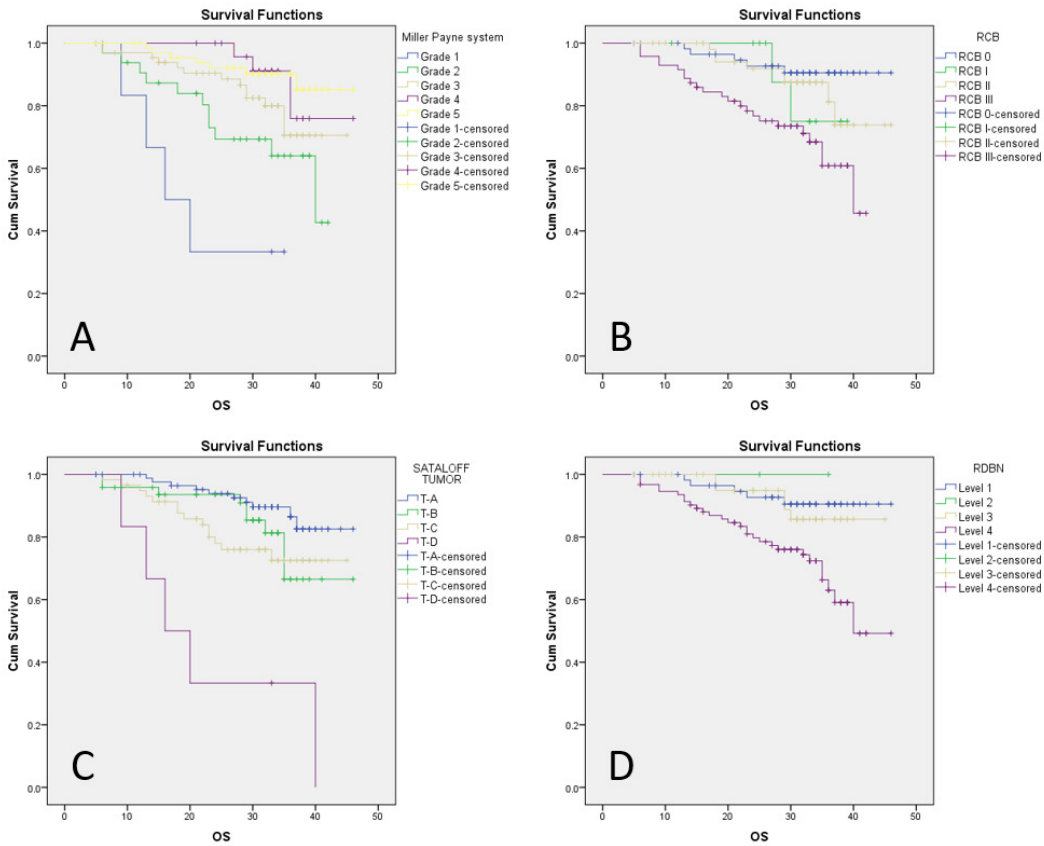

Figure 1: Overall survival (Kaplan Meier analysis) for the various grading systems. A) Miller Payne System (p<0.001); B) RCB (p=0.003); C) Sataloff tumour (p=0.001); D) RDBN (p=0.004).

Figure 2 – 178

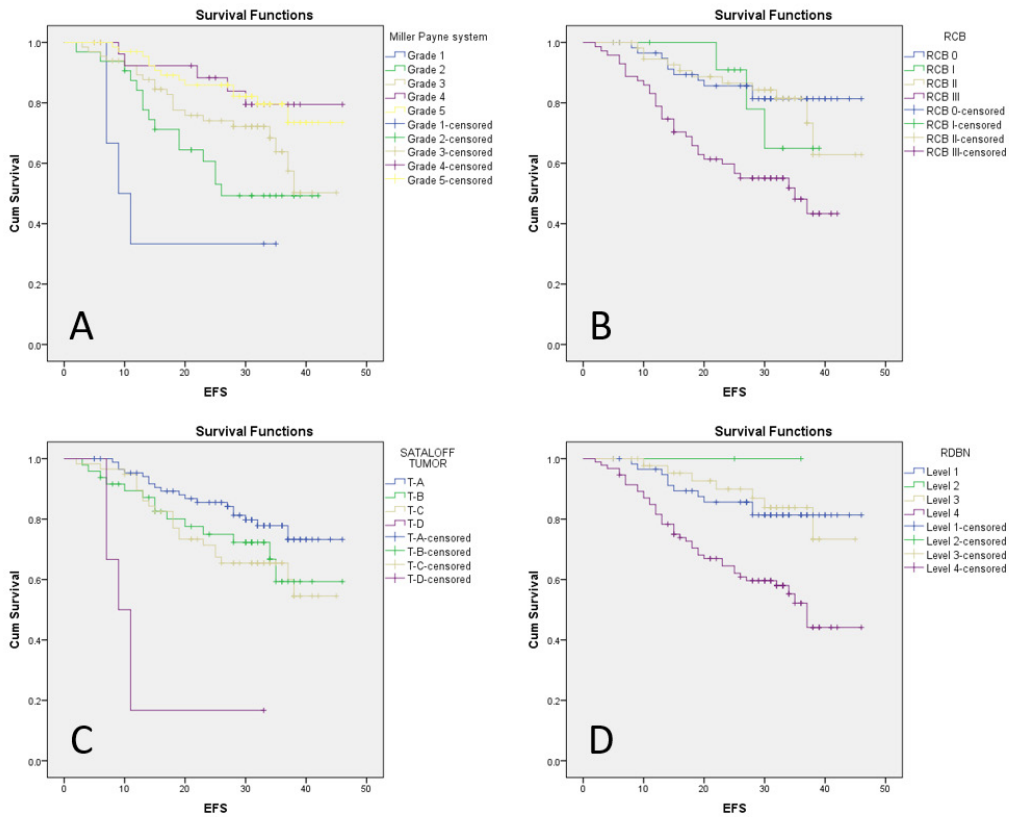

Figure 1: Event free survival (Kaplan Meier analysis) for the various grading systems. A) Miller Payne System (p<0.001); B) RCB (p<0.001); C) Sataloff tumour (p<0.001); D) RDBN (p<0.001).

Conclusions: We have demonstrated that RCB could be estimated by thorough grossing technique without prior tumor bed clipping. We found RDBN equivalent to RCB system and that it was much easier and feasible to report with limited resources.

179 Clinico-pathological Features of Breast Tumors Associated with Li-Fraumeni Syndrome

Mohan Sopanahalli Narasimhamurthy[1], Madeline Good[2], Heena Desai[3], Anh Le[4], Ira Bleiweiss[5], Kara Maxwell[2], Anupma Nayak[6]

[1]Pennsylvania Hospital of the University of Pennsylvania Health System, Philadelphia, PA, [2]University of Pennsylvania, Philadelphia, PA, [3]Perelman School of Medicine, Hospital of the University of Pennsylvania, Philadelphia, PA, [4]Hospital of the University of Pennsylvania, [5]Hospital of the University of Pennsylvania, Philadelphia, PA, [6]Perelman School of Medicine at the University of Pennsylvania, Philadelphia, PA

Disclosures: Mohan Sopanahalli Narasimhamurthy: None; Madeline Good: None; Heena Desai: None; Anh Le: None; Ira Bleiweiss: None; Kara Maxwell: None; Anupma Nayak: None

Background: Breast cancer is the most common tumor in females with Li–Fraumeni syndrome (LFS), a rare hereditary cancer syndrome caused by germline *TP53* mutations, with a median age of diagnosis in the early 30s. Unlike *BRCA1*, the morphologic features of breast cancers in LFS are not well defined. Herein, we describe the morphologic features of breast tumors in LFS patients.

Design: We retrospectively retrieved the clinical data on genetically confirmed LFS patients with breast tumors in our institution from Jan 2000 to Sept 2021. We identified 79 patients with 100 breast tumors, of which, slides from 61 tumors (44 pts) were available for pathology review. p53 immunohistochemical expression was evaluated in 24 tumors.

Results: Clinical and demographic data is summarized in Table-1. Of 79 patients, 78 were females and one male with median age of 35yrs (19 - 76yrs). Fifty patients (64%) had strong family history of cancer with ≥1 close relative with LFS spectrum tumors (range 2 - 11) (Fig. 1A). The majority of patients had missense (59, 75%), followed by large gene rearrangements (8, 10%), truncating (6, 8%), splice-site (5, 6%) and VUS (1) mutations. Of 61 reviewed tumors, 40 were invasive carcinomas (IC), 19 pure DCIS, 1 malignant phyllodes and 1 fibroadenoma (FA). IC were of ductal (35), lobular (2), mixed ductal and lobular (1), and micropapillary (2) types. Three ICs showed partial apocrine and micropapillary features and 1 partial clear cell change. All ICs were high grade, with associated DCIS in (27), LVI (16), TILs (8), and sclerotic stroma in (8). The DCIS was high grade (29), intermediate grade (16), low grade (0), with comedonecrosis (19), and with associated calcifications in (16). High risk lesions such as, radial scar (1), papilloma (3), ADH (2), and lobular neoplasia (1) were present in 7 tumors. One case showed FA containing DCIS. Biomarker status was available on all 58 IC cases in the cohort- 26(45%) luminal, 8(14%) triple negative, 10(17%) HER2+, and 14(24%) TP (triple positive). High p53 IHC nuclear expression (>50%) was seen in 16/24 tumors (all with missense mutations), whereas no protein expression (<1%, null pattern) was seen in one tumor each from carriers of large gene rearrangements and splicing mutations. Interestingly, one tumor from a patient with a truncating mutation showed overexpression (>50%) (Fig 2B).

Age, median (range in years)	35 (19-76)
Sex	
Female	78
Male	1
Race (n=76)	
Caucasian	63 (83%)
Black	9 (12%)
Asian	2 (3%)
Mixed	2 (3%)
Menopause status (n=73)	
Pre	65 (89%)
Post	8 (11%)
Previous history of cancer	35 (44%)
Family history of breast cancer	39 (49%)
Focality (n=68 tumors)	
Unifocal	52 (76%)
Multifocal	16 (24%)
Laterality (n=96 tumors)	
Bilateral	16 (17%)
synchronous	10
Consequential	6
Right	37 (38%)
left	43 (45%
Follow up	
Median (range in months)	36 (6-480)
Recurrence	3
Deceased	11
Tumor stage at presentation (n=88)	
DCIS	30 (34%)
IA	26 (30%)
II	12 (13%)
III	14 (16%)
IV	6 (7%)

Figure 1 - 179

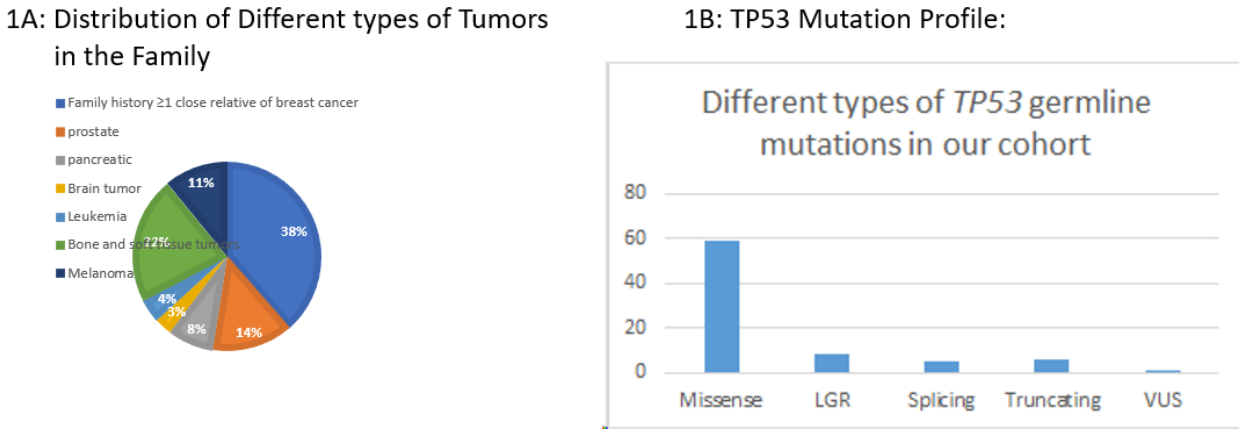

Figure 2 – 179

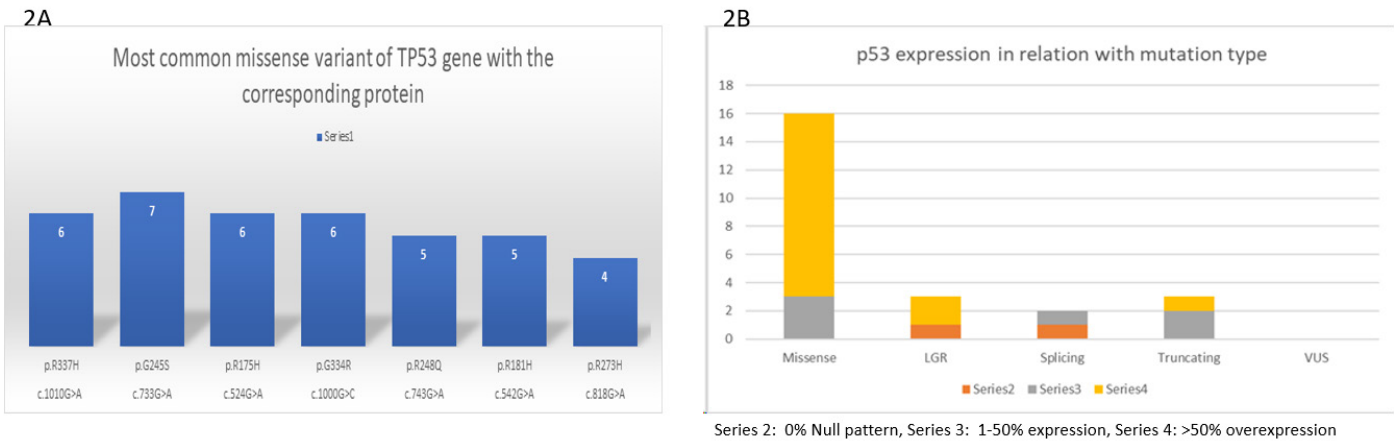

Series 2: 0% Null pattern, Series 3: 1-50% expression, Series 4: >50% overexpression

Conclusions: Invasive carcinomas in LFS patients are most often high-grade ductal type, are frequently HER2 positive, and many also show co-expression of ER. Overexpression of p53 protein on IHC correlates with the missense mutation while null pattern represents large gene rearrangements and splicing mutations.

180 PTEN Alterations in Advanced ER+ Breast Cancer: Correlation with Clinicopathologic and Molecular Features

Keith Sweeney[1], Jing Wang[1], Constance Albarracin[1], Sinchita Roy-Chowdhuri[1], Keyur Patel[1], Mark Routbort[1], Qingqing Ding[1], Yun Wu[1], Lei Huo[1], Aysegul Sahin[1], Rajyalakshmi Luthra[1], Hui Chen[1]
[1]The University of Texas MD Anderson Cancer Center, Houston, TX

Disclosures: Keith Sweeney: None; Jing Wang: None; Constance Albarracin: None; Sinchita Roy-Chowdhuri: None; Keyur Patel: *Consultant*, Astellas Pharma; *Consultant*, Novartis Pharmaceutical Corporation; Mark Routbort: None; Qingqing Ding: None; Yun Wu: None; Lei Huo: None; Aysegul Sahin: None; Rajyalakshmi Luthra: None; Hui Chen: None

Background: Resistance to hormonal therapy is a major challenge in the treatment of ER+ breast cancer (BC). A subset of ER+ BC with treatment failure show loss of ER expression (7%) or somatic *ESR1* mutation (20%) and is seen exclusively in recurrent/metastatic tumors. PTEN functions as a negative regulator of PI3K pathway and alterations may impact combined

hormonal and PI3K inhibitor therapy. Characterization of the pathologic and molecular features of BCs with PTEN alterations may aid in the early identification of ER+ BC patients at risk for a more aggressive disease course.

Design: We reviewed 372 advanced ER+ BC cases with 146-gene panel next generation sequencing (NGS) performed from 2018-2020. We selected 72 cases with *PTEN* mutation (9), deletion (10), and no alteration (53) to correlate with PTEN immunohistochemistry (IHC) expression (clone 6H2.1, Dako) and clinicopathologic and molecular features.

Results: Of the 72 cases tested by both IHC and NGS (Table 1, top), 13 showed PTEN loss, 10 *PTEN* deletion or partial deletion and 9 *PTEN* mutation. *PTEN* deletions were more prevalent in cases with PTEN loss (7/13, 54%) than in cases without PTEN loss (3/59, 5%, p<0.001). *PTEN* loss of function mutations (nonsense, indel and splice site) were more frequent in cases with PTEN loss (5/13, 38%) than without PTEN loss (1/59, 2%, p<0.001). A minority of initially ER+ BC (6/69) was found to be ER negative in recurrent/metastatic BC. Loss of ER expression occurred regardless of PTEN alteration status (5% vs 10%, Table 1, bottom). In cases with a PTEN alteration, none was HER2 overexpressed/amplified or *HER2* mutated, as compared to 13% HER2 overexpressed/amplified and 6% *HER2* mutated in those without a PTEN alteration. Concurrent *ESR1* mutations rarely occurred in patients with a PTEN alteration (1/20, 5%) as compared to patients without a PTEN alteration (10/52, 19%). There was no association between PTEN alteration and status of *PIK3CA* or *TP53* mutations.

Table 1. PTEN status by immunohistochemistry and by sequencing with correlation to clinicopathologic and molecular variables (n=72)

	PTEN loss (n=13)	**PTEN retained (n=59)**	**P-value**
***PTEN* copy number aberration, n (%)**			<0.001
Deletion or partial deletion	7 (54%)	3 (5%)	
Absent	6 (46%)	56 (95%)	
***PTEN* mutations, n (%)**			<0.001
Nonsense, indel, splice site	5 (38%)	1 (2%)	
Missense	0	3 (5%)	
Absent	8 (62%)	55 (93%)	
	PTEN alteration present (n=20)	**PTEN alteration absent (n=52)**	**P-value**
ER discordance between primary tumor and recurrent/metastatic disease, n (%)			1
ER expression preserved	18 (90%)	45 (87%)	
ER loss observed	1 (5%)	5 (10%)	
No repeat ER testing available	1 (5%)	2 (4%)	
Histologic type, n (%)			0.78
Ductal	18 (90%)	48 (92%)	
Lobular	1 (5%)	3 (6%)	
Mixed ductal and lobular	1 (5%)	1 (2%)	
Tested tissue site, n (%)			1
Primary tumor	1 (5%)	1 (2%)	
Recurrence/Metastasis	19 (95%)	51 (98%)	
Biomarker status, n (%)			0.18
ER+ HER2-	20 (100%)	45 (87%)	
ER+ HER2+	0	7 (13%)	
***HER2* somatic mutation, n (%)**			0.56
Present	0	3 (6%)	
Absent	20 (100%)	49 (94%)	
***ESR1* somatic mutation, n (%)**			0.17
Present	1 (5%)	10 (19%)	
Absent	19 (95%)	42 (81%)	
***PIK3CA* somatic mutation, n (%)**			0.57
Present	7 (35%)	14 (27%)	
Absent	13 (65%)	38 (63%)	
***TP53* somatic mutation, n (%)**			0.60
Present	7 (35%)	23 (44%)	
Absent	13 (65%)	29 (56%)	

Conclusions: Loss of PTEN IHC expression correlates with *PTEN* deletions and loss of function mutations identified by sequencing. Our results further show that PTEN alterations rarely co-exist with *ESR1* mutations in ER+ advanced BC. Thus, in metastatic/recurrent tumors, we recommend screening for PTEN alterations by both IHC and sequencing in order to identify patients at risk for impact on combined hormonal and PI3K inhibitor therapy.

181 Recurrent Challenges in the Diagnosis and Grading of Breast Phyllodes Tumors – An International Survey

Benjamin Yongcheng Tan[1], Stephen Fox[2], Sunil Lakhani[3], Puay Hoon Tan[1]
[1]Singapore General Hospital, Singapore, Singapore, [2]Peter MacCallum Cancer Centre, Melbourne, Australia, [3]The University of Queensland, Pathology Queensland, Brisbane, Australia

Disclosures: Benjamin Yongcheng Tan: None; Stephen Fox: None; Sunil Lakhani: None; Puay Hoon Tan: None

Background: Breast phyllodes tumors (PTs) are graded as benign, borderline, or malignant by analysis of multiple histological features in guidelines. Nevertheless, there is variation in PT grading and in separating cellular fibroadenoma (FA) from PT. We hypothesize this is due to pathologists differentially weighting grading criteria.

Design: To identify the hierarchy of use of diagnostic criteria, responses to a 20-question survey were collated online between June-July 2021.

Results: 213 pathologists from 29 countries responded; 54% reported 10-50 PT cases per year. Criteria considered key to PT diagnosis were: increased stromal cellularity (84%), stromal overgrowth (77%), increased stromal mitoses (68%), stromal atypia (62%), stromal fronding (59%), periductal stromal condensation (58%), and lesional heterogeneity (34%). Important grading parameters were: mitotic activity (55%), stromal overgrowth (54%), stromal atypia (51%), increased stromal cellularity (41%), and nature of tumor border (38%). 49% would diagnose malignant PT without a full array of adverse features. Common heterologous elements were: liposarcoma (28%), chondrosarcoma (26%), osteosarcoma (17%), rhabdomyosarcoma (9%). 31% were unaware that liposarcoma within a PT was insufficiently diagnostic of malignancy. 43% reported encountering epithelial malignancies in PT. 35% had reported metastatic PT, 80% being spindle cell sarcoma. 52% did not use immunohistochemistry routinely. Opinions were mixed on the role of molecular tools, concerns being lesional heterogeneity and cost. 89% used the term “cellular fibroepithelial lesion (FEL)” for difficult cases. 45% would diagnose a FEL with stromal fronding (but lacking other PT features) as FA, 35% FEL, and 17% PT. 59% deemed clinicoradiological findings diagnostically significant. 68% considered age (≥40 years) important in determining if a FEL was a FA or PT. In juvenile FELs, increased stromal cellularity (83%), fronding (52%), and mitoses (41%) were more common. 34% regarded differentiating cellular FA from PT as a specific challenge. 54% had issues assigning a borderline PT grade, due to seemingly subjective criteria.

Conclusions: Criteria for grading PT lie on a spectrum, leading to interpretive variability. PTs often exhibit intralesional heterogeneity. Cellular and juvenile FELs may have “grey zone” features. These challenges can serve as a framework for future classification work. Guidelines may benefit from outreach efforts for equitable access by pathologists in diverse settings.

182 Expanding the Spectrum of High-Grade Triple-Negative Metaplastic Breast Carcinoma: Basal-Like Myoepithelial Phenotype and More Favorable Outcome

Kriti Tiwari[1], Zachary Corey[2], Gustavo Torres[1], Wei Huang[1], Meaghan Dougher[2], Jason Aynardi[1], Julie C. Fanburg-Smith[1]
[1]Penn State Health Milton S. Hershey Medical Center, Hershey, PA, [2]Penn State College of Medicine, Hershey, PA

Disclosures: Kriti Tiwari: None; Zachary Corey: None; Gustavo Torres: None; Wei Huang: None; Meaghan Dougher: None; Jason Aynardi: None; Julie C. Fanburg-Smith: None

Background: Metaplastic breast carcinoma (MBC) is often high grade and considered unfavorable. Basal-like phenotype is shared by basaloid squamous cell carcinoma, ductal carcinoma with medullary features, and EWSR1-rearranged myoepithelial carcinoma. This study stratifies our MBC, with epithelial to mesenchymal transition, into detailed epithelial-stromal subtypes, then correlates with outcome.

Design: Cases from 2000-2019, coded as “metaplastic” and adding “medullary” carcinoma to be inclusive, were reclassified by morphology and phenotype, then correlated with clinicoradiologic outcome. A case better diagnosed as malignant phyllodes was excluded.

Results: There were 31 females, ages 33-80 (median 55) years. Tumor sizes were 0.5-22 (median 2.8) cm, smaller with medullary features. All occurred in the upper outer quadrant and were triple-negative and notably high-grade (Nottingham 8-9). Morphologic and phenotypic subtypes include the following: 1) 30% Myoepithelial carcinoma-like (MEC-L) - nodules of palisaded basal-like epithelium with central distinctive chondromyxoid change/necrosis, often with extraskeletal myxoid chondrosarcoma-like appearance. 2) 10% Predominant squamous cell with keratinization. 3) 29% Carcinoma with medullary features (MC) with (19%)

and without (10%) brisk lymphocytes. 4) 16% Mixed pattern with squamous/chondromyxoid and moat-like myxoid stromal change. 5) 3% Osteosarcomatous differentiation, heterologous. 6) 12% Sarcomatoid spindled with focal myxoid change. Those studied revealed p63+ and CK5/6+ and +/- SMA, S100, and SOX10 if medullary or myoepithelial-like phenotype. Treatment was surgery +/- chemoradiation. Subtypes 1-5 revealed lymph node (LN) and pulmonary metastases and had no evidence of disease (NED) up to 135 months follow-up. Whereas subtype 6 sarcomatoid revealed 50% died of disease (DOD) by 19 months.

Conclusions: MBC can be divided into reproducible subtypes that could include MEC-L and MC. Excluding sarcomatoid spindled, the other triple-negative and high-grade subtypes, even with LN and lung metastases, appear to have more favorable overall survival than previously considered.

183 Pathologic Findings Following Neoadjuvant Chemotherapy for Radiation-Associated Angiosarcoma of the Breast

Emily Towery[1], Leona Doyle[1], Vickie Jo[2], Chandrajit Raut[1], Stuart Schnitt[3]
[1]Brigham and Women's Hospital, Boston, MA, [2]Brigham and Women's Hospital, Harvard Medical School, Boston, MA, [3]Brigham and Women's Hospital, Dana-Farber Cancer Institute, Harvard Medical School, Boston, MA

Disclosures: Emily Towery: None; Leona Doyle: None; Vickie Jo: *Stock Ownership*, Merck and Co; Chandrajit Raut: None; Stuart Schnitt: None

Background: Radiation-associated angiosarcoma (RAS) is a rare malignant tumor that in breast typically arises secondary to radiation therapy for carcinoma and is characterized by *MYC* amplification. Most patients are initially treated with surgery, but some receive neoadjuvant chemotherapy (NAC) followed by resection. The histologic features of RAS after NAC have not been described.

Design: RAS in 14 patients treated with NAC followed by mastectomy, with available slides for review, were identified. Clinical data were obtained from medical records and pathology reports. Histologic features of the tumor bed and residual tumor (when present) were evaluated.

Results: Mean patient age was 68.9 years (range, 57-84 years)**.** RAS was diagnosed an average of 5.9 years post-radiation (range 3.3-9.6 years). All patients were treated by mastectomy after NAC with paclitaxel (9), paclitaxel and gemcitabine (2), gemcitabine and docetaxel (1), gemcitabine and doxorubicin (1), or gemcitabine (1). 3 patients had a pathologic complete response. These cases showed histologic evidence of tumor bed, with variable amounts of fibrosis, edema, benign vascular proliferation, lymphoid infiltrates, hemosiderin deposition, and hemosiderin laden macrophages. Of the 11 cases with residual RAS, tumor was confined to the skin in 7 and involved skin and breast tissue in 4. Residual RAS was most often present as scattered foci of varying size within the tumor bed; growth patterns were vasoformative in 7 cases, mixed vasoformative/solid in 3, and purely solid in 1. While most regions were histologically diagnostic of angiosarcoma, some foci were composed of highly atypical epithelioid and spindle cells, singly and in small clusters. In 5 cases, there were vessels with ectasia and/or endothelial atypia but without a dissecting growth pattern and endothelial multilayering, morphologically indeterminate between residual RAS, APRVP, and reactive vascular proliferation.

Conclusions: Residual RAS was identified in most (78.5%) mastectomy specimens after NAC. Tumor bed changes were similar to those seen after NAC for invasive breast carcinoma. Residual RAS was most often present as scattered foci within the tumor bed, some of which lacked overt diagnostic features of angiosarcoma. Careful histologic evaluation, particularly in foci close to margins, is essential to distinguish residual RAS from reactive vascular changes. Whether MYC expression may be helpful in in making this distinction warrants investigation.

184 Clinicopathological Features of Early Triple Positive Breast Cancer: An Institutional Experience

Maria Urezkova[1], Tatyana Semiglazova[1], Anna Artemyeva[1], Tatyana Soloviova[1], Asel Kudaybergenova[1], Evgeniy Imyanitov[1]

[1]N.N. Petrov National Medical Research Center of Oncology, Saint Petersburg, Russia

Disclosures: Maria Urezkova: None; Tatyana Semiglazova: None; Anna Artemyeva: None; Tatyana Soloviova: None; Asel Kudaybergenova: None; Evgeniy Imyanitov: None

Background: Breast cancer (BC) immunohistochemical (IHC) testing is a mandatory component of the clinical management of this disease. ER+/PR+/HER2- and ER-/PR-/HER2- BCs have been relatively well characterized, while so-called triple-positive (ER+/PR+/HER2+) (Figure 1) BC remains understudied.

Design: Consecutive samples of treatment-naïve ER+/PR+/HER2+ BC were obtained from pathological archive of the N.N. Petrov Institute of Oncology (St. Petersburg).

Results: We analyzed 10399 cases of BC from 2006 to 2019 y.y. Triple-positive receptor phenotype was observed in 5.2% consecutive BC (547 cases), however it was detected in to 20% of HER2+ tumors. ER+/PR+/HER2+ tended to have higher grade (grade 3: 58%), high index of proliferative activity Ki-67 (mean value: 30.76%) and high incidence of lymph node metastatic involvement among early BC cases (28.8%). The average mitotic index in the ER+/PR+/HER2+ BC was 23.7 mitoses/mm^2. ER+/PR+/HER2+ also had high amount of tumor-infiltrating lymphocytes (TILs) (Table 1). CEN17 polysomy was detected in 1 case, HER2 and TOP2A co-amplification (Figure 2) was observed in 24.6% of cases. The PIK3CA mutation was detected in 18% of cases. Adjuvant therapy consisted of combination of 3 types of drugs (hormonal, targeted and chemotherapy) in 36.6% patients, 2 types of therapy in 30% women and 1 type of therapy in 25% cases.

Table 1. Characteristics of breast cancer subtypes (median values).

BC subtype	Ki-67, %	Grade 3, %	Phh3/mm^2	CD3+, %	CD4+, %	CD8+, %	TIL's total, %
Triple positive	30.76	58	23.7	13.86	7.47	7.50	28.83
HER2+	46.88	60.3	18.39	10.71	10.43	6.03	27.17
Luminal A and B (HER2-)	17.47	22	6.95	5.81	5.73	3.51	15.05

Figure 1 - 184

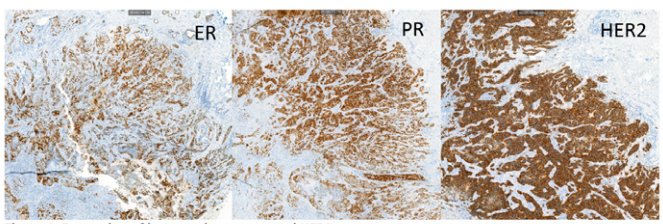

Figure 1. Expression of hormonal receptors and HER2.

Figure 2 - 184

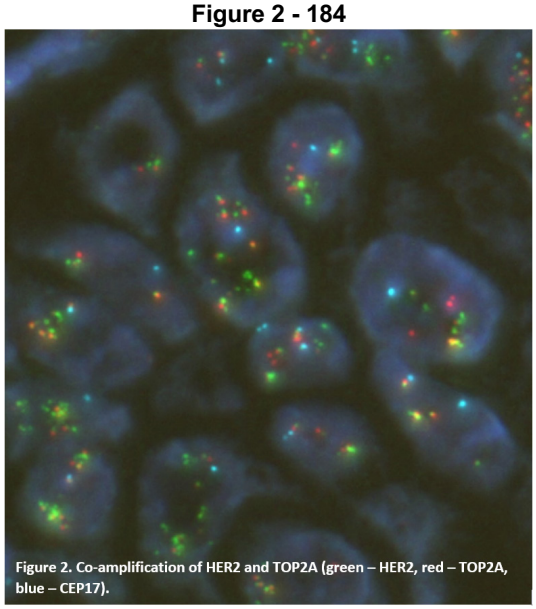

Figure 2. Co-amplification of HER2 and TOP2A (green – HER2, red – TOP2A, blue – CEP17).

Conclusions: ER+/PR+/HER2+ BCs have aggressive clinical and pathological characteristics, and could be a different entity. The frequency of PIK3CA mutations in triple positive BC is evidently lower as compared to ER+/PR+/HER2- BC.

185 A Multi-Feature AI Algorithm for Cancer Diagnosis in Breast Biopsies: A Multi-Site Clinical Validation Study

Anne Vincent-Salomon[1], Guillaume Bataillon[2], Alona Nudelman[3], Anat Albrecht Shach[4], Lucie Thibault[1], Lilach Bien[5], Ira Krasnitsky[5], Rachel Mikulinsky[5], Yuval Globerson[5], Roei Harduf[5], Shay Arbov[5], Chaim Linhart[5], Manuela Vecsler[5], Judith Sandbank[6]

[1]Institut Curie, Paris, France, [2]Institut Claudius Regaud, IUCTO, Toulouse, France, [3]Rehovot, Israel, [4]Assuta Ashdod Hospital, Ashdod, Israel, [5]Ibex Medical Analytics, Tel Aviv, Israel, [6]Maccabi Health Services, Kiriat Ono, Israel

Disclosures: Anne Vincent-Salomon: *Advisory Board Member*, Ibex; Guillaume Bataillon: None; Alona Nudelman: None; Anat Albrecht Shach: *Consultant*, IBEX Medical Analytics; Lucie Thibault: None; Lilach Bien: *Employee*, Ibex Medical Analytics; Ira Krasnitsky: None; Rachel Mikulinsky: None; Yuval Globerson: *Employee*, Ibex Medical Analytics; Roei Harduf: *Employee*, Ibex Medical Analytics; Shay Arbov: None; Chaim Linhart: *Employee*, Ibex Medical Analytics; Manuela Vecsler: *Employee*, Ibex Medical Analytics; Judith Sandbank: *Primary Investigator*, Ibex Medical Analytics

Background: Objective - This study aimed to clinically validate the performance of an AI algorithm designed to inform a pathologist's final diagnosis in the detection of invasive and in situ carcinomas in breast biopsies compared to ground truth (GT) established by multiple expert pathologists.

Design: The algorithm was based on an ensemble of convolutional neural networks previously trained on >2 million labeled image patches that were extracted from manual annotations on 2,153 H&E/HES-stained slides, selected from >115,457 breast biopsy slides. Performance of the algorithm was tested on 436 breast biopsies (841 H&E slides), including 156 invasive (including 31 rare subtypes), 135 DCIS/ADH, and 145 benign cases from two medical institutions in different geographies. All cases were distinct from those used to train the algorithm and reviewed by six pathologists from the two institutions. AI results were compared against the GT, which was established by consensus of two subspecialist breast pathologists. The study endpoints were detection of invasive carcinoma (IDC, ILC, other) and DCIS/ADH, including differentiating between low-grade DCIS/ADH and high-grade DCIS.

Results: The algorithm demonstrated high performance when compared with the GT with an AUC of 0.99 for the detection of invasive carcinoma (specificity and sensitivity of 93.6% and 95.5% respectively) and with AUC of 0.98 for the detection of DCIS. The algorithm differentiated well between subtypes/grades of invasive and in-situ cancers with an AUC of 0.97 for IDC vs. ILC and AUC of 0.92 for DCIS high grade vs. low grade/ADH, respectively. The algorithm also detected tumor-infiltrating lymphocytes with an AUC of 0.87 and fibroadenoma with an AUC of 0.88. Only 11 (7%) cases had discrepancies on invasive diagnosis (Table 1), 4 of these between invasive versus benign diagnosis encompassing one case on which the invasive component was only represented by rare lympho-vascular invasion, two cases of ILC (one with a diffuse pattern and the second in a case with granulomatous mastitis with multinucleated giant cells and hemosiderin-laden macrophages) and one rare case of tubular carcinoma surrounded by flat epithelial atypia and columnar cell lesions.

Table 1 Discrepancies between the study pathologists

Diagnosis	Diagnosis details	Discrepancies N (%)	Pathologist 1	Pathologist 2	Ground truth
Invasive vs. non-invasive		11 (7%)	153	148	156
Invasive vs. benign		4			
Invasive vs. DCIS/ADH		7			
Invasive subtypes	IDC / ILC / other	7	91 / 60 / 2	91 / 58 / 3	98 / 55 / 3
DCIS/ADH	DCIS/ADH vs. benign	14 (10.4%)	140	140	135
DCIS HG/IG vs. LG/ADH		25	87 / 53	93 /45	88 / 46
DCIS grading	DCIS HG vs. LG/ADH	10			
	DCIS IG vs. LG/ADH	15			

Conclusions: This multi-site study reports the successful clinical validation of a multi-feature AI algorithm in assisting pathologists to accurately detect invasive and in situ breast carcinoma, offering an important tool for computer-aided diagnosis in routine pathology practice.

186 Basal-Like Atypical Ductal Hyperplasia and Ductal Carcinoma In Situ: Evidence for Precursors of Basal-Like Invasive Ductal Carcinoma

Jing Wang[1], Lavinia Middleton[1]
[1]The University of Texas MD Anderson Cancer Center, Houston, TX

Disclosures: Jing Wang: None; Lavinia Middleton: None

Background: The basal-like breast cancers have been identified by gene expression profiling studies and are associated with worse overall survival. This study evaluated the characteristics of possible precursors of basal-like invasive ductal carcinomas (bIDCs) including basal-like atypical ductal hyperplasia (bADH) and ductal carcinoma in situ (bDCIS) and the significance of the expression of cytokeratin (CK) 5/6 and CK 17, commonly used markers for basal-like phenotype, in bADH and bDCIS.

Design: 10 female patients (mean, 48 years) diagnosed with bIDC and associated bDCIS and 2 females (mean,52 years) diagnosed with bADH were included. 6 patients had known family history of breast cancer. Immunohistochemical expression of estrogen receptor (ER), progesterone receptor (PR), HER2 and CK5/6 was determined in all cases and CK17 was tested in 7 IDCs and 1 ADH.

Results: IDCs were all histologic grade 3 with basal-like morphological features. The associated DCIS was cribriform or solid pattern and high nuclear grade. ER, PR and HER2 were negative in all cases (10/10). 5 patients received chemotherapy after resection. 5 patients are clinically stage IV after a follow up period of 1.6 year on average (range 0.3 to 6 years).

In IDC components, CK5/6 staining was diffusely strongly positive in 7 and patchy positive in the remaining 3 cases, while CK17 was diffusely strongly or moderately positive in 4 of 7 cases and remaining 3 with patchy staining. In bDCIS, CK5/6 staining was diffusely strongly positive in 7, patchy in 2 and negative in 1 of 10 cases, while CK17 was diffusely strongly in 1 and patchy positive in 3 of 7 cases and remaining 3 with negative staining (Table 1).

In 2 bADH cases, CK 5/6 was diffusely positive and ER and PR were negative. CK17, tested in 1 case was positive. The morphology was that of hyperchromatic cells with increased N/C ratio exhibiting rounded to cuboidal shape and intermediate grade nuclei. bADH proliferations were 2 to 3 cell layers thick and devoid of secondary lumen formation (Fig 1, 2).

Table 1 Summary of clinical pathological features of bDCIS and bADH cases and Cytokeratin expression.

Case	Age (yo)	Diagnosis	bIDC			bDCIS / bADH		Family history
			CK5/6	CK17		CK5/6	CK17	
1	55	bIDC, bDCIS	Patchy+++	++		0	Patchy+++	Yes
2	52	bIDC, bDCIS	+++	++		+++	0	No
3	59	bIDC, bDCIS	+++	+++		Patchy+++	0	No
4	50	bIDC, bDCIS	+++	+++		+++	+++	No
5	57	bIDC, bDCIS	+++	N/A		+++	N/A	No
6	56	bIDC, bDCIS	+++	N/A		+++	N/A	Yes
7	33	bIDC, bDCIS	Patchy +++	Patchy+++		+++	Patchy+++	Yes
8	46	bIDC, bDCIS	+++	N/A		+++	N/A	No
9	34	bIDC, bDCIS	+++	Patchy++		+++	0	No
10	33	bIDC, bDCIS	Patchy +++	Patchy +++		Patchy+++	Patchy +++	Yes
11	46	bADH				+++	N/A	Yes
12	58	bADH				+++	+++	Yes

Figure 1 - 186

Figure 1. H&E stained section showed bADH (case 11), original magnification, x400

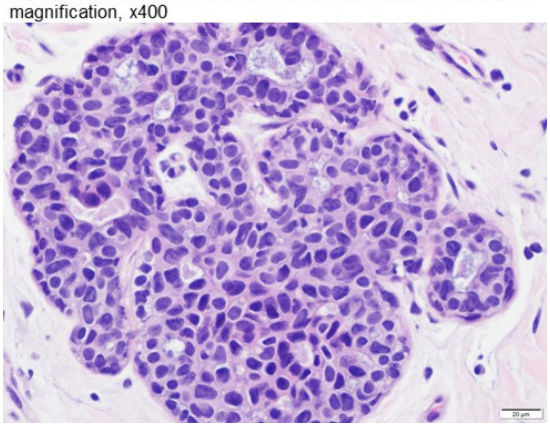

Figure 2 - 186

Figure 2. bADH (case 12) with ER and cytokeratin expression, original magnification, x200

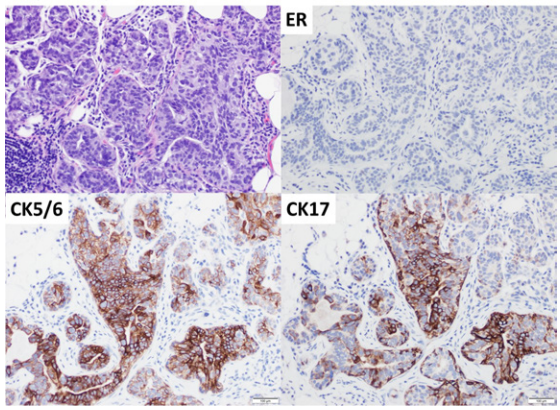

Conclusions: Our observations of atypical basal-like intraductal proliferations of intermediate nuclear grade, 2 to 3 cell layers thick with ER negative and CK 5/6 positivity is strong circumstantial evidence for a precursor basal-like ADH lesion. Importantly, there is a basal atypical intraductal lesion with diffuse CK5/6 staining, and in the context of atypical hyperplastic lesions with basal morphology, diffuse staining with CK5/6 should not confirm benignity.

187 Digital Image Analysis of HER2 Fluorescence In-Situ Hybridization: A Useful Tool to Resolve Equivocal HER2 Cases

Diane Wilcock[1], Kristina Moore[1], H. Evin Gulbahce[2], Deepika Sirohi[3]
[1]ARUP Laboratories, Salt Lake City, UT, [2]The University of Utah, Salt Lake City, UT, [3]University of Utah / ARUP, Salt Lake City, UT

Disclosures: Diane Wilcock: None; Kristina Moore: None; H. Evin Gulbahce: None; Deepika Sirohi: None

Background: The 2018 American Society of Clinical Oncologists /College of American Pathologists (ASCO/CAP) guidelines for *HER2* in breast carcinoma subdivide equivocal cases into 3 groups based on *HER2* copies and *HER2*/CEP17 ratios. These equivocal cases are challenging for manual scoring due to borderline scores, limited number of cells that can be scored, inherent scorer bias, as well as imperfect mapping of IHC and FISH slides when FISH cases are reflexed to IHC and subsequently rescored in accordance with the guidelines. Digital quantitative image analysis (QIA) allows for accurate mapping of highest areas of IHC staining to the FISH slides, a greater number of cells to be scored and better documentation than traditional manual methods. In this study we explored the utility of digital QIA in improving the *HER2* FISH reporting.

Design: *HER2* FISH slides were retrieved from the clinical workflow and sorted into their Group classifications. Forty-One Group 1, 8 Group 2, 18 Group 3, 28 Group 4, and 42 Group 5 cases were identified and imaged on a GenASIs Scan & Analysis instrument. The digital FISH QIA results were compared to the manual FISH results. Cases were considered discrepant if there was an overall change in Group Classification or ≥ ± 1 copy number difference (except for highly amplified Group 1 cases that had ≥6 *HER2* copies) and were investigated.

Results: Twenty-one cases were deemed unsuitable for digital QIA analysis (n=9 limited tumor/scattered tumor, n=5 extensive stroma, n=4 indistinct cell borders/green mist, n=2 red/green artifact, n=1 previously photobleached by manual review) and removed from the analysis. Accuracy was 91.7% for Group 1, 100% for Group 2, 84.6% for Group 3, 75% for Group 4, 100% for Group 5, with an overall accuracy of 90.3%. The main reasons for discordance were due to genetic heterogeneity (GH, n=3), tissue quality issues (n=3), and manual scoring bias (n=4).

Group (Accuracy %)	Total Cases	Discordant Case #	Reason for Discordance	Notes
Group 1: *HER2*/CEP17 ratio ≥ 2.0, *HER2*/cell ≥ 6 (91.7%)	36	1	Manual scoring bias	Unusually large tumor cells, truncation artifact
		2	Tissue issue	Indistinct cell borders plus alphoid green signals
		3	Genomic heterogeneity (GH)	Low level GH (3 vs 4 copies of *HER2*)
Group 2 *HER2*/CEP17 ratio ≥ 2.0, *HER2*/cell < 4 (100%)	8	N/A	N/A	N/A
Group 3 *HER2*/CEP17 ratio < 2.0, *HER2*/cell ≥ 6 (84.6%)	13	1	Manual scoring bias	Scattered amplified cells. Equivocal cells (~4 copies) make up majority of the tumor
		2	Tissue issue	Indistinct cell borders/large clumps of tumor cells
Group 4 *HER2*/CEP17 ratio < 2.0, *HER2*/cell ≥ 4 and < 6 (75%)	20	1	Manual scoring bias	Scattered tumor
		2	Tissue issue	Green mist/indistinct cell borders
		3	GH	<10% tumor had equivocal result. No IHC staining in these cells
		4	Manual scoring bias	Scattered highly amplified cells (~10 copies *HER2*)
		5	GH	Higher copy area was outside of IHC-circled area
Group 5 *HER2*/CEP17 ratio < 2.0, *HER2*/cell < 4 (100%)	39	N/A	N/A	N/A

Conclusions: Digital QIA has good overall accuracy and may improve targeted *HER2* FISH reading in equivocal cases which account to 22% of all FISH cases in our reference lab. Genetic heterogeneity, background on FISH slides, tissue quality that prevents accurate nuclear segmentation and inherent artifacts are some of the factors that limit use of digital QIA. Notwithstanding these limitations, digital QIA has considerable potential to improve accuracy of *HER2* FISH scoring and overcome limitations of manual scoring, especially in equivocal cases.

188 DCISionRT Testing for Patients with Ductal Carcinoma in Situ: Histopathological Correlation and Utility in Clinical Decision Making

Ariel Wu[1], Lulu Sun[2], Lulu Lai[2], Chieh-Yu Lin[3]
[1]Barnes-Jewish Hospital/Washington University, St. Louis, MO, [2]Washington University School of Medicine in St. Louis, St. Louis, MO, [3]Washington University School of Medicine, St. Louis, MO

Disclosures: Ariel Wu: None; Lulu Sun: None; Lulu Lai: None; Chieh-Yu Lin: *Consultant*, Natera

Background: Patients with breast ductal carcinoma in situ (DCIS) have up to a 50% chance of developing subsequent invasive breast cancer (IBC). There is an unmet need to identify low-risk patients who can avoid overtreatment, specifically with adjuvant radiation therapy (RT). DCISionRT is a commercially available molecular assay designed to assess future risk of DCIS and IBC. In this study, we examined the correlation of DCISionRT results with clinicopathologic features and clinical decision-making.

Design: With Institutional Review Board approval, all DCIS cases with DCISionRT testing performed as part of routine clinical practice were identified. Cases with a history of IBC, or with IBC on the immediate excision after DCIS diagnosis, were excluded. DCISionRT scores were reported as low risk (score < 3) and elevated risk (score ≥ 3). Records were reviewed for clinical data and treatment decisions. Archival slides were reviewed to confirm diagnosis, size, estrogen receptor (ER) status, margin status, presence of calcifications and necrosis. For categorical variables, statistical comparisons were made using χ^2 or Fisher's exact test. Multivariate analysis was conducted to determine predictors of DCISionRT score and to compare the score to histologic features.

Results: Forty-seven DCIS cases fit the inclusion criteria, with a mean age of 60 years (43-84) and mean size of 15.6 mm. The majority of the patients were age 50 or above (85%), ER positive (96%), and low or intermediate nuclear grade (74%).
For DCISionRT results, 25 of the cases were reported as low risk (53%) and 22 cases as elevated risk (47%). There was no statistically significant correlation of the scores with age, nuclear grade, ER positivity, size, margin status, calcifications or necrosis, although a trend was observed for elevated risk associated with age > 50 years, DCIS size > 10 mm, and necrosis. Thirty-five patients (74%) underwent adjuvant RT. The decision for RT was not significantly associated with the DCISionRT results, nor with any single clinicopathologic feature. Among the 25 patients with low-risk score, 16 (64%) received adjuvant RT. Possible reasons for RT in these cases included positive margins, >10 mm size or a borderline score (score = 3). With limited span of follow-up, none of the cases has developed recurrent DCIS or invasive/metastatic disease.

Conclusions: In our study, no clinicopathologic features correlated with DCISionRT score, and the decision for adjuvant RT was complex and multifactorial.

189 Clinicopathological and Immunohistochemical Features of Breast Extranodal Marginal Zone Lymphoma of Mucosa-associated Lymphoid Tissue: A Single Institutional Study

Mingfei Yan[1], Jing Wang[1], Hannah Gilmore[2], Philip Bomeisl[3], Aparna Harbhajanka[1]
[1]Case Western Reserve University/University Hospitals Cleveland Medical Center, Cleveland, OH, [2]University Hospitals Case Medical Center, Case Western Reserve University, Cleveland, OH, [3]University Hospitals Cleveland Medical Center, Cleveland, OH

Disclosures: Mingfei Yan: None; Jing Wang: None; Hannah Gilmore: *Speaker*, Agendia; *Advisory Board Member*, Sectra; Philip Bomeisl: *Consultant*, PathAI; Aparna Harbhajanka: None

Background: Extranodal Marginal Zone Lymphoma of Mucosa-associated Lymphoid Tissue (MALT-L) can present in various anatomical sites. However, only 3% MALT-L are found in the breast. Clinically, it may present in a similar manner as breast carcinomas. We aim to better characterize the clinicopathologic features of breast MALT-L through retrospective case reviews.

Design: A retrospective search of 56 breast lymphoma cases were performed in our institution from 2000 to 2020, including 11 MALT-L biopsy cases (19.6%). Their clinical and pathologic features were studied and characterized. Immunostains were performed for all cases.

Results: All 11 patients were female with a median age of 62-year-old. Imaging data was available for 10 patients, and all of them presented with a breast mass (table 1). Three of 10 cases showed multiple breast masses. Breast was the primary presentation in 8 patients (72.7%), while 3 (27.3%) had prior marginal zone lymphoma (MZL) in other anatomical sites. The median follow-up was 6 years, during which time 3 patients (27.3%) developed recurrent breast MALT-L, and 5 patients (45.5%) developed lymphomas in other sites (including MZL in 2 patients, diffuse large B cell lymphoma/DLBCL in 1 patient, grade 3 follicular lymphoma/FL in 1 patient, and 1 patient with no pathologic diagnosis). On histology, MALT-L in the breast most commonly showed a proliferation of monocytoid cells (fig a) with reactive germinal centers. Lymphoepithelial lesions (LEL) were identified in only 2 patients (18.2%). All cases showed typical immunophenotype, except for 2 patients (18.2%) with dim CD5 positivity (fig b). Light chain restriction was present in 7 patients (63.6%), and only 1 case (9.1%) was positive for EBER. Varying degrees of stromal sclerosis was a common finding (fig c, a), that was seen in 8 patients (72.7%). All cases were negative for CD30, except for 1 case with abundant CD30 positive cells in recurrent breast lesion (fig d). Finally, 10 patients (90.9%) were negative for IgG4. The only patient with positive IgG4 had a primary cutaneous MALT-L which is known to more likely express IgG4 than other MALT-L.

Table 1. Clinicopathologic features of breast MALT-L.

Abbreviations: F: female; s/o: suspicious of; LEL: lymphoepithelial lesion; MZL: marginal zone lymphoma; DLBCL: diffuse large B cell lymphoma; N/A: not available.

No.	Age (yr)	Gender	Primary site	Imaging impression of breast lesion	Breast recurrence	Recurrent lymphoma involving other sites	LEL	CD5	CD30	EBER ISH	IgG4	Light chain restriction	Sclerosis
1	77	F	Breast	N/A	Yes	None	Absent	Negative	Negative	Negative	Negative	Kappa	Absent
2	54	F	Breast	Irregular mass, suggest possible hematoma	No	MZL on back and left flank	Absent	Negative	Negative	Negative	Negative	Kappa	Present
3	93	F	Breast	Circumscribed mass, s/o malignancy	N/A	N/A	Absent	Negative	Negative	Negative	Negative	Polytypic	Present
4	57	F	Right cervical LN	Intramammary lymph node	None	DLBCL in spleen, diaphragm, and back	Absent	Negative	Negative	Positive	Negative	Kappa	Absent
5	59	F	Abdominal skin	Circumscribed mass, likely fibroadenoma	Yes	None	Absent	Negative	Negative, Abundant CD30+ cells in recurrent breast lesion	Negative	Positive	Kappa	Present
6	81	F	Breast	Multiple bilateral masses, possibly benign	None	FL Grade 3A in inguinal lymph node	Present	Negative	Negative	Negative	Negative	Polytypic	Present
7	62	F	Left orbital adnexa	Multiple masses, s/o malignancy	Yes	None	Absent	Dimly positive	Negative	Negative	Negative	Kappa	Present
8	76	F	Breast	Ill-defined mass, s/o malignancy	None	Diffuse lymphadenopathies, no pathology.	Absent	Negative	Negative	Negative	Negative	Lambda	Absent

9	49	F	Breast	Multiple circumscribed masses, s/o malignancy	None	None	Absent	Negative	Negative	Negative	Negative	Polytypic	Present
10	89	F	Breast	Circumscribed mass, s/o malignancy	None	None	Absent	Dimly positive	Negative	Negative	Negative	Polytypic	Present
11	56	F	Breast	Circumscribed mass, possibly benign	None	MZL in retroperitoneum and orbital lacrimal glands	Present	Negative	Negative	Negative	Negative	Kappa	Present

Figure 1 - 189

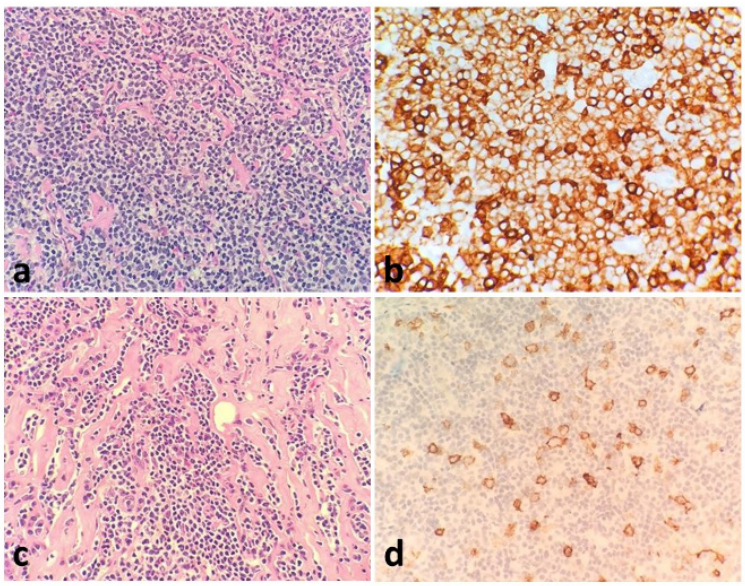

Conclusions: Low-grade lymphomas of the breast, particularly MALT-L, while rare, can present in the breast either primarily or secondarily. It is important to be cognizant of its clinical, radiologic and histologic findings, to ensure appropriate classification. Recurrences in the breast or other sites and/or transformation to a higher grade B cell lymphoma can also occur.

190 Friends in Low Places: Heterogeneity in Low ER Positive Breast Cancer

Lei Yan[1], Sarah Hackman[1], Christopher Cape[1], Alia Nazarullah[1]
[1]The University of Texas Health Science Center at San Antonio, San Antonio, TX

Disclosures: Lei Yan: None; Sarah Hackman: None; Christopher Cape: None; Alia Nazarullah: None

Background: In 2020, CAP and ASCO released guidelines for estrogen receptor (ER) testing in invasive breast cancers (IBC), including the recommendation of reporting cases with 1-10% ER positivity as ER low positive (ER-LP). The updated guidelines recommend that those patients with ER-LP IBC should be considered eligible for endocrine therapy, although the benefit of this for ER-LP IBC is controversial. ER-LP IBC is very rare, accounting for 2-3% of ER positive IBC. Core needle biopsy (CNB) is preferred for hormone receptor testing due to lower risk for cold ischemia and better tissue processing. High concordance rate (83-99%) of ER expression has been reported between CNB and surgical specimen (SS) of IBC, but majority of the studied cases are ER high positive. Due to the rarity of ER-LP IBC and tumor heterogeneity, the reproducibility of ER-LP between CNB and SS is questionable, and has not been well studied. In addition, interobserver variability (IOV) in low ER ranges is a challenge. We assessed the IOV and concordance rate of ER-LP between CNB and subsequent SS in IBC.

Design: In this retrospective study, 13 patients from 2013-2021 with prior diagnosis of ER-LP IBC on CNB, with SS showing viable tumor cells were included in the study. ER expression level by IHC was interpreted as <1% (negative), 1-10% (ER-LP) and >10% (ER-P). For CNB, the original ER expression level was reported by various surgical pathologists (P1). The CNB ER stains were reevaluated by two pathologists (P2 and P3) who routinely review breast biomarkers. ER stains were additionally performed on all SS and evaluated by P2 and P3 only. Modified Fleiss's kappa (κ) values for IOV and concordance rate ER-LP between CNB and SS were calculated.

Results: All patients were women, with median age of 49 years (range 25-87 years). The diagnoses included invasive ductal carcinoma (12) and metaplastic carcinoma (1). For IOV, P2 and P3 showed substantial agreement on CNB and excellent agreement on SS. However, the agreement between P1, P2 and P3 was only fair (Figure 1). 7 of 13 cases (54%) showed concordant ER-LP on SS (presumed true ER-LP), all of which had histologic grade 3 and negative HER2 status. Only 2 of 13 cases (15%) showed concordant ER-LP by P2 and P3 on both CNB and SS (Table 1).

Table 1. ER expression level by IHC interpreted by different pathologists

	Core needle biopsy (%)				Surgical specimen (%)	
Case Number	P1	P2	P3		P2	P3
1	1-10	>10	>10		<1	<1
2	1-10	>10	>10		1-10	1-10
3	1-10	>10	1-10		1-10	1-10
4	1-10	>10	>10		<1	<1
5	1-10	>10	>10		>10	>10
6	1-10	1-10	1-10		1-10	1-10
7	1-10	>10	>10		1-10	1-10
8	1-10	1-10	>10		1-10	1-10
9	1-10	>10	>10		1-10	1-10
10	1-10	1-10	1-10		<1	1-10
11	1-10	1-10	1-10		1-10	1-10
12	1-10	>10	>10		<1	<1
13	1-10	1-10	1-10		<1	<1

Abbreviations: ER, estrogen receptor; IHC, immunohistochemistry; P1, various surgical pathologists who previously reported breast biomarkers; P2 and P3, two pathologists who are routinely review breast markers currently in our institution.

Figure 1 - 190

Figure 1. Interobserver Variability Analysis of ER Expression of invasive breast cancer by IHC on Core Needle Biopsy

	P1, P2 and P3		P1 and P2		P1 and P3		P2 and P3	
	Kappa	Agreement (%)	Kappa	Agreement (%)	Kappa	Agreement (%)	Kappa	Agreement (%)
CNB	0.31	53.85	0.08	38.46	0.08	38.46	0.77	84.62
SS							0.88	92.31

Abbreviations: ER, estrogen receptor; IHC, immunohistochemistry; CNB, core needle biopsy; SS, surgical specimen; P1, various surgical pathologists who previously reported breast biomarkers; P2 and P3, two pathologists who are routinely review breast markers currently in our institution.

Conclusions: In ER-LP IBC, excellent agreement can be achieved between pathologists who routinely review breast biomarkers. ER-LP on CNB is variable from ER-LP on SS, and repeating ER stain on SS could be considered on all ER-LP cases.

191 "Non-Classical" HER2 Fluorescent in Situ Hybridization Categories in Breast Cancer with Clinical-Pathologic Correlation

Ellen Yang[1], Jessie Wu[2], Susan Armstrong[1], Miralem Mrkonjic[2], Gulisa Turashvili[3]
[1]University of Toronto, Toronto, Canada, [2]Mount Sinai Hospital, University of Toronto, Toronto, Canada

Disclosures: Ellen Yang: None; Jessie Wu: None; Susan Armstrong: None; Miralem Mrkonjic: None; Gulisa Turashvili: None

Background: Human Epidermal Growth Factor Receptor 2 (HER2) status in breast cancer is currently assessed based on the 2018 American Society of Clinical Oncology/College of American Pathologists (ASCO/CAP) guidelines. Although HER2 is often amplified (Group 1) or non-amplified (Group 5) by fluorescence in situ hybridization (FISH), a small subset yields "non-classical" results (Groups 2-4) requiring additional work-up with a combined reinterpretation of FISH and immunohistochemistry (IHC). We set out to assess the distribution of these "non-classical" categories with clinical-pathologic correlation.

Design: Biomarker studies of invasive breast carcinomas diagnosed between mid-2018 and 2020 were retrospectively analyzed. Clinical-pathologic features were reviewed when available. Statistical analysis was performed using Chi-square z-test and p-values of <0.05 were considered significant.

Results: Of the 3420 samples identified, 1285 (37.6%) cases were equivocal (2+) by IHC and underwent HER2 FISH. Of the 1285 cases, 214 (16.7%) yielded FISH Groups 2-4 requiring 2 reads, including 3 (1.4%) in Group 2, 25 (11.7%) in Group 3 and 186 (86.9%) in Group 4. Per the 2018 guidelines, 29 (13.6%) tumors were reclassified as amplified and 185 (86.4%) as non-amplified. The median patient age was 63 years (28-98). Most specimens were core biopsies (137, 64%). Most frequent diagnosis was primary invasive carcinoma of no special type (192, 89.7%). Group 3 tumors were higher grade than Group 4 (40% vs. 22%, p=0.05). Most cases were positive for estrogen receptor (ER; 69.6%) and progesterone receptor (PR; 58.4%). There was no statistical difference between the 3 groups for metastasis, recurrence, the presence of ductal carcinoma in situ (DCIS) or lymphovascular invasion (LVI). Systemic therapy included neoadjuvant chemotherapy in 10 (4.7%) patients with Residual Cancer Burden score of 0-II, adjuvant chemotherapy in 14 (6.5%) and hormone therapy in 12 (5.6%). Group 4 cases were more likely to receive radiotherapy than Group 3 (0% vs 9.1%, p=0.05). The median disease-free survival was 15 months (0-34) for all groups.

Table 1: Clinical-pathologic features of "non-classical" HER2 Groups 2-4

	Group 2 (ratio ≥2.0, HER2<4.0)	**Group 3 (ratio <2.0, HER2≥6.0)**	**Group 4 (ratio <2.0, HER2 ≥4.0 and <6.0)**	**Total**	**P value**
Number of cases	3	25	186	214	
Median age (yrs)	57 (47-67)	64 (38-84)	63 (28-98)	63 (28-98)	0.29
Type of specimen (no, %)					
Core biopsy	3 (100%)	18 (72%)	116 (62%)	137 (64%)	0.29
Excision	0	3 (12%)	40 (22%)	43 (20%)	0.39
Mastectomy	0	4 (16%)	28 (15%)	32 (15%)	0.76
Unknown	0	0	2 (1%)	2 (1%)	
Type of surgery (no, %)					
Excision	0	4 (16%)	52 (28%)	56 (26%)	0.26
Mastectomy	0	4 (16%)	35 (19%)	39 (18%)	0.68
Unknown	3 (100%)	17 (68%)	99 (53%)	119 (56%)	
Treatment (no, %)					
Neoadjuvant chemotherapy	0	1 (4%)	9 (5%)	10 (5%)	0.91
Adjuvant chemotherapy	0	2 (8%)	12 (6%)	14 (7%)	0.88
Hormone therapy	0	0	12 (6%)	12 (6%)	0.08
Radiotherapy	0	0	17 (9%)	17 (8%)	**0.05**
Median disease-free period (mo)	0	9 (5-17)	16 (0-34)	15 (0-34)	
Histotype (no, %)					
Invasive carcinoma of no special type	2 (67%)	22 (88%)	168 (90%)	192 (90%)	0.39
Invasive lobular carcinoma	0	0	5 (3%)	5 (2%)	0.68
Metastatic carcinoma	1 (33%)	3 (12%)	13 (7%)	17 (8%)	0.18
Nottingham grade (no, %)					
1	0	0	7 (4%)	7 (3%)	0.57
2	1 (67%)	5 (20%)	62 (33%)	68 (32%)	0.15
3	0	10 (40%)	40 (22%)	50 (23%)	**0.05**
Unknown	2 (33%)	10 (40%)	77 (41%)	89 (42%)	
Associated with ductal carcinoma in situ (DCIS)	0	8 (32%)	59 (32%)	67 (31%)	0.82
Positive lymphovascular invasion (LVI)	0	3 (12%)	30 (16%)	33 (15%)	0.56
Biomarkers (no, %)					
ER positivity	2 (67%)	16 (64%)	131 (70%)	149 (70%)	0.51
PR positivity	2 (67%)	12 (48%)	111 (60%)	125 (58%)	0.20
Unknown	1 (33%)	3 (12%)	35 (19%)	39 (18%)	

Conclusions: The "non-classical" HER2 FISH categories composed 16.7% of breast specimens with equivocal HER2 IHC requiring FISH testing, with Group 4 being the most frequent. Histologic features differed among the groups, with Group 3 tumors being higher grade than Group 4 tumors, suggesting different tumor biology. More clinical data and longer follow-up is required for sufficient treatment response correlation.

192 Cystic Neutrophilic Granulomatous Mastitis vs. Granulomatous Mastitis: Sensitivity and Specificity of 16S rRNA and Sanger Sequencing for Corynebacterium spp

Ellen Yang[1], Rob Kozak[2], Sharon Nofech-Mozes[3], Elzbieta Slodkowska[4], Anna Plotkin[1], Wedad Hanna[2], Fang-I Lu[4]
[1]University of Toronto, Toronto, Canada, [2]Sunnybrook Health Sciences Centre, Toronto, Canada, [3]University of Toronto, Sunnybrook Health Sciences Centre, Toronto, Canada, [4]Sunnybrook Health Sciences Centre, University of Toronto, Toronto, Canada

Disclosures: Ellen Yang: None; Rob Kozak: None; Sharon Nofech-Mozes: None; Elzbieta Slodkowska: None; Anna Plotkin: None; Wedad Hanna: None; Fang-I Lu: None

Background: Cystic neutrophilic granulomatous mastitis (CNGM) is a rare subtype of granulomatous mastitis (GM) characterized by cystic spaces rimmed by neutrophilic and lipogranulomatous inflammation, occasionally filled by gram-positive bacterial organism. CNGM has been associated with Corynebacterium spp, but identification of Corynebacteria can be challenging and comparison between various identification methods is lacking. We have previously examined the clinical, radiologic and pathologic features of CNGM and non-CNGM/GM cases. In this study, we analyzed the prevalence of Corynebacteria in CNGM and non-CNGM/GM cases, and compared the sensitivity and specificity of the various identification methods for Corynebacteria.

Design: A retrospective search of breast specimens with a diagnosis of granulomatous inflammation identified 82 cases from 2010-2020. 77 cases with available H&E slides were reviewed by one resident and two staff breast pathologists to reach consensus on the histologically-diagnosed CNGM cohort and non-CNGM/GM cohort. Gram stain and PCR-based identification of Corynebacteria by 16S ribosomal RNA primers (16S), were performed on Formalin-fixed, paraffin-embedded (FFPE) tissue blocks, and confirmatory Sanger sequencing (SS) was performed on cases with 16S positivity. Microbiology results were retrieved from the electronic patient records. Chi-square test was used to compare differences in the prevalence of Corynebacteria between CNGM vs non-CNGM.

Results: 29 CNGM cases and 19 non-CNGM/GM cases were identified. 3 CNGM (10%) cases were positive for Corynebacteria by microbiology culture and/or sequencing, while 2 non-CNGM/GM (11%) cases were positive for Corynebacteria; the Corynebacteria prevalence was not significantly different between these two cohorts (p=0.83). Other bacterial organisms were also detected in 5 CNGM (17%) and 8 non-CNGM/GM (42%) cases. The positivity rates for the various detection methods were 17% (8/48) for Gram stain, 38% (18/48) for 16S, 17% (8/48) for microbiology culture and 17% (8/48) for SS. Using microbiology culture and SS as the gold standards, the sensitivity and specificity of each detection method were 60% and 88% for Gram stain, 100% and 70% for 16S, 50% and 93% for microbiology culture, and 25% and 98% for SS.

Comparison between Cystic neutrophilic granulomatous mastitis (CNGM) and Non-Cystic neutrophilic granulomatous mastitis (non-CNGM/GM) cohorts

	CNGM (29)	**Non-CNGM (19)**	**Total**	**p**
+ve Gram stain (no, %)	7 (24%)	1 (5%)	8 (17%)	0.18
+ve culture (no, %)	4 (14%)	4 (21%)	8 (17%)	0.17
+ve Corynebacterial culture (no, %)	2 (7%)	2 (11%)	4 (8%)	0.65
+ve 16S (no, %)	8 (28%)	10 (53%)	18(38%)	**0.02**
+ve SS for any bacterium (no, %)	3 (10%)	5 (26%)	8 (17%)	0.08
+ve Corynbacterial SS (no, %)	2 (7%)	0	2 (4%)	0.28
+ve Corynebacterial infection (no, %)	3 (10%)	2 (11%)	5 (10%)	0.83

Conclusions: Corynebacterium was detected in 10% of CNGM and 11% of non-CNGM/GM cases. 16S on FFPE specimens was the most sensitive detection method for Corynebacteria, and SS was the most specific.

193 Ki-67 Index Regression Using Fully Convolutional Regression Network and Cancer Area Segmentation Network

Hyeon Seok Yang[1], Chan Kwon Jung[2], Tae-Yeong Kwak[3], Sun Woo Kim[1], Hyeyoon Chang[1]
[1]Deep Bio Inc., Seoul, South Korea, [2]The Catholic University of Korea, Seoul St. Mary's Hospital, Seoul, South Korea, [3]Deep Bio Inc., Guro-gu, South Korea

Disclosures: Hyeon Seok Yang: *Employee*, Deep Bio Inc.; Chan Kwon Jung: None; Tae-Yeong Kwak: *Employee*, Deep Bio Inc.; Sun Woo Kim: *Stock Ownership*, Deep Bio Inc.; Hyeyoon Chang: *Employee*, Deep Bio Inc.

Background: The Ki-67 index is commonly used as a marker of breast cancer proliferation. Direct measurement of the Ki-67 index by a pathologist is laborious and time-consuming. Automatic Ki67 index computation methods have been proposed. However, existing methods had a limitation in that the tumor area had to be manually set. In this study, we propose a deep-learning-based method for automatically estimating the Ki-67 index by using both the fully convolutional regression network (FCRN) and the cancer area segmentation network.

Design: The dataset was acquired from a set of Diaminobenzidine-Hematoxylin (DAB-H) Ki-67 immuno-stained breast cancer resection tissue slides using two microscope cameras at 40x objective lens. The first set contains 114 images of 1542x2080 pixels, and the second set contains 80 images of size 1848x2070 pixels. There are two classes: Ki-67 positive (DAB) tumor cells and Ki-67 negative (H) tumor cells. The positive and negative tumor cells were annotated by an experienced pathologist, and then the cancer area annotations were made based on those cell annotations. FCRN was used to detect stained cells and DeepLabV3 was used for cancer area segmentation. The dataset was split into train: 8, tune: 1, and validation: 1. During training, data augmentation (color jitter, random flip, and random rotation) was performed. The FCRN was trained with stochastic gradient descent (SGD) optimizer, initial learning rate 0.001, mean squared error (MSE) loss, for 200 epochs. The DeepLabV3 was trained with Adam, initial learning rate 0.002, BCEWithLogitsLoss, early stopping.

Results: We measured the mean absolute error (MAE) and coefficients of determination of Ki-67 index before and after cancer area segmentation application. In case of MAE, the error decreased from 16.36 to 15.43 for DAB, and the error decreased from 38.12 to 35.55 for H. For Coefficients of determination, DAB was improved from 0.934 to 0.942, H was similar from 0.943 to 0.943, and Ki67 index was similar from 0.980 to 0.983.

Figure 1 - 193

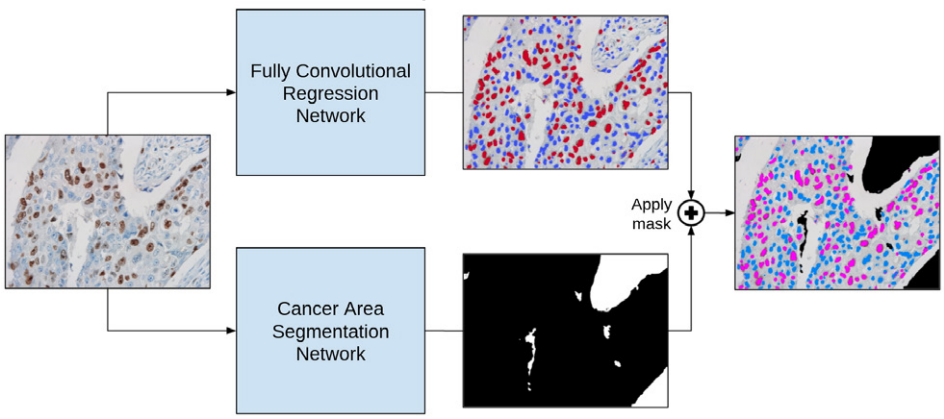

Figure 2 – 193

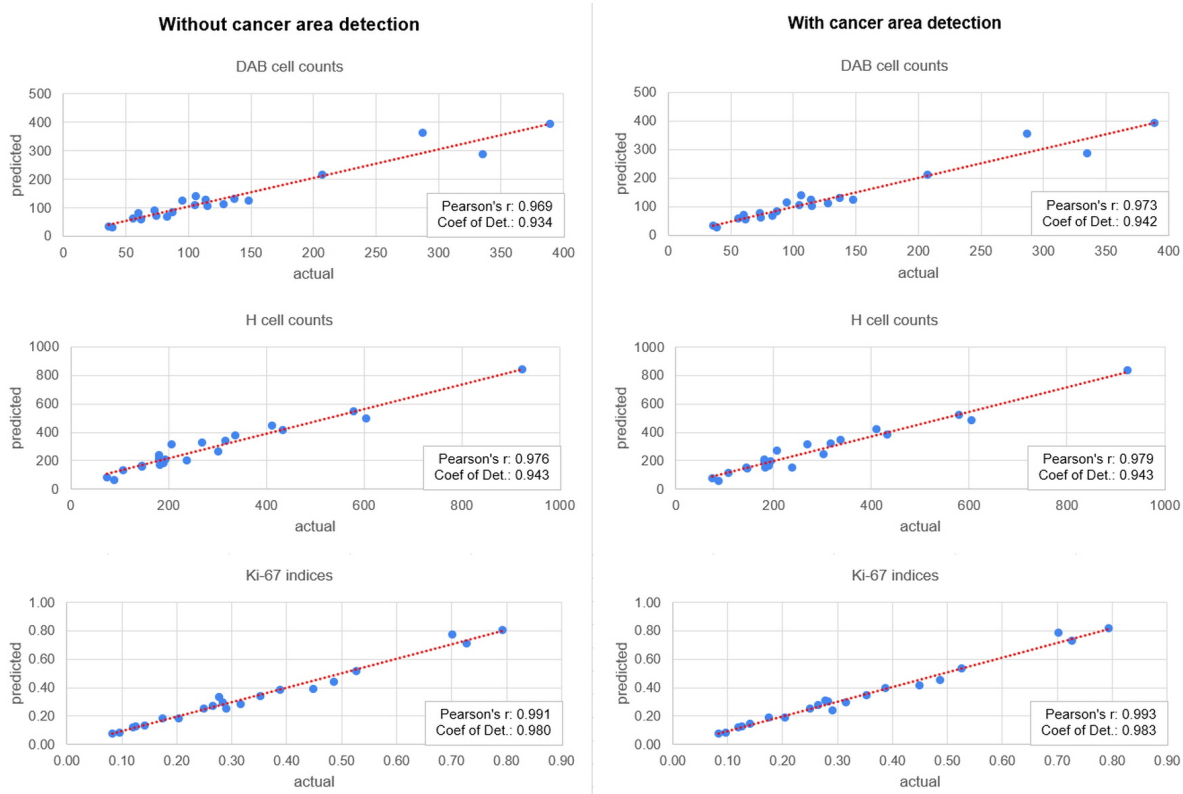

Conclusions: The automatic calculation of Ki-67 index became more accurate by applying automatic cancer area segmentation. Performance can be improved by expanding and learning with various kinds of datasets.

194 In Search for Calcifications: Do Deeper Levels Improve Diagnostic Yield in Stereotactic Core Needle Breast Biopsies?

Fazilet Yilmaz[1], Sean Hacking[1], Linda Donegan[2], Li Juan Wang[1], Evgeny Yakirevich[3], Yihong Wang[2]
[1]Alpert Medical School of Brown University, Providence, RI, [2]Brown University, Rhode Island Hospital, Providence, RI, [3]Rhode Island Hospital, Providence, RI

Disclosures: Fazilet Yilmaz: None; Sean Hacking: None; Linda Donegan: None; Li Juan Wang: None; Evgeny Yakirevich: None; Yihong Wang: None

Background: Stereotactic core needle biopsy (SCNB) is most used for mammographic calcification (calc) to rule out ductal carcinoma in situ (DCIS). In recent years, 9-gauge vacuum-assisted SCNB replaced the stereotactic 14-gauge automated biopsy, increasing the amount of tissue available for analysis. However, literature on the diagnostic yield of SCNB is very scarce. The present study evaluated the detection of calcs on a standard three levels to determine whether deeper levels improved the diagnostic yield.

Design: This retrospective study included 533 consecutive SCNBs for calc performed on 511 patients over a year period in 2020-2021. All biopsies were performed for non-mass forming calc, and 6-8 cores of tissue were obtained using a 9-gauge vacuum-assisted stereotactic biopsy. All biopsies were routinely sectioned in 3 levels at15-micron intervals. Additional 6 levels were sectioned when no calc was found.

Results: Out of 533 cases, there were 5 invasive carcinomas without DCIS (1%), 156 DCIS (15 DCIS with invasion) (29%), 55 ADH (10%), 5 FEA (1%), 25 LCIS/ALH (5%), and 287 benign (54%) (Table 1). The age of patients who underwent excision for invasive, DCIS, ADH was significantly higher of patients with benign findings (P=0.01*). The upper outer quadrant was the most frequent biopsied location, but the location/quadrant has no significance pertaining to the rate of malignancy detection. The

detection rate of calc on initial sections was 75.7% (404/533). Deeper levels were performed in 141 (26%) cases that did not contain calcs on initial levels (91%, 129/141), or while searching for a more advanced lesion (9%, 12/141). With the first 6 additional levels, calc was found in 105 cases (96%); 20 cases calc was found in additional levels (99%). Calc was not identified in 4 cases (1%) after levels and imagining the blocks. More advanced lesions were found in 20 cases with additional levels. Calc was identified and associated with all the invasive, DCIS, ADH, and FEA cases, and 8 of 25 (32%) of LCIS/ALH cases. In search for calc, the clinical management of 11 initially benign cases (2%) changed to lesions needing for excision (5 DCIS, 5 ADH, and 1 FEA).

Table 1.

	Total	Excision				Maybe excision		No excision
		INV (without DCIS)	INV (with DCIS)	DCIS	ADH	FEA	ALH/LCIS	Benign (CCC, FCC, FA)
Number of cases (N, % of total)	533	5 (1%)	15 (3%)	141(26%)	55 (10%)	5 (1%)	25 (5%)	287(54%)
Age (mean, range)	58; 30-91	59; 31-91 (*p=0.01)				57; 38-83		57: 30-86
Laterality (R; L)	277;255	109;106 (P=0.8)				16;14		152;135
Calc detected initial levels (N, % in column)	404 (75%)	5 (100%)	15 (100%)	128 +2 (92%)	34 + 8 (76%)	2+2 (80%)	6 (24%)	
Calc detected additional levels (N, % in column)	125(24%)	0	0	11 (8%)	13 (24%)	1(20%)	2 (8%)	
Change of management (N, % in column)	11 (2%)	0	0	5 (1%)	5 (9%)	1 (20%)	0	

Conclusions: Initial levels resulted in a 75% detection rate for calc. Additional levels were needed to identify the calc and increased diagnostic yield for calcs to 96%, resulting in more advanced lesions and changes from a clinical management perspective.

195 Expression of TRPS1, SOX10 and GATA3 in Different Subtypes of Metaplastic Breast Carcinoma

Esther Yoon[1], Zaibo Li[2], Lei Huo[1], Qiong Gan[1], Lavinia Middleton[1], Aysegul Sahin[1], Qingqing Ding[1]
[1]The University of Texas MD Anderson Cancer Center, Houston, TX, [2]The Ohio State University Wexner Medical Center, Columbus, OH

Disclosures: Esther Yoon: None; Zaibo Li: None; Lei Huo: None; Qiong Gan: None; Lavinia Middleton: None; Aysegul Sahin: None; Qingqing Ding: None

Background: Most metaplastic breast carcinoma (MBC)s are usually high-grade and aggressive with negative ER, PR, and HER2, and frequently lost the expression of luminal breast marker GATA3. When lacking the conventual mammary carcinoma component, it can cause a diagnostic challenge. Previously, studies found basal/myoepithelial marker SOX10 was frequently positive in some MBCs. More recently, TRPS1 was reported to be highly sensitive and specific for breast cancer. We aim to compare expression of GATA3, SOX10 and TRPS1 in the common subtypes of MBCs.

Design: Total 134 MBCs diagnosed between 2005 to 2020 were collected from our institutions, including 61 MBCs with mesenchymal differentiation (MBC-MD), 37 high-grade spindle cell carcinomas (SpCC-HG), 7 low-grade spindle cell carcinomas (SpCC-LG, including fibromatosis-like metaplastic carcinoma), 24 squamous cell carcinomas (SqCC), and 5 low-grade adenosquamous carcinomas (LGASC). Whole tissue sections were stained with GATA3, SOX10, and TRPS1 using Leica Bond Max autostainer system following standard automated protocols. Nuclear staining was considered positive for all three stains and their immunoreactive scores were calculated as the product of the percentage of positive cells (0, <1%; 1, 1%-10%; 2, 11%-50%; and 3, 51%-100%) and the staining intensity (0, negative; 1, weak; 2, moderate; and 3, strong). The scores were defined as negative (0 or 1), low positive (2), intermediate positive (3 or 4), or high positive (6 or 9).

Results: The staining results are summarized in Table 1. TRPS1 was positive in 100% of MBC-MD and 92% of SpCC-HG, which was higher than GATA3 (39% and 57%) and SOX10 (77% and 16%). For SqCC, positive TRPS1 (100%) and GATA3 (96%) were

more frequently seen than SOX10 (37%). TRPS1, GATA3 and SOX10 were all sensitive for LGASC (100%, 100% and 80%), but all less sensitive for SpCC-LG (43%, 43% and 0%). For all included cases, TRPS1 expression was predominant intermediate to high positive (116/134; 87%), however, intermediate to high positive SOX10 and GATA3 were seen in only 42% (56/134) and 37% (50/134) cases, respectively.

Table 1: Comparison of TRPS1, GATA3 and SOX10 expression in five subtypes of metaplastic breast carcinoma (n=134).

		Negative, n (%)	Positive, n (%)			Total
			Low	Intermediate	High	
TRPS1	MBC-MD	0 (0%)	1 (2%)	4 (7%)	56 (92%)	61
	SpCC-HG	3 (8%)	6 (16%)	11 (30%)	17 (46%)	37
	SpCC-LG	4 (57%)	3 (43%)	0 (0%)	0 (0%)	7
	SqCC	0 (0%)	1 (4%)	8 (33%)	15 (63%)	24
	LGASC	0 (0%)	0 (0%)	2 (40%)	3 (60%)	5
GATA3	MBC-MD	37 (61%)	11 (18%)	7 (11%)	6 (10%)	61
	SpCC-HG	16 (43%)	9 (24%)	8 (22%)	4 (11%)	37
	SpCC-LG	4 (57%)	2 (29%)	1 (14%)	0 (0%)	7
	SqCC	1 (4%)	4 (17%)	5 (21%)	14 (58%)	24
	LGASC	0 (0%)	0 (0%)	1 (20%)	4 (80%)	5
SOX10	MBC-MD	14 (23%)	2 (3%)	3 (5%)	42 (69%)	61
	SpCC-HG	31 (84%)	0 (0%)	0 (0%)	6 (16%)	37
	SpCC-LG	7 (100%)	0 (0%)	0 (0%)	0 (0%)	7
	SqCC	15 (63%)	8 (33%)	1 (4%)	0 (0%)	24
	LGASC	1 (20%)	0 (0%)	2 (40%)	2 (40%)	5

MBC-MD; Metaplastic breast carcinoma with mesenchymal differentiation; SpCC-HG: Spindle cell carcinoma, high-grade; SpCC-LG: Spindle cell carcinoma, low-grade; SqCC: Squamous cell carcinoma; LGASC: Low-grade adenosquamous carcinoma.

Figure 1 - 195

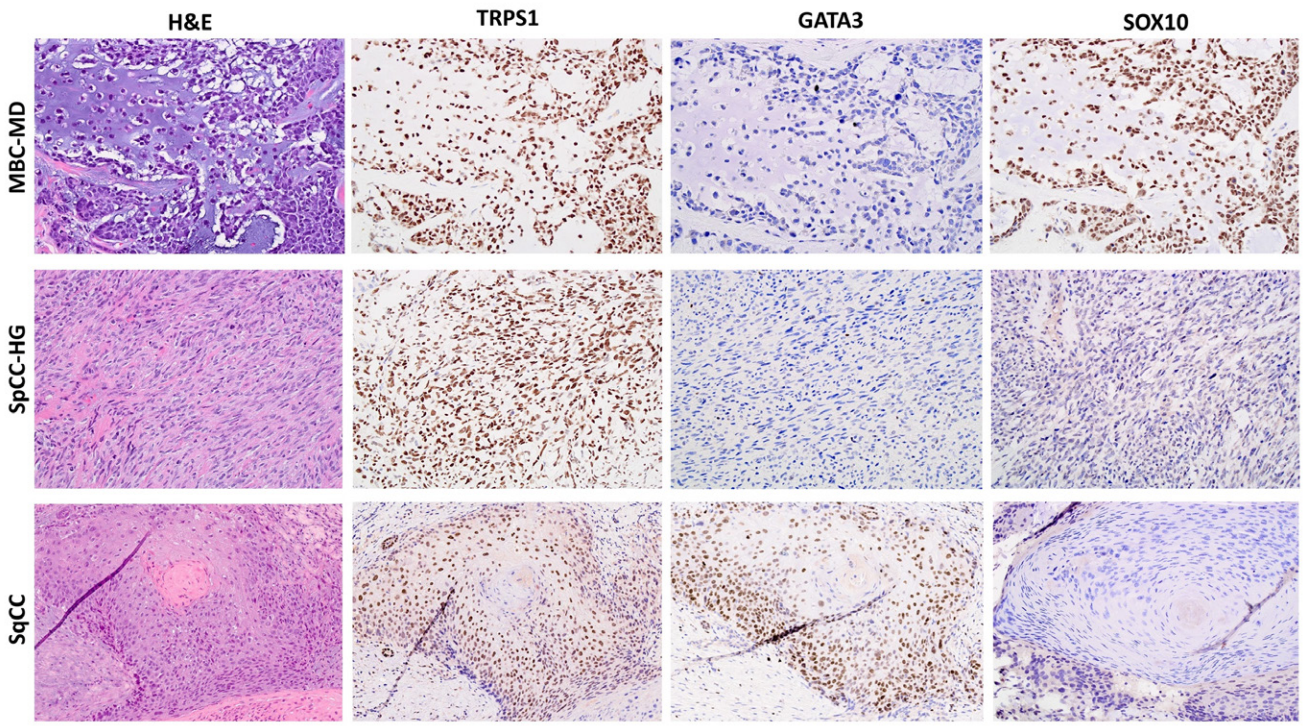

Conclusions: TRPS1 was a more sensitive and reliable diagnostic marker for MBCs than SOX10 and GATA3, especially for the most common MBCs: MBC-MD and SpCC-HG. SOX10 was relatively sensitive for MBC-MD and LGASC, while GATA3 was sensitive for SqCC and LGASC. In contrast, the sensitivity of all three markers was low in SpCC-LG, so negative staining for these markers in SpCC-LG cannot exclude breast origin. Use of TRPS1, SOX10 and GATA3 can assist in the differentiation of MBC and may contribute to our knowledge of epithelial to mesenchymal transition.

196 Expression of TRPS1, SOX10 and GATA3 in Triple Negative Invasive Ductal and Lobular Carcinomas

Esther Yoon[1], Gang Wang[2], Yun Wu[1], Hui Chen[1], Constance Albarracin[1], Erika Resetkova[1], Savitri Krishnamurthy[1], Taylor Salisbury[3], Aysegul Sahin[1], Qingqing Ding[1]
[1]The University of Texas MD Anderson Cancer Center, Houston, TX, [2]BC Cancer Vancouver Centre, Vancouver, Canada, [3]BC Cancer Agency, University of British Columbia, Vancouver, Canada

Disclosures: Esther Yoon: None; Gang Wang: None; Yun Wu: None; Hui Chen: None; Constance Albarracin: None; Erika Resetkova: None; Savitri Krishnamurthy: None; Taylor Salisbury: None; Aysegul Sahin: None; Qingqing Ding: None

Background: GATA3 is used to support the diagnosis of breast carcinoma (BC). However, the GATA3 expression level falls < 40% in all triple negative (TN) BC. SOX10 is an alternative marker for TNBC, but it can be problematic in patients with a history of melanoma. Most recently TRPS1 has been reported to be a highly sensitive and specific marker for BC. We aim to study and compare the expression of TRPS1, GATA3, and SOX10 in TNBCs, specifically, invasive breast carcinoma of no special type (IBC-NST), and invasive lobular carcinoma (ILC).

Design: We identified 105 cases of TNBCs between 2019 to 2021 from two institutions. Tissue sections of primary or metastatic TNBC cases (predominantly core biopsy without treatment) were stained with GATA3, SOX10, and TRPS1 using Leica Bond Max autostainer system following standard automated protocols. Nuclear staining was considered positive for all three stains, and their immunoreactivity scores were calculated as the product of the percentage of positive cells (0, <1%; 1, 1%-10%; 2, 11%-50%; and 3, 51%-100%) and the staining intensity (0, negative; 1, weak; 2, moderate; and 3, strong). The scores were defined as negative (0 or 1), low positive (2), intermediate positive (3 or 4), or high positive (6 or 9).

Results: The TNBC included 97 (92%) IBC-NSTs and 8 (8%) ILCs. Of the primary tumors (n=76; 72%), 95% were Nottingham histologic grade 3. All of the TN ILCs were positive for TRPS1 and GATA3, while negative for SOX10. Of the TN IBC-NSTs, TRPS1 was positive in 100% of the cases, SOX10 and GATA3 were positive in 77% and 63% of cases, respectively. One IBC-NST case was negative for both GATA3 and SOX10, while the rest of IBC-NSTs were positive for at least one of GATA3 or SOX10. For all included cases, 26% was SOX10-/GATA3 intermediate to high positive, 46% was SOX10+/GATA3 negative to low positive, 26% was intermediate to high positive for both GATA3 and SOX10. In addition, most of the TRPS1 and SOX10 positive cases demonstrated high positive scores and no case showed low positive expression.

Table 1. Expression of TRPS1, GATA3 and SOX10 in triple negative IBC-NST and ILC.

		Negative, n (%)	Positive, n (%)			Total cases
			Low	Intermediate	High	
TRPS1	All TNBC	0 (0%)	0 (0%)	4 (4%)	101 (96%)	105
	IBC-NST	0 (0%)	0 (0%)	2 (2%)	95 (98%)	97
	ILC	0 (0%)	0 (0%)	2 (25%)	6 (75%)	8
GATA3	All TNBC	36 (34%)	15 (14%)	15 (14%)	39 (37%)	105
	IBC-NST	36 (37%)	15 (15%)	14 (14%)	32 (33%)	97
	ILC	0 (0%)	0 (0%)	1 (13%)	7 (88%)	8
SOX10	All TNBC	30 (29%)	0 (0%)	8 (8%)	67 (64%)	105
	IBC-NST	22 (23%)	0 (0%)	8 (8%)	67 (69%)	97
	ILC	8 (100%)	0 (0%)	0 (0%)	0 (0%)	8

TNBC: Triple negative breast carcinoma; IBC: Invasive breast carcinoma of no special type; ILC: Invasive lobular carcinoma

Figure 1 - 196

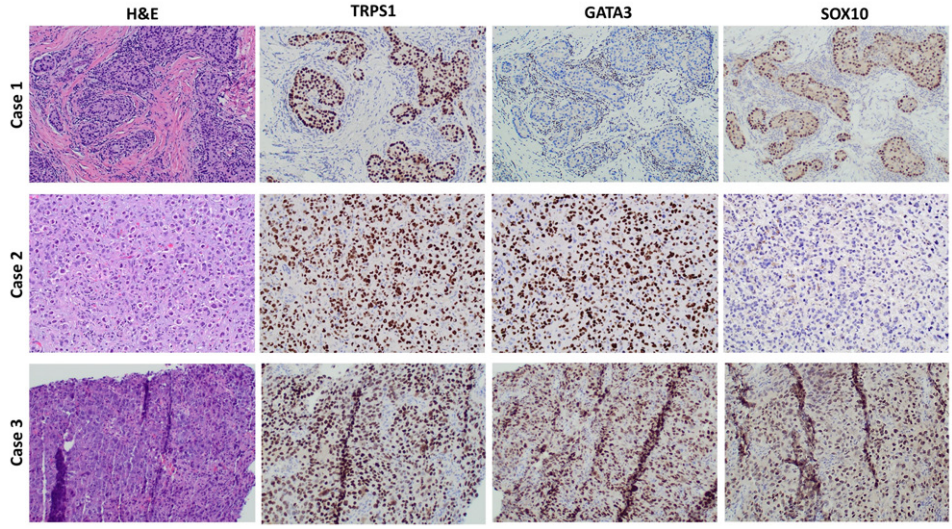

Conclusions: TRPS1 is a more sensitive marker for TNBC than previously used and more popular GATA3 or SOX10. Although GATA3 and SOX10 were co-expressed in less than one-third of the cohort, expression of luminal marker GATA3 and basal/myoepithelial marker SOX10 expression was inversely correlated in more than two-thirds of the cohort. Our findings suggest GATA3 and SOX10 can be used to distinguish these subtypes of TNBCs.

197 AI-assisted Microscope Improved the Precision of HER2 IHC 0 and 1+ of Breast Cancer

Meng Yue[1], Xinran Wang[1], Yueping Liu[1]
[1]The Fourth Hospital of Hebei Medical University, Shijiazhuang, China

Disclosures: Meng Yue: None; Xinran Wang: None; Yueping Liu: None

Background: The level of human epidermal growth factor receptor-2 (HER2) in breast cancer is an essential factor in judging the prognosis of breast cancer patients. HER2 immunohistochemistry(IHC) 1+ or 2+, but FISH negative are currently being classified as HER2-low. It showed exciting treatment results with trastuzumab deruxtecan (T-Dxd). But several investigations have shown high intraobserver and interobserver variability of HER2 diagnosis by visual examination. In this study, we aim to propose an AI-assisted microscope to improve the HER2 interpretation accuracy and consistency of IHC 0 and 1+.

Design: The AI-assisted microscope equipped a conventional microscope with AI algorithms and an augmented reality module so that pathologists can get AI results in real time. A cell-level classification based HER2 scoring algorithm was deployed on the AI assisted microscope. We organized a ring study that employed forty invasive breast carcinoma cases of non-special subtype without new adjuvant treatment and recruited 10 pathologists from 3 hospitals. In the first ring study (RS1), the pathologists read 40 HER2 through a conventional microscope. After 2 weeks of forgetting period, in the second ring study (RS2), they read the HER2 slides through an AI -assisted microscope for assisted interpretation. Interpretation accuracy, consistency and the AI acceptance rate were evaluated.

Results: The concordance evaluation of HER2 in RS2 was better than RS1 ($p < 0.001$). The consistency and accuracy of interpretation by AI-assisted microscope were further improved compared with using a conventional microscope, kappa 0.85 (0.83-0.87). The average acceptance rate of AI for all pathologists was 0.92, demonstrating that the pathologists agreed with most of the AI scoring results. AI-assisted microscope improved the precision of IHC 0 and 1+.

Figure 1 - 197

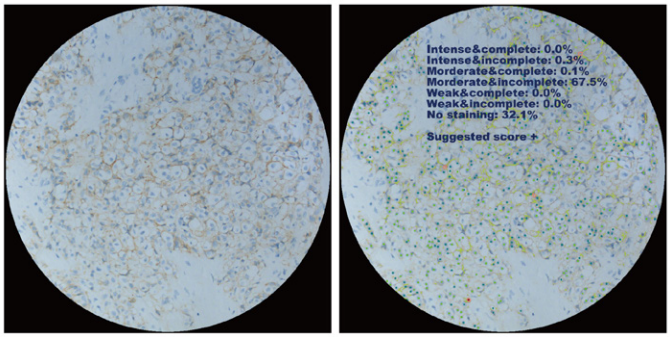

Figure 2 - 197

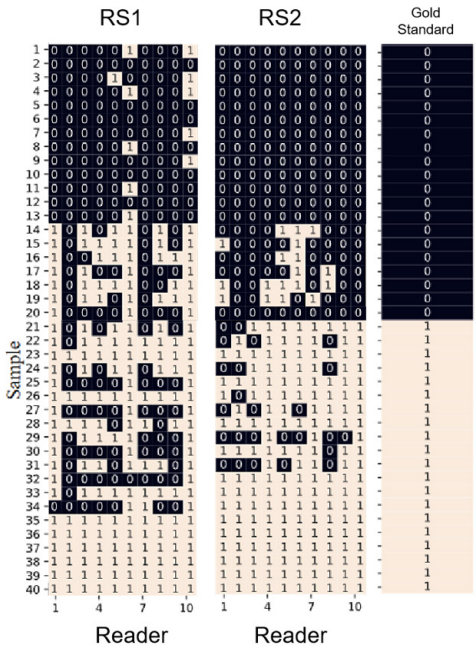

Conclusions: With the AI-assisted microscope, the accuracy and consistency of HER2 IHC 0 and 1+ among different pathologists can be significantly improved.

198 Invasive Lobular Carcinomas with Negative ER and/or HER2 Overexpression Display Frequent High Histological Grade, ILC Variant Features, and Reduced H3K27me3 Expression

Katelyn Zebrowski[1], N. Lynn Henry[1], Emily Mcmullen[2], Celina Kleer[2]
[1]Michigan Medicine, University of Michigan, Ann Arbor, MI, [2]University of Michigan, Ann Arbor, MI

Disclosures: Katelyn Zebrowski: None; N. Lynn Henry: None; Emily Mcmullen: None; Celina Kleer: None

Background: Invasive lobular carcinomas (ILC) display low grade single cancer cells with subtle infiltration, almost invariably ER/PR positive and HER2 negative. ILC may infrequently be ER/PR negative and/or overexpress HER2 (ILC with aberrant receptors). Despite the recognition of these cases, their histological and clinical features are unclear, and there are no specific biomarkers. The Polycomb group proteins regulate cell type identity through H3K27me3-mediated gene repression. High H3K27me3 was reported in ER positive breast cancer, but its expression in ILC and relationship to ER/PR/HER2 in ILC is unknown. We investigate the pathology and H3K27me3 expression of ILC with aberrant receptors.

Design: We searched the pathology files for ILC with negative ER/PR, HER2 2+, 3+, and amplified by FISH for the period 2000-2021. Three pathologists reviewed all slides and extracted clinicopathological data. E-cadherin verified ILC diagnoses. A subset of ILC with aberrant receptors and classical ILC was immunostained for H3K27me3. We blindly scored the percentage of H3K27me3 positive tumor cells as 0: <5%, 1: 5–49%, 2: 50–95%, and 3: >95%, following a published study. Data was analyzed by Chi Square and Fisher exact tests.

Results: We identified 33 ILC with aberrant receptors (24% ER negative, 58% HER2 positive, and 18% ER negative/HER2 positive). Of the ILC with aberrant receptors, 33% had histological grade 3 (of 3), and 24% had heterogeneous histology with foci of pleomorphic (24%) and solid (3%, also pleomorphic) ILC. Of the 33 cases, 52% had associated LCIS, which was pleomorphic in 29% of those cases; and 18% had associated DCIS. We found that 18% had lymph node metastases and 21% had distant metastasis. H3K27me3 was highly expressed in over 95% of tumor cells in all the classic ILC tested (6/6). In contrast, H3K27me3 expression was significantly reduced in all the ILC with aberrant receptor expression (n=10, mean staining=40%, range 5-95%), Chi square test P=0.0002.

Conclusions: ILCs with negative ER and/or HER2 overexpression have high frequency of high histological grade and display intratumoral heterogeneity with areas of pleomorphic and solid differentiation. In contrast with classical ILC, ILC with aberrant receptor expression exhibit significant reduction in H3K27me3. Ongoing studies are aimed at investigating the significance to treatment response and survival in comparison to classical ILC.

199 Biomarker Profile of Invasive Lobular Carcinoma: Pleomorphic versus Classic Subtypes, Clinicopathological Characteristics and Prognosis Analyses

Yu Zhang[1], Xiulan Luo[1], Libo Yang[2], Min Chen[1], Bing Wei[1], Zhang Zhang[1], Hong Bu[1]
[1]West China Hospital, Sichuan University, Chengdu, China, [2]West China Hospital, Sichuan University, China/The University of Texas MD Anderson Cancer Center, USA, Abidjan

Disclosures: Yu Zhang: None; Xiulan Luo: None; Libo Yang: None; Min Chen: None; Bing Wei: None; Zhang Zhang: None; Hong Bu: None

Background: Pleomorphic lobular carcinoma (PLC) is a rare subtype of invasive lobular carcinoma (ILC), considered to be more aggressive than classic ILC (C-ILC). Our aim is to compare the clinicopathological features and prognosis of PLC and C-ILC according to biomarker profile.

Design: 620 C-ILC cases and 75 PLC cases in our institution from 2010 to 2020 were included. ER, PR, HER2 and Ki67 status were detected by IHC. HER2(2+) cases were evaluated by FISH. Statistical analysis was performed with chi-square test, Kaplan-Meier test, univariate and multivariate cox regression.

Results: Compared to C-ILC, PLC patients were older (mean ages[years]: 52vs.48), had larger mean tumor size (3.3cm vs.2.6cm), higher histological grade, lower ER/PR positive rate, higher Ki67 index and HER2 positive rate (P<0.05). C-ILC was mainly classified as luminal A (374, 60.3%) and PLC was mostly luminal B (55, 73.3%). The morphological features of PLC in our study were classified as apocrine, signet-ring cells, clear cells according to cytological pattern. PLC-NOS without specific cytology was divided into solid, trabecular, alveolar and sclerotic based on growth pattern (Fig1). Luminal B PLC was more classified into trabecular (20/55, 36.4%), HER2+PLC was mostly apocrine (5/11, 45.5%), and triple-negative PLC was solid (4/9, 44.4%). Overall survival (OS) and disease-free survival (DFS) of PLC were worse than C-ILC (P<0.05). Median OS on 47 ER+PLC patients received endocrine therapy was higher than those without endocrine therapy (months: 78 vs.54) (P=0.005). ER+PLC's DFS was better than ER-PLC (P=0.034), OS and DFS were worse than matched ER+ invasive ductal carcinoma (IDC) group (P<0.05). Median OS on 8 HER2+PLC patients received HER2-targeted therapy was higher than those without targeted therapy (months: 89 vs.34) (P=0.044). HER2+PLC's OS was worse than HER2-PLC (p=0.037) and ER+PLC (p=0.028), OS and DFS were worse than matched HER2+IDC group and HER2+C-ILC (P<0.05). (Fig2) Multivariate Cox regression analysis found that HER2 status was related with OS (HR:0.08; 95%CI:0.01-0.8), histological grade was related to OS (HR: 41.9; 95%CI:3.2-555.5) and DFS (HR:5.0; 95%CI:1.4-18.3) in PLC.

Figure 1 - 199

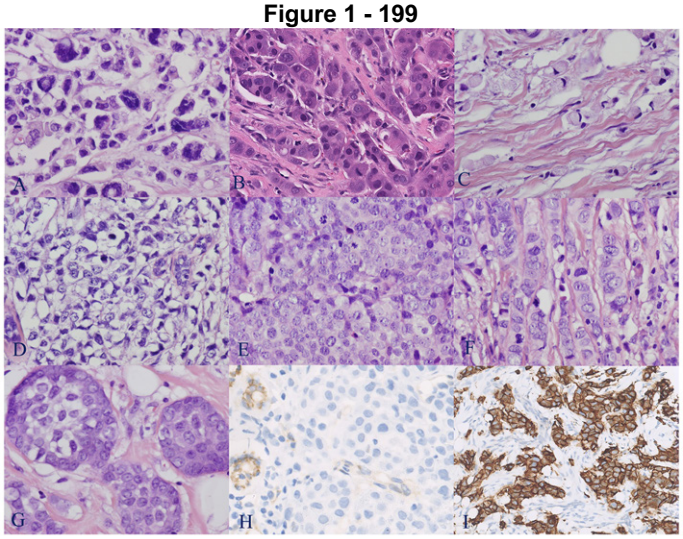

Figure 1: The representative H&E and IHC image of morphological features in PLC: Pleomorphic (A), Apocrine (B), Signet-ring cells (C), Clear cells (D), Solid (E), Trabecular (F), Alveolar (G), E-cadherin of PLC (H), HER2-positive (3+) of PLC (I).

Figure 2 – 199

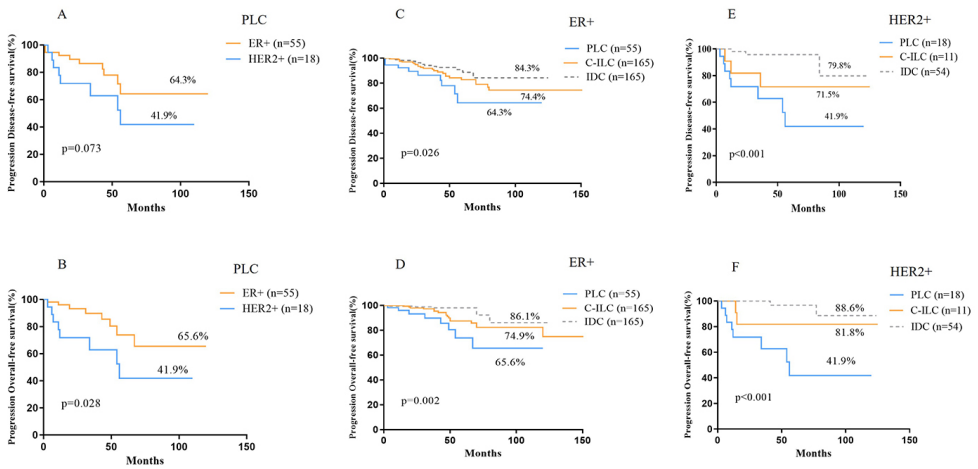

Figure 2: Kaplan-Meier survival analysis of OS and DFS between PLC, C-ILC and IDC: (A-B) DFS and OS between ER+PLC and HER2+PLC groups. (C-D) DFS and OS between ER+PLC, matched ER+C-ILC control group (1:3) and matched ER+IDC control group (1:3). (E-F) DFS and OS of HER2+PLC, matched HER2+IDC control group (1:3) and HER+C-ILC.

Conclusions: PLC was a heterogeneous cancer with high proliferative activity and invasiveness. ER-PLC had poorer DFS, HER2+PLC was associated with worse OS. PLC with grade 3 often had poorer OS and DFS. Clinical diagnosis and treatment need to strengthen the corresponding endocrine therapy or HER2-targeted therapy.

200 Breast Cancers with Reflex HER2 FISH Group 3 Results: Clinicopathological Features, Genomic Profiling and Follow-Up Outcomes

Huina Zhang[1], Rana Ajabnoor[2], Ajay Dhakal[3], Bradley Turner[1], David Hicks[1]
[1]University of Rochester Medical Center, Rochester, NY, [2]King Abdulaziz University, Jeddah, Saudi Arabia, [3]Wilmot Cancer Institute, University of Rochester Medical Center, Rochester

Disclosures: Huina Zhang: None; Rana Ajabnoor: None; Ajay Dhakal: None; Bradley Turner: None; David Hicks: *Advisory Board Member*, AstraZeneca

Background: Breast cancers with HER2 ISH Group 3 result is defined as HER2/CEP17 ratio < 2 and average HER2 copy number ≥ 6 signals/cell and accounts for 0.4-3.0% of breast cancers sent for dual-probe ISH assay. Due to the rarity, breast cancers with HER2 ISH group 3 results are little-studied, especially the long-term outcome and role of HER2 targeted therapy. We herein report the clinicopathologic, underlying genomics and follow-up outcomes of breast cancer patients with reflex HER2 group 3 FISH results.

Design: A retrospective search of the pathology laboratory information system at our institution was performed to identify breast cancer cases with Group 3 FISH results between January 2007 and March 2020. Available clinicopathologic characteristics (age, tumor size, pathologic stage and clinical stage), histomorphologic features (histologic type, histologic grade, lymphovascular invasion), prognostic variables (estrogen receptor [ER], progesterone receptor [PR], average HER2 copy number/cell, average CEP17 copy number/cell, and Ki-67) and clinical follow-up information (HER2-targeted therapy, event of local recurrence/ distant metastasis/died of disease) were collected. MammaPrint and BluePrint molecular assays were performed in a subset cases. Chi-square test was performed for categorical data and unpaired t-test was performed for numerical data. P-value < 0.05 was considered statistically significant.

Results: Fifty-two (1.8%, 52/2,874) breast cancers with HER2 FISH group 3 results were identified. Most of the FISH group 3 cases were high grade ductal carcinomas (54.6%) with positive ER expressions (89.3%). Among all the clinicopathologic variables, tumor size and clinical stage were significantly associated with disease outcomes. Average HER2 copy number failed to show any association with histologic grade, tumor size, clinical stage, hormonal receptor status or disease outcomes. Kaplan-Meier survival analysis revealed there was no statistically significant difference in overall survival and disease free survival between nineteen patients who were treated with HER2 targeted therapy and nine patients who were untreated. Out of 20 cases which were tested

for MammaPrint and BluePrint, 15 (75%) were high genomic risk, and 16 (80%) were luminal type. HER2 molecular type was only identified in 2 cases (10%) (Table 1).

Table 1. Genomic profiling of breast cancer with HER2 FISH Group 3 results

	Total (n=20)	%
MammaPrint		
Ultra Low Risk (MPI score : 0.355 to 1.0)	0	0
Low Risk (MPI score : 0.0 to 0.355)	5	25
High Risk-H1 (MPI score: 0.0 to -0.57)	13	65
High Risk-H2 (MPI score: -0.57 to -1.0)	2	10
BluePrint		
Luminal A	5	25
Luminal B	11	55
HER2 type	2	10
Basal type	2	10

Conclusions: We have presented novel clinicopathological, molecular and clinical outcome data of understudied HER2 FISH Group 3 tumors. Our results have suggested that most of breast cancers with HER2 FISH group 3 results were high-risk, luminal type disease and lack of significant benefit associated with perioperative HER2 targeted therapy in this unique cohort. Larger, more definitive study is still needed to confirm.

201 Evaluation of Lumpectomy Resection Margins for Invasive Breast Cancer: A Single Institution's Experience

Yong Zhang[1], Wei Huang[1], Tiane Chen[1], Bing Han[2]
[1]Penn State Health Milton S. Hershey Medical Center, Hershey, PA, [2]Hershey, PA

Disclosures: Yong Zhang: None; Wei Huang: None; Tiane Chen: None; Bing Han: None

Background: Breast conservation therapy (BCT) or lumpectomy followed by radiation has been established as a preferred treatment for most patients with early-stage invasive breast cancer. Lumpectomy provides the long-term equivalent survival compared to mastectomy. The main aims of lumpectomy are to obtain clean microscopic margins while maximally maintaining the cosmetic appearance of the breast. About 25% of patients after initial lumpectomy will have to undergo re-excision due to the positive margin status.

Design: To determine the factors predicting higher risk of positive resection margin, we retrospectively analyzed 193 patients who underwent initial lumpectomy for breast cancer from 2019 to 2021 at Hershey Medical Center. Based on the microscopic examination, the samples were divided into 3 subgroups with positive, close or clean margins. Positive resection margins were defined as tumor on the ink. Close margins were defined as identifying tumor cells <2 mm from the inked edge. Clean margins were verified as having tumor cells ≧2mm away from the ink. The candidate risk factors were shown in *Figure 1A*. Comparisons for these tumor characteristics were done by using Chi-square test, or Student's *t* test.

Results: Of 193 breast cancer cases, positive margin rate was 14% (*Figure 1B*). Positive margin was more frequently associated with invasive lobular carcinoma, or mixed type (invasive carcinoma with ductal and lobular features) ($p<0.0001$, *Figure 1C*). Positive margin was also significantly associated with multifocal tumor deposits ($p<0.01$, *Figure 1D*), and positive lymph node (LN) status ($p=0.03$, *Figure 1E*). Clean margin group tended to have smaller tumor size (*Figure 1F*). Other factors were not significantly associated with margin status including tumor grade (*Figure 2A*), HER2/ER/PR status (*Figure 2B*), lymphovascular invasion(LVI) (*Figure 2C*), DCIS component (*Figure 2D*), and age at diagnosis (*Figure 2E*).

Figure 1 - 201

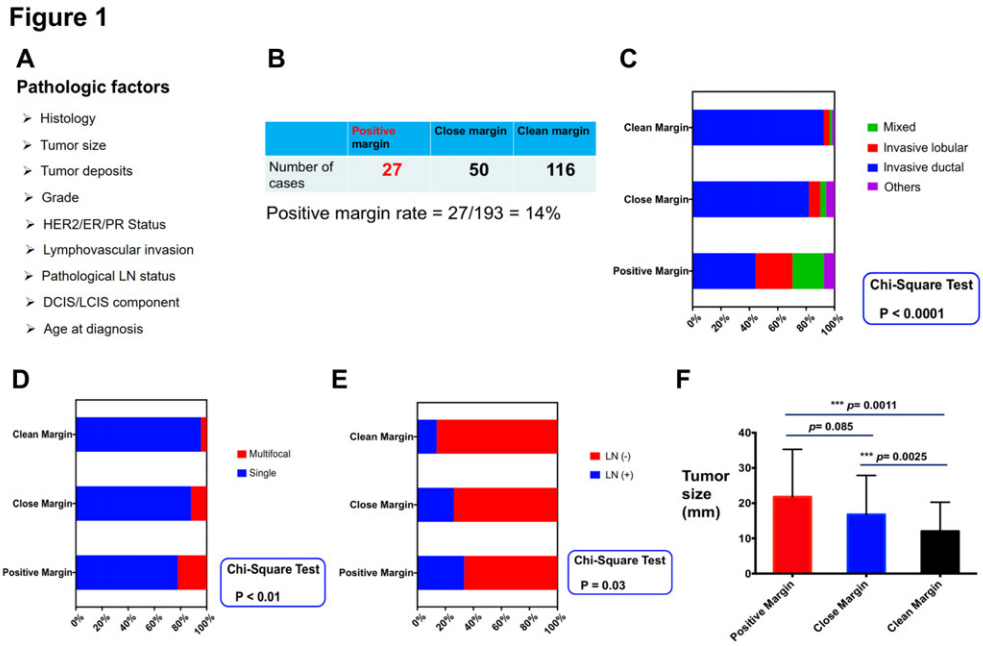

Figure 2 – 201

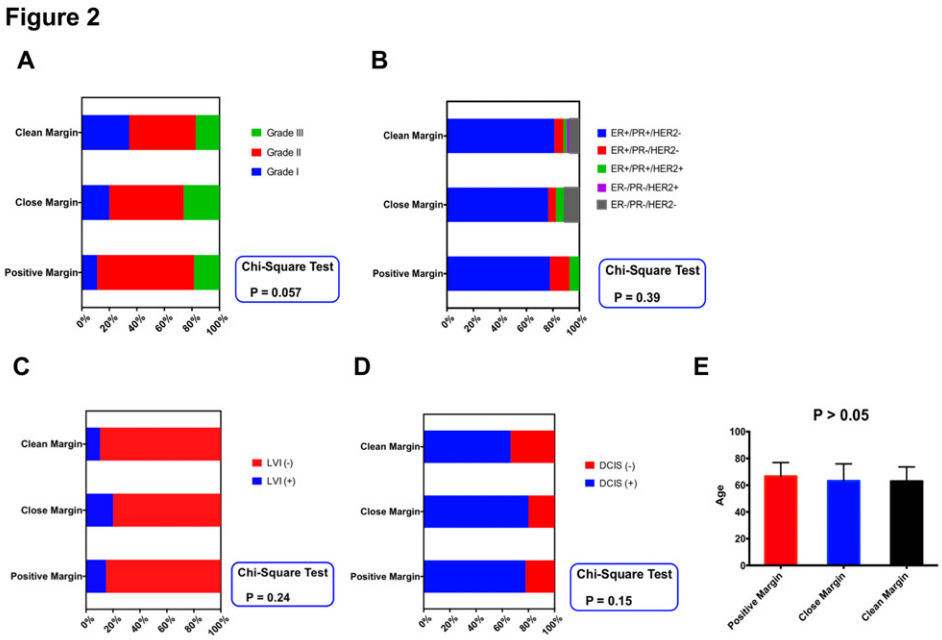

Conclusions: We demonstrated that four predictive tumor-related factors significantly associated with positive margin. Identification and comprehensive assessment of these pathological predictors are important for clinical management not only providing information to multidisciplinary team, but also facilitating surgeons to make pre-operative and intraoperative surgical decisions and reduce the chance of re-excision.

202 Identifying HER2-Low Breast Cancers by Immunohistochemistry: Inter-observer and Inter-antibody Reproducibility

Huina Zhang[1], Xi Wang[2], Hani Katerji[1], Bradley Turner[1], David Hicks[1]
[1]University of Rochester Medical Center, Rochester, NY, [2]University of Rochester, Rochester, NY

Disclosures: Huina Zhang: None; Xi Wang: None; Hani Katerji: None; Bradley Turner: None; David Hicks: *Advisory Board Member*, AstraZeneca

Background: The promising efficacy of novel HER2-targeted therapy in HER2-low breast cancers has raised the possibility of changing the interpretation of HER2 status in breast cancer into: HER2-negative (IHC score of 0), HER2-low (IHC score of 1+, or 2+ with non-amplified ISH), and HER2-positive (IHC score of 3+ or IHC score of 2+ with amplified ISH). Identifying HER2-low breast cancer under this proposed definition relies predominantly on HER2 results evaluated by semi-quantitative IHC assay. We herein investigated the inter-observer and inter-antibody reproducibility of HER2 IHC in breast cancers, with an emphasis on HER2-low breast cancers.

Design: 114 breast cancer cases with HER2 scores of 0 to 3+ were stained with both HERcepTest and 4B5 clone. All cases were independently scored by three breast pathologists using the 2018 ASCO/CAP HER2 testing guideline. The level of inter-observer agreement between observers, and the inter-antibody reproducibility between these two antibodies was evaluated by Cohen's Kappa analysis.

Results: The inter-observer agreement for HERcepTest and 4B5 clone was 74% and 69.6%, with a weighted Kappa value of 0.743 and 0.726, respectively (substantial agreement). The inter-antibody agreement between HERcepTest and 4B5 clone was 60.2%, with a weighted Kappa value of 0.430 (moderate agreement). The inter-observer agreement for HERcepTest increased from 76.7% (Kappa value: 0.447, moderate agreement) for cases with an IHC score of 0 to 1+, to 93.0% for cases with an IHC score of 2 to 3+ (Kappa value: 0.859, substantial agreement). The inter-observer agreement for 4B5 antibody showed a similar trend, increasing from 71.5% for cases with an IHC score of 0-1+ (Kappa value: 0.405, moderate agreement), to 92.4% for cases with an IHC score of 2-3+ (Kappa value: 0.845, substantial agreement). The number of cases classified as HER2-negative or HER2-low by HERceptTest ranged from 14 to 30 for HER2-negative result, and 56 to 72 for HER2-low result. There was 100% agreement between all observers for a HER2-positive result (Table 1).

Table 1: Distribution of HER2-Negative, HER2-Low and HER2-Positive cases between observers and antibodies

	HER2 Negative (IHC score of 0)	HER2 Low (IHC score of 1+, or 2+ with non-amplified FISH)	HER2 Positive (IHC score of 3+ and IHC score of 2+ with amplified FISH)	Total
HERcept				
Observer 1	14	72	28	114
Observer 2	16	70	28	114
Observer 3	30	56	28	114
4B5 clone				
Observer 1	11	75	28	114
Observer 2	11	73	28	114
Observer 3	34	52	28	114

IHC: Immunohistochemistry; FISH: Fluorescent in-situ hybridization

Conclusions: Our results reinforce there is inter-observer and inter-antibody variation in evaluation of HER2 IHC, particularly in cases with 0 to 1+ HER2 staining. Given that IHC is the primary assay used to identify HER2-low breast cancer, our results suggest that until a more consistently reproducible methodology is available, careful evaluation of HER2 IHC, with consensus between observers, may be required for the evaluation of HER2-low breast cancer.

203 Does the Status of Tumor Bed at Surgical Margins Affect Local Recurrence and Overall Prognosis in Patients Undergoing Lumpectomy Status Post Neoadjuvant Therapy?

Xiaofeng Zhao[1], Anupma Nayak[2], Ira Bleiweiss[3]
[1]Temple University Hospital, Philadelphia, PA, [2]Perelman School of Medicine at the University of Pennsylvania, Philadelphia, PA, [3]Hospital of the University of Pennsylvania, Philadelphia, PA

Disclosures: Xiaofeng Zhao: None; Anupma Nayak: None; Ira Bleiweiss: None

Background: As neoadjuvant therapy in breast cancer has gained more popularity due to its effectiveness in downstaging the tumor and providing information regarding treatment response, more breast lumpectomies status post neoadjuvant therapy are encountered in daily practice. However, consistent and reproducible pathologic assessment of response to neoadjuvant chemotherapy is hindered by a lack of universal reporting protocols. There is limited data suggesting that pathology reports should include the status of fibrotic tumor bed, particularly in tumors with swiss-cheese pattern of response. The aim of this study is to assess whether the margin positive for fibrotic bed affects local recurrence or overall prognosis in patients undergoing neoadjuvant lumpectomies.

Design: We retrospectively retrieved all breast carcinoma lumpectomy specimens status post neoadjuvant therapy over a 10-year period from the pathology archives. Clinical and pathologic features, including age, race, biomarker status, treatment, response, recurrence, survival etc. were obtained from electronic medical records. H&E Slides were reviewed by breast pathologists to evaluate the status of resection margins in relation to fibrotic tumor bed. The prognosis for each case was classified as well (disease-free for >=5 years), local recurrence, metastasis, death or lost-to-follow-up (LFU).

Results: Between July 2005 and July 2015, a total of 64 lumpectomies status post neoadjuvant therapy were retrieved (median age 56-year old, range 30-80 years). 64% of our patients were Caucasians, 30% were African Americans, 2% were Asians, and the rest were among other ethnic minorities or of unknown ethnicity. Twenty (31%) cases had pathologic complete response, including 8 (40%) cases with positive fibrotic bed margin and 12 (60%) cases with negative margins. Forty-four (69%) cases had partial pathologic response. Thirty of the specimens were found to be positive for fibrotic tumor bed at resection margins (47%) and 34 were negative (53%). The margin status for the fibrotic tumor bed did not show any correlation with the biomarker status or the prognosis of the tumor (see Table-1).

Overall prognosis	**Recurrence**	**Metastasis**	**Death**	**Disease free >5 years**	**LFU**	**P-value**
Positive fibrotic bed margin (30)	1 (3%)	6 (20%)	0 (0%)	23 (77%)	0 (0%)	>0.05
Negative fibrotic bed margin (34)	4 (12%)	9 (27%)	1 (3%)	19 (56%)	4 (12%)	
Cases with incomplete response	**Recurrence**	**Metastasis**	**Death**	**Disease free >5 years**	**LFU**	**P-value**
Positive fibrotic bed margin (22)	1 (5%)	6 (27%)	0 (0%)	15 (68%)	0 (0%)	>0.05
Negative fibrotic bed margin (22)	2 (9%)	7 (32%)	0 (0%)	12 (55%)	1 (5%)	
Fibrotic bed margin	**ER positive**	**HER2 positive**	**TN**			
Positive fibrotic bed margin (30)	11 (37%)	10 (33%)	9 (30%)			
Negative fibrotic bed margin (34)	18 (53%)	7 (21%)	9 (27%)			

Conclusions: Margins positive for fibrotic tumor bed do not cause significant difference in recurrence or overall 5-yr survival in patients with breast cancer status post neoadjuvant therapy.

204 OXC1 Predicts HER2-FISH Status in Breast Cancers with Equivocal HER2 IHC Results

Ke Zuo[1], Ming Li[1], Qianming Bai[1], Hongfen Lu[1], Xiaoyan Zhou[2], Wentao Yang[1]
[1]Fudan University Shanghai Cancer Center, Shanghai, China, [2]Fudan University Shanghai Cancer Center, Shanghai Medical College, Fudan University, Shanghai, China

Disclosures: Ke Zuo: None; Ming Li: None; Qianming Bai: None; Hongfen Lu: None; Xiaoyan Zhou: None; Wentao Yang: None

Background: In ER negative (ER^-) breast cancers, HER2 status is a determinant for patients. They can be either classified as triple negative breast cancer (TNBC) or HER2 positive cancer. Patients with TNBC are commonly involved in chemotherapy due to lack of targeted therapies. For patients with HER2 IHC 3+ or equivocal 2+ ($HER2^{IHC2+}$) with HER2 gene amplification determined by FISH assay, they can benefit from anti-HER2 targeted treatment. However, various uncertain situations are encountered in daily practice, such as heterogeneity of HER2 IHC results or failure to obtain FISH results promptly. Therefore, a quick and accurate method which can predict HER2 status is particularly important. FOXC1 is a relatively specific marker for TNBC with basal like

subtype. We speculate that breast cancer with ER$^-$HER2^{IHC2+} phenotype is likely to be finally classified as TNBC if FOXC1 is strongly positive. Thus, this study is aimed to provide a basis of FOXC1 to predict HER2 status by analyzing the correlation between the results of FOXC1 and HER2-FISH status.

Design: A retrospective cohort of 124 patients with clinical and pathological data from 2019 to 2021 were included in this study. By using Fisher's exact test or Chi-Square test, we analyzed the correlation between IHC expression status of FOXC1 and HER2-FISH results as well as with other clinicopathological parameters. Additionally, genomic sequencing information was available for 42 cases. The difference of genetic changes between FOXC1$^-$ and FOXC1$^+$ patients is analyzed.

Results: Among 124 cases of ER$^-$HER2^{IHC2+} breast cancer, there were 45 cases with positive (cutoff value ≥10%) FOXC1 expression, of which 95.6% (43/45) were HER2-FISH negative and only 4.4% (2/45) were positive. Therefore, the majority of FOXC1$^+$ cases are not accompanied by HER2 gene amplification. There was significant difference between the FOXC1$^+$ and FOXC1$^-$ data sets (P value = 0.0030) (Table1). In addition, the positive status of FOXC1 was also significantly related to histological grades, Ki67 index and AR status (all P values <0.0001) (Table1). Genomic sequencing information of 42 cases shows that 23 cases of ER$^-$HER2^{IHC2+}FOXC1$^-$ breast cancer were dominated by TP53 and PIK3CA gene mutations, while 19 cases of ER$^-$HER2^{IHC2+}FOXC1$^+$ breast cancer showed TP53 mutation as the dominant genetic change.

Table1.
Clinical and pathologic features of 124 ER$^-$HER2^{IHC2+} cases

	FOXC1 Status		
	FOXC1(-)	FOXC1(+)	P value
Median Age	62(33-88)	51(29-82)	/
T Stage			
T1	30	10	0.1479
T2	44	33	
T3	5	2	
T4	0	0	
N Stage			
N0	51	28	0.8358
N1	17	11	
N2	7	5	
N3	4	1	
Histologic Grade			
1	0	0	<0.0001
2	31	1	
3	48	44	
HER2 IHC(2+)	79	45	/
Ki-67			
≥30%	37	43	<0.0001
＜30%	42	2	
FISH Status			
non-amplified	59	43	0.0030
Amplified	20	2	
AR			
Negative	7	36	<0.0001
Positive	72	9	

Conclusions: In ER$^-$HER2^{IHC2+} cases, the expression of FOXC1 is significantly correlated with HER2-FISH-negative status, and FOXC1 can be used as a potential predictive marker.